Evolution and diversification of Amphipoda in the polar regions: the case study of *Eusirus* genus

Louraine Salabao

Laboratory of Evolutionary Ecology, FOCUS, Department of Biology, Ecology & Evolution, University of Liège, Belgium

Hasselt University, Centre for Environmental Sciences, Zoology: Toxicology and Biodiversity, Campus Diepenbeek, Belgium

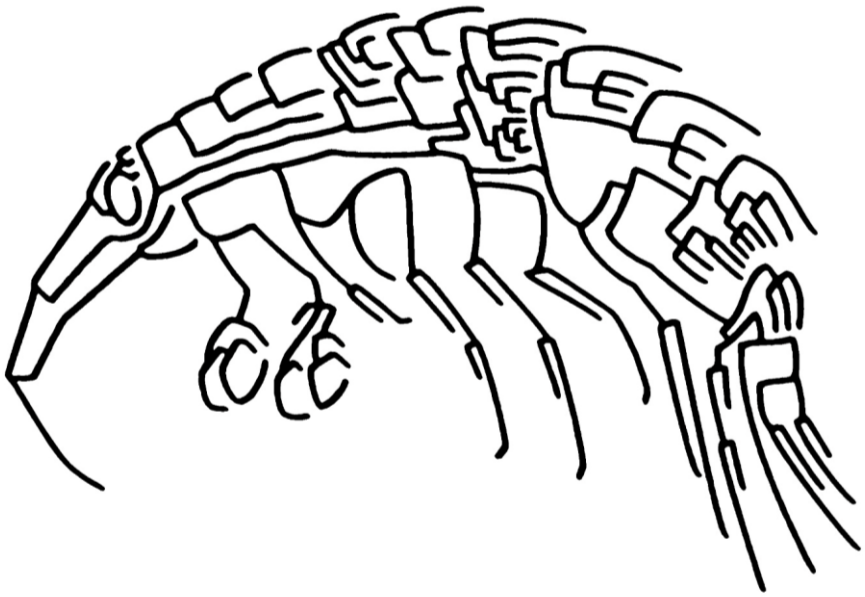

Doctoral dissertation submitted to obtain the degree of Doctor of Sciences: Biology and Doctor in Sciences

Promoters:

Dr. Isa Schön (Hasselt University/ Royal Belgian Institute of Natural Sciences)

Dr. Bruno Frederich (University of Liège)

D/2023/2451/100

Jury Composition

Dr. Jean-Christophe Plumier, President (University of Liège, Belgium)

Dr. Gilles Lepoint, Secretary (University of Liège, Belgium)

Dr. Agnès Dettai (National Museum of Natural History, Paris, France)

Dr. Nikol Kmentova (Hasselt University, Belgium)

Dr. Marie Verheye (Katholieke Universiteit Leuven, Belgium)

Dr. Bruno Frederich, Promoter (University of Liège, Belgium)

Dr. Isa Schön, Promoter (Hasselt University/Royal Belgian Institute of Natural Sciences, Belgium)

Acknowledgements

I wish to express my deepest gratitude to all the people who made this thesis possible. Most especially, I would like to extend my heartfelt thanks to the following:

Dr. Bruno Frédérich and Dr. Isa Schön, my promoters. Thank you for your constant guidance, encouragement and invaluable suggestions to improve my thesis. I am indeed very grateful and fortunate to have passionate promoters like you who were always there to help and support me through all the stages of writing my thesis.

Dr. Marie Verheye, Dr. Gilles Lepoint, and Dr. Tom Artois, my thesis committee. Thank you for constantly lending your expertise on the subject matter of my thesis and for your insightful comments which greatly helped me to improve my thesis.

My jury members, thank you for taking the time to read my thesis despite your busy schedules. Your constructive comments and invaluable suggestions were instrumental in helping me to polish my thesis.

To the various funding organizations including the Bijzonder Onderzoeksfonds (BOF) and Belgian Science Policy (Belspo) (BRAIN RECTO Project) made it possible to carry out this this research.

The Royal Belgian Institute of Natural Sciences (RBINS), freshwater biology team, and the molecular laboratory, for being instrumental in the success of my research, and I extend my heartfelt gratitude to them for hosting me and generously providing access to their advanced molecular laboratory facilities.

Cedric, thank you for sharing your expertise and knowledge on *Eusirus*.

Dr. Agnès, my warmest thanks for helping me with the sequencing of my samples.

Prof. Kochzius, Prof. Vanderpoorten, and his laboratory technician Laurent, thank you for allowing me to use your laboratory during the covid times.

Julien, thank you for helping me with the stack photography.

The different institutes and Universities who loaned me their *Eusirus* samples: Royal Belgian Institute of Natural Sciences (RBINS) through Dr. Samyn, Muséum, National d'Histoire Naturelle (MNHN) through Dr. Corbari, Centre for Biodiversity Genomics (University of Guelph,

Canada) through Dr. Dewaard and the help of Dr. Layton. Also to the Civic Museum of Natural History of Verona through Dr. Latella and Dr. Salmaso. The National Institute of Water and Atmospheric Research (NIWA, New Zealand) through Dr. Mills, Natural History Museum of Denmark through Dr. Jacobsen, Museum of Natural History Berlin through Dr. Coleman, and Hiroshima University through Dr. Tomikawa. Lastly, to Dr. Jung and Dr. Coleman for lending me your samples. This research would not have been possible without your collaboration and support.

The people on the fourth floor in RBINS and also the ones in UHasselt and ULiege, thank you for extending your help whenever I needed it.

The freshwater biology team: Jeroen, Tasnim, Marie, Dorien, Prof. Koen, Kristiaan, Tim, Joseph, and Zohra, thank you for your unwavering support. Also to Ming, thank you for your constant words of encouragement.

To the crew and the scientists during the ANTARXXVII expedition thank you for giving me a wonderful experience in Antarctica and to BELSPO which made it possible to join the expedition.

Jibi, thank you so much for being a genuine and "all seasons" friend. Thank you for always finding time to help and support me for whatever assistance I needed and whenever I needed it. Also to Fenny, Guading, Jarmak, Eduardo, Raisa, and Kyza for making my stay in Belgium enjoyable.

My family, who have always been my inspiration: Mama, Ian, Erin, Xander, Ann, Riley, Rhys, Joseph, and KD. Thank you for your incessant prayers and unwavering support. Thank you for always checking up on me despite the distance.

My husband Allen's family, Becky, Chrys, Stephanie, and Laura who have become my family, too. Thank you for your constant support and encouragement.

My husband, Allen, thank you for your love, patience and understanding. Thank you for always being there for me and for going out of your way to help me in every way you can.
いつもありがとう！

Ug labaw sa tanan, salamat sa Ginoo sa kanunayng hinabang!

Abstract

The past major climate changes have disrupted life in the polar regions and triggered different responses in marine organisms. Confronted now with fast-paced environmental changes such as global warming, understanding the adaptations and patterns of diversification in these regions with extreme environmental conditions can help to predict their possible response to future climate change. To do so, the genus *Eusirus* was chosen as a model organism because: 1) of its worldwide distribution with representatives in both polar regions; 2) local abundance and a large number of species showing high level of endemicity; 3) occupying both deep and shallow marine waters; 4) exhibiting a wide range of morphological variation; and 5) belonging to the Eusiridae family, which is a major family of polar amphipods. By combining molecular, morphological, and ecological data, this thesis aims to understand the genetic adaptations and the evolutionary processes that shaped the current diversity of the *Eusirus* amphipods in the Arctic and Southern Oceans. First, three novel complete Antarctic mitogenomes were assembled and annotated. Their analysis showed distinct features such as a lower AT-richness in the whole mitogenomes, negative GC-skews on both strands of protein coding genes, and unique gene rearrangements. These mitogenomes also shared characteristics with other amphipod mitogenomes including aberrant tRNA and short rRNA genes, which could be linked to minimalization of mitogenomes. Nucleotide diversity analysis revealed *nad6* and *atp8* to be the most variable mitochondrial regions of amphipods. In contrast, *cox1* showed low nucleotide diversity among closely and more distantly related amphipod species. Second, molecular signatures of cold adaptations were highlighted by comparing different mitogenomic features of amphipods from cold, temperate, and warm regions. Among other results, amphipods living in cold environment possessed mitogenomes with low proportions of charged amino acids and high, average ratios of non-synonymous to synonymous substitutions (ω). On the other hand, mitogenomic gene translocations and phylogenetic relationships had no distinct patterns being related to cold adaptations. Third, new phylogenetic reconstructions of *Eusirus* and a novel dated tree were produced. These data strongly supported the monophyly of the Antarctic clade whereas Arctic *Eusirus* had a polyphyletic origin. The mean age of Arctic *Eusirus* is older than Antarctic *Eusirus* despite the older existence and longer geographic isolation of Antarctica. Finally, the integration of phylogenetic information, phenotypic and ecological data identified two different

evolutionary patterns of *Eusirus* in the polar oceans. A high rate of lineage diversification coupled with low rate of morphological evolution supported a non-adaptive radiation scenario in the Antarctic clade. Even if ecology certainly played a role during the diversification of the Antarctic clade, it is hypothesized that allopatric speciation such as vicariant events following the opening of the Drake passage and the formation of the Antarctic Circumpolar Current formation mainly produced new lineages. The contrasting slower diversification rates observed in the Arctic *Eusirus* lineages could be explained by higher gene flow and higher extinction rates. Morphological and ecological diversity in the Arctic clade probably accumulated more constantly along speciation events. Despite the constant rate of lineage diversification in the Arctic *Eusirus*, the morphological and the ecological diversity were both observed to be high. This high morphological and ecological diversity in Arctic *Eusirus* could be associated to their polyphyletic origin and their older evolutionary age. Certainly, the high levels of morphological and ecological diversity in the Arctic *Eusirus* support the hypothesis that niche partitioning played a crucial role during the diversification of *Eusirus* in the Arctic. In conclusion, the multi-disciplinary approach integrating molecular, morphological, and ecological data successfully unraveled the different evolutionary patterns of the genus *Eusirus* in the two polar regions.

Table of contents

Objectives and outline of the thesis

The mode and the tempo of species diversification as well as their adaptations in the polar regions, are still poorly understood. The primary objective of the present Ph.D. thesis is to gain deeper insights into the genetic adaptations and the evolutionary processes that shaped the current diversity of the *Eusirus* amphipods in the polar regions with a multi-disciplinary approach, utilizing molecular, morphological, and ecological data.

Polar regions are characterized by extreme environmental conditions such as low temperatures. Amphipods are the main lineage of crustaceans which succeeded in these very cold marine environments. The genus *Eusirus* is a lineage of amphipods including 31 described species with a worldwide distribution. Many *Eusirus* species can be locally abundant, and many species show a high level of endemicity. They adapted to shallow and deep marine waters as well as in both Arctic and Antarctic oceans. *Eusirus* shows extensive morphological variation and belongs to the family Eusiridae, which is one of the dominant families of polar amphipod fauna. *Eusirus* thus provides the opportunity of a very interesting case study to characterize cold adaptations in amphipods and to compare the evolutionary history of marine biodiversity in both polar regions.

For this thesis, these main research questions will be addressed:

(1) To understand molecular adaptations to cold environments.

As for many taxa, the genetic adaptations of *Eusirus* to cold temperatures are still poorly known. Thus, understanding how these polar organisms adapted to cold conditions is of great interest to Science. By utilizing mitochondrial genome data (mitogenomes) of *Eusirus* and other amphipods, we can check for genetic changes in mitogenomes and possibly link these to cold adaptations.

(2) To test for the monophyly of both “polar” *Eusirus* clades and to compare the types of invasions into the Arctic and Antarctic and estimate when these invasions occurred. These questions will be answered by the production of a novel time-calibrated phylogeny.
(3) To use phylogenetic information and phenotypic data to test three evolutionary scenarios which are listed below.

(a) In the first scenario, we assume that newly available niches provided *Eusirus* to go through adaptive radiation coupled with ecological and morphological diversity.
(b) For the second scenario, we assume that *Eusirus* went through non-adaptive radiations without any partitioning of eco-morphological diversity but with allopatric speciation.
(c) In the third scenario, we postulate that *Eusirus* went through repeated convergence with parallel evolution of certain morphological or ecological traits.

In this thesis chapter, a general introduction to the study and to the polar regions is provided. This chapter also provides a summary on the morphology and ecology of amphipods in general and of *Eusirus* in particular (Chapter 1). Genetic adaptations of *Eusirus* to cold environments are poorly known. Studying mitochondrial genomes (i.e., mitogenomes) will allow us to examine some of these possible genetic adaptations. Since no mitogenomes were available for *Eusirus*, the entire mitogenomes of two *Eusirus* species were assembled and annotated *de novo* (Chapter 2). The assembled and annotated mitogenomes of these two plus another Antarctic amphipod along with other published mitogenomes from amphipods occurring in cold, temperate and warm regions were used to check for signatures of cold adaptation (Chapter 3).

The remaining part of this PhD thesis was devoted to the study of the evolutionary processes that shaped the current diversity of *Eusirus*. First, we reconstructed the evolutionary history and dated phylogenetic relationships of the genus *Eusirus* from polar and non-polar regions using mitochondrial and ribosomal DNA sequence data (Chapter 4). Morphological and ecological data were then collected to characterize and quantify the eco-morphological diversity of *Eusirus* from polar and non-polar regions. These data together with the time-calibrated phylogenies were used to identify the most likely scenario explaining the evolution and speciation in the genus *Eusirus* (Chapter 5). Novel insights of this thesis were then placed into a wider framework in a final discussion to draw more general conclusions from this study on the evolution of amphipods and polar marine organisms (Chapter 6).

Chapter 1: General Introduction

Macroevolution studies the overall patterns and processes that cause evolutionary changes at a broad scale, that is, at the species level and higher, over long periods of time (Ridley, 2003; Futuyma, 2005; Hautmann, 2020; Saupe & Myers, 2021). This includes the tempo (or the rate) of change and the mode (or the mechanism) of change (Ridley, 2003; Futuyma, 2005; Saupe & Myers, 2021). One important domain of macroevolutionary research is the study of speciation or the process by which a lineage undergoes independent divergence, forming two or more distinct lineages or species (Futuyma, 2005; Futuyma & Kirkpatrick, 2017; Saupe & Myers, 2021). Diversification is the evolutionary increase of the number of new species or lineages (Futuyma, 2005; Futuyma & Kirkpatrick, 2017). The rate of speciation could be defined by the amount of time needed for complete reproductive isolation to evolve once the process has begun, also known as the transition time or time for speciation. It could also be defined as the biological speciation interval which is the mean time between a new species' inception and its next speciation event (Futuyma, 2005). One process of speciation is adaptive radiation which is the rapid diversification of diversely adapted species when changes in the environment occur such as newly available resources, new challenges for survival allowing novel traits to be selected, and the opening of new ecological niches (Gittenberger, 1991; Schluter, 2000; Ridley, 2003; Gavrilets & Losos, 2009; Rundell & Price, 2009; Saupe & Myers, 2021). When there is diversification without significant ecological adaptations to new environmental conditions, non-adaptive radiation is said to occur (Gittenberger, 1991; Rundell & Price, 2009). In such a case, speciation may be driven by different mechanisms such as geographic isolation, genetic drift, sexual selection, polyploidy, and hybridization (Ridley, 2003; Futuyma, 2005; Butlin et al., 2009; Sobel et al., 2010; Futuyma & Kirkpatrick, 2017). Based on geography, if one population evolves when geographically isolated from the rest of its original populations, allopatric speciation is observed (Ridley, 2003; Futuyma, 2005; Mallet et al., 2009; Harrison, 2012; Saupe & Myers, 2021). Without geographic barriers, a species can undergo sympatric or parapatric speciation. Sympatric speciation occurs when a species evolves within a single geographic area (Ridley, 2003; Futuyma, 2005; Barluenga et al., 2006; Mallet et al., 2009; Harrison, 2012; Saupe & Myers, 2021). Parapatric speciation happens when two populations of a species diverge and become separate species in a shared geographical area without overlapping ranges (Ridley, 2003; Futuyma, 2005; Mallet et al., 2009; Harrison, 2012).

Drivers of speciation such as genetic drift or the random changes in the frequency of certain alleles over time due to stochastic events can lead to speciation and are often stronger in smaller populations than selection (Butlin et al., 2009; Sobel et al., 2010; Futuyma & Kirkpatrick, 2017). Natural and sexual selection also play key roles in speciation (Panhuis et al., 2001; Kirkpatrick & Ravigné, 2002; Butlin et al., 2009; Futuyma & Kirkpatrick, 2017). In natural selection, unfavorable traits are removed, and certain genetic variants are more likely to be passed on to the next generation due to their advantages in a given environment (Futuyma & Kirkpatrick, 2017; Saupe & Myers, 2021). In sexual selection, certain traits of a population can become more common due to the increase of the individual's capacity to obtain mates and successfully reproduce; this can occur through female choice and male competition (Panhuis et al., 2001; Futuyma, 2005; Ridley, 2003). Additional mechanisms of speciation are hybridization and polyploidy. Hybridization is the reproduction between two different species producing a hybrid offspring (Abbott et al., 2013) and can also result in homoploidy or polyploidy (Futuyma, 2005; Abbott et al., 2013). Polyploidy refers to an organism that possess more than two chromosome complements in its cells (Futuyma, 2005; Futuyma & Kirkpatrick, 2017). Polyploid populations can be distinct species that have different traits than their ancestral species and, in some instances, polyploid offspring can be sterile (Futuyma, 2005; Butlin et al., 2009; Futuyma & Kirkpatrick, 2017).

An important area of macroevolutionary research is the study of the evolution of biodiversity. Divergent evolution is the process by which species that share the same common ancestor become more different over time as a result to different pressures (Alcock, 2001; Futuyma, 2005; Gautam, 2020). When unrelated or distantly related organisms from different ancestral lineages evolve similar traits due to similar selective pressures in the environment, this process is called convergent evolution (Moore & Willmer, 1997; Ridley, 2003; Futuyma, 2005; Futuyma & Kirkpatrick, 2017). On the other hand, parallel evolution is defined as the evolution of similar traits of species with a common ancestor independent of each other due to similar environments (Moore & Willmer, 1997; Futuyma, 2005; Futuyma & Kirkpatrick, 2017). Extinctions are also one important area of macroevolutionary research. Depending on the intensity and timelines, extinction can occur gradually with a mild to moderate intensity which is also referred as background extinction while mass extinctions occur periodically and with great intensity (Saupe & Myers, 2021; Futuyma & Kirkpatrick, 2017). Evolutionary

replacements can take place as a result of extinction allowing other species to radiate and fill the newly available niches, which were formerly occupied by the now extinct species (Ridley, 2003).

Since Darwin, there have been many macroevolutionary studies investigating diversification in terrestrial and aquatic environments. Some examples include the study of the *Euhadra* Japanese land snails that showed parallel evolution of the chirality or the direction of the coiling of shells which evolved to favor genetically dominant chirality as determined by a single gene speciation (Ueshima & Asami, 2003). Another example is cichlid fish undergoing sympatric speciation in the crater lakes in Cameroon (Schliewen et al. 1994; Schliewen et al., 2001) and the Midas cichlid species complex (*Amphilophus* sp.) in Nicaraguan crater lakes (Barluenga et al., 2006). Non-allopatric speciation was also documented in the Hawaiian *Cellana* limpet species (Bird et al., 2011). Other examples of adaptive radiations showing variations in the bill morphology were reported from Hawaiian honeycreepers (Lovette et al., 2002) and Darwin's finches (Burns et al., 2002). Adaptive radiations of cichlids in Lake Victoria, Lake Malawi and Lake Tanganyika have also been recorded which may have been facilitated by ancient hybridization events (Meier et al., 2017; Irisarri et al., 2018; Svardal et al., 2021)

Despite these numerous studies conducted in different environments, very little is known on how the diversity in the polar regions evolved, particularly in the polar oceans (Lörz & Held, 2004; Clarke & Crame, 2010; Hardy et al., 2011). This scarcity in knowledge can be attributed to the extreme conditions and the presence of sea ice cover making it more difficult to study these regions (Clarke & Crame, 2010; Thatje, 2012; Legezyñska et al., 2020). Tectonic and climatic histories of these polar regions have played a crucial role in the evolution of the polar marine fauna (Marincovich et al., 1985; Clarke & Crame, 1989; Golikov & Scarlato, 1989; Dunton, 1992; Knox, 2006; Hardy et al., 2011; Crame et al., 2014; Crame, 2018). Past climatic changes have triggered different responses in marine fauna with some species surviving *in situ* while others retreated into different refugia (Thatje et al., 2005, 2008; Barnes & Kulinski 2010; Hardy et al., 2011; Allcock & Strugnell 2012). Confronted now with fast-paced environmental changes like global warming (Aronson et al., 2007; Gilg et al., 2012; Gutt et al. 2015), knowledge on how these organisms managed to survive climate changes in the past can help us to predict how the marine fauna will respond in the future (Parmesan, 2006; Dam, 2013; Reusch, 2014).

1. Antarctica

1.1. Evolution in the Southern Ocean

During the Mesoproterozoic (about 1.6-1 billion years ago), the crust of East Antarctica was formed by the amalgamation of Archean nuclei which became a part of the supercontinent Gondwana at the end of Precambrian (about 600 million years ago; mya) (Dalziel, 1992). Around 180 mya, Gondwana started to break up creating a seaway in the middle of West (South America and Africa) and East (Antarctica, Australia, India and New Zealand) Gondwana (Storey, 2005; Lurcock & Florindo, 2017). The break-up of Gondwana led to extensive shallow waters in the Mesozoic (Clarke & Crame, 1989) and in the late Mesozoic, in-situ adaptive radiation was suggested to start based on the observation of many closely related species such as pycnogonid, gastropods, echinoderms, ascidians, and notothenioid fish found in the shallow Antarctic and sub-Antarctic waters (Clarke & Crame, 1989; Clarke, 1990; Arntz et al., 1995; Knox, 2006). According to fossil evidence, Antarctica had a relatively warm temperature during this time and a relatively rich and diverse marine fauna (Clarke, 1990; Clarke & Crame, 1989).

During the Cretaceous-Palaeogene (K–Pg) boundary, a mass extinction occurred about 66 mya (Renne et al., 2013). In Antarctica, two separate extinction events were suggested during this time and attributed to the eruption of the Deccan Traps volcanic province and the Chicxulub meteorite impact; the latter was also linked to a major global warming event (Petersen et al., 2016). These mass extinction events were followed by global evolutionary radiation and the establishment of some elements of the modern Antarctic fauna (e.g. Neogastropods) (Crame et al., 2014; Crame, 2018).

The Drake passage opened later around Eocene-Oligocene (34-26 mya) when South America and Antarctica separated which led to the formation of the Antarctic circumpolar current (ACC) around the Oligocene (31-26 mya), geologically and thermally isolating Antarctica (Latimer & Filippelli, 2002; Lawver & Gahagan, 2003; Storey, 2005; Hodel et al., 2021; Vincze et al., 2021). This created a major marine biological barrier preventing gene flow (Thornhill et al., 2008), a prerequisite for vicariance and subsequent allopatric speciation. In contrast, Rogers (2007) and Crame (1999) suggested that the opening of Drake passage and the formation of the ACC could also have allowed dispersal to occur. During the Eocene-Oligocene

transition, subsequent cooling resulted in significant extinction and ecological reorganization in many biological groups (Coxall & Pearson, 2007). Records of extinction of warm-adapted marine taxa were mostly obtained around the end of the middle Eocene and middle Oligocene (Prothero, 1994). These extinctions were replaced by species being adapted to cold climates (Keller et al., 1992; Hutchinson et al., 2021).

During the end of the Pleistocene to Holocene (about 70,000 to 10,000 years ago), most of the Antarctic shelf was covered with grounded ice masses and the rest with ice shelves (Ingólfsson, 2004; Thatje et al., 2008). This period was characterized by low food availability and primary production was absent in sea-ice covered zones, which starved the benthic communities but promoted the evolution of feeding mechanisms of these organisms (Thatje et al., 2008). Thatje et al. (2005; 2008) suggested that benthic communities were able to survive this period by migrating to the deep sea followed by recolonization of the Antarctic margins during subsequent interglacial periods or migrating from one isolated shelter in the shelf to another during diachronous ice advances and retreats. Thatje et al. (2008) also pointed out that recolonization to the shallow water niches that opened during the following deglaciation period was likely pioneered by species with adaptable life cycles and the ability to disperse and radiate in the subsequent interglacial.

The geographic isolation and the long history of cooling and repeated glaciation events could have driven allopatric speciation in the Antarctic taxa which acted as a taxonomic diversity pump and resulted in the current high degree of endemism in Antarctica (Clarke & Crame, 1989; Knox, 2006; Rogers, 2007).

1.2. Physical Geography

Antarctica is a continent located almost entirely within the Antarctic Circle at 66°33’ south (Figure 1). The continent has an area of 14 million km^2 and is mostly covered with massive ice sheets with a mean thickness of approximately 2.1 kilometers (Gonzalez & Vasallo, 2020). It is divided into East and West Antarctica by the transantarctic mountains and is surrounded by the Southern Ocean (Thomas et al., 2008; Gonzalez & Vasallo, 2020).

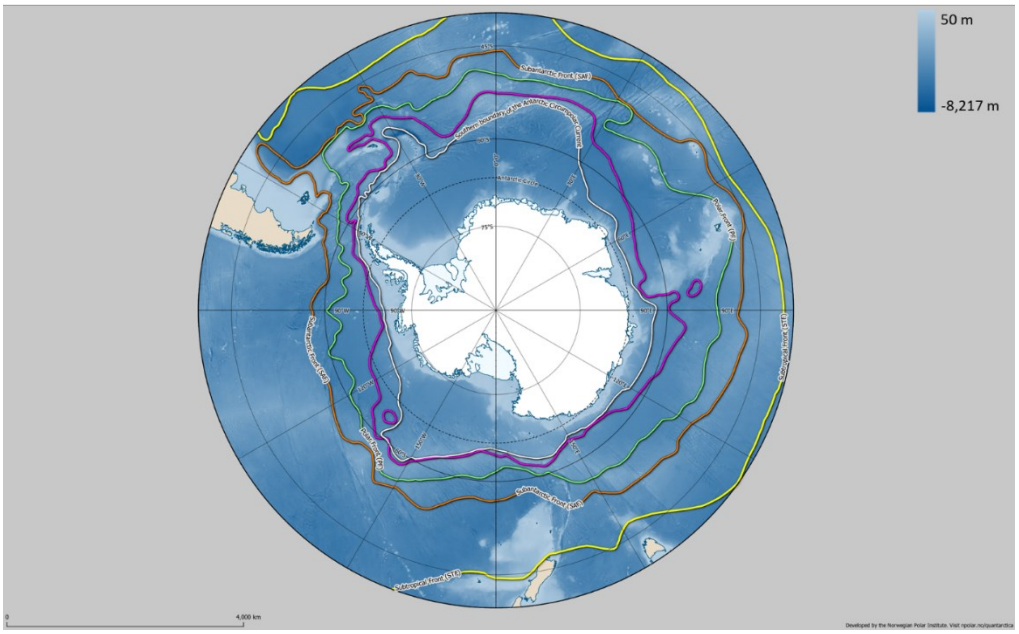

Figure 1. Map of Antarctica showing the Southern boundary of the Antarctic Circumpolar Current (ACC) (white) and the Southern Ocean fronts: Southern ACC front (pink), Polar front (green), Subantarctic front (orange), and Subtropical front (yellow). This illustration has been made with Quantarctica (Matsuoka et al., 2018) using the detailed basemap (Norwegian Polar Institute, 2018) and the datasets Southern Ocean fronts (Orsi et al., 1995) and Antarctic Digital Database/Quantarctica (Matsuoka et al., 2018), compiled Hillshades and Elevation Model mosaics from ETOPO1 (Amante & Eakins, 2009), IBCSO (Arndt et al., 2013), and RAMP2 (Liu et al., 2001).

The Southern Ocean is defined as the ocean between the 60° south latitude and the coast of Antarctica as described by the International Hydrographic Organization (IHO) (https://iho.int). Beyond the northern border of the 60° south latitude, the Southern Ocean is linked with the South Atlantic Ocean, the Indian Ocean, and the South Pacific Ocean (IHO, 2001). The Southern Ocean is also bordered by the Antarctic Polar Front (APF) towards the Northern edge. North of the APF, the sub-Antarctic region is located (Knox, 2006; Thomas et al., 2008). The IHO has furthermore created different subdivisions of the Southern Ocean into seas, straits and gulfs (see Figure 2).

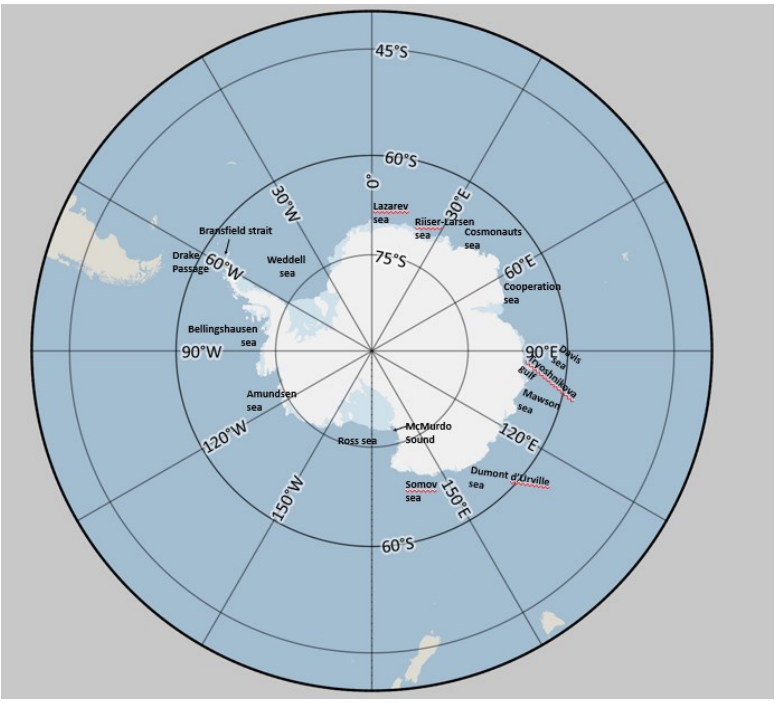

Figure 2. Map of the Southern Ocean showing the different subdivisions as defined by the IHO (2001). Illustration have been made with Quantarctica (Matsuoka et al., 2018) using the dataset Antarctic Digital Database/Quantarctica (Matsuoka et al., 2018).

1.3. Climate

1.3.1. Ice and snow cover

Almost the entire Antarctic continent is covered with large ice sheets amounting to about 26 million km^3 (Gonzalez & Vasallo, 2020). The Southern Ocean surrounding the continent freezes in winter, then doubling the continent's frozen area (Thomas et al., 2008; Gonzalez & Vasallo, 2020). The maximum sea ice extent of about 18 million km^2 is observed in September and mostly melted in the summer, reaching its minimum of about 3 million km^2 in February (Vaughan et al., 2013; Gonzalez & Vasallo, 2020). One of the factors driving climate variability is the higher albedo of the ice. The high reflectivity (albedo) in solar radiation causes much of the solar radiation reaching the Earth to be lost to space resulting in low temperatures and low heat redistributions through air and ocean currents (Eicken et al., 1995; Worby et al., 1996; AMAP, 1998; Parkinson, 2014).

Snow accumulation in the Antarctic is highly variable with snow cover contributing to about a third or a half of the sea ice thickness (Eicken et al., 1995; Massom et al., 1997). The snow in Weddell Sea contributes about 8% to the total ice mass (Eicken et al., 1995). Similar to ice cover, snow has a high albedo, and its accumulation can result in a net cooling effect on the global climate (Massom et al., 1997). The high albedo of snow greatly reduces the absorbed

solar radiation at the surface resulting in the cooling of the surface and the atmosphere (Ledley, 1991). Snow also serves as a protective buffer during spring or summer, delaying the melting of surface sea ice (Massom et al., 1997).

1.3.2. Temperature

The majority of Antarctica has an ice-cap climate (category EF in the Köppen climate classification) (Kottek et al., 2006) with monthly mean temperatures not exceeding 0°C except for some coastal areas which have a tundra climate (category ET) characterized by a mean temperature between 0 and 10°C during the warmest month (Kottek et al., 2006; Peel et al., 2007; Gonzalez & Vasallo, 2020). Summer temperatures reach more than 0°C and last for 3-4 months in the Southern Ocean islands, 2-3 months in the West part of the Antarctic Peninsula and 1-2 months on the East side of the Peninsula. Average winter temperatures vary between -5 and -10°C in the Southern Ocean islands, and are colder at the East side of the Antarctic Peninsula compared to the Western side (Gonzalez & Vasallo, 2020).

Effects of climate change have especially been observed in the polar regions, with an increasing temperature trend in Antarctica resulting in a fast rate of ice loss and sea level rise (Gonzalez & Vasallo, 2020; Hughes et al., 2021). A 25-year study (since 1992) has shown that temperatures in the sub-Antarctic waters have increased about 0.29 ± 0.09 °C per decade and sub-surface sub-Polar deep waters about 0.04 ± 0.01 °C per decade, while a decrease in the near-surface sub-Polar waters (of about -0.7 ± 0.04 °C per decade) has been recorded (Auger et al., 2021). Thinning of the West Antarctica ice sheets has been observed to increase, particularly at the bottom of the ice shelves and is attributed to the intrusion of relatively warm water into the subshelf cavities; this causes basal melting, subsequently resulting in the retreat of ice sheet grounding lines and reduced basal traction (Gonzalez & Vasallo, 2020).

1.3.3. Precipitation and wind

Precipitation in Antarctica mainly comes in the form of snow or as rain in the summer, with most precipitation occurring in the coastal areas while it is rare in the plateau (Gonzalez & Vasallo, 2020; Vignon et al., 2021). Precipitation can influence the variation of the surface albedo, can speed up glacier retreat due to surface ice melting and can increase freshwater input into Antarctic lakes and oceans (Pollard et al., 2015; Vignon et al., 2021).

The wind speeds in Antarctica greatly vary due to the frequent presence of cyclones (Gonzalez & Vasallo, 2020). Strong katabatic winds persist at the steep edge of Antarctica (Thomas et al., 2008) which are stronger in the winter than in summer (Gonzalez & Vasallo, 2020). They have been found to cause snowfall sublimation (i.e. conversion of snow into vapor) in the atmosphere which could possibly counterbalance the predicted increase of precipitation in a warming climate (Grazioli et al., 2017). Antarctica is also influenced by westerly winds which frequently get obstructed by the mountain range in the Antarctic Peninsula; if they gain sufficient velocity to surpass the mountain ranges, they can sometimes result in dry and warm winds on the leeward side (Parish, 1983; Gonzalez & Vasallo, 2020). These winds known as foehn winds affect the surface melting of the Eastern side of the Antarctic Peninsula shelf (Gonzalez & Vasallo, 2020).

1.4. Physical Oceanography

The Antarctic circumpolar current (ACC) is the largest ocean current and is wind-driven, flowing from west to east (clockwise), and allowing the exchange of water between oceans (Orsi et al., 1995; Klinck & Nowlin, 2001; Barker et al., 2007; Hassold et al., 2009). The current extends from the sea surface to the sea floor (Barker et al., 2007; Hassold et al., 2009) where its strongest flow is near the surface with recorded speeds between 0.25 and 0.4 m/sec (Klinck & Nowlin, 2001). The formation of the ACC is linked to the Antarctic continental glaciation as it decreases the meridional heat transport across the Southern Ocean (Barker et al., 2007).

A counter-current of the ACC is the Antarctic Coastal Current (ACoC) causing East Wind Drift in Antarctica (Knox, 2006; Núñez-Riboni & Fahrbach, 2009; Anderson, 2010). The Antarctic coastal current is a surface current that flows from east to west (counterclockwise) and has been found to have the strongest current closer to the coast and close to the edge of the continental shelf (Anderson, 2010). The current affects the Southern Ocean as it keeps the warm deep water away from the ice shelf cavity of the Weddell Sea through depressing the thermocline (Núñez-Riboni & Fahrbach, 2009). The current is also major transporter of warm deep water into the formation area of the Weddell Sea's deep water and to the Antarctic bottom water in the southwestern Weddell Sea (Foster & Carmack, 1976; Núñez-Riboni & Fahrbach, 2009).

There are several ocean fronts and zones in the Southern Ocean (Figure 1) characterized by their distinct vertical stratification of salinity and temperature in surface and middle water columns (Anderson, 2010). These zones are separated by fronts being associated with certain water mass properties and defined by increase in flow velocity (Sokolov & Rintoul, 2009; Stupnikova et al., 2018).

The following water masses are recognized in the Southern Ocean: Antarctic Surface Waters, Subantarctic Intermediate Waters, Antarctic Bottom Waters, Antarctic Circumpolar Deep Waters, and Warm Deep Waters (Figure 3) (Knox, 2006; Anderson, 2010).

Where the Warm Deep Water upwells, lies the Antarctic Divergence and this zone is characterized by high nutrient concentrations, minimal oxygen concentrations and a temperature maximum (Anderson, 2010). The cold, oxygen-rich and fresh Antarctic Surface Water comes from the Antarctic continent and flows north towards the Polar Front until it meets with the Subantarctic Surface Water at the region of convergence known as the Antarctic convergence or Polar Front (PF) where it starts to sink and forms the low salinity Subantarctic intermediate water (Knox, 2006; Anderson, 2010). The high-salinity Warm Deep Water flowing from the Atlantic, Pacific and Indian oceans mixes with the Antarctic waters making up the Circumpolar Deep Water, which is the dominant water mass in the Southern Ocean (Knox, 2006; Anderson, 2010). The border between Circumpolar Deep Water and the Warm Deep Water is indicated by a temperature maximum and oxygen minimum while the border between Warm Deep Water and the Antarctic Surface Water corresponds to a minimum temperature layer (Anderson, 2010). The downslope movement and mixing of Circumpolar Deep Water and saline shelf water forms the very cold Antarctic Bottom Water and it is mostly generated in the Weddell Sea but also in the Ross Sea and off Wilkes Land (Knox, 2006; Anderson, 2010). The border between Circumpolar Deep Water and Antarctic Bottom Water coincides with a minimum temperature layer (Anderson, 2010).

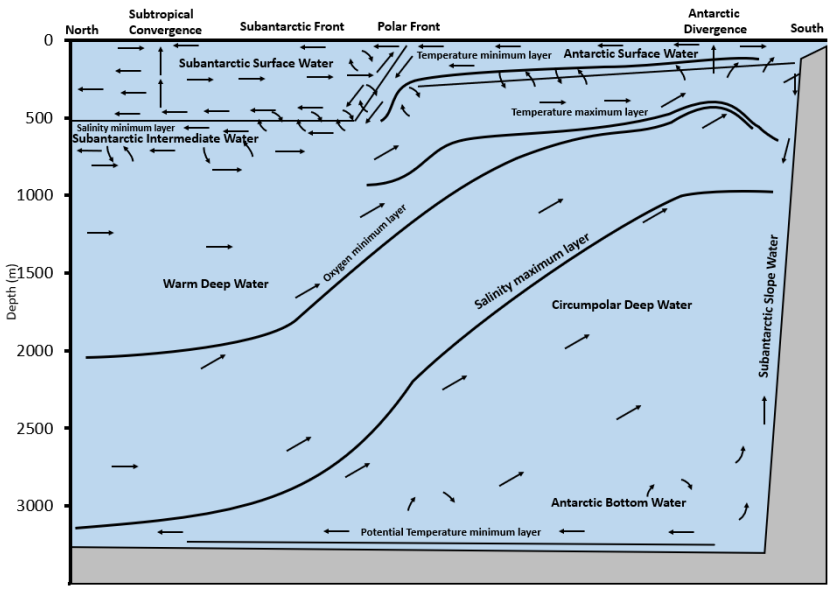

Figure 3. Illustration of the water masses in the Southern Ocean, adapted from Anderson, 2010 as cited from Gordon, 1967.

2. Arctic

2.1. Evolution in the Arctic Ocean

The formation of the Arctic basin started during the Mesozoic about 200 mya and was characterized by the breakup of the Pangea and the primary stages of the opening of the Amerasian basin (Khain & Filatova, 2010; Lebedeva-Ivanova, 2010; Serreze & Barry, 2005) followed later by the formation of the Eurasian basin in the Cenozoic.

In the late Cretaceous, the Arctic Ocean formed two large seaways: the Western Interior seaway and the Turgay Strait which allowed limited connections to the other oceans and may have served as subtropical migration routes for Arctic species with phylogenetic affinities to warm-water taxa (Dunton, 1992). It was also around this time when the deep-water connection between the North Pacific Ocean and Arctic Ocean closed (about 80-100 mya) which prevented further exchange of the bathyal and abyssal fauna of the two oceans (Marincovich et al., 1990; Dunton, 1992; Bodil et al., 2011). The closure of the deep-water connection and the limited connections through the seaways may have significantly isolated the Arctic Ocean around the Cretaceous (Marincovich et al., 1985; Dunton, 1992). Moreover, the isolation of the North Pacific led the cool-water fauna to evolve around 40 mya which later served as a significant seed stock for the invasion of the Arctic Ocean and the North Atlantic in the late Cenozoic (Dunton, 1992).

The Western Interior seaway later closed during the end of the Cretaceous to early Paleocene (about 65.5-70.6 mya) further isolating the Arctic Ocean (O'Regan et al., 2011). In the late Paleocene (about 56 mya), the North Atlantic rapidly widened into the Arctic Ocean caused by spreading of the sea floor (Brozena et al., 2003; O'Regan et al., 2011). Around the same time, the Arctic experienced periods of global warmth with rising of sea surface temperatures, absence of ice, increase in the sea level, and anoxic conditions in the ocean (Sluijs et al., 2006; Sluijs et al., 2009; O'Regan et al., 2011). This resulted in the disappearance of fauna being adapted to more saline conditions and an increase of fauna with adaptations to less-saline conditions due to an increase in freshwater influx (Sluijs et al., 2006; Sluijs et al., 2009). Such a change was, for example, observed in sedimentary records of dinocysts with marine dinocysts species being absent and an abundance of subtropical dinocyst species and dinocyst species that tolerate low surface water salinities and require high nutrient conditions (Sluijs et al., 2009). Benthic foraminiferal lineages were also absent suggesting anoxic bottom water conditions (Sluijs et al., 2006; Sluijs et al., 2009). Around the late Eocene or Oligocene, the Turgay Strait closed (Marincovich et al., 1985).

Around the Eocene, the Fram strait was formed along with declining temperatures, allowing the exchange of biota between the North Atlantic Ocean and the Arctic Ocean (Wilce, 1990; Dunton, 1992; Kuklinski et al., 2013). The continued temperature decline enabled the cool-temperate Arctic biota of Northern Atlantic origin to prevail, especially during the late Miocene (Wilce, 1990; Dunton, 1992). The Bering Strait later opened in the late Miocene and earliest Pliocene (approximately 7.4-3.5 million years ago) (Vermeij, 1991; Marincovich & Gladenkov, 1999; Serreze & Barry, 2005; Adey et al., 2008; Meltofte et al., 2013) which permitted the entry of the North Pacific biota to the ice-free Arctic and the North Atlantic Oceans (Wilce, 1990; Dunton, 1992). During this time, the high-latitude biota of the Arctic, North Atlantic and the North Pacific Oceans reached their highest level of diversity (Dunton, 1992).

Repeated ice expansions and retreats occurred during the Quaternary which caused the Arctic shelf fauna assemblages to be almost eliminated (Dunton, 1992; Kuklinski et al., 2013). The few shelf fauna survivors found refuge in the North Atlantic and North Pacific, in the ice-free shelf sites of the East Siberian and Beaufort Seas or in the deeper bathyal areas of the Eurasian areas; they later reinvaded the Arctic shelves (Golikov & Scarlato, 1989; Dunton, 1992). Hardy

et al. (2011) suggested that these glaciation/deglaciation events could have contributed to the current overall genetic diversity in the Arctic. The retreat of some fauna into different isolated refugia during glaciation events could have led to vicariant effects increasing the genetic dissimilarity among different regional populations. However, populations that were unable to disperse and survive may have experienced genetic bottlenecks. Re-invasion and mixing of isolated populations could again have occurred during periods of deglaciation allowing interbreeding of some species while other divergent lineages remained distinct.

2.2. Physical Geography

The Arctic region is geographically defined as the area north of the Arctic circle (66°33' north) where there is at least one day in the year when the sun does not set (Thomas et al., 2008) (Figure 4). The Arctic circle encompasses a land area of 14.8 million km^2 and an ocean area of 13 million km^2 (Kullerud et al., 2013). There are also several other definitions of the boundaries of the Arctic region based on the tree line, which is the northern boundary where trees do not grow and is located in the transition area between the continuous boreal forest and tundra (AMAP 1997; AMAP, 1998). Another definition for the Arctic region refers to the 10°C July isotherm or the area in the north that has an average temperature of 10°C in July (AMAP, 1998; AMAP 1997; CAFF 2001). The Arctic can also be delineated into high and low Arctic regarding its latitudinal, environmental, climatic and biological characteristics, with the high Arctic (polar desert) having more extreme conditions, supporting fewer vegetation and animals than the low Arctic (AMAP, 1998; Serreze & Barry, 2005). The sub-Arctic, which is above 50° north is usually defined by the existence of patchy permafrost (AMAP 1997; Hoberg et al., 2003).

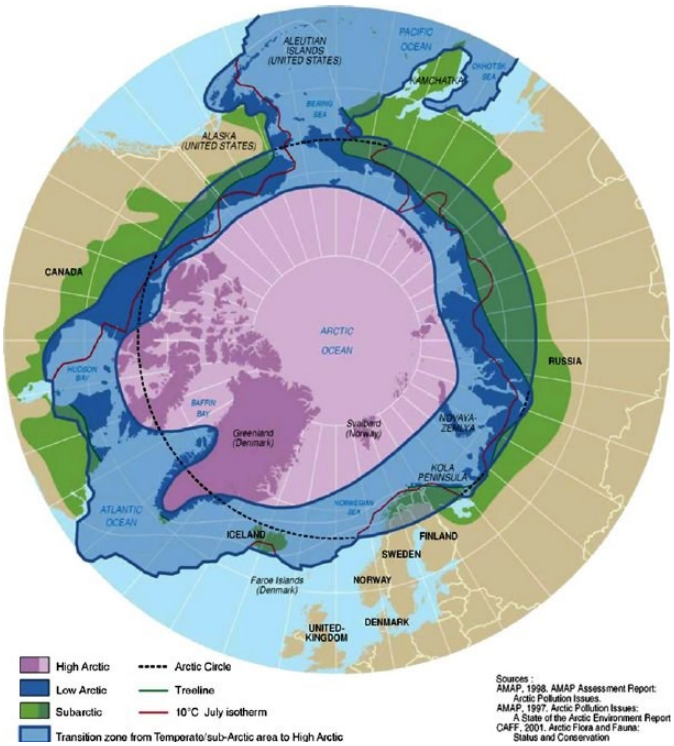

Figure 4. Map showing the Arctic and sub-Arctic regions as defined by the AMAP, 1998, the AMAP 1997, and the CAFF 2001. Delimitations are defined by the Arctic circle (broken black lines), tree line (green line), and isotherm (magenta line) and the following biogeographical regions: High Artic (dark and light magenta), low Arctic (dark blue), Sub-Arctic (dark and light green), and Transition zone (light blue). Figure from Hoberg et al. (2003).

The nearly land-locked Arctic Ocean is located in the Arctic region, and has a water surface area of approximately 14.7 million km^2 (Shiklomanov et al., 2000) which is bordered by land (Jakobsson & Macnab, 2006; Timmermans & Marshall, 2020; Lenn et al., 2022). The Arctic Ocean is also sometimes called the Arctic Mediterranean with the inclusion of the Nordic Seas (Norwegian, Iceland, and Greenland seas) as defined by the IHO (Jakobsson, 2002; Timmermans & Marshall, 2020; Eldevik et al., 2020). This definition of the Arctic Ocean by the IHO includes the entire Hudson Bay and Strait and covers up to 60°N in Davis Strait (IHO, 2001).

The Arctic Ocean is composed of 50% shallow shelf seas and 50% deep basins (Mauritzen et al., 2013); these basins are divided into major basins and sub-basins (Figure 5). The Lomonosov Ridge which stretches from the northern Greenland to the Laptev shelf separates the two major basins: the Eurasian and Amerasian Basins. The Nansen Basin (4000 m deep) and Amundsen Basin (depth of 4500 m) are located in the Eurasian Basin and are divided by the Gakkel Ridge (about 4000 meters) while the Canada and Makarov basins (both approximately 4000 m deep) are found in the Amerasian Basin and are separated by the Alpha and Mendeleyev Ridges (about 2200 meters) (Korhonen et al., 2013; Mauritzen et al., 2013; Coakley et al., 2016; Timmermans & Marshall, 2020; Wiers, 2020).

In the north of Eurasia, the shallow and broad (approximately 500 kilometers (km) wide) shelf seas are found: the Barents Sea (200-300 m deep), the Kara Sea (depth of 50-100), the Laptev Sea (<50 m deep), the East Siberian Sea (<50 m deep), and the Chuckchi Sea (50-100 m deep). The Alaskan Sea and Beaufort Sea shelves in the North of Amerasia are narrower (approximately <100 km wide) (Serreze & Barry, 2005; Mauritzen et al., 2013; Wiers, 2020). The Nordic Seas, separated by bathymetric ridges, comprise the Greenland Sea (3500 m deep), the Lofoten Basin (3000 m deep), the Norwegian Basin (3500 m deep), and the Iceland Sea (2000 m deep).

The warmer and highly saline water of the North Atlantic Ocean flows into the Nordic Seas via the Greenland-Scotland Ridge and enters the Arctic Ocean through the Fram Strait and the Barents Sea opening; North Pacific Ocean water with low salinity comes into the Arctic Ocean through the Bering Strait while water of the Arctic Ocean exits through the channels of the Canadian Arctic Archipelago and the Fram Strait (Mauritzen et al., 2013; Woodgate, 2013; Timmermans & Marshall, 2020; Wiers, 2020).

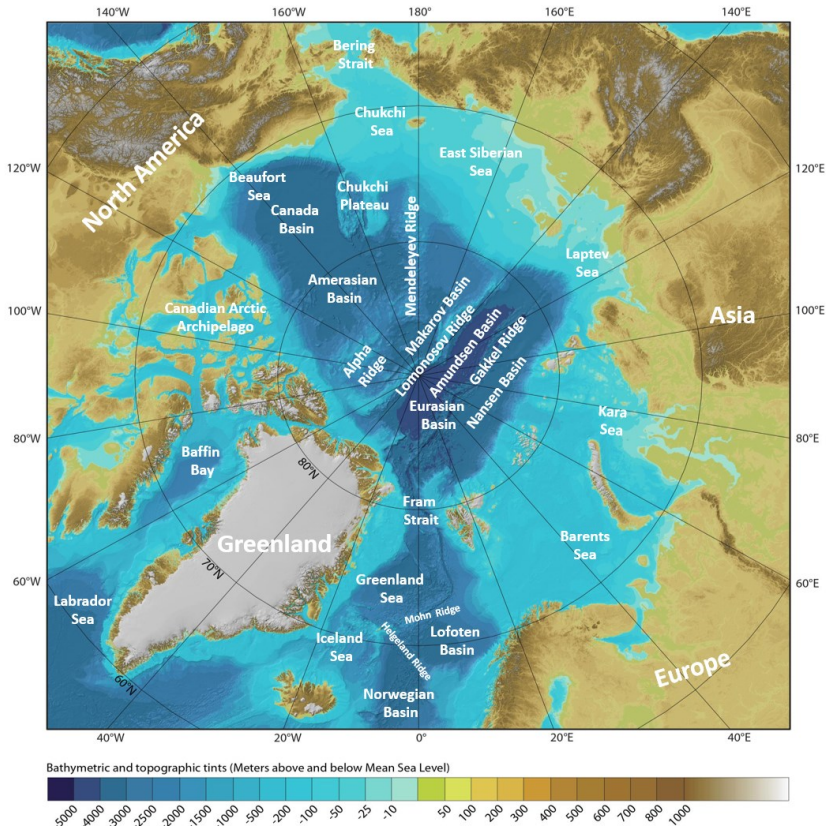

Figure 5. Map of the Arctic Ocean showing the major basins, sub-basins and ridges. Map, IBCAO grids, Bathymetry, and topography are from Jakobsson et al. (2012).

2.3. Climate

2.3.1. Ice and snow cover

Floating sea ice covers the Arctic Ocean all year long and permafrost lies beneath the majority of the Arctic land. Most of the mean sea ice cover is concentrated in the Arctic Ocean, including an area of 8 million km^2 to 15 million km^2 in September and March, respectively, with the overall surface varying each year (Serreze & Barry, 2005). Permanent land ice occupies mainly the vast area of Greenland (termed as Greenland ice sheet) encompassing an area of 1.71 million km^2 (Bamber et al., 2001; Serreze & Barry, 2005). Sub-Polar ice caps, glaciers, and ice sheets are primarily found in the mountainous areas of the Siberian and Canadian archipelagos as well as in Svalbard and Iceland (Serreze & Barry, 2005). Permafrost allows the rapid transport of precipitation and meltwater into streams affecting the seasonality river discharge and rates of evaporation. The perennial sea ice cover reflects the solar radiation back in summer (albedo effect) and restricts the heat exchange between the atmosphere and the warmer water masses in winter affecting the climate of the region as well as of the world (Perovich et al., 2008)

Snow cover plays an important role in the Arctic climate as most of the Arctic is covered with snow for at least 6-8 months of the year (Serreze & Barry, 2005). The insulating effect of the snow cover prevents the near-surface ground from deep freezing affecting ecological and biogeochemical processes (Callaghan et al., 2011). The water stored in the form of snow gets released through river discharges in spring and summer, influences the vertical structure of the Arctic Ocean and contributes to the formation of the sea ice cover. The influx of fresh water creates a stable surface layer in the cold Arctic Ocean because there is limited vertical mixing between the lighter fresh water and the denser more saline water below it. This stable surface layer coupled with cold winter air temperatures allows easy formation of sea ice (Serreze & Barry, 2005).

2.3.2. Temperature

Surface air temperature varies per region and season. The mean temperature in the central Arctic is -30 to -35°C in winter and between 0 to 2°C in summer (AMAP, 1998). Most of the Arctic Ocean reaches temperatures below the freezing point in mid-August and the Arctic coast from Taymyr eastwards up to 120°W by mid-September (Serreze & Barry, 2005).

Similar to the surface air temperature, the ocean temperature also changes from year to year. The recorded average temperature in the Canada Basin varies from -1 to 0.5°C at 203 meters (m) depth and -0.5 to 1.5°C at 369 m depth (Farmer et al., 2011). Areas in the Arctic Ocean showed cooling of up to c. 0.5°C every 10 years from 1930-1965 while water temperatures were increasing from 1965-1995. The increase in the upper ocean summertime warming since 1965 has caused a decrease of subsequent ice growth in winter of about 0.75 meters (Steele et al., 2008).

2.3.3. Precipitation and wind

The recorded yearly precipitation varies for most of the Arctic and amounts to about 300-400 mm in the central Arctic Ocean and >200 mm in the Canadian Arctic Archipelago and Beaufort Sea. The further an Arctic region is located from the ocean, the lower the amount of precipitation, with a decline in a west-east direction across the continent following the movement of the low pressure systems (AMAP, 1998).

Surface winds play a crucial role in the high-latitude circulation and are linked to cyclones and ocean wave heights (Vavrus & Alkama, 2021). In the winter, cyclonic disturbances result in higher wind speeds with the highest values recorded in the Barents Sea, Kap Farvell, southeastern Greenland, and the Bering Sea with a speed of >11 m per second (Serreze & Barry, 2005). Winds influence the sea surface stability, ice drift, formation of polynyas and increase the mixing of the water column (AMAP, 1998).

2.4. Physical Oceanography

The physical oceanography of the Arctic Ocean is affected by freshwater discharge, net precipitation and the cycle of sea ice formation and melting. The Arctic Ocean receives about 11% of the world's freshwater discharge from rivers reaching the highest discharge during terrestrial snowpack melting in June (Serreze & Barry, 2005; McClelland et al., 2012). The inflow of low salinity water from the North Pacific Ocean to the Arctic Ocean also contributes to the influx of freshwater into the Arctic Ocean (Serreze & Barry, 2005; Timmermans & Marshall, 2020). Moreover, precipitation over the Arctic Ocean exceeds evaporation, also accounting for additional freshwater input (Serreze & Barry, 2005; Rudels, 2012). Sea ice melting adds to the freshwater influx into the Arctic Ocean and inhibits vertical mixing while the sea ice formation increases salinity, leading to increased density of the surface layer and

vertical mixing (Serreze & Barry, 2005). These factors result in a strong stratification of the water masses in the Arctic Ocean (Rudels, 2009), which can be categorized into five vertical layers (Figure 6):

1) Comprising the upper c. 50 m, the polar mixed layer (PML) is characterized by its low salinity.
2) The 100-250 m thick, halocline layer is characterized by its close to freezing temperatures and increasing salinity with increasing depths.
3) The Atlantic layer with a thickness of 400-700 m has a subsurface water temperature of more than 0°C.
4) The intermediate water transfers freely across the Lomonosov ridge.
5) Bottom deep-water layers are found in different Arctic basins.

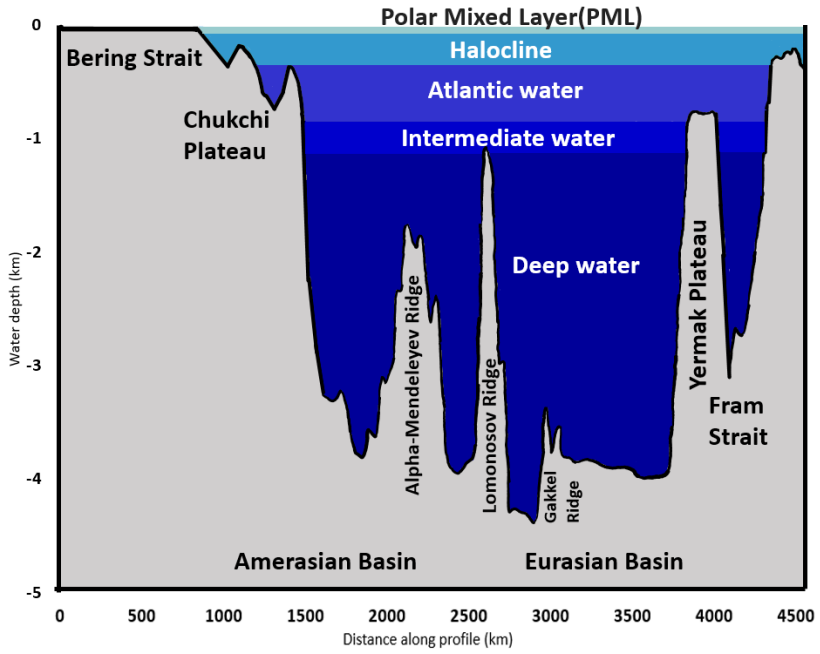

Figure 6. Five vertical layers of the water masses in the Arctic Ocean as proposed by Rudels (2009). Illustration adapted from Wiers (2020).

Surface or near surface circulation in the Arctic Ocean (Figure 7) is driven by wind force and is defined by anticyclonic flow of the Beaufort gyre into the Canadian Basin and the Transpolar Drift (TPD) which transports water and sea ice from the Canada Basin to the Fram Strait (Serreze & Barry, 2005; Rudels, 2009; Timmermans & Marshall, 2020; Wiers, 2020).

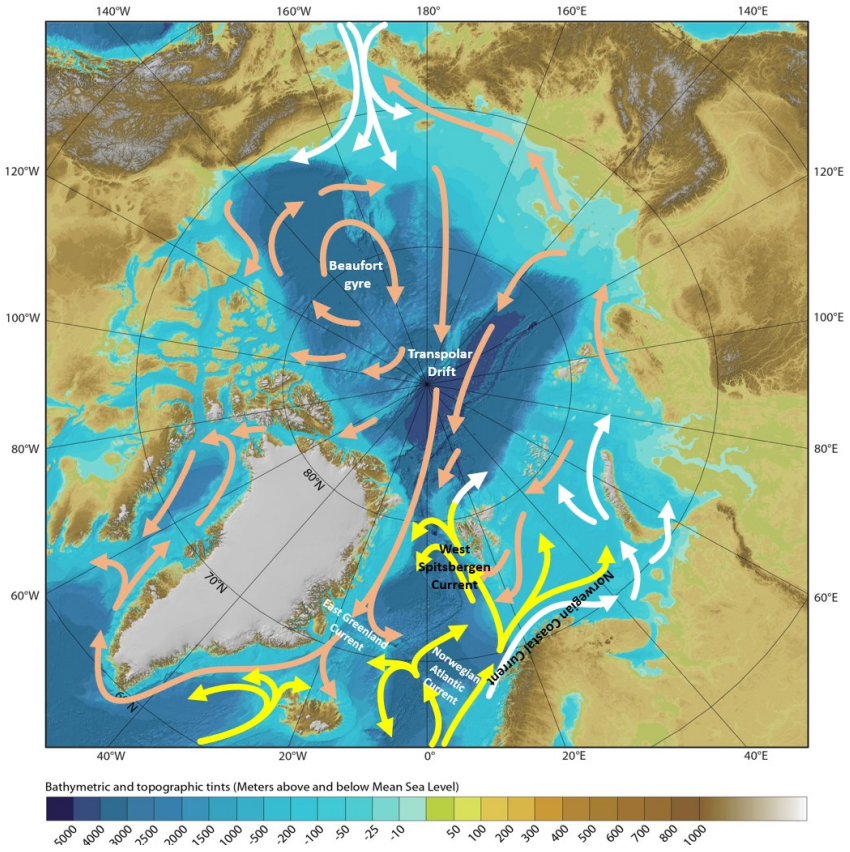

Figure 7. Surface or near surface and subsurface circulation of the Atlantic waters as discussed by Rudels (2009). The different arrow colors represent the warm Atlantic Current (yellow), the cold, less-saline Polar and Arctic currents (orange), and transformed currents with low salinities (white). Illustration adapted from Rudels (2009). Map, IBCAO grids, Bathymetry, and Topography from Jakobsson et al., (2012).

3. Marine fauna of the polar regions

The polar oceans harbor a diverse marine fauna with a higher endemism found in the Antarctic compared to the Arctic (Eastman, 2005; Sirenko, 2009; Clarke & Crame, 2010; Baird et al., 2011; Legezyñska et al., 2020; Rabosky, 2022). The high endemism in the Antarctic is attributed to its older geological age and its long history of isolation (Piepenburg, 2005; Josefson et al., 2013; Legezyñska et al., 2020; Rabosky, 2022). Different taxa dominate these polar oceans with most species having been recorded in the benthic realm (Piepenburg, 2005; Barnes et al., 2009; De Broyer & Danis, 2011; Barnes & Tarling, 2017) and estimates on the overall richness of the benthic fauna have shown to be generally similar at both poles (Piepenburg, 2005; Clarke & Crame, 2010; Rabosky, 2022). The benthic fauna in the Arctic is dominated by certain taxa such as crustaceans, mollusks, annelids, and polychaetes (Sirenko, 2001; Piepenburg, 2005; Clarke & Crame, 2010) while bryozoans, cnidarians (i.e. hydrozoans and anthozoans), ascidians, sponges, crustaceans (i.e. isopods and amphipods), polychaetes,

and pycnogonids dominate the Antarctic (Clarke & Johnston, 2003; Griffiths, 2010; Kaiser et al., 2013).

4. Crustaceans

Crustaceans are classified under the subphylum Crustacea and are one of the major groups of the phylum Arthropoda (Boore et al., 1998; Martin & Davis, 2001; Thorp & Covich, 2001; Duffy & Thiel, 2007). Moreover, Crustacea and Hexapoda are members of the pancrustacean clade (Duffy & Thiel, 2007). As classified by Martin & Davis (2001), there are six classes that are included in the subphylum Crustacea, namely: Branchiopoda, Remipedia, Cephalocarida, Maxillopoda, Ostracoda, and Malacostraca.

The major body parts of a crustacean are composed of a cephalon or head, and a trunk which is usually separated into thorax and abdomen except for remipedes and ostracods (Brusca & Brusca, 2003). Crustaceans exhibit a great diversity of body forms (Brusca & Brusca, 2003; Watling & Thiel, 2013) and are mostly found in the aquatic environments with some also occurring in terrestrial habitats (Brusca & Brusca, 2003). Crustaceans are important components of the pelagic, benthic, and sea-ice communities in the polar regions (Arndt & Swadling, 2006; Legezyñska et al., 2020). They usually have higher abundance and biomass than other metazoans (Arndt & Swadling, 2006) with comparable species richness at both poles (Legezyñska et al., 2020; Rabosky, 2022). In the Arctic Ocean, crustaceans have the greatest diversity of species in the pelagic, benthic, and sea-ice domains (Josefson et al., 2013; Legezyñska et al., 2020), with the malacostracans specifically being the most diverse in the benthic realm (Legezyñska et al., 2020). The majority of the crustacean species in the Southern Ocean are peracarids, particularly amphipods and isopods with more benthic and benthopelagic species compared to the number of pelagic species (Legezyñska et al., 2020). Brooding behaviour, which limits dispersal capacity and leads to reproductive isolation, has been associated with the high species richness of these benthic amphipods and isopods in the Antarctic (Rogers, 2007; Baird et al., 2011; Legezyñska et al., 2020). As a result, there is decreased gene flow between populations which promotes speciation (Baird et al., 2011; Legezyñska et al., 2020). Moreover, glaciation cycles in the past could have acted as a "diversity pump" resulting in high species diversity of benthic biota in the Antarctic (Thatje et al., 2005; Baird et al., 2011). The current Arctic crustaceans are of Atlantic and Pacific origin with few

endemic species which is explained by the geological history of the Arctic Ocean and fewer dispersal events (Josefson et al., 2013; Legezyñska et al., 2020). The Arctic diversity has also been formed by a series of glacial and interglacial cycles causing extinction and immigration events (Clarke & Crame, 2010; Josefson et al., 2013). Given that crustaceans have high species richness and complex evolutionary histories in the polar regions, they offer suitable models for comparing patterns of diversification between the two regions. Moreover, crustaceans have exhibited genetic adaptations in response to cold conditions (Zhao et al., 2015; Naumenko et al., 2017; Greco et al., 2021). One group of crustaceans are the amphipods that live in a wide range of environments including extremely cold environments (Gradinger, 2001; Väinölä et al., 2008; Lowry et al., 2007; Lan et al., 2016; Li et al., 2019a; Li et al., 2019b) thus, providing a good model system to study these kinds of adaptations.

5. Amphipods

5.1. Taxonomy

The order Amphipoda is classified under the superorder Pericarida and currently contains 10,428 formally described species (Horton et al., 2022). Amphipoda have historically been divided into three to four suborders: Gammaridea Latreille, 1802; Caprellidea Leach, 1814; Hyperiidea Milne Edwards, 1830; and Ingolfiellidea Hansen, 1903 (Barnard, 1969; Dahl, 1977; Lincoln, 1979; Bowman & Abele, 1982; Barnard & Karaman, 1983; and Barnard & Karaman, 1991). The establishment of the fourth suborder, Ingolfiellidea, by Hansen (1903) was questioned by several authors as for example Dahl (1977). Bowman & Abele (1982) incorporated the Ingolfiellidea within the Gammaridea. This was later changed by Barnard & Karaman (1983), who proposed to combine part of the old Gammaridea with the Caprellidea in the suborder Corophiidea. However, other authors have continued to use the four suborders (Barnard, 1969; Lincoln, 1979; Barnard & Karaman, 1991; and Martin & Davis, 2001). Myers and Lowry (2003) later classified the suborder Caprellidea into a superfamily within the suborder Corophiidea. The Senticaudata suborder was also erected by Lowry and Myers (2013), incorporating families that were formerly classified as Gammaridea. The most recent classification by Lowry and Myers (2017) recognizes six suborders in the Amphipoda: Pseudingolfiellidea, Hyperiidea, Colomastigidea, Hyperiopsidea, Senticaudata, and Amphilochidea.

5.2. Morphology

Morphological descriptions provided hereafter are derived from Chapman (2007) and Lincoln (1979) and all figures (nrs 8-9) are from Chapman (2007).

Amphipod bodies are generally laterally compressed and have a typical body plan that is divided into three parts: 1) head, 2) pereon/thorax, 3) pleon/abdomen (Figure 8). The head is more correctly called cephalothorax since the head is fused to the first pereon segment. The head has a spine-like or triangular process called the rostrum that is usually present on the anterodorsal margin, between the bases of the first antennae. The head also bears two sessile eyes, two pairs of antennae, and various mouthparts.

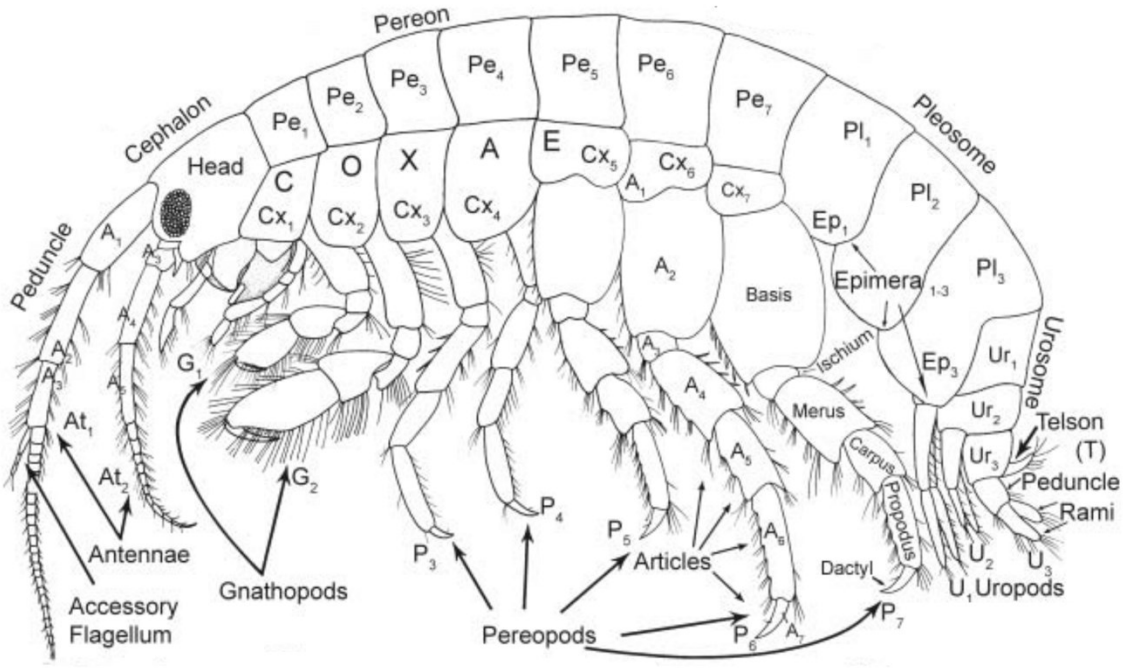

Figure 8. General morphology of a Gammaridean amphipod (Chapman, 2007).

Eye size and shape vary and consist of many ommatidia although eyes can also be absent in certain amphipods. The antennae have osmoregulatory and chemosensory functions. Antenna 1 has a peduncle of three articles and a flagellum. A small accessory flagellum can also be present at the distal part of the third peduncle article. Antennae 2 is composed of five peduncular articles and a flagellum.

The mouthparts of amphipods are involved in feeding function and consist of the upper lip (labrum), mandibles, lower lip (labium), maxilla 1, maxilla 2, and maxillipeds (Figure 9). The upper lip is attached to the epistome and is located at the anterior border of the mouth. The

mandibles, along with the upper and lower lip surround the opening of the mouth part. The mandibles usually consist of a distal toothed process called incisor, an articulated accessory plate called *lacinia mobilis* and a medial process called molar with accessory spines found between *lacinia mobilis* and molar. The mandible typically also has a tri-articulate palp attached to the outer border. The lower lip is found behind the mandibles and is located at the posterior border of the mouth. Maxilla 1 is found next to the lower lip and has an inner and outer plate and a palp. Maxilla 2 only consists of the inner and outer plate. A pair of maxillipeds forms the posterior surface of the buccal mass and is each composed of an inner and outer plate and an articulated palp.

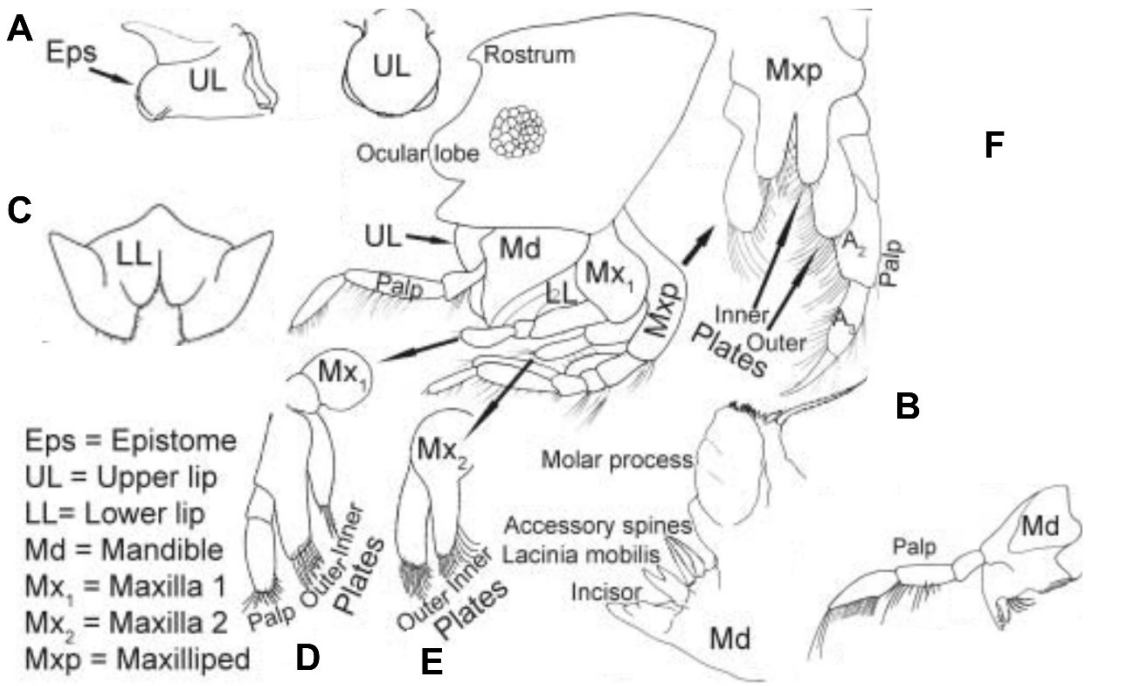

Figure 9. General mouthparts of an amphipod. A) Upper lip, B) Mandible, C) Lower lip (labium), D) Maxilla 1, E) Maxilla 2, and F) Maxillipeds (Chapman, 2007).

The pereon (or thorax) is comprised of seven segments with seven pairs of walking legs called pereopods attached to it. The first two pairs are called gnathopods and function mainly for feeding, cleaning, defense, and reproductive activities whereas the succeeding pereopods 3-7 are primarily for attachment, mobility, and nest or tube construction. Each pereopod has seven articles: coxa, basis, ischium, merus, carpus, propodus, and dactyl. The coxae are the first article being fused to the body and are often expanded to form rather large coxal plates. Usually situated at the inner base of the coxal plates 2-7 are the respiratory coxal gills or

branchiae. In females, the oostegites (which form the brood pouch or marsupium) are typically medially attached to coxal plates 2-5 while in males, a penial process (or penes) hangs ventrally from the 7th segment between the coxae.

The pleon is composed of six segments, with the first three pairs making up the pleosome and the last three the urosome. The anterior pleosome has epimeral plates and paired pleopods which are mainly used for swimming but also aerate the gills and ventilate the marsupium in females. The posterior urosome bears three pairs of uropods. Their main function is to allow amphipods to adhere to the substratum but it can also assist in swimming, burrowing, and tube-dwelling. The posterior end of the urosome is called the telson.

5.3. Ecology

Amphipods have a wide geographic distribution and inhabit a broad range of different habitats (Li et al., 2019b). They are found in almost all aquatic, some terrestrial and some subterranean habitats (Väinölä et al., 2008). Their presence in extreme environments such as below the polar sea ice (Macnaughton et al., 2007; Krapp et al., 2008), in deep abyssal trenches (Lan et al., 2016; Li et al., 2019a) and hydrothermal vents (Kniesz et al., 2022) has been well documented. Amphipods play an important role in aquatic food webs and have diverse trophic types, including detritivores, herbivores, omnivores, scavengers, predators, suspension- and deposit-feeders (Nyssen, 2005; Väinölä et al., 2008; Legeżyńska et al., 2012).

In terms of food preference, amphipods can be detritivorous, feeding on dead organic matter or detritus (Dauby et al. 2001; Platvoet et al., 2009) or herbivorous, feeding mainly on plants (Cruz-Rivera & Hay, 2001; Dauby et al. 2001; Nyssen, 2005). They can also be omnivorous, feeding on organic matter as well as scavenge and prey on other plants and animals (Thorp & Rogers, 2010).

Even if ecomorphological studies are limited in amphipods (e.g. Fišer et al., 2015; Zakšek et al., 2019; Copilaş-Ciocianu et al., 2021), some links can be found between their diet and feeding habits. Suspension-feeders are weakly motile or sedentary and consume particulate organic matter that sunk from the surface. Deposit-feeders scrape on the sea floor to collect particles originating from the water column or the breakdown of benthic organisms (Dauby et al. 2001; Nyssen, 2005; Riisgård & Schotge, 2007). Scavengers can be obligate with mainly feeding on dead organisms or facultative taking advantage of available food, and also

employing other feeding strategies such as predation and necrophagy (Dauby et al. 2001; Seefeldt et al., 2017). Some predatory amphipods are weakly motile but can walk around to search and capture food with their gnathopods and feed mainly on small living benthos. Others called grazers or browsers are predators that consume only a part of sedentary organisms as food without killing their prey while macropredators search actively or ambush their preys. Depending on the food availability, some predators can also resort to carrion in their diet (Dauby et al. 2001).

5.4. Phylogeny and Evolution of Amphipods

Amphipoda diverged from Ingolfiellida around the Permian period (about 280 mya) (Copilaş-Ciocianu et al., 2020). This coincides with the recorded Pericarida radiation being based on the first appearance of peracarid fossils (Schram, 1986; Poore, 2005). Amphipoda later began radiating around 240 mya following the Permian-Triassic mass extinction with four main pulses of diversification assumed to have occurred from middle Jurassic to the late Cretaceous (Copilaş-Ciocianu et al., 2020).

The reproductive strategies of amphipods such as brooding behavior, the lack of a free-swimming larval stage, and extended parental care limit their dispersal capacity (Väinölä et al., 2008; Baird et al., 2011; Copilaş-Ciocianu et al., 2020) making it likely that intraspecific genetic variation is highly structured (Baird et al., 2011). Moreover, their weak dispersal capabilities can lead to isolated populations, thus influencing their high diversification and distribution patterns which depict past events (Hou et al., 2014; Copilaş-Ciocianu et al., 2019; Copilaş-Ciocianu et al., 2020).

6. Genus *Eusirus*

The genus *Eusirus,* Krøyer, 1845 comprises a total of thirty-one formally described species (Wang et al., 2021) and is distributed worldwide (Verheye, 2011; Jung et al., 2016; Peña Othaitz & Sorbe, 2020). It currently has ten species from Antarctica, namely: *Eusirus antarcticus* Thomson,1880, *Eusirus bouvieri* Chevreux, 1911, *Eusirus giganteus* Andres, Lörz & Brandt, 2002, *Eusirus laevis* Walker, 1903, *Eusirus laticarpus* Chevreux, 1906, *Eusirus microps* Walker, 1906, *Eusirus perdentatus* Chevreux, 1912, *Eusirus pontomedon* Verheye & d'Udekem d'Acoz, 2020, *Eusirus propeperdentatus* Andres, 1979, and *tridentatus* Bellan-

Santini & Ledoyer, 1974 (Andres et al., 2002; De Broyer et al., 2007; Verheye, 2011; Peña Othaitz & Sorbe, 2020; Verheye & D'Udekem D'Acoz, 2020). *Eusirus laevis* Walker, 1903 is a species with uncertain status as it was described from a small juvenile specimen only (Monod, 1926; De Broyer, 1983). Also, depending on the authors, *Eusirus tridentatus* Bellan-Santini and Ledoyer,1974 and *Eusirus microps* Walker 1906 have been considered as two separate or the same species (Krapp et al., 2008; Verheye, 2011). Barnard and Karaman (1991) treated *E. tridentatus* Bellan-Santini and Ledoyer, 1974 and *E.microps* Walker 1906 as separate species while De Broyer and Jazdzewski (1993) synonymized *E. tridentatus* Bellan-Santini and Ledoyer,1974 and *E. microps* Walker. In this study, we treat *E. tridentatus* and *E. microps* as synonymous species in agreement with De Broyer and Jazdzewski (1993). *Eusirus giganteus* Andres, Lörz & Brandt, 2002 is morphologically rather similar to *Eusirus perdentatus* Chevreux, 1912 although *E. giganteus* is bigger than *E. perdentatus*. This similarity has caused both species to be taxonomically mixed up (Andres et al., 2002; De Broyer et al. 2007; Verheye & D'Udekem D'Acoz, 2020). *Eusirus perdentatus* is a synonym to *Eusirus splendidus* Chilton, 1912. Antarctic *Eusirus* species are distributed in the Antarctic and the sub-Antarctic regions at varying depths from 0-2000 m (De Broyer, 1983; De Broyer et al., 2007; Verheye, 2011; Peña Othaitz & Sorbe, 2020; Verheye & d'Udekem d'Acoz, 2020).

The application of molecular approaches to Antarctic *E. perdentatus* and *E. giganteus* showed the presence of multiple cryptic species with *E. perdentatus* comprising three putative genetic species (clades P1-P3) and *E. giganteus* four to five genetic putative genetic species (clades G1-G4a and G4b) (Baird et al., 2011; Verheye & D'Udekem D'Acoz, 2020). The P1 clade of *E. perdentatus* has an unknown phenotype and can only be recognized from DNA sequence data while clade P2 has been identified as the true *E. perdentatus.* Verheye & D'Udekem D'Acoz (2020) later formally described the putative *E. perdentatus* clade P3 as a new species called *Eusirus pontomedon* Verheye & d'Udekem d'Acoz, 2020. The components of the *E. giganteus* complex still need to be formally described but Verheye & D'Udekem D'Acoz (2020) have already reported minor morphological differences and recommended a thorough morphological analysis.

The number of Arctic *Eusirus* species varies depending on the author but only four species can be found in the Arctic Register of Marine Species (https://www.marinespecies.org/arms) (Sirenko et al., 2022) namely: *Eusirus cuspidatus* Krøyer, 1845, *Eusirus holmii* Hansen, 1887,

Eusirus minutus G.O. Sars, 1893, *Eusirus propinqvus* Sars, 1893. However, based on Thurston (2009) and Palerud & Vader (1991) there are nine *Eusirus* species recorded in the Arctic, namely *Eusirus abyssi* Stephensen, 1944, *Eusirus biscayensis* Bonnier, 1896, *Eusirus cuspidatus* Krøyer, 1845, *Eusirus holmii* Hansen, 1887, *Eusirus minutus* G.O. Sars, 1893, *Eusirus leptocarpus* G.O. Sars, 1893, *Eusirus propinqvus* Sars, 1893, *Eusirus longipes* Boeck, 1861, and *Eusirus tjalfiensis* Stephensen, 1912. *Eusirus longipes* Boeck, 1861 is synonymous with *Eusirus bidens* Heller, 1867 and *Eusirus helvetiae* Spence Bate, 1862. These Arctic species are distributed in the Arctic and sub-Arctic regions and have also been recorded outside of these regions as in the Northeast Atlantic Ocean, South African seas, the Mediterranean sea, and Japan seas at depths of 22-4330 m (Della Valle, 1893; Palerud & Vader, 1991; Bousfield & Hendrycks, 1995; Golovan et al., 2013; Peña Othaitz & Sorbe, 2020). No presence of cryptic species has yet been documented for Arctic *Eusirus* species though different eye shape and color as well as variation in body color of *E. holmii* from different habitats could indicate the presence of cryptic diversity (Macnaughton et al., 2007; Hop et al., 2021).

There are other described *Eusirus* species that are not found in the Antarctic or the Arctic and are classified here as non-polar species. These species include: *Eusirus bathybius* Schellenberg, 1955, *Eusirus bonnieri* Peña Othaitz & Sorbe, 2020, *Eusirus bulbodigitus* Jung, Kim, Soh & Yoon, 2016, *Eusirus columbianus* Bousfield & Hendrycks, 1995, *Eusirus crosnieri* Ledoyer, 1978, *Eusirus fragilis* Birstein & M. Vinogradov, 1960, *Eusirus hirayamae* Bousfield & Hendrycks, 1995, *Eusirus latirostris* Ledoyer, 1982, *Eusirus liui* Wang, Sha & Ren, 2021, *Eusirus meteorae* Andres, 1996, *Eusirus nevandis* J.L. Barnard, 1961, and *Eusirus parvus* Pirlot, 1934 (Pirlot, 1934; Schellenberg, 1955; Birstein & Vinogradov, 1960; Barnard, 1961; Ledoyer, 1978; Ledoyer, 1982; Bousfield & Hendrycks, 1995; Andres, 1996; Jung et al., 2016; Peña Othaitz & Sorbe, 2020; Wang et al., 2021). These non-polar species are found in the Puerto Rico Trench, the Tonga Trench, the Northwest and Northeast Pacific Ocean, the Indian Ocean, the Northeast Atlantic Ocean around Alaska, the Pyrdz Bay, the Greenland-Iceland-Faeroe-Ridge (GIF-Ridge), and the Flores sea at depths from 0 to 7900 m (Bousfield & Hendrycks, 1995; Weisshappel, 2000; Arndt & Swadling, 2006; Peña Othaitz & Sorbe, 2020).

Eusirus species are mainly benthic to benthopelagic but some are also found to be only pelagic (De Broyer, 1983, De Broyer et al., 2007, Andres et al., 2002, Peña Othaitz & Sorbe, 2020, Verheye & D'Udekem D'Acoz, 2020, Barnard, 1961, Arndt & Swadling, 2006, Ohtsuka et al.,

2004, Schellenberg, 1927, Carrassón & Matallanas, 2002, Jung et al., 2016, Vinogradov, 2004). Some *Eusirus* species are also known to switch to a sympagic lifestyle or live in association with sea ice (Arndt & Swadling, 2006; Macnaughton et al., 2007; Kiko et al., 2008; Krapp et al., 2008; Kosobokova et al., 2011; Peña Othaitz & Sorbe, 2020) and can survive at temperatures as low as -2°C (Aarset & Torres, 1989). These species are primarily predators feeding on living polychaetes, zooplankton, and crustaceans, primarily on other amphipods (Klages & Gutt 1990; Dauby et al. 2001; Nyssen et al., 2002; De Broyer et al., 2004; Nyssen, 2005; Michel et al., 2020), but can also consume a wide range of other food items (Graeve et al., 2001; Nyssen, 2005; Macnaughton et al., 2007; Smoot, 2015; Macdonald et al., 2010; Michel et al., 2020). These *Eusirus* species can also shift to deposit feeding or scavenging and can show necrophagous behavior (Klages & Gutt 1990 ; Gromisz et al., 1996; Takeuchi et al., 2002; De Broyer et al., 2004). As is obvious from these descriptions, the current knowledge on the ecology and biology of *Eusirus* species is still very limited which can among other reasons be attributed to their low population abundances (Peña Othaitz & Sorbe, 2020).

Eusirus bouvieri *Eusirus giganteus* G2

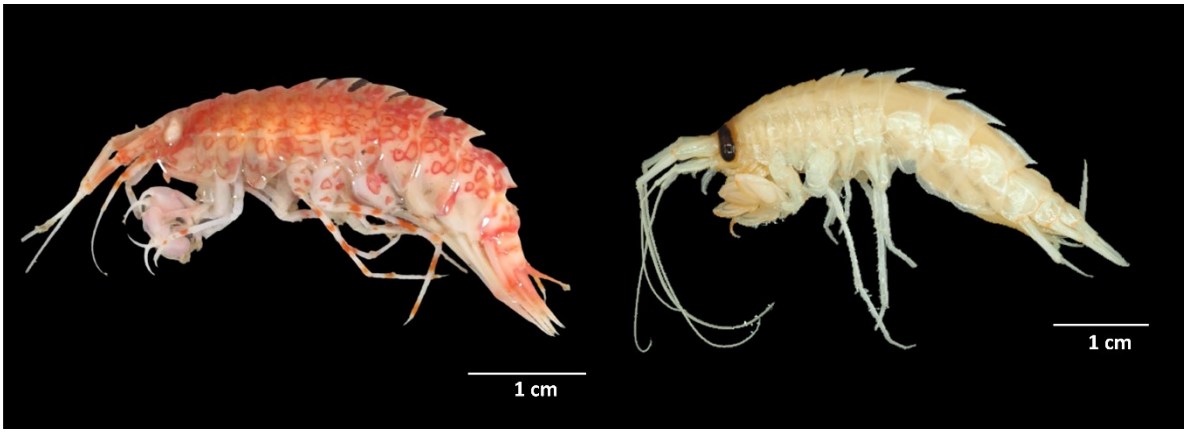

Eusirus perdentatus *Eusirus propeperdentatus*

Figure 10. Some photos of the *Eusirus* specie (photos taken by Louraine Salabao)

Objectives

The overarching goal of this thesis is to add to our understanding of the genetic adaptations and the evolutionary processes that shaped the current diversity of the *Eusirus* amphipods in the Arctic and Southern Oceans. Specifically, I would like to check for signatures of cold-adaptations using mitogenomes. I would also like to test for the monophyly of the Arctic and Antarctic *Eusirus* clades and examine if types of invasions are the same in both polar regions. I aim to date the timing of these invasions from a time-calibrated phylogeny. Lastly, I will test whether the *Eusirus* clade diversity have evolved through adaptive radiation, non-adaptive radiation, or parallel convergence by combining phylogenetic data, ecological and trophic data, and morphological information.

The genus *Eusirus* was chosen as a model organism to identify cold adaptations in amphipods and understand the evolutionary history of marine biodiversity in polar regions because: 1) this genus has a worldwide distribution and has representatives in both polar regions; 2) locally abundant and many species show a high level of endemicity; 3) they occupy both the deep and shallow marine waters; 4) they exhibit a wide range of morphological variation; and 5) they are members of the Eusiridae family, which is a major family of polar amphipods.

References

Aarset, A. V., & Torres, J. J. 1989. Cold resistance and metabolic responses to salinity variations in the amphipod Eusirus antarcticus and the krill Euphausia superba. Polar Biology, 9(8), 491–497.

Abbott, R., Albach, D., Ansell, S., Arntzen, J. W., Baird, S. J., Bierne, N., Boughman, J., Brelsford, A., Buerkle. C. A., Buggs, R. , Butlin, R. K. , Dieckmann, U., Eroukhmanoff, F., Grill, A., Cahan, S. H., Hermansen J. S., Hewitt, G., Hudson A. G., Jiggins C., Jones, J., Keller, B., Marczewski, T., Mallet, J., Martinez-Rodriguez, P., Möst, M., Mullen, S., Nichols, R., Nolte, A. W., Parisod, C., Pfennig, K., Rice, A. M., Ritchie, M. G., Seifert, B., Smadja, C. M., Stelkens, R., Szymura, J. M., Väinölä, R., Wolf, J. B. W., & Zinner, D. 2013. Hybridization and speciation. Journal of evolutionary biology, 26(2), 229-246.

Adey, W. H., Lindstrom, S. C., Hommersand, M. H., & Müller, K. M. 2008. The Biogeographic origin of arctic endemic seaweeds: a thermogeographic view 1. Journal of Phycology, 44(6), 1384-1394.

Alcock, J. 2001. Animal behavior: An evolutionary approach, Tenth Edition. Sunderland: Sinauer associates.

Allcock, A. L., & Strugnell, J. M. 2012. Southern Ocean diversity: new paradigms from molecular ecology. Trends in ecology & evolution, 27(9), 520-528.

Amante, C. and B. W. Eakins. 2009. ETOPO1 1 Arc-Minute Global Relief Model: Procedures, Data Sources and Analysis. NOAA Technical Memorandum NESDIS NGDC-24, 19 pp.

AMAP (Arctic Monitoring and Assessment Programme). 1997. Arctic Pollution Issues: A State of the Arctic Environment Report. Arctic monitoring and Assessment Programme (AMAP), Oslo, Norway. xii+188.

AMAP (Arctic Monitoring and Assessment Programme). 1998. AMAP Assessment Report: Arctic Pollution Issues. Arctic Monitoring and Assessment Programme (AMAP), Oslo, Norway. xii+859.

Anderson, J. 2010. Antarctic Marine Geology. Cambridge: Cambridge University Press.

Andres, H.G. 1979. Gammaridea (Amphipoda, Crustacea) der Antarktis-Expedition 1975/1976. Auswertung der Dauerstation sudlich von Elephant Island. Meeresforschung. 27(3): 88-102.

Andres, H.G. 1996. A new pelagic eusirid amphipod, Eusirus meteorae, from the tropical NE-Atlantic (Crustacea, Gammaridea). Mitteilungen des Hamburger Zoologisches Museum und Institut, 93, 83–90.

Andres, H. G., Lörz, A. N., & Brandt, A. 2002. A common but undescribed huge species of Eusirus Krøyer. 1845. (Crustacea, Amphipoda, Eusiridae) from Antarctica. Mitteilungen aus dem Hamburgischen Zoologischen Museum und Institut, 99, 109-126.

Arndt, C. E., & Swadling, K. M. 2006. Crustacea in Arctic and Antarctic sea ice: distribution, diet and life history strategies. Advances in marine biology, 51, 197-315.

Arndt, J.E, Schenke, H. W., Jakobsson, M., Nitsche, F.O., Buys, G., Goleby, B, Rebesco, M., Bohoyo, F., Hong, J.K., Black, J., Greku, R.K., Udintsev, G.B, Barrios, F., Reynoso-Peralta, W., Taisei, M., Wigley, R. 2013. The International Bathymetric Chart of the Southern Ocean (IBCSO) - digital bathymetric model. PANGAEA.

Arntz, W. E., Brey, T., & Gallardo, V. A. 1995. Antarctic zoobenthos. Oceanographic Literature Review, 8(42), 668.

Aronson, R. B., Thatje, S., Clarke, A., Peck, L. S., Blake, D. B., Wilga, C. D., & Seibel, B. A. 2007. Climate change and invasibility of the Antarctic benthos. Annu. Rev. Ecol. Evol. Syst., 38, 129-154.

Auger, M., Morrow, R., Kestenare, E., Sallée, J. B., & Cowley, R. 2021. Southern Ocean in-situ temperature trends over 25 years emerge from interannual variability. Nature communications, 12(1), 1-9.

Baird, H. P., Miller, K. J., & Stark, J. S. 2011. Evidence of hidden biodiversity, ongoing speciation and diverse patterns of genetic structure in giant Antarctic amphipods. Molecular Ecology, 20(16), 3439-3454.

Bamber, J. L., Layberry, R. L., & Gogineni, S. P. 2001. A new ice thickness and bed data set for the Greenland ice sheet: 1. Measurement, data reduction, and errors. Journal of Geophysical Research: Atmospheres, 106(D24), 33773-33780.

Barker, P. F., Filippelli, G. M., Florindo, F., Martin, E. E., & Scher, H. D. 2007. Onset and role of the Antarctic Circumpolar Current. Deep Sea Research Part II: Topical Studies in Oceanography, 54(21-22), 2388-2398.

Barluenga, M., Stölting, K. N., Salzburger, W., Muschick, M., & Meyer, A. 2006. Sympatric speciation in Nicaraguan crater lake cichlid fish. Nature, 439(7077), 719-723.

Barnard, J.L. 1961 Gammaridean Amphipoda from depths of 400 to 6000 m. Galathea Report, 5, 23–128.

Barnard, J.L., 1969. The families and genera of marine gammaridean Amphipoda. Smithsonian Institution Press, Washington.

Barnard, J. L., & Karaman, G. S. 1983. Australia as a major evolutionary centre for Amphipoda (Crustacea). Memoirs of the Australian Museum, 18, 45-61.

Barnard, J. and G. Karaman. 1991. The Families and Genera of Marine Gammaridean Amphipoda (except Marine Gammaroids), Part 1,2 Records of the Australian Museum Supplement, 13, 1-866.

Barnes, D. K., Kaiser, S., Griffiths, H. J., & Linse, K. 2009. Marine, intertidal, freshwater and terrestrial biodiversity of an isolated polar archipelago. Journal of Biogeography, 36(4), 756-769.

Barnes, D. K., & Kuklinski, P. 2010. Bryozoans of the Weddell Sea continental shelf, slope and abyss: did marine life colonize the Antarctic shelf from deep water, outlying islands or in situ refugia following glaciations?. Journal of Biogeography, 37(9), 1648-1656.

Barnes, D. K., & Tarling, G. A. 2017. Polar oceans in a changing climate. Current Biology, 27(11), R454-R460.

Bate, C. S. 1862. Catalogue of the Specimens of Amphipodous Crustacea in the Collection of the British Museum. order of the Trustees [by Taylor and Francis].154-155.

Bellan-Santini, D.; Ledoyer, M. 1974. Gammariens (Crustacea,Amphipoda) des Iles Kerguelen et Crozet. Tethys. 5(4): 635-708.

Bird, C. E., Holland, B. S., Bowen, B. W., & Toonen, R. J. 2011. Diversification of sympatric broadcast‐spawning limpets (Cellana spp.) within the Hawaiian archipelago. Molecular Ecology, 20(10), 2128-2141.

Birstein, J.A. & Vinogradov, M.E. 1960 Pelagicheskie gammaridy tropicheskoi chasti Tixogo Okeana. Akademiia Nauk SSSR, Instituta Okeanologii, Trudy, 34, 165–241.

Bodil, B. A.,Ambrose, W. G.,Bergmann, M., Clough, L. M.,Gebruk, A. V.,Hasemann, C., Iken, K., Klages, M., MacDonald, I. R., Renaud, P. E., Schewe, I., Soltwedel, T., & Włodarska-Kowalczuk, M. 2011. Diversity of the arctic deep-sea benthos. Marine Biodiversity, 41(1), 87–107.

Boeck, A. 1861. Bermærkninger Angaaende de Ved de Norske Kyster forekommende Amphipoder. Forhandlinger ved de Skandinaviske Naturforskeres Ottende Møde, 8, 631–677.

Bonnier, J. 1896. Edriophthalmes. In: Kœlher, R. (Ed.), Résultats scientifiques de la campagne du "Caudan" dans le Golfe de Gascogne. Annales de l'Université de Lyon, Masson et Cie ed., Paris, 527–689.

Boore, J. L., Lavrov, D. V., & Brown, W. M. 1998. Gene translocation links insects and crustaceans. Nature, 392(6677), 667-668.

Bousfield E.L. & Hendrycks E.A. 1995. The amphipod superfamily Eusiroidea in the North American Pacific region. I. Family Eusiridae: systematics and distributional ecology. Amphipacifica, 1, 4, 3-59.

Bowman, T. E., & Abele, L. G. 1982. Classification of the recent Crustacea. The biology of Crustacea, 1, 1-27.

Brozena, J. M., Childers, V. A., Lawver, L. A., Gahagan, L. M., Forsberg, R., Faleide, J. I., & Eldholm, O. 2003. New aerogeophysical study of the Eurasia Basin and Lomonosov Ridge: Implications for basin development. Geology, 31(9), 825-828.

Brusca, R. C. & G.J., Brusca. 2003. Invertebrates (2nd ed.). Sinauer Associates Inc., Sunderland, Massachusetts, United States. pp. 1-878.

Burns, K. J., Hackett, S. J., & Klein, N. K. 2002. Phylogenetic relationships and morphological diversity in Darwin's finches and their relatives. Evolution, 56(6), 1240-1252.

Butlin, R., Bridle, J., & Schluter, D. (Eds.). 2009. Speciation and patterns of diversity. Cambridge University Press. 1-351.

CAFF (Conservation of Arctic Flora and Fauna). 2001. Arctic Flora and Fauna: Status and Conservation.

Callaghan, T. V., Johansson, M., Brown, R. D., Groisman, P. Y., Labba, N., Radionov, V., Bradley, R. S., Blangy, S., Bulygina, O. N., Christensen, T. R., Colman, J. E., Essery, R. L. H., Forbes, B. C., Forchhammer, M. C., Golubev, V. N., Honrath, R. E., Juday, G. P., Meshcherskaya, A. V., Phoenix, G. K., Pomeroy, J., Rautio, A., Robinson, D.A., Schmidt, N.M., Serreze, M.C., Shevchenko, V.P., Shiklomanov, A.I., Shmakin, A.B., Sköld, P., Sturm, M., Woo, M. & Wood, E. F. 2011. Multiple Effects of Changes in Arctic Snow Cover. AMBIO, 40(S1), 32–45.

Carrassón, M., & Matallanas, J. 2002. Feeding habits of Cataetyx alleni (Pisces: Bythitidae) in the deep western Mediterranean. Scientia Marina, 66(4), 417-421.

Chapman, J. W. 2007. Amphipoda: Chapter 39 of The Light and Smith Manual: Intertidal Invertebrates from Central California to Oregon. Completely Revised and Expanded.

Chevreux, E. 1906. Crustacés amphipodes. In: Expédition antarctique française (1903–1905) commandée par le Dr Jean Charcot. Sciences Naturelles: Documents Scientifiques. Masson, Paris. 100.

Chevreux, E. 1911. Sur quelques amphipodes des îles Sandwich du Sud. An. Mus. Nac. Bs. As, 21, 403-407.

Chevreux, E. 1912. Deuxième expédition dans l'Antarctique, dirigée par le Dr. Charcot, 1908-1910. Diagnoses d'amphipodes nouveaux. Bulletin du Museum National d'Histoire Naturelle. 18(4): 208-218.

Clarke, A. 1990. Temperature and evolution: Southern Ocean cooling and the Antarctic marine fauna. In Antarctic ecosystems. Springer, Berlin, Heidelberg. 9-22.

Clarke, A. & Crame, J. A. 1989. The origin of the Southern Ocean marine fauna. Geological Society, London, Special Publications, 47(1), 253–268.

Clarke, A., & Crame, J. A. 2010. Evolutionary dynamics at high latitudes: speciation and extinction in polar marine faunas. Philosophical Transactions of the Royal Society B: Biological Sciences, 365(1558), 3655-3666.

Clarke, A., & Johnston, N. M. 2003. Antarctic marine benthic diversity. In Oceanography and Marine Biology, An Annual Review, Volume 41 .CRC Press. pp. 55-57.

Coakley, B., Brumley, K., Lebedeva-Ivanova, N., & Mosher, D. 2016. Exploring the geology of the central Arctic Ocean; understanding the basin features in place and time. Journal of the Geological Society, 173(6), 967-987.

Copilaș-Ciocianu, D., Sidorov, D.A., Gontcharov, A.A. 2019. Adrift across tectonic plates: molecular phylogenetics supports the ancient Laurasian origin of old limnic crangonyctid amphipods. Org. Divers. Evol. 19, 191–207.

Copilaş-Ciocianu, D., Borko, Š., & Fišer, C. 2020. The late blooming amphipods: global change promoted post-Jurassic ecological radiation despite Palaeozoic origin. Molecular Phylogenetics and Evolution, 143, 106664.

Copilaş-Ciocianu, D., Boros, B. V., & Šidagytė-Copilas, E. 2021. Morphology mirrors trophic niche in a freshwater amphipod community. Freshwater Biology, 66(10), 1968-1979.

Coxall, H. K., & Pearson, P. N. 2007. The Eocene-Oligocene transition. Deep time perspectives on climate change: Marrying the signal from computer models and biological proxies, 351-387.

Crame, J. A. 2018. Key stages in the evolution of the Antarctic marine fauna. Journal of Biogeography, 45(5), 986-994.

Crame, J. A., Beu, A. G., Ineson, J. R., Francis, J. E., Whittle, R. J., & Bowman, V. C. 2014. The early origin of the Antarctic marine fauna and its evolutionary implications. PloS one, 9(12), e114743. 1-22.

Cruz-Rivera, E. & Hay, M. E. 2001. Macroalgal traits and the feeding and fitness of an herbivorous amphipod: the roles of selectivity, mixing, and compensation. Marine Ecology Progress Series, 218, 249-266.

Dahl, E. 1977. The amphipod functional model and its bearing upon systematics and phylogeny. Zool. Scr. 6, 221-228.

Dalziel, I. W. 1992. Antarctica: a tale of two supercontinents?. Annual Review of Earth and Planetary Sciences, 20, 501.

Dam, H. G. 2013. Evolutionary adaptation of marine zooplankton to global change. Annual review of marine science, 5, 349-370.

Dauby, P., Scailteur, Y., & De Broyer, C. 2001. Trophic diversity within the eastern Weddell Sea amphipod community. Hydrobiologia, 443(1), 69-86.

De Broyer, C. 1983. Recherches sur la systémique et l'évolution des crustacés amphipodes gammarides antarctiques et subantarctiques (Doctoral dissertation, UCL-Université Catholique de Louvain).

De Broyer, C. & Jazdzewski, K. 1993. A checklist of the Amphipoda (Crustacea) of the Southern Ocean. In: Studiedocumenten van het Koninklijk Belgisch Institut voor Natuurwetenschappen, vol. 73. Royal Belgian Institute for Natural Sciences, Brussels. 1-154.

De Broyer, C., Nyssen, F., & Dauby, P. 2004. The crustacean scavenger guild in Antarctic shelf, bathyal and abyssal communities. Deep Sea Research Part II: Topical Studies in Oceanography, 51(14-16), 1733-1752.

De Broyer, C., Lowry, J. K., Jazdzewski, K., & Robert, H. 2007. Census of Antarctic Marine Life. Synopsis of the Amphipoda of the Southern Ocean. Vol. 1. Part 1: Catalogue of the Gammaridean and Corophiidean Amphipoda of the Southern Ocean with Distribution and Ecological Data, by C. de Broyer, JK Lowry, K Jazdzewski and H. Robert. Institut Royal des Sciences Naturelles de Belgique.

De Broyer, C., & Danis, B. 2011. How many species in the Southern Ocean? Towards a dynamic inventory of the Antarctic marine species. Deep sea research Part II: Topical studies in oceanography, 58(1-2), 5-17.

Della Valle, A. 1893. Gammarini del Golfo di Napoli: monografia (Vol. 1). R. Freidländer.52, 147,669.

Duffy, J. E., & Thiel, M. (Eds.). 2007. Evolutionary ecology of social and sexual systems: crustaceans as model organisms. Oxford University Press.

Dunton, K. 1992. Arctic biogeography: the paradox of the marine benthic fauna and flora. Trends in Ecology & Evolution, 7(6), 183-189.

Eastman, J. T. 2005. The nature of the diversity of Antarctic fishes. Polar biology, 28(2), 93-107.

Eicken, H., Fischer, H., & Lemke, P. 1995. Effects of the snow cover on Antarctic sea ice and potential modulation of its response to climate change. Annals of Glaciology, 21, 369-376.

Eldevik, T., Smedsrud, L., Li, C., Årthun, M., Madonna, E., & Svendsen, L. 2020. The Arctic Mediterranean. In C. Mechoso (Ed.), Interacting Climates of Ocean Basins: Observations, Mechanisms, Predictability, and Impacts. Cambridge: Cambridge University. 186-215.

Farmer, J. R., Cronin, T. M., De Vernal, A., Dwyer, G. S., Keigwin, L. D., & Thunell, R. C. 2011. Western Arctic Ocean temperature variability during the last 8000 years. Geophysical Research Letters, 38(24).

Fišer, C., Luštrik, R., Sarbu, S., Flot, J. F., & Trontelj, P. 2015. Morphological evolution of coexisting amphipod species pairs from sulfidic caves suggests competitive interactions and character displacement, but no environmental filtering and convergence. PLoS One, 10(4), e0123535.

Foster, T. D., & Carmack, E. C. 1976. Frontal zone mixing and Antarctic Bottom Water formation in the southern Weddell Sea. In Deep Sea Research and Oceanographic Abstracts. Elsevier. Vol. 23, No. 4, 301-317.

Futuyma, D. J. 2005. Evolution. Sinauer Associates. Sunderland, Massachusetts, U.S.A. pp. 502-518.

Futuyma, D.J. & Kirkpatrick, M. 2017. Evolution (Fourth Edition). Sinauer Associates, Inc. Sunderland, Massachusetts, U.S.A. 1-725.

Gautam, P. 2020. Divergent Evolution. In: Vonk, J., Shackelford, T. (eds) Encyclopedia of Animal Cognition and Behavior. Springer, Cham.

Gavrilets, S., & Losos, J. B. 2009. Adaptive radiation: contrasting theory with data. Science, 323(5915), 732-737.

Gilg, O., Kovacs, K. M., Aars, J., Fort, J., Gauthier, G., Grémillet, D., Ims, R.A., Meltofte, H., Moreau, J., Post, E., Schmidt, N.M., Yannic, G., & Bollache, L. 2012. Climate change and the ecology and evolution of Arctic vertebrates. Annals of the New York Academy of Sciences, 1249(1), 166-190.

Gittenberger, E. 1991. What about non-adaptive radiation?. Biological Journal of the Linnean Society, 43(4), 263-272.

Golikov, A. N., & Scarlato, O. A. 1989. Evolution of Arctic ecosystems during the Neogene period. In The Arctic Seas. Springer, Boston, MA. 257-279.

Golovan, O. A., Błażewicz-Paszkowycz, M., Brandt, A., Budnikova, L. L., Elsner, N. O., Ivin, V. V., Lavrenteva, A. V., Malyutina, M. V., Petryashov, V. V., & Tzareva, L. A. 2013. Diversity and distribution of peracarid crustaceans (Malacostraca) from the continental slope and the deep-sea basin of the Sea of Japan. Deep Sea Research Part II: Topical Studies in Oceanography, 86–87, 66–78.

Gonzalez, S., & Vasallo, F. 2020. Antarctic climates. Encyclopedia of the World's Biomes. Elsevier. 595-605

Gordon, A. L. 1967. Structure of Antarctic Waters Between 20°Wand 170°W. Antarctic Map Folio Series - Folio 6. American Geographical Society, New York, 10 pp.

Gradinger, R. R. 2001. Adaptation of Arctic and Antarctic ice metazoa to their habitat. Zoology, 104(3-4), 339-345.

Graeve, M., Dauby, P., & Scailteur, Y. 2001. Combined lipid, fatty acid and digestive tract content analyses: a penetrating approach to estimate feeding modes of Antarctic amphipods. Polar biology, 24(11), 853-862.

Grazioli, J., Madeleine, J. B., Gallée, H., Forbes, R. M., Genthon, C., Krinner, G., & Berne, A. 2017. Katabatic winds diminish precipitation contribution to the Antarctic ice mass balance. Proceedings of the National Academy of Sciences, 114(41), 10858-10863.

Greco, S., Agostino, E. D., Manfrin, C., Gaetano, A. S., Furlanis, G., Capanni, F., Santovito, G., Edomi, P., Giulianini, P.G., & Gerdol, M. 2021. RNA-sequencing indicates high hemocyanin expression as a key strategy for cold adaptation in the Antarctic amphipod Eusirus cf. giganteus Clade g3. Biocell, 45(6), 1611-1619.

Griffiths, H. J. 2010. Antarctic marine biodiversity–what do we know about the distribution of life in the Southern Ocean?. PloS one, 5(8), e11683.

Gromisz, S. Wlodarska M., Weslawski J.M. 1996. A comparison of the macrofaunal community structure and diversity in two arctic glacial bays -a 'cold' one off Franz Josef Land and a 'warm' one off Spitsbergen. OCEANOLOGIA, No.38 (2). 259.

Gutt, J., Bertler, N., Bracegirdle, T. J., Buschmann, A., Comiso, J., Hosie, G., Isla, E., Schloss, I.R., Smith, C.R., Tournadre, J., & Xavier, J. C. 2015. The Southern Ocean ecosystem under multiple climate change stresses – an integrated circumpolar assessment. Global Change Biology, 21(4), 1434-1453.

Hansen, H.J. 1887. Oversigt over de paa Dijmphna-Togtet indsamlede Krebsdyr. In: Lütken, C.F. (Ed.), Dijmphna-Togtets Zoologisk-Botaniske Udbytte. I Kommission hos H. Hagerup, Kjøbenhavn. 183–286.

Hansen, H. J. 1903. The Ingolfiellidae, fam. n., a new type of Amphipoda. Zoological Journal of the Linnean Society, 29(188), 117-133.

Hardy, S. M., Carr, C. M., Hardman, M., Steinke, D., Corstorphine, E., & Mah, C. 2011. Biodiversity and phylogeography of Arctic marine fauna: insights from molecular tools. Marine Biodiversity, 41(1), 195-210.

Harrison, R. G. 2012. The language of speciation. Evolution, 66(12), 3643-3657.

Hassold, N. J., Rea, D. K., van der Pluijm, B. A., & Parés, J. M. 2009. A physical record of the Antarctic Circumpolar Current: Late Miocene to recent slowing of abyssal circulation. Palaeogeography, Palaeoclimatology, Palaeoecology, 275(1-4), 28-36.

Hautmann, M. 2020. What is macroevolution?. Palaeontology, 63(1), 1-11.

Hoberg, E. P., Kutz, S. J., Galbreath, K. E., & Cook, J. 2003. Arctic biodiversity: from discovery to faunal baselines-revealing the history of a dynamic ecosystem. Journal of Parasitology, 89(Suppl), S84-S95.

Hodel, F., Grespan, R., de Rafélis, M., Dera, G., Lezin, C., Nardin, E., Rouby, D., Aretz, M., Steinnman, M., Buatier, M., Lacan, F., Jeandel, C., & Chavagnac, V. 2021. Drake Passage gateway opening and Antarctic Circumpolar Current onset 31 Ma ago: The message of foraminifera and reconsideration of the Neodymium isotope record. Chemical Geology, 570, 120171.

Hop, H., Vihtakari, M., Bluhm, B. A., Daase, M., Gradinger, R., & Melnikov, I. A. 2021. Ice-associated amphipods in a pan-Arctic scenario of declining sea ice. Frontiers in Marine Science, 8, 743152.

Horton, T.; Lowry, J.; De Broyer, C.; Bellan-Santini, D.; Coleman, C.O.; Corbari, L.; Costello, M.J.; Daneliya, M.; Dauvin, J.-C.; Fišer, C.; Gasca, R.; Grabowski, M.; Guerra-García, J.M.; Hendrycks, E.; Hughes, L.; Jaume, D.; Jazdzewski, K.; Kim, Y.-H.; King, R.; Krapp-Schickel, T.; LeCroy, S.; Lörz, A.-N.; Mamos, T.; Senna, A.R.; Serejo, C.; Sket, B.; Souza-Filho, J.F.; Tandberg, A.H.; Thomas, J.D.; Thurston, M.; Vader, W.; Väinölä, R.; Vonk, R.; White, K.; Zeidler, W. 2022. World Amphipoda Database. Accessed at https://www.marinespecies.org/amphipoda on 2022-04-14.

Hou, Z., Li, J., & Li, S. 2014. Diversification of low dispersal crustaceans through mountain uplift: a case study of Gammarus (Amphipoda: Gammaridae) with descriptions of four novel species. Zoological Journal of the Linnean Society, 170(4), 591-633.

Hughes, K. A., Convey, P., & Turner, J. 2021. Developing resilience to climate change impacts in Antarctica: An evaluation of Antarctic Treaty System protected area policy. Environmental Science & Policy, 124, 12-22.

Hutchinson, D. K., Coxall, H. K., Lunt, D. J., Steinthorsdottir, M., de Boer, A. M., Baatsen, M., von der Heydt, A., Huber, M., Kennedy-Asser, A. T., Kunzmann, L., Ladant, J. B., Lear, C. H., Moraweck, K., Pearson, P. N., Piga, E., Pound, M. J., Salzmann, U., Scher, H. D., Sijp, W. P., Śliwińska, K.K., Wilson, P.A., & Zhang, Z. 2021. The Eocene–Oligocene transition: a review of marine and terrestrial proxy data, models and model–data comparisons. Climate of the Past, 17(1), 269–315.

IHO (International Hydrographic Office). 2001. S-23 ‘‘Limits of Ocean and Seas’’, draft 4th Edition.

Incze, L. S., Lawton, P., Ellis, S. L., & Wolff, N. H. 2010. Biodiversity knowledge and its application in the Gulf of Maine area. Life in the world's oceans: diversity, distribution and abundance. Wiley Blackwell Scientific Publications, London, 49.

Ingólfsson, Ó. 2004. Quaternary glacial and climate history of Antarctica. Developments in Quaternary sciences, 2, 3-43.

Irisarri, I., Singh, P., Koblmüller, S., Torres-Dowdall, J., Henning, F., Franchini, P., Fischer, C., Lemmon, A.R., Lemmon, E.M., Thallinger, G.G., Sturmbauer, C., & Meyer, A. 2018. Phylogenomics uncovers early hybridization and adaptive loci shaping the radiation of Lake Tanganyika cichlid fishes. Nature communications, 9(1), 3159.

Jakobsson, M. 2002. Hypsometry and volume of the Arctic Ocean and its constituent seas. Geochemistry, Geophysics, Geosystems, 3(5), 1-18.

Jakobsson, M., & Macnab, R. 2006. A comparison between GEBCO sheet 5.17 and the International Bathymetric Chart of the Arctic Ocean (IBCAO) version 1.0. Marine Geophysical Researches, 27(1), 35-48.

Jakobsson, M., L. A. Mayer, B. Coakley, J. A. Dowdeswell, S. Forbes, B. Fridman, H. Hodnesdal, R. Noormets, R. Pedersen, M. Rebesco, H.-W. Schenke, Y. Zarayskaya A, D. Accettella, A. Armstrong, R. M. Anderson, P. Bienhoff, A. Camerlenghi, I. Church, M. Edwards, J. V. Gardner, J. K. Hall, B. Hell, O. B. Hestvik, Y. Kristoffersen, C. Marcussen, R. Mohammad, D. Mosher, S. V. Nghiem, M. T. Pedrosa, P. G. Travaglini, & P. Weatherall. 2012. The International Bathymetric Chart of the Arctic Ocean (IBCAO) Version 3.0, Geophysical Research Letters.

Josefson, A.B., V. Mokievsky, M. Bergman, M.E. Blicher, B. Bluhm, S. Cochrane, N. V. Denisenko, C. Hasemann, L.L. Jorgensen, M. Klages, I. Schewe, M.K. Sejr, T. Soltwedel, and M. Wlodarska-Kowalczuk. 2013. Marine Invertebrates. Pages 277–309 in H. Melforte,editor. Arctic Biodiversity Assessment. Status and Trends in Arctic Biodiversity. Conservation of Arctic Flora and Fauna, Akureyri, Iceland.

Jung, T. W.; Kim, M.-S.; Soh, H.-Y.; Yoon, S. M. 2016. A new species of Eusirus from Jeju Island, Korea (Crustacea, Amphipoda, Eusiridae). ZooKeys.(640), 19-35.

Kaiser, S., Brandão, S. N., Brix, S., Barnes, D. K., Bowden, D. A., Ingels, J., Leese, F., Schiaparelli, S., Arango, C.P., Badhe, R., Bax, N., Blazewicz-Paszkowycz, M., Brandt, A., Brenke, N., Catarino, A.I., David, B., De Ridder, C., Dubois, P., Ellingsen, K.E., Glover, A.G., Griffiths, H.J., Gutt, J., Halanych, K.M., Havermans, C., Held, C., Janussen, D., Lörz, A., Pearce, D.A., Pierrat, B., Riehl, T., Rose, A., Sands, C.J., Soler-Membrives, A., Schüller, M., Strugnell, J.M., Vanreusel, A., Veit-Köhler, G., Wilson, N.G., & Yasuhara, M. 2013. Patterns, processes and vulnerability of Southern Ocean benthos: a decadal leap in knowledge and understanding. Marine biology, 160(9), 2295-2317.

Keller, G., MacLeod, N., & Barrera, E. 1992. Eocene-Oligocene Faunal Turnover in Planktic Foraminifera and Antarctic Glaciation. In D. R. Prothero & W. A. Berggren (Eds.), Eocene-Oligocene Climatic and Biotic Evolution. Princeton University Press. 218–244.

Khain, V. E., & Filatova, N. I. 2010. Oceanic basins in prehistory of the evolution of the Arctic Ocean. In Doklady Earth Sciences. Vol. 432, No. 2, 742-745.

Kiko, R., Michels, J., Mizdalski, E., Schnack-Schiel, S. B., & Werner, I. 2008. Living conditions, abundance and composition of the metazoan fauna in surface and sub-ice layers in pack ice of the western Weddell Sea during late spring. Deep Sea Research Part II: Topical Studies in Oceanography, 55(8-9), 1000-1014.

Kirkpatrick, M., & Ravigné, V. 2002. Speciation by natural and sexual selection: models and experiments. the american naturalist, 159(S3), S22-S35.

Klages, M., & Gutt, J. 1990. Observations on the feeding behaviour of the Antarctic gammarid Eusirus perdentatus Chevreux, 1912 (Crustacea: Amphipoda) in aquaria. Polar Biology, 10(5), 359-364.

Klinck, L., & Nowlin Jr, W. D. 2001. Southern Ocean-Antarctic Circumpolar Current. Encyclopedia of Oceanography, 151-159.

Kniesz, K., Jażdżewska, A. M., Martínez Arbizu, P., & Kihara, T. 2022. DNA Barcoding of Scavenging Amphipod Communities at Active and Inactive Hydrothermal Vents in the Indian Ocean. Frontiers in Marine Science, 1904.

Knox, G.A. 2006. Biology of the Southern Ocean, Second Edition. CRC Press, Boca Raton.

Korhonen, M., Rudels, B., Marnela, M., Wisotzki, A., & Zhao, J. 2013. Time and space variability of freshwater content, heat content and seasonal ice melt in the Arctic Ocean from 1991 to 2011. Ocean Science, 9(6), 1015-1055.

Kosobokova, K. N., Hopcroft, R. R., & Hirche, H. J. 2011. Patterns of zooplankton diversity through the depths of the Arctic's central basins. Marine Biodiversity, 41(1), 29-50.

Kottek, M., Grieser, J., Beck, C., Rudolf, B., & Rubel, F. 2006. World map of the Köppen-Geiger climate classification updated.

Krapp, R. H., Berge, J., Flores, H., Gulliksen, B., & Werner, I. 2008. Sympagic occurrence of Eusirid and Lysianassoid amphipods under Antarctic pack ice. Deep Sea Research Part II: Topical Studies in Oceanography, 55(8-9), 1015-1023.

Krøyer, H. 1845. Karcinologiske Bidrag (Fortsaettelse). Naturhistorisk Tidsskrift Ser. II. 1: 453-638.

Kuklinski, P., Taylor, P. D., Denisenko, N. V., & Berning, B. 2013. Atlantic origin of the Arctic biota? Evidence from phylogenetic and biogeographical analysis of the cheilostome bryozoan genus Pseudoflustra. PLoS One, 8(3), e59152. 1-25.

Kullerud, L., Corell, R., Barry, T., Eamer, J., Hislop, L., Melillo, J., Nellemann, C., Neretin, L., Reiersen, L., & Samseth, J. 2013. The View from the Top: Searching for Responses to a Rapidly Changing Arctic.

Lan, Y., Sun, J., Bartlett, D. H., Rouse, G. W., Tabata, H. G., & Qian, P. Y. 2016. The deepest mitochondrial genome sequenced from Mariana Trench Hirondellea gigas (Amphipoda). Mitochondrial DNA Part B, 1(1), 802-803.

Latimer, J. C., & Filippelli, G. M. 2002. Eocene to Miocene terrigenous inputs and export production: geochemical evidence from ODP Leg 177, Site 1090. Palaeogeography, Palaeoclimatology, Palaeoecology, 182(3-4), 151-164.

Lawver, L. A., & Gahagan, L. M. 2003. Evolution of Cenozoic seaways in the circum-Antarctic region. Palaeogeography, Palaeoclimatology, Palaeoecology, 198(1-2), 11-37.

Lebedeva-Ivanova, N. 2010. Geophysical studies bearing on the origin of the Arctic Basin (Doctoral dissertation, Acta Universitatis Upsaliensis).

Ledley, T. S. 1991. Snow on sea ice: Competing effects in shaping climate. Journal of Geophysical Research: Atmospheres, 96(D9), 17195-17208.

Ledoyer, M. 1978. Contribution à l'étude des amphipodes gammariens profonds de Madagascar (Crustacea). Tethys, 8, 365– 382.

Ledoyer, M. 1982. Crustacés amphipodes gammariens, familles des Acanthonotozomatidae à Gammaridae. Faune de Madagascar, 59 (1), 1–598.

Legeżyńska, J., Kędra, M., & Walkusz, W. 2012. When season does not matter: summer and winter trophic ecology of Arctic amphipods. Hydrobiologia, 684(1), 189-214.

Legezyñska, J., De Broyer, C., & Wesławski, J. M. 2020. Invasion of the poles. The Natural History of the Crustacea: Evolution and Biogeography of the Crustacea, 216-246.

Lenn, Y. D., Fer, I., Timmermans, M. L., & MacKinnon, J. A. 2022. Mixing in the Arctic Ocean. In Ocean Mixing. Elsevier. 275-299.

Li, J. Y., Zeng, C., Yan, G. Y., & He, L. S. 2019a. Characterization of the mitochondrial genome of an ancient amphipod Halice sp. MT-2017 (Pardaliscidae) from 10,908 m in the Mariana Trench. Scientific reports, 9(1), 1-15.

Li, J. Y., Song, Z. L., Yan, G. Y., & He, L. S. 2019b. The complete mitochondrial genome of the largest amphipod, Alicella gigantea: Insight into its phylogenetic relationships and deep sea adaptive characters. International journal of biological macromolecules, 141, 570-577.

Lincoln, R. J. 1979. British marine amphipoda: Gammaridea (Vol. 818). British Museum (Natural History).10, 402-403.

Liu, H., K. Jezek, B. Li, and Z. Zhao. 2001. Radarsat Antarctic Mapping Project Digital Elevation Model Version 2. [indicate subset used]. Boulder, Colorado USA: National Snow and Ice Data Center.

Lörz, A. N., & Held, C. 2004. A preliminary molecular and morphological phylogeny of the Antarctic Epimeriidae and Iphimediidae (Crustacea, Amphipoda). Molecular Phylogenetics and Evolution, 31(1), 4-15.

Lovette, I. J., Bermingham, E., & Ricklefs, R. E. 2002. Clade-specific morphological diversification and adaptive radiation in Hawaiian songbirds. Proceedings of the Royal Society of London. Series B: Biological Sciences, 269(1486), 37-42.

Lurcock, P. C., & Florindo, F. 2017. Antarctic climate history and global climate changes. Oxford University Press.

Lowry, J. K., Jazdzewski, K., & Robert, H. 2007. Synopsis of the Amphipoda of the Southern Ocean. C. De Broyer (Ed.). Koninklijk Belgisch Instituut voor Naruurwetenschappen.

Lowry, J. K., & Myers, A. A. 2013. A phylogeny and classification of the Senticaudata subord. nov. Crustacea: Amphipoda. Zootaxa, 3610(1), 1-80.

Lowry, J. K., & Myers, A. A. 2017. A phylogeny and classification of the Amphipoda with the establishment of the new order Ingolfiellida (Crustacea: Peracarida). Zootaxa, 4265(1), 1-89.

Macdonald, T. A., Burd, B. J., Macdonald, V. I., & Van Roodselaar, A. 2010. Taxonomic and feeding guild classification for the marine benthic macroinvertebrates of the Strait of Georgia, British Columbia (p. 63). Fisheries and Oceans Canada= Pêches et océans Canada. 1-63.

Macnaughton, M. O., Thormar, J., & Berge, J. 2007. Sympagic amphipods in the Arctic pack ice: redescriptions of Eusirus holmii Hansen, 1887 and Pleusymtes karstensi (Barnard, 1959). Polar Biology, 30(8), 1013-1025.

Mallet, J., Meyer, A., Nosil, P., & Feder, J. L. 2009. Space, sympatry and speciation. Journal of evolutionary biology, 22(11), 2332-2341.

Marincovich Jr, L., Brouwers, E. M., & Carter, L. D. 1985. Early Tertiary marine fossils from northern Alaska: implications for Arctic Ocean paleogeography and faunal evolution. Geology, 13(11), 770-773.

Marincovich L Jr, Brouwers EM, Hopkins DM, McKenna MC. 1990. Late Mesozoic and Cenozoic paleogeographic and paleoclimatic history of the Arctic Ocean Basin, based upon shallow-water marine faunas and terrestrial vertebrates. In: Gantz A, Johnson L, Sweeny JF (eds) The Arctic Ocean Region. The Geology of North America, vol. L. Geological Society of America, Boulder, Colorado. 403–426.

Marincovich, L., & Gladenkov, A. Y. 1999. Evidence for an early opening of the Bering Strait. Nature, 397(6715), 149-151.

Martin, J.W. & Davis, E.D. 2001. An updated classification of the recent Crustacea. Natural History Museum of Los Angeles County, Science Series, 39, 1-124.

Massom, R. A., Drinkwater, M. R., & Haas, C. 1997. Winter snow cover on sea ice in the Weddell Sea. Journal of Geophysical Research: Oceans, 102(C1), 1101-1117.

Matsuoka, K., Skoglund, A., Roth, G., de Pomereu, J., Griffiths, H., Headland, R., … Melvær, Y. 2018. Quantarctica. Norwegian Polar Institute. https://doi.org/10.21334/npolar.2018.8516e961.

Mauritzen, C., Rudels, B., & Toole, J. 2013. The Arctic and Subarctic oceans/seas. In International Geophysics. Academic Press. Vol. 103, 443-470.

McClelland, J. W., Holmes, R. M., Dunton, K. H., & Macdonald, R. W. 2012. The Arctic ocean estuary. Estuaries and Coasts, 35(2), 353-368.

Meier, J. I., Marques, D. A., Mwaiko, S., Wagner, C. E., Excoffier, L., & Seehausen, O. 2017. Ancient hybridization fuels rapid cichlid fish adaptive radiations. Nature communications, 8(1), 14363.

Meltofte, H., Barry, T., Berteaux, D., Bültmann, H., Christiansen, J. S., Cook, J. A., Dahlberg, A.,Daniëls, F. J. A., Ehrich, D., Fjeldså, J.,Friðriksson, F., Ganter, B., Gaston, A. J., Gillespie, L. J., Grenoble, L., Hoberg, E.P., Hodkinson, I. D., Huntington, H. P., Ims, R.A., Josefson, A.B., Kutz, S. J., Kuzmin, S.L., Laidre, K. L., Lassuy, D. R., Lewis, P. N., Lovejoy, C., Michel, C., Mokievsky, V., Mustonen, T., Payer, D. C., Poulin, M., Reid, D. G., Reist, J. D., Tessler, D. F. & Wrona, F. J. 2013. Arctic Biodiversity Assesment. Synthesis. Conservation of Arctic Flora and Fauna (CAFF).

Michel, L. N., Nyssen, F. L., Dauby, P., & Verheye, M. 2020. Can mandible morphology help predict feeding habits in Antarctic amphipods?. Antarctic Science, 32(6), 496-507.

Monod T. 1926. Tanaidacés, Isopodes et Amphipodes. Expédition Antarctique Belge. Résultats du Voyage de la Belgica en 1897-1899. 54-55.

Moore, J., & Willmer, P. 1997. Convergent evolution in invertebrates. Biological Reviews, 72(1), 1-60.

Myers, A. A., & Lowry, J. K. 2003. A phylogeny and a new classification of the Corophiidea (Amphipoda). Journal of crustacean biology, 23(2), 443-485.

Naumenko, S. A., Logacheva, M. D., Popova, N. V., Klepikova, A. V., Penin, A. A., Bazykin, G. A., Etingova, A.E., Mugue, N.S., Kondrashov, A.S., & Yampolsky, L. Y. 2017. Transcriptome‐based phylogeny of endemic Lake Baikal amphipod species flock: fast speciation accompanied by frequent episodes of positive selection. Molecular ecology, 26(2), 536-553.

Norwegian Polar Institute. 2018. Accessed at https://www.npolar.no/

Núñez-Riboni, I., & Fahrbach, E. 2009. Seasonal variability of the Antarctic Coastal Current and its driving mechanisms in the Weddell Sea. Deep Sea Research Part I: Oceanographic Research Papers, 56(11), 1927-1941.

Nyssen, F., Brey, T., Lepoint, G., Bouquegneau, J. M., De Broyer, C., & Dauby, P. 2002. A stable isotope approach to the eastern Weddell Sea trophic web: focus on benthic amphipods. Polar Biology, 25(4), 280-287.

Nyssen, F. 2005. Role of benthic amphipods in Antarctic trophodynamics: a multidisciplinary study (Doctoral dissertation, Université de Liège).

Ohtsuka, S., Hanamura, Y., Nagasawa, K., Horiguchi, T., & Suzaki, T. 2004. First record of the occurrence of an ellobiopsid Thalassomyces marsupii Kane on a new host of hyperiid amphipod in Japanese waters. Plankton Biology and Ecology, 51(2), 110-112.

O'Regan, M., Williams, C. J., Frey, K. E., & Jakobsson, M. 2011. A synthesis of the long-term paleoclimatic evolution of the Arctic. Oceanography, 24(3), 66-80.

Orsi, A. H., Whitworth III, T., & Nowlin Jr, W. D. 1995. On the meridional extent and fronts of the Antarctic Circumpolar Current. Deep Sea Research Part I: Oceanographic Research Papers, 42(5), 641-673.

Palerud, R., & Vader, W. 1991. Marine Amphipoda Gammaridea in north-east Atlantic and Norwegian Arctic. p. 1-54.

Panhuis, T. M., Butlin, R., Zuk, M., & Tregenza, T. 2001. Sexual selection and speciation. Trends in ecology & evolution, 16(7), 364-371.

Parish T.R. 1983. The influence of the Antarctic peninsula on the wind field over the Western Weddell Sea. Journal of Geophysical Research 88: 2684–2692.

Parkinson, C. L. 2014. Global sea ice coverage from satellite data: Annual cycle and 35-yr trends. Journal of Climate, 27(24), 9377-9382.

Parmesan, C. 2006. Ecological and evolutionary responses to recent climate change. Annu. Rev. Ecol. Evol. Syst., 37, 637-669.

Peel, M. C., Finlayson, B. L., & McMahon, T. A. 2007. Updated world map of the Köppen-Geiger climate classification. Hydrology and earth system sciences, 11(5), 1633-1644.

Peña Othaitz J. & Sorbe J.C. 2020. Eusirus bonnieri sp. nov. (Crustacea: Amphipoda: Eusiridae), a new deep species from the southeastern Bay of Biscay (NE Atlantic Ocean). Zootaxa. 4751(2): 238-256.

Perovich, D. K., Richter‐Menge, J. A., Jones, K. F., & Light, B. 2008. Sunlight, water, and ice: Extreme Arctic sea ice melt during the summer of 2007. Geophysical Research Letters, 35(11).

Petersen, S. V., Dutton, A., & Lohmann, K. C. 2016. End-Cretaceous extinction in Antarctica linked to both Deccan volcanism and meteorite impact via climate change. Nature communications, 7(1), 1-9.

Piepenburg, D. 2005. Recent research on Arctic benthos: common notions need to be revised. Polar Biology, 28(10), 733-755.

Pirlot, J.M. 1934. Les amphipodes de l'expédition du Siboga. Deuxième partie. Les amphipodes gammarides II. Les amphipodes de la mer profonde 2. (Hyperiopsidae, Pardaliscidae, Astyridae nov. fam., Tironidae, Calliopiidae, Paramphithoidae, Amathillopsidae nov. fam., Eusiridae, Gammaridae, Aoridae, Photidae, Ampithoidae, Jassidae). Siboga Expeditie, 33, 167–235.

Platvoet, D., Van Der Velde, G., Dick, J. T., & Li, S. 2009. Flexible omnivory in Dikerogammarus villosus (Sowinsky, 1894)(Amphipoda)-amphipod pilot species project (AMPIS) Report 5. Crustaceana, 703-720.

Pollard, D., DeConto, R. M., & Alley, R. B. 2015. Potential Antarctic Ice Sheet retreat driven by hydrofracturing and ice cliff failure. Earth and Planetary Science Letters, 412, 112–121.

Poore, G. C. B. 2005. Peracarida: monophyly, relationships and evolutionary success. Nauplius, 13(1), 1-27.

Prothero, D. R. 1994. The late Eocene-Oligocene extinctions. Annual Review of Earth and Planetary Sciences, 22, 145-165.

Rabosky, D. L. 2022. Evolutionary time and species diversity in aquatic ecosystems worldwide. Biological Reviews, 97(6), 2090-2105.

Renne, P. R., Deino, A. L., Hilgen, F. J., Kuiper, K. F., Mark, D. F., Mitchell, W. S., Morgan, L. E., Mundil, R., & Smit, J. 2013. Time Scales of Critical Events Around the Cretaceous-Paleogene Boundary. Science, 339(6120), 684–687.

Reusch, T. B. 2014. Climate change in the oceans: evolutionary versus phenotypically plastic responses of marine animals and plants. Evolutionary applications, 7(1), 104-122.

Ridley, M. 2003. Evolution (Third edition). Blackwell Science Limited. pp. 521-643.

Riisgård, H. U., & Schotge, P. 2007. Surface deposit feeding versus filter feeding in the amphipod Corophium volutator. Marine Biology Research, 3(6), 421-427.

Rogers, A. D. 2007. Evolution and biodiversity of Antarctic organisms: a molecular perspective. Philosophical transactions of the royal society B: Biological sciences, 362(1488), 2191-2214.

Rudels, B. 2009. Arctic Ocean Circulation. In Encyclopedia of Ocean Sciences. Elsevier. 211–225.

Rudels, B. 2012. Arctic Ocean circulation and variability–advection and external forcing encounter constraints and local processes. Ocean Science, 8(2), 261-286.

Rundell, R. J., & Price, T. D. 2009. Adaptive radiation, nonadaptive radiation, ecological speciation and nonecological speciation. Trends in Ecology & Evolution, 24(7), 394-399.

Sars, G.O. 1893. An account of the Crustacea of Norway with short descriptions and figures of all the species. Amphipoda. Cammemeyers, Christiana and Copehangen, 1: 415-423.

Saupe, E. E., & Myers, C. E. 2021. Macroevolution. Evolutionary Developmental Biology: A Reference Guide, 149-167.

Schellenberg, A. 1927. Amphipoda des nordischen Plankton. Nordisches Plankton, 20: 708-710.

Schellenberg, A. 1955. Amphipoda. Reports of the Swedish Deep-Sea Expedition 1947–1948, 2 (Zoologii), 2, 181–195.

Schliewen, U. K., Tautz, D., & Pääbo, S. 1994. Sympatric speciation suggested by monophyly of crater lake cichlids. Nature, 368(6472), 629-632.

Schliewen, U., Rassmann, K., Markmann, M., Markert, J., Kocher, T., & Tautz, D. 2001. Genetic and ecological divergence of a monophyletic cichlid species pair under fully sympatric conditions in Lake Ejagham, Cameroon. Molecular Ecology, 10(6), 1471-1488.

Schluter, D. 2000. The ecology of adaptive radiation. OUP Oxford.

Schram, F. R. 1986. Crustacea. Oxford University Press, New York, xii, p. 606.

Seefeldt, M. A., Campana, G. L., Deregibus, D., Quartino, M. L., Abele, D., Tollrian, R., & Held, C. 2017. Different feeding strategies in Antarctic scavenging amphipods and their implications for colonisation success in times of retreating glaciers. Frontiers in Zoology, 14(1), 1-15.

Serreze, M. C., & Barry, R. G. 2005. The Arctic climate system. Cambridge University Press.

Shiklomanov, I. A., Shiklomanov, A. I., Lammers, R. B., Peterson, B. J., & Vorosmarty, C. J. 2000. The dynamics of river water inflow to the Arctic Ocean. In The freshwater budget of the Arctic Ocean. Springer, Dordrecht. 281-296.

Sirenko, B. I. (Ed.). 2001. List of species of free-living invertebrates of Eurasian Arctic seas and adjacent deep waters. Moscow: Russian Academy of Science, Zoological Institute.

Sirenko, B. I. 2009. Main differences in macrobenthos and benthic communities of the Arctic and Antarctic, as illustrated by comparison of the Laptev and Weddell Sea faunas. Russian Journal of Marine Biology, 35(6), 445-453.

Sirenko, B.I.; Clarke, C.; Hopcroft, R.R.; Huettmann, F.; Bluhm, B.A.; Gradinger, R. (eds). 2022. The Arctic Register of Marine Species (ARMS) compiled by the Arctic Ocean Diversity (ArcOD). Accessed at https://www.marinespecies.org/arms on 2022-12-14.

Sluijs, A., Schouten, S., Pagani, M., Woltering, M., Brinkhuis, H., Damsté, J. S. S., Dickens, G. R., Huber, M., Reichart, G. J., Stein, R., Matthiessen, J., Lourens, L. J., Pedentchouk, N., Backman, J., & Moran, K. 2006. Subtropical Arctic Ocean temperatures during the Palaeocene/Eocene thermal maximum. Nature, 441(7093), 610–613.

Sluijs, A., Schouten, S., Donders, T. H., Schoon, P. L., Röhl, U., Reichart, G. J., Sangiorgi, F., Kim, J. H., Sinninghe Damsté, J. S., & Brinkhuis, H. 2009. Warm and wet conditions in the Arctic region during Eocene Thermal Maximum 2. Nature Geoscience, 2(11), 777–780.

Smoot, C. A. 2015. Contemporary mesozooplankton communities of the Beaufort Sea. University of Alaska Fairbanks.

Sobel, J. M., Chen, G. F., Watt, L. R., & Schemske, D. W. 2010. The biology of speciation. Evolution, 64(2), 295-315.

Sokolov, S., & Rintoul, S. R. 2009. Circumpolar structure and distribution of the Antarctic Circumpolar Current fronts: 1. Mean circumpolar paths. Journal of Geophysical Research: Oceans, 114(C11).

Steele, M., Ermold, W., & Zhang, J. 2008. Arctic Ocean surface warming trends over the past 100 years. Geophysical Research Letters, 35(2).

Stephensen, K. 1912. Report on the Malacostraca collected by the 'Tjalfe'-expedition, under the direction of cand. mag. Ad. S. Jensen, especially at W Greenland. Videnskabelige Meddelelser fra Dansk Naturhistorik Forening, 64, 57–134.

Stephensen, K. 1944. Crustacea Malacostraca VIII (Amphipoda IV). Danish Ingolf-Expedition, 3 (13), 1–51.

Storey, B.C. 2005. Encyclopedia of Geology. Antarctic. Elsevier. 132–140.

Stupnikova, A. N., Tarakanov, R. Y., Kulagin, D. N., & Vereshchaka, A. L. 2018. Factors maintaining the identity of mesoplankton communities: cool evidence from the Drake Passage. Hydrobiologia, 809(1), 221-232.

Svardal, H., Salzburger, W., & Malinsky, M. 2021. Genetic variation and hybridization in evolutionary radiations of cichlid fishes. Annual Review of Animal Biosciences, 9, 55-79.

Takeuchi, I., Watanabe, K., Tanimura, A., & Fukuchi, M. 2002. Assemblages of necrophagous animals off Enderby Land, east Antarctica. In Ecological Studies in the Antarctic Sea Ice Zone. Springer, Berlin, Heidelberg. 97-103.

Thatje, S. 2012. Effects of capability for dispersal on the evolution of diversity in Antarctic benthos. pp. 470-482.

Thatje, S., Hillenbrand, C. D., & Larter, R. 2005. On the origin of Antarctic marine benthic community structure. Trends in Ecology & Evolution, 20(10), 534-540.

Thatje, S., Hillenbrand, C. D., Mackensen, A., & Larter, R. 2008. Life hung by a thread: endurance of Antarctic fauna in glacial periods. Ecology, 89(3), 682-692.

Thomas, D. N., Fogg, G. E., Convey, P., Fritsen, C. H., Gili, J. M., Gradinger, R., Laybourn-Parry, J., Reid, K. & Walton, D. W.H. 2008. The biology of polar regions. OUP Oxford.

Thomson G.M. 1880. New species of Crustacea from New Zealand. Annals and Magazine of Natural History, (ser.5) 6 (31): 1-6.

Thornhill, D. J., Mahon, A. R., Norenburg, J. L., & Halanych, K. M. 2008. Open‐ocean barriers to dispersal: A test case with the Antarctic Polar Front and the ribbon worm Parborlasia corrugatus (Nemertea: Lineidae). Molecular ecology, 17(23), 5104-5117.

Thorp, J. H., & Covich, A. P. 2001. Ecology and Classification of North American Freshwater Invertebrates (Second Edition). Academic press.

Thorp, J. H., & Rogers, D. C. (Eds.). 2010. Field guide to freshwater invertebrates of North America. Academic Press.

Thurston, M. 2009. Key to the genera and species of Eusiridae from the Arctic Ocean and Norwegian Sea. Deep-sea workshop. Skibotn: Unpublished.

Timmermans, M. L., & Marshall, J. 2020. Understanding Arctic Ocean circulation: A review of ocean dynamics in a changing climate. Journal of Geophysical Research: Oceans, 125(4), e2018JC014378. 1-35.

Ueshima, R., & Asami, T. 2003. Single-gene speciation by left–right reversal. Nature, 425(6959), 679-679.

Väinölä, R., Witt, J. D. S., Grabowski, M., Bradbury, J. H., Jazdzewski, K., & Sket, B. 2008. Global diversity of amphipods (Amphipoda; Crustacea) in freshwater. Hydrobiologia, 595, 241-255.

Vaughan, D.G., J.C. Comiso, I. Allison, J. Carrasco, G. Kaser, R. Kwok, P. Mote, T. Murray, F. Paul, J. Ren, E. Rignot, O. Solomina, K. Steffen & T. Zhang. 2013: Observations: Cryosphere. In: Climate Change 2013: The Physical Science Basis. Contribution of Working Group I to the Fifth Assessment Report of the Intergovernmental Panel on Climate Change [Stocker, T.F., D. Qin, G.-K. Plattner, M. Tignor, S.K. Allen, J. Boschung, A. Nauels, Y. Xia, V. Bex and P.M. Midgley (eds.)]. Cambridge University Press, Cambridge, United Kingdom and New York, NY, USA. 317-382.

Vavrus, S. J., & Alkama, R. 2021. Future trends of arctic surface wind speeds and their relationship with sea ice in CMIP5 climate model simulations. Climate Dynamics, 1-16.

Verheye ML. 2011. Systématique et diversité génétique des Eusirus de l'Océan Austral (Crustacea, Amphipoda, Eusiridae). Mémoire présenté en vue de l'obtention du diplôme de Master en Biologie des Organismes et Ecologie. Louvainla- Neuve: Université Catholique de Louvain-la-Neuve.

Verheye, M. L., & D'Udekem D'Acoz, C. 2020. Integrative taxonomy of giant crested Eusirus in the Southern Ocean, including the description of a new species (Crustacea: Amphipoda: Eusiridae). Zoological Journal of the Linnean Society, 193(1), 31-77.

Vermeij, G. J. 1991. Anatomy of an invasion: the trans-Arctic interchange. Paleobiology, 17(3), 281-307.

Vignon, É., Roussel, M. L., Gorodetskaya, I. V., Genthon, C., & Berne, A. 2021. Present and future of rainfall in Antarctica. Geophysical Research Letters, 48(8), e2020GL092281. 1-13.

Vincze, M., Bozóki, T., Herein, M., Borcia, I. D., Harlander, U., Horicsányi, A., ... & Pálfy, J. 2021. The Drake Passage opening from an experimental fluid dynamics point of view. Scientific reports, 11(1), 1-11.

Vinogradov, G. M. 2004. Near-bottom and pelagic gammaridean amphipods in the western Indian Ocean. South African Museum. 1-69.

Walker, A. O. 1903. Amphipoda of the 'Southern Cross' Antarctic Expedition. Zoological Journal of the Linnean Society, 29(187), 38-64.

Walker, A. O. 1906. Preliminary descriptions of new species of Amphipoda from the 'Discovery' Antarctic Expedition, 1902-1904. Annals and Magazine of Natural History, (Ser. 7). 17: 452-458.

Wang, Y., Sha, Z., & Ren, X. 2021. A new species of Eusirus (Amphipoda, Amphilochidea, Eusiridae) described from a hydrothermal vent in the Okinawa Trough, North-West Pacific. Crustaceana, 94(11-12), 1395-1405.

Watling, L., & Thiel, M. (Eds.). 2013. Functional morphology and diversity. The Natural History of the Crustacea (Vol. 1). Oxford University Press. pp. 1-515.

Weisshappel, J. B. 2000. Distribution and diversity of the hyperbenthic amphipod family Eusiridae in the different seas around the Greenland-Iceland-Faeroe-Ridge. Sarsia, 85(3), 227-236.

Wiers, S. 2020. The Arctic Ocean Palaeomagnetic Record: A Stratigraphic Approach (Doctoral dissertation, Acta Universitatis Upsaliensis).

Wilce, R. T. 1990. Role of the Arctic Ocean as a bridge between the Atlantic and Pacific Oceans: fact and hypothesis. In Evolutionary biogeography of the marine algae of the North Atlantic. Springer, Berlin, Heidelberg. 323-347.

Woodgate, R. 2013. Arctic Ocean circulation: Going around at the top of the world. Nature Education Knowledge, 4(8), 8.

Worby, A. P., Jeffries, M. O., Weeks, W. F., Morris, K., & Jana, R. 1996. The thickness distribution of sea ice and snow cover during late winter in the Bellingshausen and Amundsen Seas, Antarctica. Journal of Geophysical Research: Oceans, 101(C12), 28441-28455.

Zakšek, V., Delić, T., Fišer, C., Jalžić, B., & Trontelj, P. 2019. Emergence of sympatry in a radiation of subterranean amphipods. Journal of Biogeography, 46(3), 657-669.

Zhao, Q., Pan, L., Ren, Q., & Wang, L. 2015. Identification of genes differentially expressed in swimming crab Portunus trituberculatus response to low temperature. Aquaculture, 442, 21-28.

Chapter 2: Describing novel mitochondrial genomes of Antarctic amphipods*

Louraine Salabao[1,2], Tim Plevoets[3], Bruno Frédérich[1], Gilles Lepoint[4], Marc Kochzius[5] & Isa Schön[2,6]

Admiralty Bay, Antarctica (taken by Louraine Salabao)

*The text of this chapter has been published, with some modifications.

This is an Accepted Manuscript of an article published by Taylor & Francis in *Journal of Mitochondrial DNAPart B on 10 May 2022*, available online:
https://www.tandfonline.com/doi/full/10.1080/23802359.2022.2073837

[1] Laboratory of Evolutionary Ecology, FOCUS, Department of Biology, Ecology & Evolution, University of Liège, B-4000 Liège, Belgium

[2] Centre for Environmental Sciences, Zoology: Toxicology and Biodiversity, Campus Diepenbeek, Agoralaan Gebouw D - B-3590 Diepenbeek

[3] Flanders Research Institute for Agriculture, Fisheries and Food, Unit Animal Sciences - ILVO Marine Research, Jacobsenstraat 1, 8400 Oostende, Belgium

[4] Laboratoire d'Ecologie Trophique et Isotopique (LETIS), FOCUS, Université de Liège, B-4000 Liège, Belgium

[5] Marine Biology, Vrije Universiteit Brussel (VUB),Pleinlaan 2, 1050 Brussels, Belgium

[6] Royal Belgian Institute of Natural Sciences, OD Nature, Freshwater Biology, Vautierstraat 29, 1000 Brussels, Belgium

Abstract

To date, only one mitogenome from an Antarctic amphipod has been published. Here, novel complete mitochondrial genomes (mitogenomes) of two morphospecies are assembled, namely, *Charcotia amundseni* and *Eusirus giganteus*. For the latter species, we have assembled two mitogenomes from different genetic clades of this species. The lengths of *Eusirus* and *Charcotia* mitogenomes range from 15,534 to 15,619 base pairs and their mitogenomes are composed of 13 protein coding genes, 22 transfer RNAs, 2 ribosomal RNAs, and 1 putative control region (CR). Some tRNAs display aberrant structures suggesting that minimalization is also ongoing in amphipod mitogenomes. The novel mitogenomes of the two Antarctic species have features distinguishing them from other amphipod mitogenomes such as a lower AT-richness in the whole mitogenomes and a negative GC- skew in both strands of the protein coding genes. The genetically most variable mitochondrial regions of amphipods are *nad6* and *atp8*, while *cox1* shows low nucleotide diversity among closely and more distantly related species. In comparison to the pancrustacean mitochondrial ground pattern, *E. giganteus* shows a translocation of the *nad1* gene, while *cytb* and *nad6* genes are translocated in *C. amundseni*. Phylogenetic analysis based on mitogenomes illustrates that *Eusirus* and *Charcotia* cluster together with other species belonging to the same amphipod superfamilies. In the absence of reference nuclear genomes, mitogenomes can be useful to develop markers for studying population genetics or evolutionary relationships at higher taxonomic levels.

Introduction

Mitogenome DNA sequence data or parts of mitogenomes have been widely used to reconstruct evolutionary relationships or detect cryptic diversity (Caterino et al., 2000; Tang et al., 2020). For instance, in amphipods, sequencing mitochondrial *cox1* or *cytb* together with nuclear genes (e.g. 18S, 28S, ITS2) has revealed cryptic species of *Hyalella* S.I. Smith, 1874 (Witt et al., 2006), *Caprella penantis* Leach, 1814 (Pilar Cabezas et al., 2013), *Gammarus fossarum* Koch, 1836 (Grabowski et al., 2017) and some *Eusirus* Krøyer, 1845 species (Baird et al., 2011). Molecular data from 13 protein coding genes of *Alicella gigantea* Chevreux, 1899 (Li et al., 2019b), Baikalian amphipods (Romanova et al., 2016), *Gammarus roeselii* Gervais, 1835 (Cormier et al., 2018), *Halice* sp. Boeck, 1871 (Li et al., 2019a), Metacrangonyctidae

Boutin & Messouli, 1988 (Bauzà-Ribot et al., 2012), and from all mitochondrial genes (protein coding genes, rRNA, and tRNA) of *Gammarus pisinnus* Hou, Li & Li, 2014 and *Gammarus lacustris* G.O. Sars, 1863 (Sun et al., 2020) have been used to reconstruct evolutionary relationships. The broad application of molecular data from mitogenomes can be explained by several advantages, which the mitogenome has compared to the nuclear genome. These include its simpler structure, conserved gene content and limited size (Boore, 1999; Li et al., 2019b; Krebes and Bastrop, 2012) facilitating sequencing of mitogenomes from those species for which reference nuclear genomes are not yet available. The uniparental, usually maternal inheritance of mitogenomes furthermore simplifies analyses because recombination is either totally absent or very rare (Barr et al., 2005; Lin and Danforth, 2004). The relatively high evolutionary rate of mitogenomes generating relative large genetic differences makes mitogenomic DNA sequence data furthermore suitable for studies at the genus or species level investigating population genetic or and phylogeographic patterns (Ballard and Whitlock, 2004; Krebes and Bastrop, 2012; Tang et al., 2020; Li et al., 2019a). The inclusion of whole mitogenomes has resulted in phylogenies with better statistical supports (Haran et al., 2013; López-López and Vogler, 2017) and clearer phylogeographic patterns (Keis et al., 2013). Moreover, despite the highly conserved gene content of the mitogenome, gene order has been found to be variable and can provide additional data for reconstructing phylogenetic relationships and evolutionary histories (Cormier et al., 2018; Krebes and Bastrop, 2012; Zhang et al., 2020).

Amphipods are widely distributed crustaceans inhabiting a range of different habitats (Väinölä et al., 2008; Li et al., 2019b). In Antarctica, amphipods are among the most diverse components of the benthic community (Gallardo, 1987) and show high levels of endemism (Knox and Lowry, 1977) making them ideal model organisms to study evolutionary patterns and divergences based on mitogenomes. Currently, there is only one published complete mitogenome of an Antarctic amphipod, namely of *Gondogeneia antarctica* Chevreux, 1905 (Shin et al., 2012), and no mitogenomes are yet available for abundant amphipods of the genera *Eusirus* Krøyer, 1845 and *Charcotia* Chevreux, 1905.

In this paper, we have assembled and analyzed complete mitogenomes of three Antarctic amphipods from two morphospecies (*Charcotia amundseni* d'Udekem d'Acoz, Schön and Robert, 2018 and *Eusirus giganteus* Lörz and Brandt, 2002) and two genetic clades of the latter

species. Our aims are to (1) provide full mitogenomic data of selected amphipod species for future research and (2) compare gene content and order with published amphipod mitogenomes to unravel shared and unique patterns of mitogenome evolution in amphipods.

Materials and methods

Sample collection

Specimens of two species of Antarctic amphipods, *Charcotia amundseni* d'Udekem d'Acoz, Schön and Robert, 2018 and two genetic clades of *Eusirus giganteus* Andres, Lörz and Brandt, 2002 (G1 and G2; which might resemble different genetic species (Verheye and D'Udekem D'Acoz, 2021) have been collected during different Antarctic expeditions (Table 1) and are curated in the collections of the Royal Belgian Institute of Natural Sciences, Brussels, Belgium.

Table 1. Sampling details of specimens analysed in this study, including the date of sample, expedition, locality, geographical coordinates, voucher ID provided by Royal Belgian Institute of Natural Sciences (RBINS), and gear used during sampling. *Eusirus* cf. *giganteus* (G1) and *E.* cf. *giganteus* (G2) are taxonomically undescribed putative species that belong to *E. giganteus* complexes as verified genetically by Baird et al. (2011) and Verheye and D'Udekem D'Acoz (2021).

Species	Date collected	Expedition	Locality, coordinates	Voucher ID	Gear
Eusirus cf. *giganteus (G1)*	23/02/2013	PS81, ANT-XXIX-3	Bransfield Strait, 62° 43.73' S 57° 29.04' W	INV. 122797 spec. C	Agassiz trawl
Eusirus cf. *giganteus (G2)*	15/01/2008	CEAMARC	Adélie Coast, 66°10'14.3"S 139°21'11.3"E	MNHN-IU-2019-3365	Beam trawl
Charcotia amundseni	23/12/2008	BELARE 08-09	Crown Bay, 70°S 23°E	INV.180000	Baited trap

Eusirus amphipods belong to the superfamily Eusiroidea Stebbing, 1888. *Eusirus* cf. *giganteus* has previously been confused with *Eusirus perdentatus* Chevreux, 1912 due to small morphological differences (Andres et al., 2002). The genetic study of Baird et al. (2011) reveals cryptic diversity of *Eusirus giganteus* including the so-called clades G1- G4, and the existence of a species complex is supported by Verheye and D'Udekem D'Acoz (2021). The same authors report that potential *Eusirus giganteus* species that still need to be formally described showed at least minor morphological differences and different color morphs but that a thorough morphological analysis of the putative genetic species is still required. Given the possibility of

multiple cryptic species, we follow here the suggestion of Greco et al. (2021) to use the name *Eusirus* cf. *giganteus* in our study. Our other target species, *Charcotia amundseni,* belongs to the superfamily Lysianassoidea Dana, 1849. The genus *Charcotia* has formerly been known as *Waldeckia* (Chevreux, 1906) but recently has undergone a change in nomenclature (D'Udekem D'Acoz et al., 2018) which we follow here.

Mitochondrial genome sequencing, assembly, annotation and analyses

DNA has been extracted from a pleopod of each specimen using the DNeasy *Blood* & *Tissue Kit (Qiagen,* Germany*) for both Eusirus cf. giganteus clades and the* Qiamp DNA Minikit (*Qiagen*, Germany) for *Charcotia amundseni* following the manufacturer's protocol. DNA concentration and quality have been checked with a Nanodrop ND-1000 Spectrophotometer (ThermoFisher Scientific, USA) and a Qubit 2.0 fluorometer (Life Technologies, USA).

A low coverage skimming sequencing approach has been applied at the Genomics Core at the KU Leuven (Leuven, Belgium) using an Illumina HiSeq2500 sequencing platform in the 2x125 bp mode. Samples were indexed separately as unique libraries. Reads have been quality-checked using FASTQC (Andrews, 2010) and pre-processed with Geneious Prime 2019 v1.8.0 (https://www.geneious.com) by merging paired reads, removing duplicates and trimming of low-quality ends using the BBDuk trimmer in Geneious with the minimum quality set to 20. These pre-processed reads have then been used for *de novo* assemblies in MITObim v1.9.1 (Hahn et al., 2013) with the MIRA 4.0.2 (Chevreux et al., 1999) assembler with default settings (kmer size=31) and an iteration limit of 100. The *Onisimus nanseni* G.O. Sars, 1900 mitogenome (GenBank accession number FJ555185.1) which belongs to the same superfamily as *Charcotia* and a partial 16S to COI sequence of *Eusirus perdentatus* have been used as seed references. The longest resulting contigs from the *de novo* assembly have been imported into Geneious and further assembled with the "map to reference" approach with medium-low sensitivity and 50 iterations. Identity of the resulting consensus sequences have been verified with BLAST searches (Altschul et al., 1997). Automatic annotation has subsequently been conducted with the MITOS web server, versions 1 and 2 (Bernt et al., 2013). The identity of the *rrnL* region of both *Eusirus* species has been confirmed by BLAST searches only, since it has not been annotated by MITOS. The resulting annotations have been viewed and gene boundaries manually corrected in Geneious. The boundaries of the 13 protein coding genes

and 2 rRNA genes have been identified by comparing alignments of the novel assemblies with mitochondrial genes of other amphipod species. Protein coding genes boundaries have been further corrected by avoiding any overlap with the subsequent tRNA gene and by noticing any partial stop codons (T or TA). Such partial stop codons are atypical features of mitochondrial protein coding genes (Cameron, 2014). Transfer RNA (tRNA) genes and their secondary structures have been predicted with MitFI (Jühling et al., 2012) in the MITOS pipeline and further verified with ARWEN 1.2.3 (Laslett and Canbäck, 2008). Potential control regions (CRs) have been identified from their typical features such as high AT content, poly-T stretches and hairpin structures (Zhang and Hewitt, 1997).

Gene orders of the novel mitogenome assemblies were compared to the putative pancrustacean ground pattern which is derived from both Crustacea and Hexapoda (often referred to as pancrustacea) as they share the same ground pattern in terms of their mitochondrial gene order (Kilpert and Podsiadlowski, 2006; Boore et al., 1998). Possible gene rearrangements have been analyzed with the CREx web service (Bernt et al., 2007). CREx utilizes a strong common interval tree to heuristically deduce the plausible rearrangement scenarios to change one gene order to another (Bernt et al., 2007). AT and GC-skew have been calculated using the formulas of Perna and Kocher (1995): AT skew = [A - T]/[A + T] and GC skew = [G - C]/[G + C]. Only other amphipod species with complete and published mitogenomes have been analysed for their AT and GC skew (Supplementary table 1). Nucleotide diversity (π) has been computed for each protein coding gene with DnaSP v6.12.03 (Rozas et al., 2017).

To verify the phylogenetic position of the studied species, the three novel and assembled mitogenomes were supplemented with data from other amphipod species for phylogenetic reconstructions. Published amino acid sequences of 13 protein coding genes were obtained from GenBank and aligned separately for each gene using MAFFT v7.0 online (Katoh et al., 2019), together with the amino acid sequences of the current study. The resulting alignments were concatenated with Geneious Prime 2019 v1.8.0 (https://www.geneious.com) and trimmed with Bioedit v7.2.5 (Hall, 1999) with additional checking by eye. The MtArt+G+F was chosen as the best fitting model of molecular evolution as identified with ModelGenerator v0.85 (Keane et al., 2006) using four discrete categories for gamma distribution. Phylogenetic analyses based on maximum likelihood methods were carried out using PhyML v3.0 (Guindon and Gascuel, 2003) with 1000 bootstrap replications. Bayesian inference was conducted with

MrBayes v3.2.7 (Ronquist and Huelsenbeck, 2003) with 1 million generations, tree sampling every 1000th generation and 10% of the initial trees being discarded as burn-in.

Results

Mitogenome organization

The total length of the obtained complete mitochondrial genomes of *Eusirus* cf. *giganteus* (G1), *Eusirus* cf. *giganteus* (G2), and *Charcotia amundseni* is 15,558, 15,534, and 15,619 bp, respectively (Genbank accession nos. OK489458, OK489459, OK489457, respectively) which is within the range of complete mitogenomes from other amphipods (13,517-18,424 bp) (Table 2). The three newly assembled mitogenomes are each composed of 13 protein coding genes, 22 tRNAs and 2 rRNAs. For *E.* cf. *giganteus*, 23 genes are encoded on the positive (+) strand and 14 on the negative (–) strand while 17 genes are encoded on the + strand and 20 on the – strand in *C. amundseni* (Figure 1a and b, Supplementary table 2). A putative control region (CR) has also been identified in all three mitogenomes and is located between *trnS2* and *rrnL* in *Eusirus* and between *trnF* and *nad5* in *C. amundseni*. The mitogenome also contains 20 intergenic regions for *E.* cf. *giganteus* and 18 intergenic regions for *C. amundseni*. The whole mitogenomes of the two species show AT-richness of 61.9% for *E.* cf. *giganteus* and 68.7% for *C. amundseni*, respectively, which contributes to the positive AT skew (0.008 to 0.092) and negative GC skew (-0.317 to -0.201) values observed in the three mitogenomes (Table 2). A relatively high AT content is also observed in the complete mitogenomes of other amphipod species varying from 61.09 to 77% (Table 2).

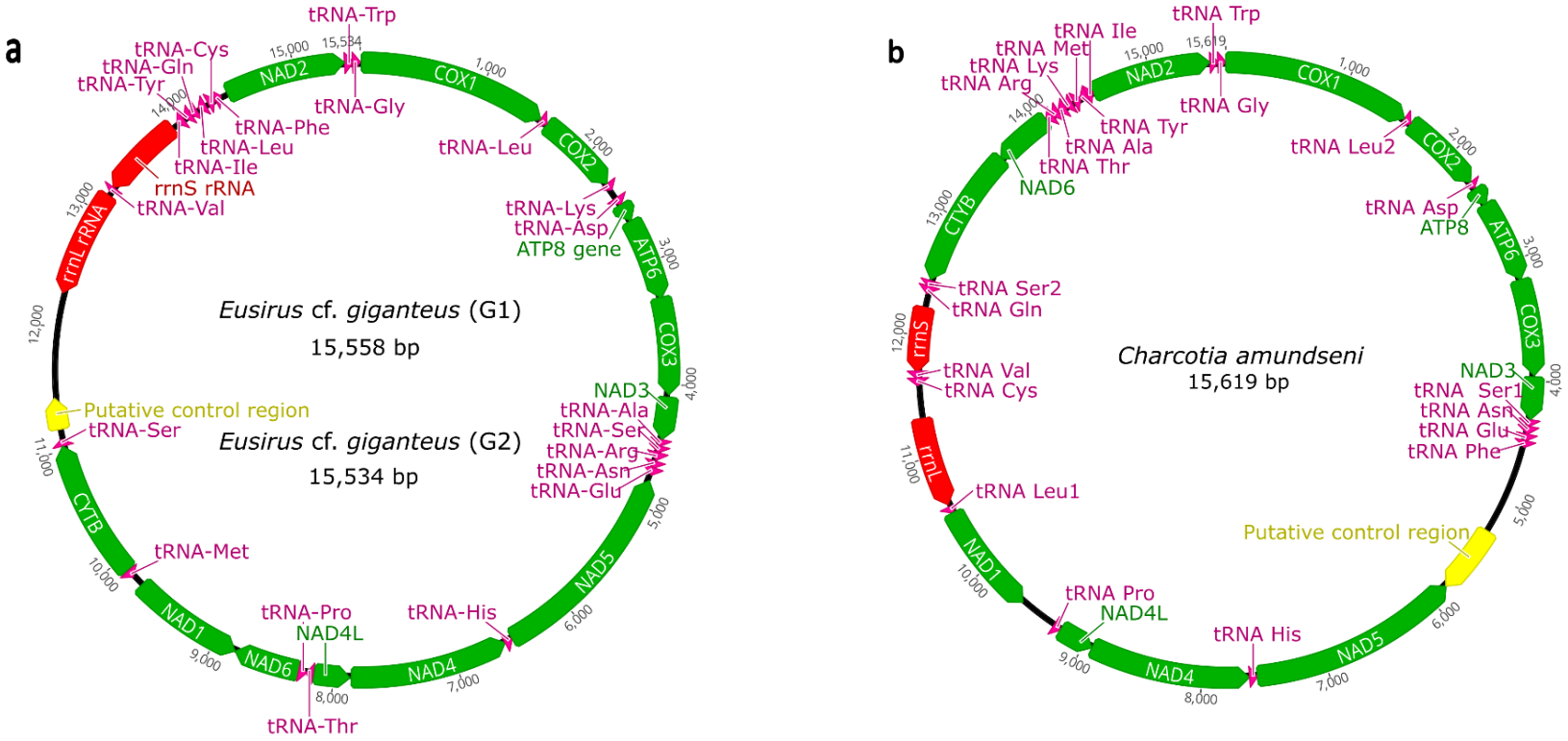

Figure 1. Structural organisation of the complete mitochondrial genome of **a** *Eusirus* cf. *giganteus* (G1) and *Eusirus* cf. *giganteus* (G2) **b** *Charcotia amundseni*. Protein coding genes are indicated in green, ribosomal RNAs (rRNAs) in red, transfer RNAs (tRNAs) in pink, and the putative control region (CR) in yellow. Direction of transcription is indicated by the arrowheads.

Table 2. Gene lengths, AT content, and AT and GC skews of *E.* cf. *giganteus* (G1), *E.* cf. *giganteus* (G2) and *C. amundseni* and 40 other amphipod species with complete, published mitogenomes (for details of the analysed species, see supplementary table 1). Target species of the current study are indicated in bold.

		Whole mitogenome			Protein-coding genes			tRNA genes			rRNA genes		
Species	**Length**	**A+T%**	**AT skew**	**GC skew**	**A+T%**	**AT skew**	**GC skew**	**A+T%**	**AT skew**	**GC skew**	**A+T%**	**AT skew**	**GC skew**
***Eusirus* cf. *giganteus* (G1)**	**15,558**	**61.90**	**0.008**	**-0.201**	**59.60**	**-0.003**	**-0.207**	**66.20**	**0.063**	**-0.096**	**69.70**	**0.020**	**-0.260**
***Eusirus* cf. *giganteus* (G2)**	**15,534**	**61.90**	**0.012**	**-0.201**	**59.60**	**-0.007**	**-0.208**	**66.20**	**0.066**	**-0.098**	**69.70**	**0.021**	**-0.261**
Charcotia amundseni	**15,619**	**68.70**	**0.092**	**-0.317**	**67.30**	**0.115**	**-0.312**	**69.90**	**0.058**	**-0.220**	**70.80**	**0.057**	**-0.310**
Alicella gigantea	16,851	68.44	0.071	-0.301	66.12	-0.122	0.007	65.52	0.027	0.106	69.59	-0.135	0.335
Ampithoe lacertosa	14,607	77.00	0.066	-0.153	72.10	0.071	-0.157	75.55	0.092	-0.071	80.17	0.073	-0.216
Bahadzia jaraguensis	14,657	69.67	0.037	-0.431	68.48	0.040	-0.454	71.85	0.018	-0.184	72.43	0.076	-0.477
Brachyuropus grewingkii	17,118	62.24	0.003	-0.307	60.20	-0.015	-0.295	65.41	0.025	-0.157	66.36	0.074	-0.383
Caprella mutica	15,427	68.00	-0.020	-0.170	67.70	-0.140	-0.110	72.00	0.010	-0.112	72.40	-0.050	-0.170
Caprella scaura	15,079	66.43	-0.015	-0.134	64.24	-0.028	-0.136	71.09	0.025	-0.139	71.77	0.024	-0.149
Epimeria cornigera	14,391	68.11	0.034	-0.357	66.92	0.039	-0.373	69.72	0.031	-0.140	73.54	0.019	-0.384
Eulimnogammarus cyaneus	14,370	67.59	-0.019	-0.251	66.78	-0.040	-0.246	66.69	0.017	-0.132	71.81	0.095	-0.377
Eulimnogammarus verrucosus	15,314	68.96	-0.007	-0.238	66.63	-0.023	-0.249	67.42	0.022	-0.090	69.54	0.072	-0.348
Eulimnogammarus vittatus	15,534	67.42	-0.014	-0.222	65.59	-0.033	-0.226	67.30	0.013	-0.122	71.30	0.072	-0.341
Eurythenes magellanicus	14,988	61.15	0.044	-0.388	59.26	0.040	-0.399	64.70	0.042	-0.202	64.65	0.074	-0.443
Eurythenes maldoror	14,976	61.53	0.067	-0.430	59.81	-0.152	-0.065	64.65	0.042	0.077	64.86	-0.073	0.459
Gammarus duebeni	15,651	64.00	-0.016	-0.223	61.00	-0.038	-0.229	64.00	0.031	-0.121	65.00	0.037	-0.345
Gammarus fossarum	15,989	65.14	0.018	-0.261	62.56	0.011	-0.268	66.28	0.027	-0.175	72.46	0.022	-0.269
Gammarus lacustris	15,333	64.30	0.014	-0.263	62.09	-0.027	-0.272	65.20	0.021	-0.132	68.50	0.013	-0.305
Gammarus pisinnus	15,907	70.00	-0.068	-0.310	68.01	-0.090	-0.332	68.88	0.023	-0.120	73.55	-0.051	-0.322
Gammarus roeselii	16,073	66.80	0.016	-0.259	64.38	0.012	-0.266	65.82	0.048	-0.151	69.93	0.087	-0.362
Gmelinoides fasciatus	18,114	65.87	-0.027	-0.223	63.29	-0.020	-0.296	66.47	0.058	-0.137	69.00	0.031	-0.332
Gondogeneia antarctica	18,424	70.10	-0.006	-0.290	67.00	-0.016	-0.314	69.65	0.021	-0.116	70.25	-0.007	-0.261
Grandidierella fasciata	14,656	67.56	0.058	-0.189	65.32	0.060	-0.179	71.26	0.169	-0.184	74.88	0.070	-0.329
Grandidierella japonica	14,930	66.91	0.097	-0.189	64.94	0.098	-0.184	70.73	0.088	-0.161	72.30	0.136	-0.263
Grandidierella osakaensis	14,658	70.90	0.037	-0.182	69.30	0.042	-0.172	75.75	0.057	-0.093	75.79	0.029	-0.325
Grandidierella rubroantennata	14,469	74.14	0.056	-0.232	73.28	0.059	-0.234	76.25	0.065	-0.102	77.00	0.062	-0.344
Haploginglymus sp.	15,000	68.53	0.041	-0.396	66.61	0.037	-0.413	71.06	0.021	-0.212	74.26	0.096	-0.450
Hyalella azteca	15,991	61.09	-0.066	0.052	59.59	-0.102	0.086	65.83	0.013	0.049	64.33	0.053	0.041
Metacrangonyx boveei	15,012	72.59	-0.009	0.005	70.28	-0.017	0.036	75.58	0.036	0.022	75.27	0.024	-0.252
Metacrangonyx longipes	14,113	76.03	-0.020	-0.040	75.33	-0.170	0.080	78.01	0.050	0.180	78.70	0.028	-0.271
Metacrangonyx nicoleae tamri	13,517	74.02	-0.049	0.111	73.92	-0.083	0.163	76.75	0.004	0.043	78.25	0.015	-0.139
Metacrangonyx repens	14,355	76.88	-0.025	-0.014	76.00	-0.038	0.020	78.91	0.007	-0.007	79.22	0.022	-0.280

Metacrangonyx spinicaudatus	15,037	74.79	0.010	-0.139	73.25	0.010	-0.126	78.17	0.031	-0.056	77.42	0.013	-0.352
Onisimus nanseni	14,734	70.30	-0.004	-0.198	68.60	-0.011	-0.189	73.07	0.004	-0.112	76.25	0.009	-0.286
Pallaseopsis kesslerii	15,759	63.10	0.010	-0.182	61.13	-0.018	-0.184	67.52	0.063	-0.069	64.87	0.071	-0.241
Platorchestia japonica	14,780	72.58	0.015	-0.237	70.61	0.002	-0.237	76.68	0.055	-0.131	75.40	0.069	-0.338
Platorchestia parapacifica	14,787	74.80	0.011	-0.253	73.18	-0.002	-0.253	76.69	0.035	-0.110	77.19	0.066	-0.330
Pleonexes koreana	14,645	73.20	0.071	-0.206	70.20	0.078	-0.221	74.70	0.083	-0.044	79.00	0.072	-0.263
Pseudocrangonyx daejeonensis	15,069	68.00	0.003	-0.350	66.31	-0.006	-0.350	69.37	0.038	-0.223	73.27	0.034	-0.441
Pseudoniphargus daviui	15,157	68.70	-0.002	-0.314	66.40	-0.024	-0.317	70.40	0.015	-0.168	73.80	0.076	-0.433
Stygobromus indentatus	14,638	69.00	0.016	-0.270	67.40	0.007	-0.275	71.60	-0.009	-0.173	74.50	0.081	-0.356
Stygobromus tenuis potomacus	14,915	69.00	0.020	-0.275	67.20	0.012	-0.284	71.00	0.008	-0.156	73.20	0.095	-0.383
Trinorchestia longiramus	15,401	71.20	0.039	-0.277	68.60	0.030	-0.291	74.00	0.067	-0.112	73.90	0.101	-0.325

Gene order and rearrangements

A translocation of *nad1* gene in *E.* cf. *giganteus* is observed while *cytb* and *nad6* are translocated in *C. amundseni* as compared to the pancrustacean ground pattern (Figure 2). We furthermore also find shifts in the position of tRNAs and the control region in *E.* cf. *giganteus* and *C. amundseni* as compared to the pancrustacean ground pattern (Figure 2). While also *trnG* has been translocated in the three species investigated here, we find other tRNA gene strings consisting of *trnA*, *trnS1*, *trnR*, *trnN*, and *trnE* for *E.* cf. *giganteus* and *trnS1*, *trnN*, *trnE*, and *trnF* for *C. amunseni* (Figure 2). Similar with the pancrustacean ground pattern, the *trnV* is located between the *rrnL* and *rrnA* genes in *E.* cf. *giganteus* while *trnC* and *trnV* are inserted between these genes in *C. amundseni* (Figure 2).

Results of the CREx analyses indicate that *E.* cf. *giganteus* and *C. amundseni* have undergone multiple transpositions and rearrangements relative to the pancrustacean ground pattern (Supplementary figures 1a and b).

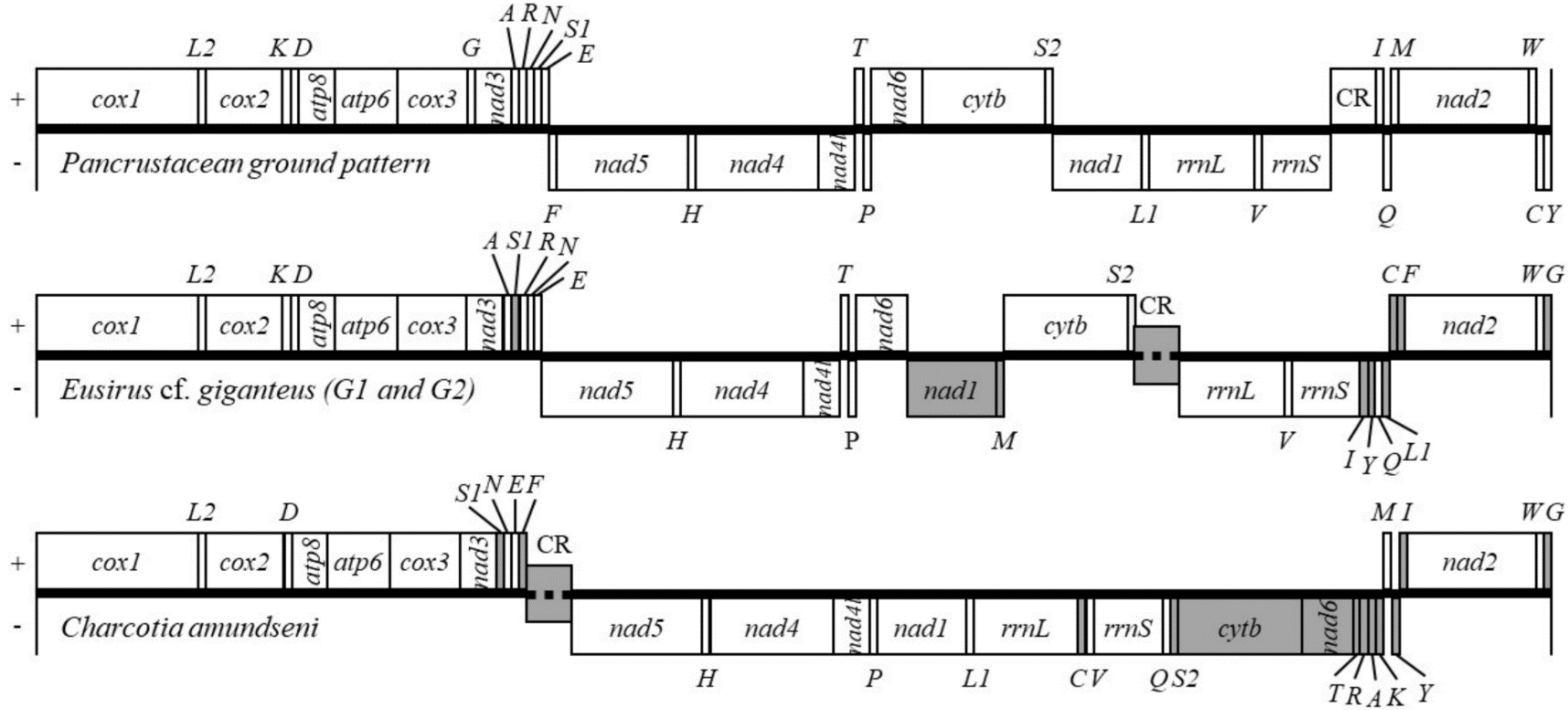

Figure 2. Organization of mitochondrial genomes of the three Antarctic amphipod species in this study in comparison to the putative pancrustacean ground pattern. Grey-colored genes indicate changes of gene order relative to the putative pancrustacean ground pattern. Genes on the (+) strand are found above the line while genes on the (-) strand are found below the line. tRNA genes are labeled using their single-letter amino acid code: G - Glycine, P - Proline, A - Alanine, V - Valine, L1 - Leucine1, L2 - Leucine2 , I - Isoleucine, M - Methionine, C - Cysteine, F - Phenylalanine, Y - Tyrosine, W - Tryptophan, H - Histidine, K - Lysine, R - Arginine, Q - Glutamine, N - Asparagine, E - Glutamic Acid, D - Aspartic Acid, S1 - Serine 1, S2 - Serine2, T - Threonine.

Protein coding genes

The most frequent start codon in *E.* cf. *giganteus* and *C. amundseni* is ATG (Supplementary table 2). Defining the protein coding gene boundaries following a tRNA results in a few partial or incomplete stop codons (T or TA). The AT content of the protein coding genes of the three amphipod mitogenomes is estimated as 59.6% for *E.* cf. *giganteus* (G1 and G2) and 67.3% for *C. amundseni* (Table 2). Mitochondrial genomes of the two species in this study have negative GC skew values in the protein coding genes encoded on both strands (Table 3).

Table 3. AT and GC skews of the protein-coding genes of *E.* cf. *giganteus* (G1), *E.* cf. *giganteus* (G2) and *C. amundseni* encoded in the positive and negative strands

Species	+		-	
	AT skew	**GC skew**	**AT skew**	**GC skew**
Eusirus cf. *giganteus* (G1)	-0.144	-0.143	0.220	-0.315
Eusirus cf. *giganteus* (G2)	-0.147	-0.144	0.215	-0.315
Charcotia amundseni	-0.052	-0.244	0.253	-0.38

The highest AT content is found in the third codon position of *C. amundseni* and the second codon position of *E.* cf. *giganteus* while the lowest AT content is observed in the first codon position in all three species. (Table 4).

Table 4. AT content (%) in three codon positions of the mitochondrial protein coding genes in *E.* cf. *giganteus* (G1 and G2) and *C. amundseni*

Species	First codon position	Second codon position	Third codon position
Eusirus cf. *giganteus* (G1)	57.91	61.18	59.88
Eusirus cf. *giganteus* (G2)	57.89	61.12	59.87
Charcotia amundseni	64.08	65.19	72.61

Ribosomal RNA

The two ribosomal RNA (*rrnS* and *rrnL*) genes in the three mitogenomes are located on the negative (-) strand. In the two *Eusirus* species, the length of both RNAs is 681 bp and 871 bp, respectively (Supplementary table 2). Unlike in *E.* cf. *giganteus*, the two mitochondrial rRNAs of *C. amundseni* are shorter (529 bp and 739 bp) (Supplementary table 2). The mitochondrial rRNA genes of the two amphipod species in this study also show a high AT content with 69.7% for *E.* cf. *giganteus* (G1 and G2) and 70.8% for *C. amundseni*.

Transfer RNA

In the three mitogenomes of this study, 22 tRNAs are present with a length ranging from 52 to 67 base pairs (Supplementary table 2). The AT content of tRNAs of *E.* cf. *giganteus* is 66.2% and 69.9% for *C. amundseni* (Table 2). In *E.* cf. *giganteus*, 14 tRNAs are encoded in the + strand and 8 in the - strand. In *C. amundseni* 10 tRNAs are encoded in the + and 12 in the - strand. Typical clover leaf secondary structures are observed in most predicted tRNAs although some tRNAs show wobble base pairs, atypical pairing or the DHU and TΨC arm are missing (Supplementary figure 2a-2c). More specifically, the DHU arm is missing in *trnS1*, *trnS2* and *trnV* of *E.* cf. *giganteus* (Supplementary figures 2a and b) and *trnS1*, *trnS2*, and *trnI* of *C. amundseni* (Supplementary figure 2c). We also find that the TΨC loop is absent in *trnK*, *trnD*, *trnN*, *trnM*, *trnS2*, *trnI* and *trnQ* of *E.* cf. *giganteus* (Supplementary figures 2a and b) and in *trnD*, *trnH*, *trnL1*, *trnC*, *trnV*, *trnQ*, *trnK*, *trnM* of *C. amundseni* (Supplementary figure 2c).

Nucleotide diversity

When estimating nucleotide diversity (π) between the two *Eusirus* genetic clades, we observe high values for *nad6* (0.013), *nad5* (0.012), and *nad1* (0.011) (Figure 3a) and low ones for *nad4* (0.002), *nad3* (0.003), *nad2* (0.004), and *cox1* (0.005) with *nad4* (0.002) being the least variable. We also find high variability in *nad6* (0.569), *atp8* (0.566), and nad2 (0.515) between *C. amundseni* and *E.* cf. *giganteus* (G1) and low variability in *cox1* (0.279), *cytb* (0.328), and *cox3* (0.342) (Figure 3b). Moreover, between *C. amundseni* and *E.* cf. *giganteus* (G2), high variability is observed in *nad6* (0.567), *atp8* (0.560), and *nad2* (0.515) while the lowest variability is found in *cox1* (0.28), *cytb* (0.327), and *cox3* (0.343) (Figure 3b).

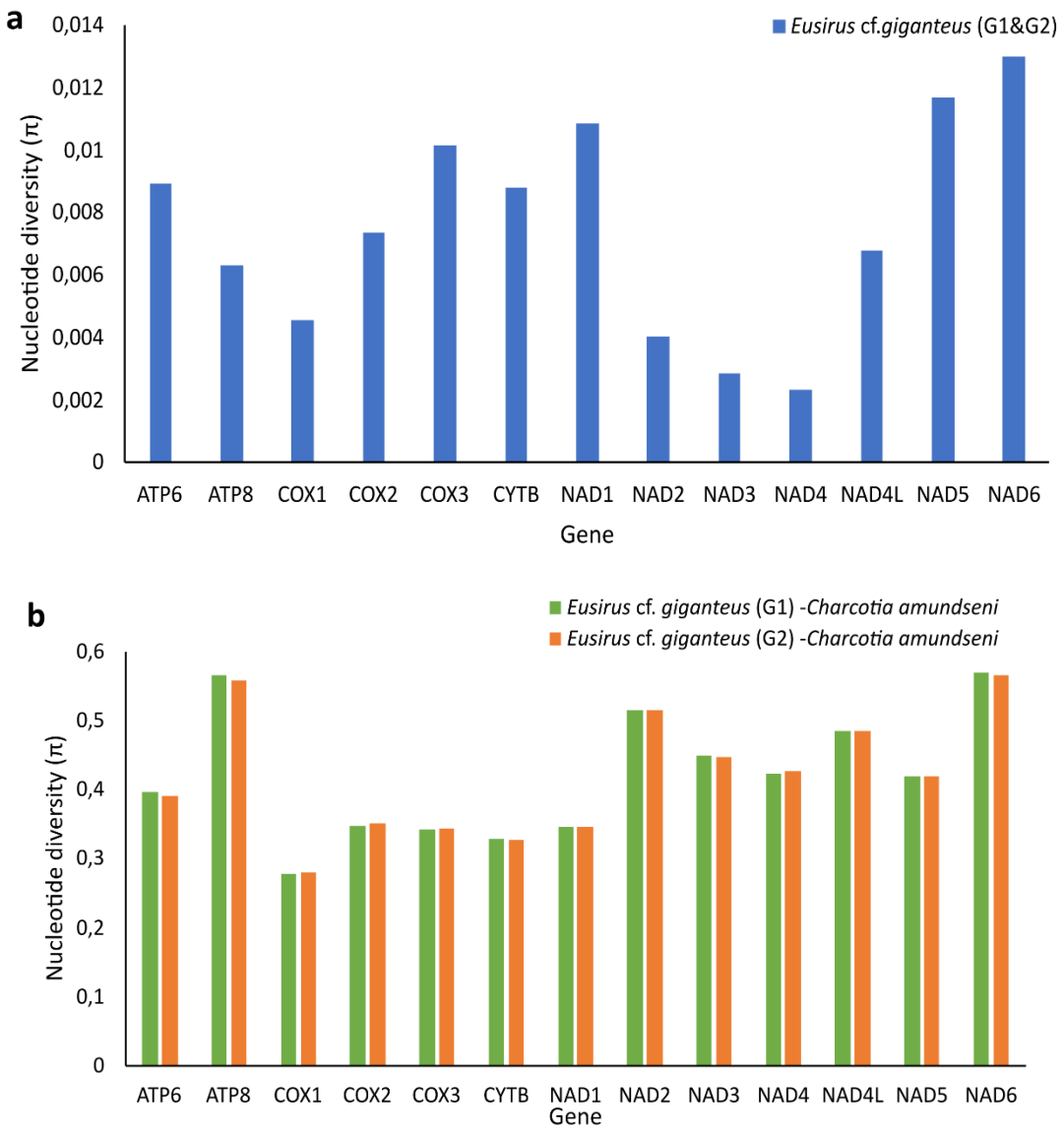

Figure 3. Nucleotide diversity (π) for the mitochondrial protein coding genes estimated **a** between *Eusirus* cf. *giganteus* G1 and G2; **b** between *Charcotia amundseni* and *Eusirus* cf. *giganteus* G1 (green) and *Charcotia amundseni* and *Eusirus* cf. *giganteus* G2 (orange).

Phylogenetic analysis

Phylogenetic analysis revealed that the phylogenetic grouping follows the superfamily identity and fall under different family groups (Figure 4). The two genetic clades of *Eusirus* cf. *giganteus* G1 and G2 under family Eusiridae, cluster together. They belong to the superfamily Eusiroidea and are found to be closely related to both *Epimeria frankei* Beermann and Raupach, 2018 in Beerman, Westbury, Hofreiter, Hilgers, Deister, Neumann and Raupach, 2018 and *Epimeria cornigera* Fabricius, 1779 (family Epimeriidae Boeck, 1871) from the Iphimedioidea Boeck, 1871 superfamily. Similarly, *Charcotia amundseni* from family Lysianassidae Dana, 1849 is

clustering together with *Eurythenes magellanicus* H. Milne Edwards, 1848 and *Eurythenes maldoror* d'Udekem d'Acoz and Havermans, 2015 (family Eurytheneidae Stoddart and Lowry, 2004), *Hirondellea gigas* Birstein and Vinogradov, 1955 (family Hirondelleidae Lowry and Stoddart, 2010), and *Onisimus nanseni* G.O. Sars, 1900 (family Uristidae Hurley, 1963) and all belonging to the superfamily Lysianassoidea.

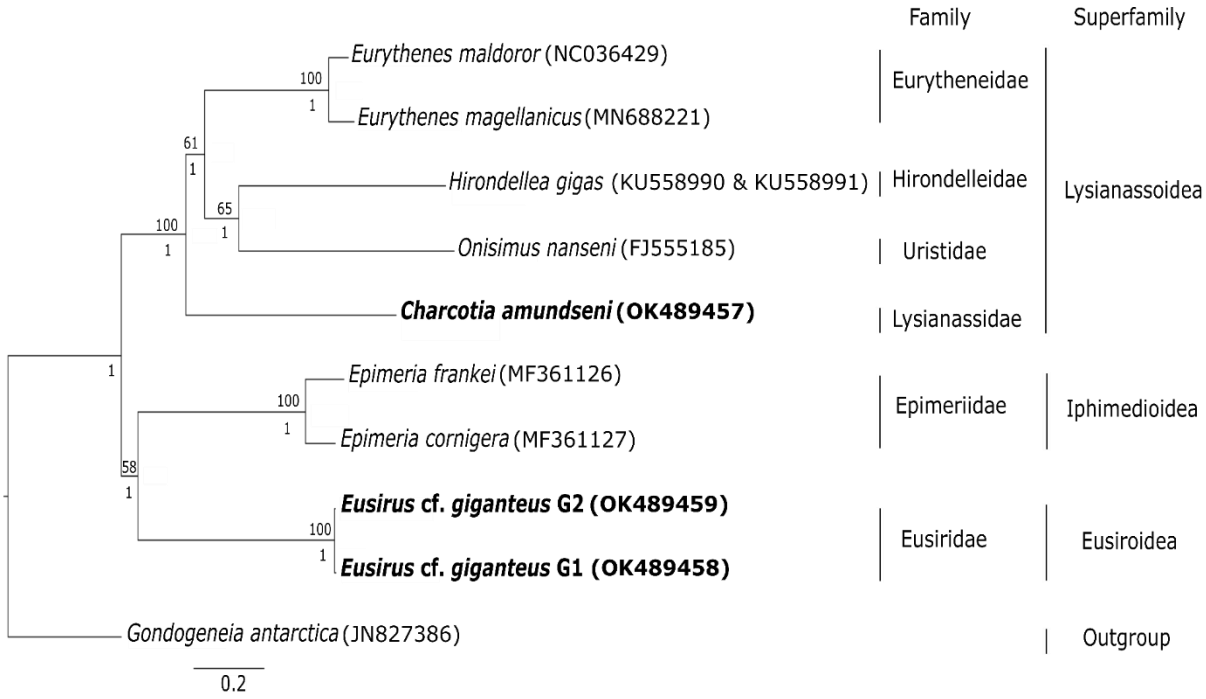

Figure 4. Phylogenetic tree based on the concatenated 13 protein-coding genes amino acid alignment using maximum likelihood and Bayesian methods. Only bootstrap values of ≥50 (above the nodes) and posterior probabilities >0.80 (below the nodes) are shown. Scale bar corresponds to the number of substitutions per site. Target species of the current study are indicated in bold. The Genbank accession numbers for the mitochondrial genomes are shown in the parenthesis.

Discussion

In the current study, we have assembled and annotated novel complete mitogenomes from two Antarctic amphipod species with a low coverage skimming sequencing approach. We have obtained very low percentages of ambiguities (<0.01%) illustrating that this cost efficient approach is very successful. Besides our study, only two complete mitogenomes from amphipods of the polar regions are currently available, namely from *Gondogeneia antarctica* Chevreux, 1905 from Antarctica (Shin et al., 2012) and *Onisimus nanseni* G.O. Sars, 1900 from the Arctic (Ki et al., 2010). Our study thus provides important novel genomic data for further research and the first complete mitogenomes of the widely spread amphipod genera *Eusirus*

and *Charcotia*. Our comparisons of mitogenomes between two genetic clades, possibly resembling two different genetic species of *E.* cf. *giganteus* illustrate that mitogenomic features such as length, gene order, AT content and tRNA structure are similar at the intraspecific level (Table 2, Figure 2, Figure 2, Table 4, Supplementary figure 2a and b).

All three newly obtained mitogenomes are with 15,534 and 15,619 bp at the middle range of reported lengths of published amphipod mitogenomes (14,113 bp to 18,424 bp) (Romanova et al., 2016; Li et al., 2019b). The observed AT-richness of the mitogenomes of the current study (61.9% and 68.7%) is slightly lower than in other studies based on complete (Table 2) and incomplete amphipod mitogenomes where AT range between 69.79% and 74.35% (Li et al., 2019a). However our data are in line with Wilson et al. (2000) reporting such an AT-rich bias as typical for arthropods.

The negative GC- skews on both strands of the protein coding genes of the two species in this study differ from the so far known common Malacostraca pattern where genes encoded on the + strand usually exhibit negative and genes encoded on the - strand positive GC-skews (Hassanin, 2006). The strand bias in nucleotide composition of metazoan mitogenomes is attributed to varying mutational pressure during replication or transcription (Pons et al., 2014; Hassanin et al., 2005). Future research will need to test if these factors are responsible for the different GC patterns observed in the two Antarctic amphipod species of the current study.

Gene order and rearrangements

The translocations of *trnG* and a commonly derived pattern of a gene string consisting of *trnA*, *trnS1*, *trnN*, *trnE*, and *trnR* are presumed to be apomorphic features of certain amphipods (Kilpert and Podsiadlowski, 2010; Krebes and Bastrop, 2012; Li et al., 2019a). The two studied species exhibit the translocation of *trnG* relative to the pancrustacean ground pattern. However, the altered tRNA gene order of the two species results in a unique tRNA string that is dissimilar to the apomorphic gene string of *trnA*, *trnS1*, *trnN*, *trnE*, and *trnR*. Moreover, the observed *rrnL-trnV-rrnS* pattern of *E.* cf. *giganteus* is known to be common in most Malacostraca (Ki et al, 2010) and is also observed in the pancrustacean ground pattern. This is however not the case for *C. amundseni* with the *trnC* being present. In addition, the large-scale gene reversals that have been found in three species have also been observed in *Halice sp.* Boeck, 1871 (Li et al., 2019a). It may be attributed to intramitochondrial recombination

allowing breaking and rejoining of the mitochondrial genome (Dowton and Austin, 1999, Li et al., 2019a)

rRNA genes

The shortest complete *rrnL* in amphipods of 577 bp is currently known from *Hirondellea gigas* Birstein and Vinogradov, 1955 (Lan et al., 2016), which is much shorter than the *rrnL* that has been found in the species of the current study. On the other hand, the *rrnS* of *C. amundseni* has with 529 bp the same length as *Alicella gigantea* (Li et al., 2019b) which has so far been the shortest reported *rrnS* length in amphipods. Also, the shortest total length of *rrnL* and *rrnS* together has been described from the amphipod *Hirondellea gigas* Birstein and Vinogradov, 1955 (Lan et al., 2016) with 1120 bp, and we find that the total length of the two rRNAs in *C. amundseni* is with 1268 bp rather similar. Short rRNA genes have also been observed in *Gammarus duebeni* Lilljeborg, 1852 (Krebes and Bastrop, 2012) where they have been attributed to a minimization strategy of the mitogenome.

tRNA secondary structures

Aberrant tRNA structures as we find them in the three novel mitogenomes are common. Jühling et al. (2012) have described a loss of a D-domain in *trnS1* in almost all metazoan while the D-domain in *trnS2* has only been lacking in Lophotrochozoa and Ecdysozoa. Mitogenome studies of other amphipod species also report the lack of the DHU arm in *trnS1* and *trnS2* in *Epimeria cornigera* Fabricius, 1779, *Epimeria frankei* Beermann and Raupach, 2018 in Beerman, Westbury, Hofreiter, Hilgers, Deister, Neumann and Raupach, 2018 (Beermann et al., 2018), *Caprella scaura* Templeton, 1836 (Ito et al., 2010) and “Metacrangonyx boveii” (Pons et al., 2014) and in *trnV* in *Brachyuropus grewingkii* Dybowsky, 1874, *Acanthogammarus victorii* Dybowsky, 1874, *Eulimnogammarus cyaneus* Dybowsky, 1874, and *Garjajewia cabanisii* Dybowsky, 1874 (Romanova et al., 2016), *Halice* sp. Boeck, 1871 (Li et al., 2019a) and “Metacrangonyx boveii” (Pons et al., 2014). The absence of the TΨC loop is another aberrant and common structure in amphipods that has also been observed in *trnC*, *trnE*, and *trnT* of *Caprella mutica* Schurin, 1935 (Kilpert and Podsiadlowski, 2010), *trnQ* and *trnV* of *Gammarus duebeni* Lilljeborg, 1852 (Krebes and Bastrop, 2012), and *trnC*, *trnQ*, *trnK*, and *trnF* of *Onisimus nanseni* G.O. Sars, 1900 (Ki et al, 2010). The pressure for minimization of the mitogenome has been put forward as one of the explanations for these aberrant tRNA structures (Yamazaki et

al., 1997). Other explanations could be replication slippage resulting in sequence deletions or insertions (Macey et al., 1997). Despite these aberrant structures in tRNAs, these are most likely still functional (Watanabe et al., 2014).

Nucleotide diversity

Information on nucleotide diversity can be helpful for the design of new molecular markers (Romanova et al., 2016; Zhang et al., 2018). Here, we have shown that the most variable mitogenes of *Eusirus* for intraspecific comparisons between genetic clades are *nad6*, *nad5*, and *nad1* while for comparisons between *Eusirus* and *Charcotia, atp8*, *nad6* and *nad2* are most variable, which could be suitable for future phylogeographic and population genetic studies. Contrary, the least variable mitogenes for *Eusirus* are *nad4*, *nad3*, *nad2*, and *cox1* and for interspecies comparisons between *Eusirus* and *Charcotia cox1*, *cytb*, and *cox3* could be more suitable for future deep phylogeny investigations. Surprisingly, despite its wide use in DNA barcoding initiatives (Witt et al., 2006; Hebert et al., 2003), the *cox1* gene appears to have relatively low nucleotide diversities between closely and distantly related amphipods. Consistent with our results, also Romanova et al. (2016) describe the mitogenes *atp8*, *nad2*, *nad4l*, *nad5*, *nad6* as most variable in Baikalian amphipods and *cox* genes to be less variable, with *cox1* having the lowest nucleotide diversity.

Phylogenetic analysis

Our evolutionary tree (Figure 4) constructed from mitochondrial protein coding genes is well supported and shows phylogenetic clades according to amphipod superfamily identity. Moreover, our results are congruent to the current taxonomic classification where the species were categorized into their respective family and superfamily (Horton et al., 2021). Previous classification have placed *Eusirus* in the same Eusiroidea superfamily as *Epimeria* (Bousfield, 1978) while the recent classification have placed *Eusirus* under superfamily Eusiroidea and *Epimeria* under Iphimedioidea (Lowry and Myers, 2017). Phylogenetic evidence using 18S rDNA have shown that *Eusirus* has a close relationship with *Epimeria* which showed a well-supported clade of Eusiridae, Calliopiidae, Astyridae, Iphimediidae, Epimeriidae and Pleustidae families (Englisch, 2001). Phylogenetic evidence using 13-protein coding genes further corroborates these close relationships (Figure 4).

Our grouping of *Charcotia amundseni* with other species from the superfamily Lysianassoidea (Figure 4) is supported with the morphological phylogeny of Lowry and Myers (2017), which characterized this superfamily as often having a type 3 lysianassoid calceolus and a cleft telson. Molecular phylogenetic analyses using concatenated 16S-COX1-18S data in Ritchie et al. (2015) show clustering of families and superfamilies similar to our study which further backs up our results. The phylogenetic grouping of the two morphospecies invested here based on the three novel mitogenomes thus follow the expected patterns according to taxonomic relationships.

Conclusions

The current study provides three additional novel complete mitogenomes of Antarctic amphipod species and the first complete mitogenomes of the abundant amphipod genera *Eusirus* and *Charcotia*. In comparison to other published amphipod mitogenomes, the novel mitogenomes show distinct features such as a lower AT-richness in their whole mitogenomes, negative GC- skews on both strands of the protein coding genes, and unique gene rearrangements. The novel mitogenomes also share characteristics with other amphipod mitogenomes including aberrant tRNA and short rRNA genes, which could be linked to minimalization of mitogenomes. Moreover, the estimation of the nucleotide diversity (π) provides information to choose mitogenes as most suitable markers for future phylogenetic studies of amphipods. The novel mitogenomes are certainly useful for future phylogenetic analyses as it put the investigated species into phylogenetic positions matching superfamily and family identity.

References

Altschul, S. F., Madden, T. L., Schäffer, A. A., Zhang, J., Zhang, Z., Miller, W., & Lipman, D. J. 1997. 366Gapped BLAST and PSI-BLAST: a new generation of protein database search programs. *Nucleic Acids Research*, *25*(17), 3389–3402.

Andres, H. G., Lörz, A. N., & Brandt, A. 2002. A common but undescribed huge species of Eusirus Krøyer, 1845 (Crustacea, Amphipoda, Eusiridae) from Antarctica. *Mitteilungen aus dem Hamburgischen Zoologischen Museum und Institut*, *99*, 109-126.

Andrews, S. 2010. FastQC: A Quality Control Tool for High Throughput Sequence Data [Online]. Available online at: http://www.bioinformatics.babraham.ac.uk/projects/fastqc/

Baird, H. P., Miller, K. J., & Stark, J. S. 2011. Evidence of hidden biodiversity, ongoing speciation and diverse patterns of genetic structure in giant Antarctic amphipods. *Molecular Ecology*, *20*(16), 3439-3454.

Ballard, J. W. O., & Whitlock, M. C. 2004. The incomplete natural history of mitochondria. *Molecular ecology*, *13*(4), 729-744.

Barr, C. M., Neiman, M., & Taylor, D. R. 2005. Inheritance and recombination of mitochondrial genomes in plants, fungi and animals. *New Phytologist*, *168*(1), 39-50.

Bauzà-Ribot, M. M., Juan, C., Nardi, F., Oromí, P., Pons, J., & Jaume, D. 2012. Mitogenomic phylogenetic analysis supports continental-scale vicariance in subterranean thalassoid crustaceans. *Current Biology*, *22*(21), 2069-2074.

Beermann, J., Westbury, M. V., Hofreiter, M., Hilgers, L., Deister, F., Neumann, H., & Raupach, M. J. 2018. Cryptic species in a well-known habitat: applying taxonomics to the amphipod genus Epimeria (Crustacea, Peracarida). *Scientific reports*, *8*(1), 1-26.

Bernt, M., Merkle, D., Ramsch, K., Fritzsch, G., Perseke, M., Bernhard, D., Schlegel, M., Stadler, P.F., Middendorf, M. 2007. CREx: inferring genomic rearrangements based on common intervals. *Bioinformatics*, *23*(21), 2957–2958.

Bernt, M., Donath, A., Jühling, F., Externbrink, F., Florentz, C., Fritzsch, G., Pütz, J., Middendorf, M., Stadler, P. F. 2013. MITOS: Improved de novo metazoan mitochondrial genome annotation. *Molecular Phylogenetics and Evolution*, *69*(2), 313–319.

Boore, J. L., Lavrov, D. V., & Brown, W. M. 1998. Gene translocation links insects and crustaceans. *Nature*, *392*(6677), 667-668.

Boore, J. L. 1999. Animal mitochondrial genomes. *Nucleic acids research*, *27*(8), 1767-1780.

Bousfield, E.L., 1978. A revised classification and phylogeny of amphipod crustaceans. Royal Society of Canada, Ottawa.

Cameron, S. L. 2014. How to sequence and annotate insect mitochondrial genomes for systematic and comparative genomics research. *Systematic Entomology*, *39*(3), 400-411.

Caterino, M. S., Cho, S., & Sperling, F. A. 2000. The current state of insect molecular systematics: a thriving Tower of Babel. *Annual review of entomology*, *45*(1), 1-54.

Chevreux E. 1905. Diagnoses d'amphipodes nouveaux provenant de l'expédition antarctique du Français. I. Lysianassidae. Bulletin de la Société Zoologique de France 30: 159–165.

Chevreux, B., Wetter, T., & Suhai, S. 1999. Genome sequence assembly using trace signals and additional sequence information. In *German conference on bioinformatics* (Vol. 99, No. 1, pp. 45-56).

Cormier, A., Wattier, R., Teixeira, M., Rigaud, T., & Cordaux, R. 2018. The complete mitochondrial genome of *Gammarus roeselii* (Crustacea, Amphipoda): insights into mitogenome plasticity and evolution. *Hydrobiologia*, *825*(1), 197-210.

Dowton, M., & Austin, A. D. 1999. Evolutionary dynamics of a mitochondrial rearrangement" hot spot" in the Hymenoptera. *Molecular Biology and Evolution*, *16*(2), 298-309.

D'Udekem D'Acoz, C., Schon, I., & Robert, H. 2018. The genus Charcotia Chevreux, 1906 in the Southern Ocean, with the description of a new species (Crustacea, Amphipoda, Lysianassoidea). BELGIAN JOURNAL OF ZOOLOGY, 148(1), 31–82.

Englisch, U., 2001. Analyse der Phylogenie der Amphipoda (Crustacea, Malacostraca) mit Hilfe von Sequenzen des Gens der RNA der kleinen ribosomalen Untereinheit. Dissertation, Ruhr-Universität Bochum, Lehrstuhl für Spezielle Zoologie1-312.

Gallardo, V. A. 1987. The sublittoral macrofaunal benthos of the Antarctic shelf. *Environment International*, *13*(1), 71-81.

Grabowski, M., Mamos, T., Bącela-Spychalska, K., Rewicz, T., & Wattier, R. A. 2017. Neogene paleogeography provides context for understanding the origin and spatial distribution of cryptic diversity in a widespread Balkan freshwater amphipod. *PeerJ*, *5*, e3016.

Greco, S., D'Agostino, E., Manfrin, C., Gaetano, A. S., Furlanis, G., Capanni, F., Santovito, G., Edomi, P., Giulianini, P.G., & Gerdol, M. 2021. RNA-sequencing Indicates High Hemocyanin Expression as a Key Strategy for Cold Adaptation in the Antarctic Amphipod *Eusirus* cf. *giganteus* Clade g3.

Guindon, S., & Gascuel, O. 2003. A simple, fast, and accurate algorithm to estimate large phylogenies by maximum likelihood. *Systematic biology*, *52*(5), 696-704.

Hahn, C., Bachmann, L., & Chevreux, B. 2013. Reconstructing mitochondrial genomes directly from genomic next-generation sequencing reads--a baiting and iterative mapping approach. *Nucleic Acids Research*, *41*(13), e129–e129.

Hall, T.A. 1999. BioEdit: a user-friendly biological sequence alignment editor and analysis program for Windows 95/98/NT. Nucl. Acids. Symp. Ser. 41:95-98.

Haran, J., Timmermans, M. J., & Vogler, A. P. 2013. Mitogenome sequences stabilize the phylogenetics of weevils (Curculionoidea) and establish the monophyly of larval ectophagy. *Molecular Phylogenetics and Evolution*, *67*(1), 156-166.

Hassanin, A., Leger, N, & Deutsch, J. 2005. Evidence for multiple reversals of asymmetric mutational constraints during the evolution of the mitochondrial genome of Metazoa, and consequences for phylogenetic inferences. *Systematic biology*, *54*(2), 277-298.

Hassanin, A. 2006. Phylogeny of Arthropoda inferred from mitochondrial sequences: strategies for limiting the misleading effects of multiple changes in pattern and rates of substitution. *Molecular phylogenetics and evolution*, *38*(1), 100-116.

Hebert, P. D., Cywinska, A., Ball, S. L., & DeWaard, J. R. 2003. Biological identifications through DNA barcodes. Proceedings of the Royal Society of London. Series B: Biological Sciences, 270(1512), 313-321.

Horton, T., Lowry, J., De Broyer, C., Bellan-Santini, D., Coleman, C.O., Corbari, L., Costello, M.J., Daneliya, M., Dauvin, J.-C., Fišer, C., Gasca, R., Grabowski, M., Guerra-García, J.M., Hendrycks, E., Hughes, L., Jaume, D., Jazdzewski, K., Kim, Y.-H., King, R., Krapp-Schickel, T., LeCroy, S., Lörz, A.-N., Mamos, T., Senna, A.R., Serejo, C., Sket, B., Souza-Filho, J.F., Tandberg, A.H., Thomas, J.D., Thurston, M., Vader, W., Väinölä, R., Vonk, R., White, K., Zeidler, W. 2021. World Amphipoda Database. Accessed at http://www.marinespecies.org/amphipoda on 2021-11-23.

Ito, A., Aoki, M. N., Yokobori, S. I., & Wada, H. 2010. The complete mitochondrial genome of Caprella scaura (Crustacea, Amphipoda, Caprellidea), with emphasis on the unique gene order pattern and duplicated control region. *Mitochondrial DNA*, *21*(5), 183-190.

Jühling, F., Pütz, J., Bernt, M., Donath, A., Middendorf, M., Florentz, C., & Stadler, P. F. 2012. Improved systematic tRNA gene annotation allows new insights into the evolution of mitochondrial tRNA structures and into the mechanisms of mitochondrial genome rearrangements. *Nucleic Acids Research*, *40*(7), 2833–2845.

Katoh, K., Rozewicki, J., & Yamada, K. D. 2019. MAFFT online service: multiple sequence alignment, interactive sequence choice and visualization. *Briefings in bioinformatics*, *20*(4), 1160-1166.

Keane, T. M., Creevey, C. J., Pentony, M. M., Naughton, T. J., & Mclnerney, J. O. 2006. Assessment of methods for amino acid matrix selection and their use on empirical data shows that ad hoc assumptions for choice of matrix are not justified. *BMC evolutionary biology*, *6*(1), 29.

Keis, M., Remm, J., Ho, S. Y., Davison, J., Tammeleht, E., Tumanov, I. L., Saveljev, A.P., Männil, P., Kojola, I., & Abramov A.V. 2013. Complete mitochondrial genomes and a novel spatial genetic method reveal cryptic phylogeographical structure and migration patterns among brown bears in north-western Eurasia. *Journal of Biogeography*, *40*(5), 915-927.

Ki, J. S., Hop, H., Kim, S. J., Kim, I. C., Park, H. G., & Lee, J. S. 2010. Complete mitochondrial genome sequence of the Arctic gammarid, *Onisimus nanseni* (Crustacea; Amphipoda): Novel gene structures and unusual control region features. *Comparative Biochemistry and Physiology Part D: Genomics and Proteomics*, *5*(2), 105-115.

Kilpert, F., & Podsiadlowski, L. 2006. The complete mitochondrial genome of the common sea slater, *Ligia oceanica* (Crustacea, Isopoda) bears a novel gene order and unusual control region features. Bmc Genomics, 7(1), 1-18.

Kilpert, F., & Podsiadlowski, L. 2010. The mitochondrial genome of the Japanese skeleton shrimp *Caprella mutica* (Amphipoda: Caprellidea) reveals a unique gene order and shared apomorphic translocations with Gammaridea. *Mitochondrial DNA*, *21*(3-4), 77-86.

Knox, G. A., & Lowry, J. K. 1977. A comparison between the benthos of the Southern Ocean and the North Polar Ocean with special reference to the Amphipoda and the Polychaeta. *Polar oceans. Arctic Institute of North America, Calgary*, 423-462.

Krebes, L., & Bastrop, R. 2012. The mitogenome of *Gammarus duebeni* (Crustacea Amphipoda): A new gene order and non-neutral sequence evolution of tandem repeats in the control region. *Comparative Biochemistry and Physiology Part D: Genomics and Proteomics*, *7*(2), 201-211.

Lan, Y., Sun, J., Bartlett, D. H., Rouse, G. W., Tabata, H. G., & Qian, P. Y. 2016. The deepest mitochondrial genome sequenced from Mariana Trench *Hirondellea gigas* (Amphipoda). *Mitochondrial DNA Part B*, *1*(1), 802-803.

Laslett, D., & Canbäck, B. 2008. ARWEN: A program to detect tRNA genes in metazoan mitochondrial nucleotide sequences. In *Bioinformatics (Oxford, England)* (Vol. 24).

Li, J. Y., Zeng, C., Yan, G. Y., & He, L. S. 2019a. Characterization of the mitochondrial genome of an ancient amphipod *Halice* sp. MT-2017 (Pardaliscidae) from 10,908 m in the Mariana Trench. *Scientific reports*, *9*(1), 1-15.

Li, J. Y., Song, Z. L., Yan, G. Y., & He, L. S. 2019b. The complete mitochondrial genome of the largest amphipod, *Alicella gigantea*: Insight into its phylogenetic relationships and deep sea adaptive characters. *International journal of biological macromolecules*, *141*, 570-577.

Lin, C. P., & Danforth, B. N. 2004. How do insect nuclear and mitochondrial gene substitution patterns differ? Insights from Bayesian analyses of combined datasets. *Molecular phylogenetics and evolution*, *30*(3), 686-702.

López-López, A., & Vogler, A. P. 2017. The mitogenome phylogeny of Adephaga (Coleoptera). *Molecular Phylogenetics and Evolution*, *114*, 166-174.

Lowry, J. K., & Myers, A. A. 2017. A Phylogeny and Classification of the Amphipoda with the establishment of the new order Ingolfiellida (Crustacea: Peracarida). *Zootaxa*, *4265*(1), 1-89.

Macey, J. R., Larson, A., Ananjeva, N. B., & Papenfuss, T. J. 1997. Replication slippage may cause parallel evolution in the secondary structures of mitochondrial transfer RNAs. *Molecular Biology and Evolution*, *14*(1), 30-39.

Perna, N. T., & Kocher, T. D. 1995. Patterns of nucleotide composition at fourfold degenerate sites of animal mitochondrial genomes. *Journal of Molecular Evolution*, *41*(3), 353–358.

Pilar Cabezas, M., Cabezas, P., Machordom, A., & Guerra-García, J. M. 2013. Hidden diversity and cryptic speciation refute cosmopolitan distribution in *Caprella penantis* (Crustacea: Amphipoda: Caprellidae). *Journal of Zoological Systematics and Evolutionary Research*, *51*(2), 85-99.

Pons, J., Bauzà-Ribot, M. M., Jaume, D., & Juan, C. 2014. Next-generation sequencing, phylogenetic signal and comparative mitogenomic analyses in Metacrangonyctidae (Amphipoda: Crustacea). *BMC genomics*, *15*(1), 566.

Ritchie, H., Jamieson, A. J., & Piertney, S. B. 2015. Phylogenetic relationships among hadal amphipods of the Superfamily Lysianassoidea: Implications for taxonomy and biogeography. *Deep Sea Research Part I: Oceanographic Research Papers*, *105*, 119-131.

Romanova, E. V., Aleoshin, V. V., Kamaltynov, R. M., Mikhailov, K. V., Logacheva, M. D., Sirotinina, E. A., Gornov, A.Y., Anikin, A.S., & Sherbakov, D. Y. 2016. Evolution of mitochondrial genomes in Baikalian amphipods. *BMC genomics*, *17*(14), 1016.

Ronquist F, Huelsenbeck JP. 2003. MRBAYES 3: Bayesian phylogenetic inference under mixed models. Bioinformatics. 19:1572–1574.

Rozas, J., Ferrer-Mata, A., Sánchez-DelBarrio, J.C., Guirao-Rico, S., Librado, P., Ramos-Onsins S.E., Sánchez-Gracia, A. 2017. DnaSP v6: DNA Sequence Polymorphism Analysis of Large Datasets. *Mol. Biol. Evol.* 34: 3299-3302.

Shin, S. C., Cho, J., Lee, J. K., Ahn, D. H., Lee, H., & Park, H. 2012. Complete mitochondrial genome of the Antarctic amphipod *Gondogeneia antarctica* (Crustacea, amphipod). *Mitochondrial DNA*, *23*(1), 25-27.

Sun, S., Wu, Y., Ge, X., Jakovlić, I., Zhu, J., Mahboob, S., Al-Ghanim, K.A., Al-Misned, F., & Fu, H. 2020. Disentangling the interplay of positive and negative selection forces that shaped mitochondrial genomes of *Gammarus pisinnus* and *Gammarus lacustris*. *Royal Society Open Science*, *7*(1), 190669.

Tang, Y., Zheng, X., Liu, H., & Sunxie, F. 2020. Population genetics and comparative mitogenomic analyses reveal cryptic diversity of *Amphioctopus neglectus* (Cephalopoda: Octopodidae). *Genomics*, *112*(6), 3893-3902.

Väinölä, R., Witt, J. D. S., Grabowski, M., Bradbury, J. H., Jazdzewski, K., & Sket, B. 2008. Global diversity of amphipods (Amphipoda; Crustacea) in freshwater. In *Freshwater Animal Diversity Assessment*. Springer, Dordrecht. 241-255.

Verheye, M. L., & D'Udekem D'Acoz, C. 2021. Integrative taxonomy of giant crested *Eusirus* in the Southern Ocean, including the description of a new species (Crustacea: Amphipoda: Eusiridae). *Zoological Journal of the Linnean Society*. 193(1): 31–77.

Watanabe, Y. I., Suematsu, T., & Ohtsuki, T. 2014. Losing the stem-loop structure from metazoan mitochondrial tRNAs and co-evolution of interacting factors. *Frontiers in genetics*, *5*, 109.

Wilson, K., Cahill, V., Ballment, E., & Benzie, J. 2000. The complete sequence of the mitochondrial genome of the crustacean Penaeus monodon: are malacostracan crustaceans more closely related to insects than to branchiopods?. *Molecular Biology and Evolution*, *17*(6), 863-874

Witt, J. D., Threloff, D. L., & Hebert, P. D. 2006. DNA barcoding reveals extraordinary cryptic diversity in an amphipod genus: implications for desert spring conservation. *Molecular ecology*, *15*(10), 3073-3082.

Yamazaki, N., Ueshima, R., Terrett, J. A., Yokobori, S. I., Kaifu, M., Segawa, R., Kobayashi, T., Numachi, K., Ueda, T., & Nishikawa, K. 1997. Evolution of pulmonate gastropod mitochondrial genomes: comparisons of gene organizations of Euhadra, Cepaea and Albinaria and implications of unusual tRNA secondary structures. *Genetics*, *145*(3), 749-758.

Zhang, D. X., & Hewitt, G. M. 1997. Insect mitochondrial control region: a review of its structure, evolution and usefulness in evolutionary studies. *Biochemical Systematics and Ecology*, *25*(2), 99-120.

Zhang, D., Li, W. X., Zou, H., Wu, S. G., Li, M., Jakovlić, I., Zhang, J., Chen, R., & Wang, G. T. 2018. Mitochondrial genomes of two diplectanids (Platyhelminthes: Monogenea) expose paraphyly of the order Dactylogyridea and extensive tRNA gene rearrangements. *Parasites & vectors*, *11*(1), 1-13.

Zhang, Z., Xing, Y., Cheng, J., Pan, D., Lv, L., Cumberlidge, N., & Sun, H. 2020. Phylogenetic implications of mitogenome rearrangements in East Asian potamiscine freshwater crabs (Brachyura: Potamidae). *Molecular Phylogenetics and Evolution*, *143*, 106669.

Chapter 3: Evidence for cold adaptations in amphipod mitochondrial genomes

Louraine Salabao[1,2], Bruno Frédérich[1], Gilles Lepoint[3] & Isa Schön[2,4]

Bransfield Strait, Antarctica (taken by Louraine Salabao)

[1] Laboratory of Evolutionary Ecology, FOCUS, Department of Biology, Ecology & Evolution, University of Liège, B-4000 Liège, Belgium

[2] Centre for Environmental Sciences, Zoology: Toxicology and Biodiversity, Campus Diepenbeek, Agoralaan Gebouw D - B-3590 Diepenbeek

[3] Laboratoire d'Ecologie Trophique et Isotopique (LETIS), FOCUS, Université de Liège, B-4000 Liège, Belgium

[4] Royal Belgian Institute of Natural Sciences, OD Nature, Freshwater Biology, Vautierstraat 29, 1000 Brussels, Belgium

Abstract

Amphipods are malacostracan crustaceans that occupy a wide range of mostly marine and freshwater habitats, and can live under extreme conditions such as in the Arctic, Antarctic or the deep sea. Although this makes them good model organisms to study the molecular features of thermal adaptations, transcriptomic data or good quality genomes of this crustacean group are still rare, and even more so for species from extreme environments. Given the increasing availability of mitogenomes, also from amphipods, mitogenomic data can be used instead to examine potential thermal adaptations since mitochondrial genes are involved in the oxidative phosphorylation process for energy production. In this study, we analysed published mitogenomes of amphipods from cold, temperate, and warm regions to test for cold-adaptations by comparing different mitogenome features and by constructing phylogenies. We featured molecular patterns for cold adaptations in mitogenomes of amphipods. On one hand, we observed significantly lower proportions of charged amino acids in amphipods from cold regions and evidence for purifying selection in all amphipod mitogenomes. Additionally, a higher average non-synonymous/synonymous substitutions (ω) was observed in the amphipods from the cold regions. On the other hand, no grouping of species from cold regions was observed in the reconstructed phylogeny nor did we find any general patterns of gene translocations that could be linked to cold adaptation. We show that mitogenomes can be used as an alternative to study cold adaptations in species for which high quality genomic data are not yet available. Additional data from other taxa occurring in cold regions could strengthen our conclusions for molecular signatures of cold adaptations in mitogenomes.

Introduction

Mitochondria are involved in a wide range of cellular processes (Harada et al., 2019) including genes that are engaged in oxidative phosphorylation. This process occurs through the electron transport chain's (ETC) creation of a trans-membrane proton gradient which generates adenosine triphosphate (ATP) (Silva et al., 2014). Consequently, mitochondria play a key role in energy production (Vakifahmetoglu-Norberg et al., 2017). The formation of ETC involves protein complexes that are encoded in both nuclear DNA and mitochondrial DNA (Ballard & Whitlock, 2004; Fontanillas et al., 2005; Silva et al., 2014). In general, mitochondrial genomes

(mitogenomes) contain 13 protein coding genes all involved in electron transport, two rRNAs, 22 mitochondrial-specific tRNAs, and a non-coding region that regulates transcription and replication (Ballard & Whitlock, 2004; Fontanillas et al., 2005; Carapelli et al., 2013). The adaptive evolution of the mitochondrial genes that are involved in oxidative phosphorylation has been linked to different environmental conditions including heat and cold stress, which could possibly indicate thermal adaptations (Doi et al., 1999; Sebastian et al., 2020). Positive selection in genes that are involved in oxidative phosphorylation has been reported, as for example in *nad1*, *nad3*, and *nad4* mitochondrial genes in Atlantic salmon (Consuegra, et al., 2015) and the *cytb* gene in European anchovy (Silva et al., 2014). The positive selection in these genes has been suggested to be linked to the need for higher metabolic efficiency and ATP production, or the production of a thermogenic mechanism in order to thrive at low temperatures (Consuegra, et al., 2015; Carapelli et al., 2019).

Amphipods are malacostracan crustaceans that occupy a wide range of mostly marine habitats although they are also found in freshwater and terrestrial habitats (Väinölä, et al., 2007). They can live under extreme environmental conditions as in the Arctic (Gradinger, 2001) and Antarctic (Gradinger, 2001; Lowry et al., 2007) or the deep sea (Lan et al., 2016; Li et al., 2019a; Li et al., 2019b), making them good model organisms to study thermal adaptations. For Amphipoda in general, few high quality genomes or transcriptomes are yet available, and with one exception (Kang et al. 2015), these genomic resources are still lacking for taxa from extreme environments. Given the increasing availability of mitogenomes, also from amphipods, such mitogenomic data can be used instead to examine potential thermal adaptation. Two studies have already demonstrated specific thermal adaptations including positive selection in the membrane and substrate-level ATP synthases subunits of the amphipods from the stenotherm lake Baikal (Naumenko et al. 2017) and the translocation of ND6 in Antarctic nototheniid fish (Mark et al. 2012). Thermal adaptations can also be derived from specific amino acid compositions in mitogenomes as has been demonstrated for the deep sea amphipod *Alicella gigantea,* with less frequent charged amino acids (Li et al., 2019b), and mitogenomes of Antarctic notothenioid fish favoring the amino acids methionine, serine and isoleucine (Berthelot et al., 2019). In this study, we aim to test for signatures of cold adaptations in mitogenomes of amphipods from cold regions by reconstructing phylogenies and comparing molecular features of amphipod mitogenomes from regions with cold,

temperate and warm temperatures. Based on other mitogenome studies on animals from low temperature habitats, we expect that similar cold adaptations in amphipods led to (1) specific patterns of mitochondrial amino acid content and polarity; (2) positive selection in mitochondrial protein coding genes of amphipods from cold regions; and (3) certain mitochondrial gene translocations.

Materials and Methods

Amphipod mitogenome data

Amino acid and DNA sequence data from a total of 59 published amphipod mitogenome were downloaded from GenBank (For an overview of accession numbers see Table 1) for further analyses. All 59 mitogenomes contained the 13 protein coding genes but only 46 were complete. The sampling location of each species was used to categorize the species' ecoregions based on Spalding et al. (2007) and Abell et al. (2008). These ecoregions were then used to classify amphipods into species from cold, temperate, and warm regions (Table 1) for further comparisons. When a species did not classify into any ecoregion because its sampling location was not classified into any ecoregions, the published information of the sampling location was used.

Table 1. Species list of mitogenomes used for analysis including the eco-region, category, mitogenome coverage, and the GenBank accession number.

Species	Eco-region	Category	Mitogenome	Genbank
Acanthogammarus victorii	Lake Baikal	Cold	Partial	KX341962
Alicella gigantea	Mariana Islands	Cold	Complete	MK215211
Ampithoe lacertosa	Sea of Japan	Temperate	Complete	MK215645
Bahadzia jaraguensis	Hispaniola	Warm	Complete	FR872382
Brachyuropus grewingkii	Lake Baikal	Cold	Complete	KP161875
Caprella mutica	North Sea	Temperate	Complete	GU130250
Caprella scaura	Central Kuroshio Current	Temperate	Complete	AB539699
Charcotia amundseni	East Antarctic Dronning Maud Land	Cold	Complete	OK489457
Epimeria cornigera	North Sea	Temperate	Complete	MF361127
Epimeria frankei	North Sea	Temperate	Partial	MF361126
Eulimnogammarus cyaneus	Lake Baikal	Cold	Complete	KX341964
Eulimnogammarus verrucosus	Lake Baikal	Cold	Complete	KF690638
Eulimnogammarus vittatus	Lake Baikal	Cold	Complete	KM287572
Eurythenes magellanicus	Gulf of Tonkin	Cold	Complete	MN688221
Eusirus cf. giganteus clade G1	South Shetland Islands	Cold	Complete	OK489458
Eusirus cf. giganteus clade G2	East Antarctic Wilkes Land	Cold	Complete	OK489459
Gammarus duebeni	Iceland–Jan Mayen	Cold	Complete	JN704067
Gammarus fossarum	Central and Western Europe	Temperate	Complete	KY197961
Gammarus lacustris	Upper Brahmaputra	Warm	Complete	MK354235
Gammarus pisinnus	Lower Huang He	Temperate	Complete	MK354236
Gammarus roeselii	Central and Western Europe	Temperate	Complete	MG779536
Garjajewia cabanisii	Lake Baikal	Cold	Partial	KX341965
Gmelinoides fasciatus	Lake Baikal	Cold	Complete	KX341966
Gondogeneia antarctica	South Shetland Islands	Cold	Complete	JN827386
Grandidierella fasciata	Central Kuroshio Current	Temperate	Complete	LC500464
Grandidierella osakaensis	Central Kuroshio Current	Temperate	Complete	LC546828
Grandidierella rubroantennata	Central Kuroshio Current	Temperate	Complete	LC500463
Halice sp.	Mariana Islands	Cold	Partial	MH294484
Hirondellea gigas	Mariana Islands	Cold	Partial	KU558991 & KU558990
Hyalella lucifugax	Lake Titicaca	Temperate	Partial	LT594767
"Longipodacrangonyx stocki"	Atlantic Northwest Africa	Temperate	Partial	HE860496
"Metacrangonyx boutini boutini"	Atlantic Northwest Africa	Temperate	Partial	HE860497

"Metacrangonyx boveei"	Atlantic Northwest Africa	Temperate	Complete	HE860498
Metacrangonyx dominicanus	Hispaniola	Warm	Complete	HE860499
Metacrangonyx goulmimensis	Atlantic Northwest Africa	Temperate	Complete	HE860501
Metacrangonyx ilvanus	Italian Peninsula & Islands	Temperate	Complete	HE860503
Metacrangonyx longicaudus	Atlantic Northwest Africa	Temperate	Complete	HE860509
Metacrangonyx longipes	Eastern Iberia	Temperate	Complete	AM944817
"Metacrangonyx nicoleae tamri"	Atlantic Northwest Africa	Temperate	Complete	HE860504
"Metacrangonyx notenboomi"	Atlantic Northwest Africa	Temperate	Complete	HE860513
Metacrangonyx panousei	Atlantic Northwest Africa	Temperate	Complete	HE860510
"Metacrangonyx paurosexualis"	Atlantic Northwest Africa	Temperate	Partial	HE860507
Metacrangonyx remyi	Atlantic Northwest Africa	Temperate	Complete	HE860512
Metacrangonyx repens	NO ECOREGION*	Warm	Complete	HE860495
Metacrangonyx samanensis	Hispaniola	Warm	Partial	HE860505
Metacrangonyx spinicaudatus	Atlantic Northwest Africa	Temperate	Complete	HE860506
Onisimus nanseni	Arctic	Cold	Complete	FJ555185
Pallaseopsis kessleri	Lake Baikal	Cold	*Complete*	*KX341968*
Platorchestia japonica	Eastern Yellow Sea Drainages	Temperate	Complete	MG010370
Platorchestia parapacifica	Eastern Yellow Sea Drainages	Temperate	Complete	MG010371
Pleonexes koreana	Sea of Japan	Temperate	Complete	MK265245
Pseudocrangonyx daejeonensis	Eastern Yellow Sea Drainages	Temperate	Complete	MH229998
Pseudoniphargus daviui	Eastern Iberia	Temperate	Complete	FR872383
Pseudoniphargus gorbeanus	Eastern Iberia	Temperate	Partial	LN871176
Pseudoniphargus sorbasiensis	Southern Iberia	Temperate	Partial	LN871175
Stygobromus foliatus	Chesapeake Bay	Temperate	Partial	KU869713
Stygobromus indentatus	Chesapeake Bay	Temperate	Complete	KU869711
Stygobromus tenuis potomacus	Chesapeake Bay	Temperate	Complete	KU869712
Trinorchestia longiramus	Sea of Japan	Temperate	Complete	MH542431

* Groundwater mean value is 24.6°C (Herrera & Custodio, 2014)

Species names in quotes and not in italics denote taxa not formally described yet (Bauzà-Ribot et al., 2012).

Codon usage

To analyse the codon usage, the 13 protein coding gene DNA sequences were used except for the data of *Epimeria frankei* (GenBank accession nr. MF361126) which were excluded due to a high number of ambiguities; this left 58 amphipod mitochondrial DNA sequences for analysis. Codon usage was analysed with the Sequence Manipulation Suite (Stothard, 2000) which determines the frequencies of codons that code for the same amino acid and will assess the sequence preference for selected amino acids. From these frequencies, the amino acid proportions were calculated for each individual amino acid and the amino acid groups with different properties (i.e. nonpolar, polar-uncharged and charged amino acids) (Reece et al., 2013). The amino acid proportions for each individual amino acid and the amino acid groups with different properties were statistically compared among the three groups of amphipod species from cold, temperate, warm regions with a one-way ANOVA followed by a post hoc Tukey HSD tests for multiple comparison of means in R version 3.61 (R Core Team, 2019).

Testing for signals of selection at the molecular level

The DNA sequences of the 13 mitochondrial protein coding gene were aligned separately per gene with MUSCLE in MEGA X (Kumar et al., 2018). The alignments were concatenated with Geneious Prime 2019 v1.8.0. and used for further analysis in EasyCodeML version 1.4 (Gao et al., 2019) together with the phylogenetic tree. Estimating the ratio of the non-synonymous/synonymous substitutions (ω) allows to investigate the patterns of selection acting on the protein coding genes with $\omega = 1$ indicate a neutral evolution while $\omega < 1$ indicate a negative or purifying selection, and $\omega > 1$ indicate positive (adaptive or diversifying) selection (Garvin et al., 2011; Jeffares et al., 2015; Sun et al., 2020). Two branch models, the one-ratio model (M0) and the free-ratio model (M1) were compared to test whether the dn/ds ratio (ω) differed among the branches of the tree. The one-ratio model (M0) assumes that all branches have the same dn/ds ratio (ω) while independent dn/ds ratios (ω) for each branch are assumed for the free-ratio model (M1). To assess the significant difference between the two models, a likelihood ratio test (LRT) was conducted. Average ω for amphipods from the cold, temperate, and warm regions were statistically compared with one-way ANOVA followed by a post hoc Tukey HSD tests for multiple comparison of means in R software.

Phylogenetic analyses

Phylogenetic reconstructions were based on the amino acid sequences of 13 protein coding genes and gene boundaries from defined according to the information in GenBank. *Limnoria quadripunctata* (Genbank no. KF704000), *Ligia oceanica* (Genbank no. DQ442914), and *Trachelipus rathkii* (Genbank no. KR013001) are the three Isopoda species that were used as outgroups. All amino acid sequences were aligned separately for each gene using MUSCLE (Edgar, 2004) in MEGA X (Kumar et al., 2018) and concatenated with Geneious Prime 2019 v1.8. The best fitting model of molecular evolution for each partition was identified with PartitionFinder v2.1. (Lanfear et al., 2016). Phylogenetic analyses based on maximum likelihood were carried out with RAxML v8 (Stamatakis, 2014) implemented in the CIPRES web portal (Miller et al., 2010) with 1000 bootstrap replications. Trees based on Bayesian inference were constructed with MrBayes v3.2 (Ronquist et al., 2012) in the CIPRES web portal with 10 million generations, sampling every 5000 generations and discarding 10% of the initial trees as burnin. The convergence of parameters and effective sample size were examined with Tracer version 1.7.1 (Rambaut et al., 2018). Resulting trees were viewed and edited in FigTree v1.4.4 (http://tree.bio.ed.ac.uk/software/figtree/) and with Inkscape v1.0.1 (https://inkscape.org).

Rearrangements of mitogenome gene order

CREx (Bernt et al., 2007) was used to examine complete mitogenomes for possible gene rearrangements by comparing them to the pancrustacean ground pattern. In the CREx program, species with incomplete genes are excluded from the analysis as this hampers pairwise comparisons. For comparing the gene orders, CREx creates a distance matrix with the number of common intervals. A higher common interval value indicates a more similar gene order with the highest resulting value of 1400 when the gene orders are identical. For further comparisons, the mean of the common intervals in comparison to the pancrustacean ground pattern was calculated for the three amphipod groups and statistically compared with a one-way ANOVA in R version 3.61.

Results

Codon usage

No significant differences among amphipods from cold, temperate, and warm regions were found when comparing preferences for individual amino acids (one-way ANOVA, p-value = 1) (Figure 1). Figure 2c illustrates the significantly lower proportion of charged amino acids in amphipods from cold regions (10.24 ± 0.21%) than from temperate regions (10.51 ± 0.29) (Tukey HSD test, p-value= 0.01). The amino acid proportions of non-polar (one-way ANOVA, p-value=0.35) and polar-uncharged (one-way ANOVA, p-value=0.72) amino acids did not differ significantly among the three groups (Figure 2a, b).

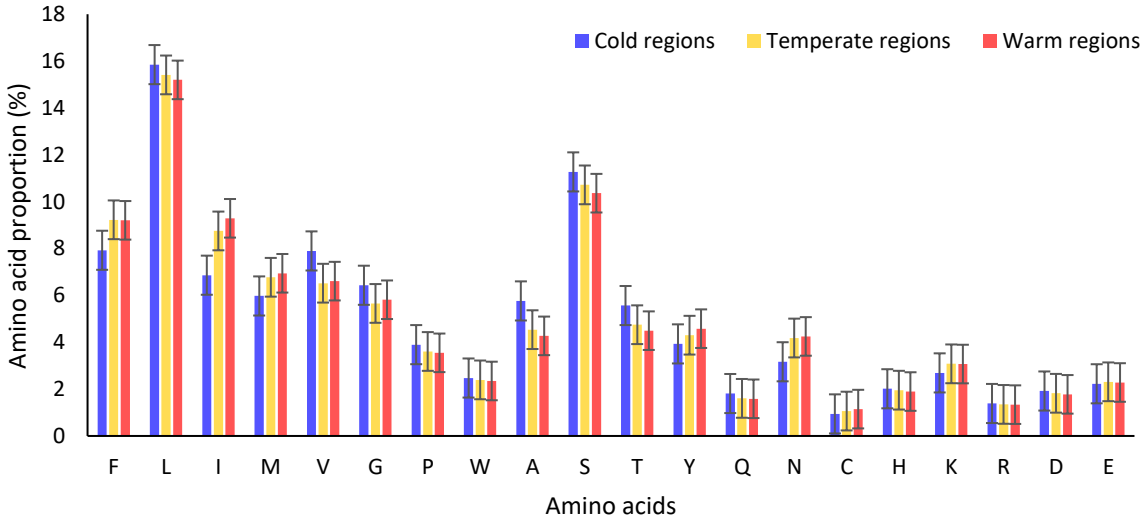

Figure 1. Proportions of individual amino acids of amphipod species from cold (blue), temperate (yellow), and warm (red) regions. Amino acid identities are indicated by single letter codes: G - Glycine, P - Proline, A - Alanine, V - Valine, L - Leucine, I - Isoleucine, M - Methionine, C - Cysteine, F - Phenylalanine, Y - Tyrosine, W - Tryptophan, H - Histidine, K - Lysine, R - Arginine, Q - Glutamine, N - Asparagine, E - Glutamic Acid, D - Aspartic Acid, S - Serine, T - Threonine. Amphipods from cold, temperate, and warm regions did not differ significantly in the proportions of individual amino acids (one-way ANOVA, p-value = 1).

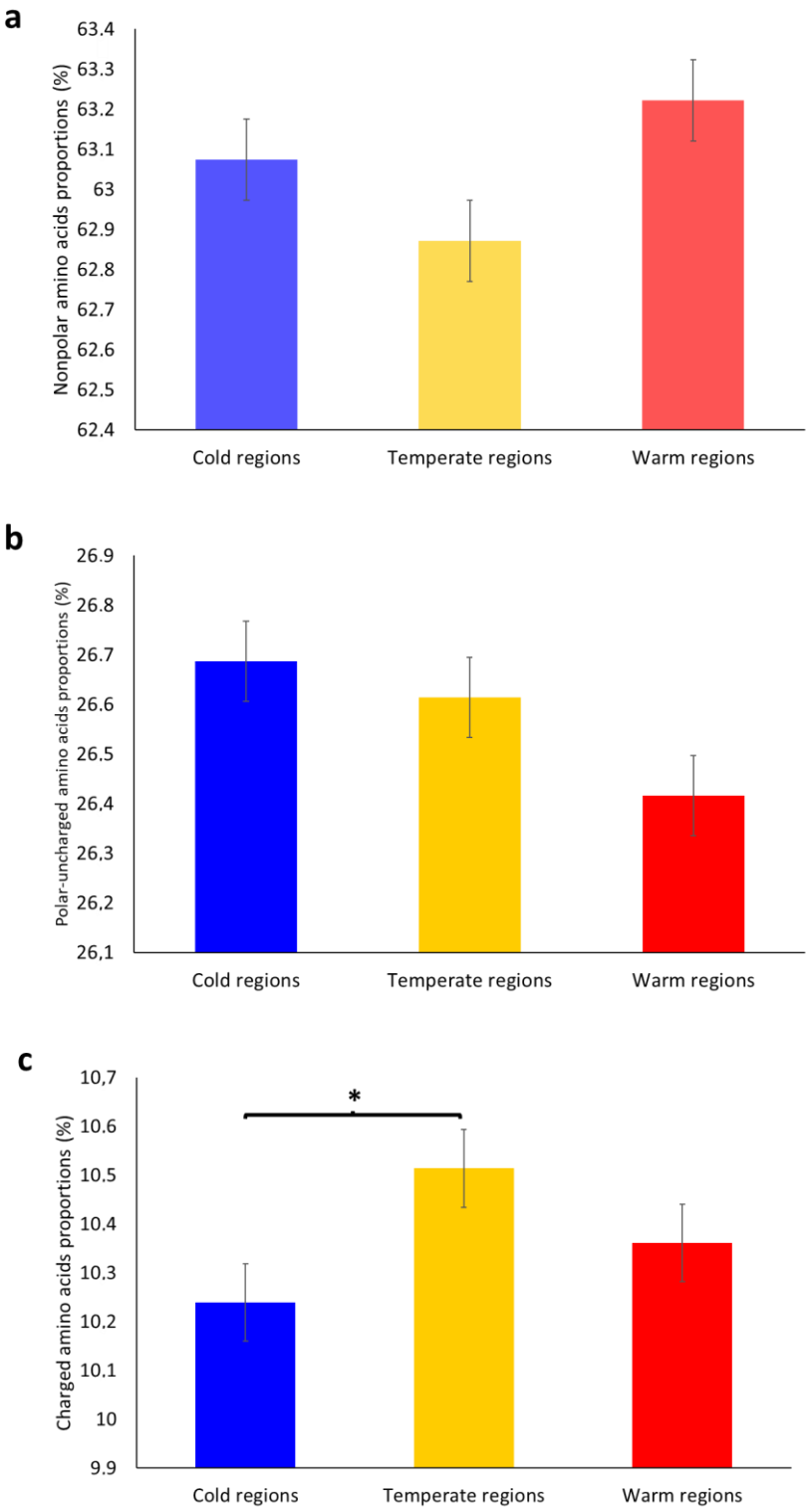

Figure 2. The proportions of a) non-polar and b) polar-uncharged c) charged amino acids of amphipod species from cold (blue), temperate (yellow), and warm (red) regions. No significant differences were found among the species from cold, temperate, and warm regions for non-polar (p=0.35) and polar-uncharged (p=0.72). Significant differences were only observed in the proportions of charged amino acids between amphipods from cold and temperate regions (p= 0.01). Significant differences are indicated by *.

Signals of selection at the molecular level

A likelihood ratio test (Table 2) revealed a significant difference between the one-ratio model (M0) and free-ratio model (M1) (p-value < 0.001) indicating different dn/ds ratios (ω) among different branches of the phylogenetic tree. All ω values were smaller than one (Figure 3) indicating that these branches are under negative or purifying selection. Amphipods from cold regions had an average ω of 0.051 which was significantly higher than that of amphipods from temperate regions, which showed an average ω of 0.032 (Tukey HSD test, p-value < 0.001). Amphipods from warm regions had an average ω of 0.037, a value between these two other means. These differences as compared to the average ω of amphipods from cold (Tukey HSD test, p-value= 0.17) and temperate (Tukey HSD test, p-value= 0.79) regions was not significant.

Table 2. Results of the likelihood ratio test between the one-ratio model (M0) and free-ratio model (M1) estimating ω for branches of the phylogenetic tree

Model	np	LnL	ω	Model comparison	LRT P-value
One‑ratio model (M0)	124	-408149.161419	0.05334	Model 0 vs. M1	< 0.001
Free-ratio model (M1)	245	-405034.579461			

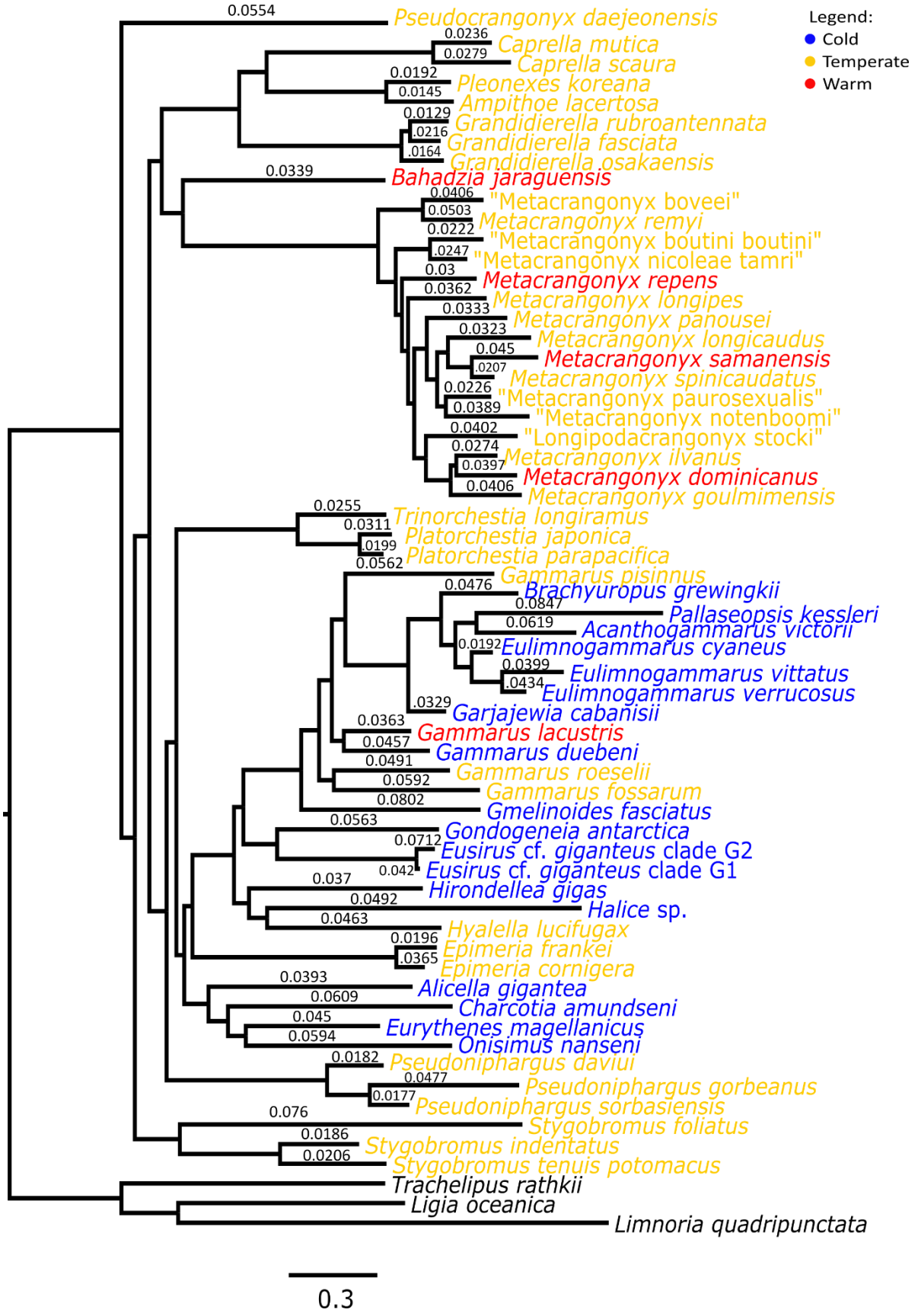

Figure 3. Phylogenetic tree with different dn/ds ratio (ω) displayed on top of each branch. Amphipods from cold regions are indicated in blue, from temperate regions in yellow, and from warm regions in red.

Phylogenetic analyses

Phylogenetic reconstructions of the relationships of the analysed amphipods species based on the amino acids alignment of 13 concatenated protein-coding genes showed no clear phylogenetic clustering of amphipods from cold regions regardless which phylogenetic method was used (Figures 3 & 4). Indeed, some species from temperate regions and one species from warm environments were grouped with the clade of species living in cold environments.

Mitochondrial gene order and rearrangements

Translocations of the mitochondrial genes *trnG*, *trnC*, and *trnY* are observed in all amphipods regardless from which region they originate (Supplementary figure 3). No specific pattern of gene translocations can been detected from amphipods from cold regions only.

The gene order of *Eulimnogammarus cyaneus*, *Eulimnogammarus verrucosus*, *Gammarus duebeni*, *Gammarus fossarum*, *Gammarus lacustris*, and *Gammarus pisinnus* showed the highest similarity to the pancrustacean ground pattern with 464 common intervals (Supplementary figure 4).

The mean common interval was also calculated for each of the three groups (i.e. amphipods from cold, temperate, and warm regions) in comparison to the pancrustacean ground pattern. No significant differences were observed among the three amphipod groups (Kruskal-Wallis rank sum test, p-value = 0.388) (Figure 5).

Figure 4. Phylogenetic tree based on the concatenated amino acid alignment of the 13 mitochondrial protein coding genes using ML and BI methods. Only bootstrap values of ≥50 (above the nodes) and posterior probabilities >0.80 (below the nodes) are shown. The scale bar corresponds to the number of substitutions per site. Amphipod species from cold regions are indicated in blue, from temperate regions in yellow, and from warm regions in red.

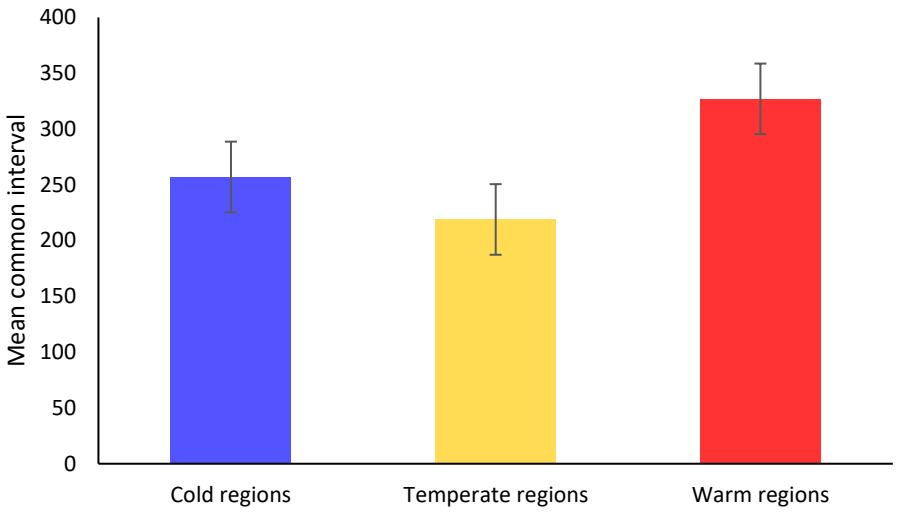

Figure 5. Mean common interval of mitochondrial gene arrangements as compared to the pancrustacean pattern for amphipod from cold, temperate, and warm regions.

Discussion

Codon usage

Amino acid usage and properties have been identified to affect protein function (Metpally et al., 2009; Berthelot et al., 2019) and can thus provide information on adaptations to certain environmental conditions (Venev & Zeldovich, 2018). There was no significant difference in the preference of individual amino acid among amphipods from cold, temperate, and warm regions. Regarding amino acid properties, a significantly lower proportions of charged amino acids was found for amphipods from cold regions (Figure 2), which could be regarded as a signal for cold-adaptation in amphipods. Similarly, lower proportions of charged amino acids were also reported by Li et al. (2019a) for non-hadal and hadal amphipods as well as by Li et al. (2019b) for both abyssal and hadal amphipods as compared to species from shallow waters. Additional studies on psychrophiles or organisms that thrive in cold environments showed less preference for charged amino acids (Gianese et al., 2001; Methé et al., 2005; Goldstein, 2007; Metpally et al., 2009). Taken together, our results and these studies highly suggest that lower proportions of charged amino acids could be related to cold adaptations. Charged amino acids are involved in electrostatic interactions for ion pairs and H bonds that are necessary for protein stabilization, especially at high temperatures (Kumar et al., 2000; Gianese et al., 2001).

Thus, reducing the number and strength of these electrostatic interactions should increase protein flexibility which is required for cold adaptations (Gianese et al., 2001).

Synonymous and non-synonymous substitution rates

Estimated ω values of <1 for all branches in the tree indicate that these branches are under negative or purifying selection and that there is minimal accumulation of non-synonymous substitutions (Jeffares et al., 2015). Similar patterns of purifying selection have been reported for mitogenomes of the amphipods *Gammarus pisinnus* and *Gammarus lacustris* (Sun et al., 2020) and other invertebrates (Du et al., 2017; Vanhove et al., 2018; Sun et al., 2019). Synonymous substitutions exceeding the non-synonymous substitutions is a common pattern (Choudhuri, 2014) with purifying selection being suggested as the major force shaping molecular evolution of mitogenomes (Sun et al., 2020) to maintain vital mitochondrial gene functions (Ballard & Whitlock, 2004; Castellana et al., 2011). Our results thus confirm this general expectation. On the other hand, despite the <1 average ω values observed, amphipods from the cold regions still showed higher average ω compared to the amphipods from the temperate and warm regions. This higher average ω could be attributed to the lower average synonymous substitutions (ds) (Parker et al., 2018). This could also indicate relatively weaker degree of purifying selection (Jeffares et al., 2015) acting on the genes of the amphipods from the cold regions compared to the amphipods from the temperate and warm regions. Similar case of lower average synonymous substitutions (ds) was also observed in the cold-tolerant species of *Drosophila* (Parker et al., 2018) which could indicate signatures of cold-adaptation.

Phylogenetic analyses

We expected that species with similar environmental adaptations would cluster together in the phylogeny, reflecting their close evolutionary relationships influenced by similar ecological pressures. This pattern was however, not observed in our results. The absence of any obvious pattern of the species from the cold regions also indicates that no signal for cold adaptation was detected in the amino acid sequences. However, amino acid composition might still be functionally important as lower preference for charged amino acid was observed. Moreover, other factors might have driven these evolutionary relationships other than environmental conditions such as ecological convergence of parallel adaptation which might further obscure

the expected clustering pattern as species may develop similarities in ecology in response to similar environmental pressures (Hibbitts & Fitzgerald, 2005; Derome & Bernatchez, 2006).

Mitochondrial gene order and rearrangements

No apparent pattern of gene translocations was observed for amphipods from the three different groups. These results did not support the hypothesis that closely related species tend to have similar gene rearrangements. This could be attributed differences in the evolutionary history of the species (Hurst et al., 2004; Lajoie et al., 2010). Moreover, the lack of any differences in gene translocations for amphipods from regions with cold or warm temperatures could at least partly also be explained by the small number of species studied here: mitogenomes were only available for 18 amphipod species from the cold and five from warm regions as compared to 36 species from temperate regions. The results of our study should be treated with some caution and for further in-depth examinations of additional amphipod mitogenomes are required to confirm our results on possible signals for cold adaptations in amphipod mitogenomes.

Conclusions

Our results provide evidence for certain molecular signatures of cold adaptations in amphipod mitogenomes such as low proportions of charged amino acids and a high average non-synonymous/synonymous substitutions (ω). We proved also evidence for negative or purifying selection. Increasing the number of mitogenomes for amphipod species from cold and warm regions could improve the strengths of statistical analyses for possible signals of thermal adaptations and provide a more balanced dataset for comparisons. Despite these limitations, this study illustrates that mitogenomes are a suitable resource to test for thermal adaptations, especially for species for which full genomic data are not yet available.

References

Abell, R., Thieme, M. L., Revenga, C., Bryer, M., Kottelat, M., Bogutskaya, N., ... & Petry, P. 2008. Freshwater ecoregions of the world: a new map of biogeographic units for freshwater biodiversity conservation. *BioScience*, *58*(5), 403-414.

Ballard, J. W. O., & Whitlock, M. C. 2004. The incomplete natural history of mitochondria. *Molecular ecology*, *13*(4), 729-744.

Bauzà-Ribot, M. M., Juan, C., Nardi, F., Oromí, P., Pons, J., & Jaume, D. 2012. Mitogenomic phylogenetic analysis supports continental-scale vicariance in subterranean thalassoid crustaceans. Current Biology, 22(21), 2069-2074.

Bernt, M., Merkle, D., Ramsch, K., Fritzsch, G., Perseke, M., Bernhard, D., … & Middendorf, M. 2007. CREx: inferring genomic rearrangements based on common intervals. *Bioinformatics*, *23*(21), 2957-2958.

Berthelot, C., Clarke, J., Desvignes, T., William Detrich III, H., Flicek, P., Peck, L. S., ... & Clark, M. S. 2019. Adaptation of proteins to the cold in Antarctic fish: A role for Methionine?. Genome biology and evolution, 11(1), 220-231.

Boore, J. L., Lavrov, D. V., & Brown, W. M. 1998. Gene translocation links insects and crustaceans. Nature, 392(6677), 667-668.

Carapelli, A., Torricelli, G., Nardi, F., & Frati, F. 2013. The complete mitochondrial genome of the Antarctic sea spider *Ammothea carolinensis* (Chelicerata; Pycnogonida). Polar biology, 36(4), 593-602.

Carapelli, A., Fanciulli, P. P., Frati, F., & Leo, C. 2019. Mitogenomic data to study the taxonomy of Antarctic springtail species (Hexapoda: Collembola) and their adaptation to extreme environments. *Polar Biology*, *42*(4), 715-732.

Castellana, S., Vicario, S., & Saccone, C. 2011. Evolutionary patterns of the mitochondrial genome in Metazoa: exploring the role of mutation and selection in mitochondrial protein-coding genes. *Genome biology and evolution*, *3*, 1067-1079.

Choudhuri, S. 2014. Fundamentals of molecular evolution. *Bioinformatics for beginners*.

Consuegra, S., John, E., Verspoor, E., & de Leaniz, C. G. 2015. Patterns of natural selection acting on the mitochondrial genome of a locally adapted fish species. Genetics Selection Evolution, 47(1), 1-10.

Derome, N., & Bernatchez, L. 2006. The transcriptomics of ecological convergence between 2 limnetic coregonine fishes (Salmonidae). Molecular Biology and Evolution, 23(12), 2370-2378.

Doi, A., Suzuki, H., & Matsuura, E. T. 1999. Genetic analysis of temperature-dependent transmission of mitochondrial DNA in Drosophila. *Heredity*, *82*(5), 555-560.

Du, C., Zhang, L., Lu, T., Ma, J., Zeng, C., Yue, B., & Zhang, X. 2017. Mitochondrial genomes of blister beetles (Coleoptera, Meloidae) and two large intergenic spacers in Hycleus genera. *BMC genomics*, *18*(1), 1-15.

Edgar, R. C. 2004. MUSCLE: Multiple sequence alignment with high accuracy and high throughput. Nucleic Acids Research, 32(5), 1792-1797.

Fontanillas, P., Depraz, A., Giorgi, M. S., & Perrin, N. 2005. Nonshivering thermogenesis capacity associated to mitochondrial DNA haplotypes and gender in the greater white‐toothed shrew, Crocidura russula. *Molecular Ecology*, *14*(2), 661-670.

Gao, F., Chen, C., Arab, D. A., Du, Z., He, Y., & Ho, S. Y. 2019. EasyCodeML: A visual tool for analysis of selection using CodeML. *Ecology and Evolution*, *9*(7), 3891-3898.

Garvin, M. R., Bielawski, J. P., & Gharrett, A. J. 2011. Positive Darwinian selection in the piston that powers proton pumps in complex I of the mitochondria of Pacific salmon. PloS one, 6(9), e24127.

Gianese, G., Argos, P., & Pascarella, S. 2001. Structural adaptation of enzymes to low temperatures. *Protein engineering*, *14*(3), 141-148.

Gradinger, R. R. 2001. Adaptation of Arctic and Antarctic ice metazoa to their habitat. *Zoology*, *104*(3-4), 339-345.

Goldstein, R. A. 2007. Amino‐acid interactions in psychrophiles, mesophiles, thermophiles, and hyperthermophiles: insights from the quasi‐chemical approximation. *Protein science*, *16*(9), 1887-1895.

Harada, A. E., Healy, T. M., & Burton, R. S. 2019. Variation in thermal tolerance and its relationship to mitochondrial function across populations of *Tigriopus californicus*. *Frontiers in physiology*, *10*, 213.

Herrera, C., & Custodio, E. 2014. Groundwater flow in a relatively old oceanic volcanic island: The Betancuria area, Fuerteventura Island, Canary Islands, Spain. Science of the Total Environment, 496, 531-550.

Hibbitts, T. J., & Fitzgerald, L. A. 2005. Morphological and ecological convergence in two natricine snakes. Biological Journal of the Linnean Society, 85(3), 363-371.

Hurst, L. D., Pál, C., & Lercher, M. J. 2004. The evolutionary dynamics of eukaryotic gene order. Nature Reviews Genetics, 5(4), 299-310.

Jeffares, D. C., Tomiczek, B., Sojo, V., & Reis, M. D. 2015. A beginners guide to estimating the non-synonymous to synonymous rate ratio of all protein-coding genes in a genome. In *Parasite genomics protocols*. Humana Press, New York, NY. pp. 65-90.

Kang, S., Kim, S., & Park, H. 2015. Transcriptome of the Antarctic amphipod Gondogeneia antarctica and its response to pollutant exposure. Marine genomics, 24, 253-254.

Kumar, S., Stecher, G., Li, M., Knyaz, C., & Tamura, K. 2018. MEGA X: molecular evolutionary genetics analysis across computing platforms. *Molecular biology and evolution*, *35*(6), 1547.

Kumar, S., Tsai, C. J., & Nussinov, R. 2000. Factors enhancing protein thermostability. *Protein engineering*, *13*(3), 179-191.

Lajoie, M., Bertrand, D., & El-Mabrouk, N. 2010. Inferring the evolutionary history of gene clusters from phylogenetic and gene order data. Molecular biology and evolution, 27(4), 761-772.

Lan, Y., Sun, J., Bartlett, D. H., Rouse, G. W., Tabata, H. G., & Qian, P. Y. 2016. The deepest mitochondrial genome sequenced from Mariana Trench Hirondellea gigas (Amphipoda). *Mitochondrial DNA Part B*, *1*(1), 802-803.

Lanfear, R., Frandsen, P. B., Wright, A. M., Senfeld, T., & Calcott, B. 2016. Partition Finder 2: new methods for selecting partitioned models of evolution for molecular and morphological phylogenetic analyses. Molecular biology and evolution.

Li, J. Y., Zeng, C., Yan, G. Y., & He, L. S. 2019a. Characterization of the mitochondrial genome of an ancient amphipod *Halice* sp. MT-2017 (Pardaliscidae) from 10,908 m in the Mariana Trench. *Scientific reports*, *9*(1), 1-15.

Li, J. Y., Song, Z. L., Yan, G. Y., & He, L. S. 2019b. The complete mitochondrial genome of the largest amphipod, *Alicella gigantea*: Insight into its phylogenetic relationships and deep sea adaptive characters. *International journal of biological macromolecules*, *141*, 570-577.

Lowry, J. K., Jazdzewski, K., & Robert, H. 2007. *Synopsis of the Amphipoda of the Southern Ocean*. C. De Broyer (Ed.). Koninklijk Belgisch Instituut voor Naruurwetenschappen.

Mark, F. C., Lucassen, M., Strobel, A., Barrera-Oro, E., Koschnick, N., Zane, L., ... & Papetti, C. 2012. Mitochondrial function in Antarctic nototheniids with ND6 translocation. PloS one, 7(2), e31860.

Methé, B. A., Nelson, K. E., Deming, J. W., Momen, B., Melamud, E., Zhang, X., ... & Fraser, C. M. 2005. The psychrophilic lifestyle as revealed by the genome sequence of Colwellia psychrerythraea 34H through genomic and proteomic analyses. *Proceedings of the National Academy of Sciences*, *102*(31), 10913-10918.

Metpally, R. P. R., & Reddy, B. V. B. 2009. Comparative proteome analysis of psychrophilic versus mesophilic bacterial species: Insights into the molecular basis of cold adaptation of proteins. *BMC genomics*, *10*(1), 1-10.

Miller, M. A., Pfeiffer, W., & Schwartz, T. 2010. "Creating the CIPRES Science Gateway for inference of large phylogenetic trees" in Proceedings of the Gateway Computing Environments Workshop (GCE), 14 Nov. 2010, New Orleans, LA. pp 1 - 8.

Naumenko, S. A., Logacheva, M. D., Popova, N. V., Klepikova, A. V., Penin, A. A., Bazykin, G. A., Etingova, A.E., Mugue, N.S., Kondrashov, A.S., & Yampolsky, L. Y. 2017. Transcriptome‐based phylogeny of endemic Lake Baikal amphipod species flock: fast speciation accompanied by frequent episodes of positive selection. Molecular ecology, 26(2), 536-553.

Parker, D. J., Wiberg, R. A. W., Trivedi, U., Tyukmaeva, V. I., Gharbi, K., Butlin, R. K., Hoikkala, A., Kankare, M., & Ritchie, M. G. 2018. Inter and intraspecific genomic divergence in Drosophila montana shows evidence for cold adaptation. Genome Biology and Evolution, 10(8), 2086-2101.

R Core Team. 2019. R: A language and environment for statistical computing. R Foundation for Statistical Computing, Vienna, Austria. URL (http://www.R-project.org/).

Rambaut, A., Drummond, A. J., Xie, D., Baele, G., & Suchard, M. A. 2018. Posterior summarization in Bayesian phylogenetics using Tracer 1.7. Systematic biology, 67(5), 901-904.

Reece, J. B., Urry, L. A., Cain, M. L., Minorsky, P. V., & Jackson, R. B. 2013. *Campbell Biology 10th Edition* (Vol. 2). Benjamin Cummings. Pearson Education, Incorporated. pp. 75-77.

Ronquist, F., Teslenko, M., van der Mark, P., Ayres, D. L., Darling, A., Hohna, S., Larget, B., Liu, L., Suchard, M. A., Huelsenbeck, J. P. 2012. MrBayes 3.2: efficient bayesian phylogenetic inference and model choice across a large model space. Syst Biol. 61(3):539-542.

Sebastian, W., Sukumaran, S., Zacharia, P. U., Muraleedharan, K. R., Dinesh Kumar, P. K., & Gopalakrishnan, A. 2020. Signals of selection in the mitogenome provide insights into adaptation mechanisms in heterogeneous habitats in a widely distributed pelagic fish. *Scientific reports*, *10*(1), 1-14.

Silva, G., Lima, F. P., Martel, P., & Castilho, R. 2014. Thermal adaptation and clinal mitochondrial DNA variation of European anchovy. *Proceedings of the Royal Society B: Biological Sciences*, *281*(1792), 20141093.

Spalding, M. D., Fox, H. E., Allen, G. R., Davidson, N., Ferdaña, Z. A., Finlayson, M. A. X., ... & Robertson, J. 2007. Marine ecoregions of the world: a bioregionalization of coastal and shelf areas. *BioScience*, *57*(7), 573-583.

Stamatakis, A. 2014. RAxML version 8: a tool for phylogenetic analysis and post-analysis of large phylogenies. Bioinformatics, 30(9), 1312-1313.

Stothard, P. 2000. The sequence manipulation suite: JavaScript programs for analyzing and formatting protein and DNA sequences. BioTechniques 28: 1102-1104.

Sun, S. E., Sha, Z., & Wang, Y. 2019. Divergence history and hydrothermal vent adaptation of decapod crustaceans: A mitogenomic perspective. PloS one, 14(10), e0224373.

Sun, S., Wu, Y., Ge, X., Jakovlić, I., Zhu, J., Mahboob, S., ... & Fu, H. 2020. Disentangling the interplay of positive and negative selection forces that shaped mitochondrial genomes of *Gammarus pisinnus* and *Gammarus lacustris*. *Royal Society Open Science*, *7*(1), 190669.

Väinölä, R., Witt, J. D. S., Grabowski, M., Bradbury, J. H., Jazdzewski, K., & Sket, B. 2007. Global diversity of amphipods (Amphipoda; Crustacea) in freshwater. In *Freshwater Animal Diversity Assessment*. Springer, Dordrecht. pp. 241-255.

Vakifahmetoglu-Norberg, H., Ouchida, A. T., & Norberg, E. 2017. The role of mitochondria in metabolism and cell death. *Biochemical and biophysical research communications*, *482*(3), 426-431.

Vanhove, M. P., Briscoe, A. G., Jorissen, M. W., Littlewood, D. T. J., & Huyse, T. 2018. The first next-generation sequencing approach to the mitochondrial phylogeny of African monogenean parasites (Platyhelminthes: Gyrodactylidae and Dactylogyridae). *BMC genomics*, *19*(1), 1-16.

Venev, S. V., & Zeldovich, K. B. 2018. Thermophilic adaptation in prokaryotes is constrained by metabolic costs of proteostasis. *Molecular biology and evolution*, *35*(1), 211-224.

Chapter 4: Origin and diversification of *Eusirus* amphipods in the polar regions

Louraine Salabao[1,2], Isa Schön[2,4], Gilles Lepoint[3], Marie Verheye[4,5], Agnes Dettai[6], & Bruno Frédérich[1]

King George Island near Machu Picchu Scientific Base, Antarctica (taken by Louraine Salabao)

[1] Laboratory of Evolutionary Ecology, FOCUS, Department of Biology, Ecology & Evolution, University of Liège, B-4000 Liège, Belgium

[2] Centre for Environmental Sciences, Zoology: Toxicology and Biodiversity, Campus Diepenbeek, Agoralaan Gebouw D - B-3590 Diepenbeek

[3] Laboratoire d'Ecologie Trophique et Isotopique (LETIS), FOCUS, Université de Liège, B-4000 Liège, Belgium

[4] Royal Belgian Institute of Natural Sciences, OD Nature, Freshwater Biology, Vautierstraat 29, 1000 Brussels, Belgium

[5] Department of Biology, Ecology, Evolution and Biodiversity Conservation unit, Katholieke Universiteit Leuven, Charles Deberiotstraat 32, 3000, Leuven, Belgium

[6] Muséum national d'Histoire naturelle (MNHN), UMR 7205 ISYEB (MNHN, CNRS, Sorbonne Unversité des Antilles), Paris, France

Abstract

The polar oceans harbor a rich faunal diversity, which is composed of lineages from multiple origins. The evolution of this fauna is possibly linked to the tectonic, climatic, and glacial history of these polar oceans. The genus *Eusirus* amphipods has a global distribution with species occurring in both polar oceans. This distribution together with its low dispersal capacity makes *Eusirus* a good model organism to provide novel insights into the origin and the diversification of benthos from both polar oceans. To do so, phylogenetic reconstructions of *Eusirus* were produced by using DNA sequence data from ribosomal 18S and 28S together with the mitochondrial COI and COII genes. The obtained phylogenies support the monophyly of the Antarctic *Eusirus* clade and show polyphyly for the group of Arctic species. Interestingly, the time-calibrated phylogeny indicates that the Arctic *Eusirus* are older than their Antarctic congeners. The origin of the Antarctic clade around the Oligocene coincides with the opening of the Drake passage and the formation of the Antarctic circumpolar current (ACC). In contrast, Arctic *Eusirus* species show a varied history of lineage splitting and appear to have originated prior to the glacial/interglacial periods. Finally, the detected high rates of lineage diversification in the Antarctic clade could be attributed to the vicariant events and ecological opportunities brought about by the climatic and geological changes in the Antarctic.

Introduction

The polar oceans harbor a diverse marine fauna which is probably shaped by their tectonic, climatic, and glacial history (Sirenko, 2009; Clarke & Crame, 2010; Hardy et al., 2011; Legezyñska et al., 2020; Rabosky, 2022). However, Antarctica has higher endemism compared to the Arctic which is attributed to its older geological age and its long history of geographic isolation (Eastman, 2005; Piepenburg, 2005; Sirenko, 2009; Baird et al., 2011; Legezyñska et al., 2020; Rabosky, 2022). The Antarctic marine fauna has been considered to have evolved *in situ* since the late Mesozoic or even earlier (Clarke & Crame, 1989; Arntz et al., 1995; Knox, 2006). Some Antarctic lineages were found to be of Gondwanan origins and probably emerged through vicariance when Gondwana went through subsequent fragmentations (Knox & Lowry, 1977; Clarke & Crame, 1989; Clarke & Johnston, 2003; Williams et al., 2003; Sirenko, 2009; Clarke & Crame, 2010; Legezyñska et al., 2020). Thermal isolation of the Antarctic following

the Drake passage opening and the formation of the Antarctic circumpolar current (ACC) around the Eocene to Oligocene led to vicariant speciation in some marine lineages (Rogers, 2007; Thornhill et al., 2008). However, dispersal of organisms with planktonic larvae may still have been possible (Beu et al., 1997; Crame, 1999; Barnes et al., 2006) and even taxa that do not have this type of planktonic larvae may still have been able to disperse through kelp-rafting (Helmuth et al., 1994; Smith, 2002; Waters, 2008). Some taxa could migrate from the Magellan region to Antarctica through the Scotia Arc prior to the thermal isolation of Antarctica (Knox & Lowry, 1977; Legezyñska et al., 2020). The decreasing temperatures around the Eocene-Oligocene caused extinctions in certain lineages and provided new opportunities for speciation in others (Brandt, 1999; Rogers, 2007; Verheye et al., 2017). During the repeated ice expansions and retreats, it was suggested that some benthic organisms had undergone polar emergences (the colonization of the Antarctic shelf from the deep sea) through the Circumpolar Deep Water while others went through polar submergences (the colonization of the deep sea from the shelf) through the Antarctic Bottom Water (Thatje et al., 2005; 2008; Strugnell et al., 2008; Strugnell et al., 2011; Verheye et al., 2017). The pre-adaptation to low temperature tolerance of deep sea species also facilitated the movement to the shelf (Knox & Lowry, 1977). Some taxa also migrated from one isolated shelter in the shelf to another during diachronous ice advances and retreats (Thatje et al., 2005). Moreover, these repeated glaciation events could have driven allopatric speciation in the Antarctic taxa acting as a taxonomic diversity pump (Clarke & Crame, 1989; Knox, 2006; Rogers, 2007).

The native fauna of the Arctic Ocean evolved during preglacial periods and eventually adapted to lower temperatures during the Ice ages (Zenkevitch, 1963; Knox & Lowry, 1977). The formation of the Fram strait and the declining temperatures around the Eocene (Serreze & Barry, 2005) permitted the exchange of fauna between the North Atlantic Ocean and the Arctic Ocean (Wilce, 1990; Dunton, 1992; Hardy et al., 2011; Kuklinski et al., 2013) while the opening of the Bering Strait in the late Miocene (Marincovich & Gladenkov, 1999; Serreze & Barry, 2005) allowed the fauna from the North Pacific Ocean to enter the Arctic and the North Atlantic oceans (Wilce, 1990; Dunton, 1992; Hardy et al., 2011). Dispersal and colonization of these taxa were possible with the aid of ocean currents, with some of the sessile or sedentary marine fauna with planktonic larval forms were also able to disperse resulting in genetic connectivity among Arctic, North Pacific, and North Atlantic faunas (Hardy et al., 2011). The

harsh conditions during the Quaternary glaciation/deglaciation events nearly eliminated the Arctic shelf faunal assemblages (Golikov & Scarlato, 1989; Dunton, 1992; Legezyñska et al., 2020), with only few shelf taxa finding refuge in ice-free shelf sites, with some moving into deeper areas and later re-invading the Arctic shelves (Golikov & Scarlato, 1989; Dunton, 1992). The retreat of some taxa into isolated refugia during glaciations facilitated vicariant effects. During deglaciations, re-invasions allowed the interbreeding of some species while other divergent lineages remained distinct (Hardy et al., 2011). Overall, the fauna of both the Southern Ocean and the Arctic Ocean is thus comprised of a mixture of taxa from multiple origins (Zenkevitch, 1963; Knox & Lowry, 1977; Clarke & Crame, 1989; Dunton, 1992; Clarke & Crame, 2010; Hardy et al., 2011; Legezyñska et al., 2020).

The amphipod genus *Eusirus* Krøyer, 1845 is comprised of thirty-one nominal species occurring worldwide (Verheye, 2011; Jung et al., 2016; Peña Othaitz & Sorbe, 2020; Wang et al., 2021) with ten described species from the Antarctic (Verheye, 2011; Jung et al., 2016; Peña Othaitz & Sorbe, 2020). The so far investigated *Eusirus* representatives of the Southern Ocean were found to be monophyletic (Verheye, 2011; Lecointre et al., 2013) and thus fulfill the criteria of a species flock — a group of closely related species that arose and diversified in a specific region, in this case the Southern Ocean (Lecointre et al., 2013). By using COI and 28S sequence data, Verheye (2011) found two putative genetic species of the *Eusirus perdentatus* complex and three putative genetic species of the *Eusirus giganteus* complex. These were later confirmed by using COI, CytB, and ITS2 DNA sequence data which revealed three putative genetic species of the *Eusirus perdentatus* complex and four or five putative genetic species of *Eusirus giganteus* complex suggesting that the species richness of this genus is still underestimated (Baird et al., 2011; Verheye & D'Udekem D'Acoz, 2020). The number of Arctic species varies depending on the authors: four species are found in the Arctic Register of Marine Species (ARMS, https://www.marinespecies.org/arms) (Sirenko et al., 2022) while nine species are mentioned by Thurston (2009) and Palerud & Vader (1991). *Eusirus* species are generally benthic to bentho-pelagic, and their brooding behaviour limits dispersal capacity (Baird et al., 2011). The global distribution of the genus *Eusirus*, with representative species found in the Southern and Arctic Oceans, along with its low dispersal capacity makes the genus a good model to study the origin and diversification of benthos in the two polar oceans.

In this study, we focus on the origin and the diversification of the genus *Eusirus* in the polar regions. We reconstructed a phylogeny of *Eusirus* using DNA sequence data from the complete mitochondrial COI and COII genes and from the nuclear ribosomal 18S and 28S regions for specimens from the Arctic and the Antarctic as well as from non-polar *Eusirus* species. We utilized substitution rates as well as geological and secondary calibrations to date the phylogenetic tree and subsequently, we explored the tempo of lineage diversification. Our aims were to: 1) test if polar *Eusirus* are mono- or polyphyletic and 2) assess whether there are any diversification bursts in the historical patterns of the polar *Eusirus* diversifications, especially during the early history of the polar oceans and in connection with climate events.

Materials and Methods

Taxon Sampling

Antarctic samples were collected from different localities in Antarctica (see Table 1 and supplementary table 3): the Amundsen Sea (JR179 expedition), Elephant Island and North of South Georgia and the South Sandwich Islands (JR144 (BIOPEARL I) expedition), Adelie Coast (CEAMARC expedition), North of Bouvet Island (ANT-XXII-3 (ANDEEP III) expedition), the Weddell Sea (PS118 expedition), North of the Antarctic Peninsula and Larsen B (ANT-XXIII/8 expedition), Larsen A and East Weddell Sea (ANT-XXIV/2 (ANDEEP SYSTCO) and ANT-XXI/2 (BENDEX), ANTXXVII/3 expeditions), Southern Weddell Sea (ANT-XXIX-9 expedition), Southeast of Clarence Island, Joinville Island, the Drake Passage (ANTXXIX-3 expedition), and South of South Georgia and the South Sandwich Islands (ANT-XIX/5 (LAMPOS) expedition). Arctic samples were collected from Resolute Bay, Canada and Malangen, and Kvalsund in Norway (no data on expeditions are available; Table 1 and supplementary table 3).

Other samples were collected in the deep sea of the Northern Pacific Ocean (SO239-171, SO239-133, SO239-118, and SO239-20 expeditions) and Japan (TRV Toyoshio-maru, Hiroshima University) (Table 1 and supplementary table 3). The taxonomic identity of twelve specimens could not be determined at the species level. All specimens were preserved in 95-100% ethanol. Vouchers are available at the Royal Belgian Institute of Natural Sciences (RBINS, Brussels, Belgium), the Muséum National d'Histoire Naturelle (MNHN, Paris, France), the

Centre for Biodiversity Genomics (University of Guelph, Canada), and Hiroshima University (Japan) (see Table 1 and supplementary table 3 for details).

Acknowledging that the information provided by ARMS does not necessarily reflect an approved consensus among taxonomists, I will follow the classification from Thurston (2009) and Palerud & Vader (1991) recognizing nine species in the Arctic. The study sample covers eight out of the ten (80%) described species from the Antarctic, and one undescribed *Eusirus* species while three out of the nine (33.3%) described species from the Arctic are included in the study. Additionally, five undescribed non-polar *Eusirus* species are sampled in this study.

Table 1. Overview of the number of sequenced *Eusirus* specimens per putative genetic species and information on the species' locality. Detailed information of each specimen can be found in Supplementary Table 3.

Species name	Locality	Number of sequenced pecimen
Eusirus microps	Antarctica	3
Eusirus propeperdentatus	Antarctica	3
Eusirus laticarpus 1	Antarctica	6
Eusirus laticarpus 2	Antarctica	3
Eusirus perdentatus	Antarctica	5
Eusirus pontomedon	Antarctica	3
Eusirus antarcticus	Antarctica	5
Eusirus bouvieri 1	Antarctica	4
Eusirus bouvieri 2	Antarctica	6
Eusirus giganteus G1	Antarctica	6
Eusirus giganteus G2	Antarctica	4
Eusirus giganteus G3	Antarctica	2
Eusirus giganteus G4a	Antarctica	5
Eusirus giganteus G4b	Antarctica	4
Eusirus sp. 1	Antarctica	4
Eusirus cuspidatus	Arctic	4
Eusirus propinqvus	Arctic	3
Eusirus minutus	Arctic	5
Eusirus sp. 3	Non-polar	1
Eusirus sp. 5	Non-polar	1
Eusirus sp. 4	Non-polar	1
Eusirus sp. 7	Non-polar	1
*Eusirus sp.*6	Non-polar	1
Rhachotropis schellenbergi (outgroup)	Antarctica	2
Rhachotropis antarctica (outgroup)	Antarctica	2

DNA extraction, PCR amplification, and sequencing

DNA was extracted from a pleopod of each specimen using the DNeasy Blood & Tissue Kit (Qiagen, Germany) following the manufacturer's protocol. DNA concentration and quality were checked with a Nanodrop ND-1000 Spectrophotometer (ThermoFisher Scientific, USA) and a Qubit 2.0 fluorometer (Life Technologies, USA). The entire mitochondrial cytochrome oxidase subunit I (COI, ~1537 bp) and cytochrome oxidase subunit II (COII, ~678 bp) genes as well as two partial nuclear ribosomal DNA 28S (~1400 bp) and 18S (~2200 bp) segments were amplified by Polymerase chain reaction (PCR). Each 20 µL PCR reaction contained 10 µL of 2X Phusion Flash PCR Master Mix, 0.6 µL of $MgCl_2$, 1 µL of each primer, and 1-7 µL of DNA extracts. All PCRs were performed in a T personal Thermoblock (Biometra).

The COI to COII fragment was amplified using the primers CrustCOIF (Teske et al., 2006) and the newly designed *Eusirus*-specific primer COX2_R 5'-TCAKARRATAGGGGCTATTTGAGG-3'. PCR amplification conditions included an initial denaturation for 10 seconds at 98°C, followed by 40 cycles of denaturation for 1 second at 98°C, annealing at 55°C for 5 seconds, extension at 72 °C for 1 minute and 15 seconds, and a final extension at 72°C for 1 minute. The 28S rDNA fragment was amplified using the 28S amphipod-specific primers 5'-GGGACTACCCGCTGAACTTAAGCAT-3' and 5'-GTCTTTCGCCCCTATGCCCAACTG-3' (Verheye et al., 2016), and the 18S rDNA fragment using the 18S-Universal/Reverse primers from Englisch (2001). The PCR amplification conditions for 28S rDNA and 18S rDNA were similar to those of COI and COII except for a higher annealing temperature of 50°C for 28S rDNA. To ensure the absence of contamination, a negative control was included in each PCR reaction. Amplicons were visualized in Midori Green-stained (Nippon Genetics) 1% agarose gels to assess the success of the PCR and the length of the amplicons. Amplicons were sent to the National Museum of Natural History (MNHN) in Paris, France for sequencing with a Miseq 2x250 standard V2.

Sequence assembly and alignment

The obtained raw DNA sequences were processed using Geneious Prime 2019 v1.8.0 (https://www.geneious.com) with the settings "paired reads, merging paired reads, trimming of low quality ends with the minimum quality set to 20" using the BBDuk trimmer in Geneious. The "map to reference" approach was used to assemble the sequences using the medium-low

sensitivity parameters with the maximum of mismatches per read set to 5% with 25 iterations. The COI to COII segment from the complete mitogenomes of two *Eusirus* cf. *giganteus* G1 and G2 (GenBank accession nrs. OK489458 and OK489459, respectively) was used as a reference sequence to assemble the mitochondrial COI to COII fragment. The complete 18S sequences of *Eusirus* cf. *microps* and *Eusirus perdentatus* (GenBank accession nrs. DQ378011 and DQ378012, respectively) were used for the 18S sequence assembly while the 28S partial sequence of *Eusirus giganteus* (GenBank accession nr. KT808714) was used for the 28S sequence assembly. The assembled COI to COII fragment was sent to MITOS web server version 2 (Donath et al., 2019) for automatic annotations. Additional annotations were conducted using the 'annotate from database' option in Geneious and compared with the annotations from MITOS. The COI and COII annotated sequences were also subjected to BLASTN searches (Altschul et al., 1997) to verify the identity of the sequences. Similarly, the 18S and 28S assembled sequences were subjected to BLASTN searches (Altschul et al., 1997) to check for annotations and to verify the identity of the sequence data. The annotated COI to COII fragments were further verified through BLASTP searches.

Sequences for each gene were subsequently aligned separately with the outgroups *Rhachotropis schellenbergi* and *Rhachotropis antarctica*. *Rhachotropis* sequences for 18S and 28S were retrieved from GenBank. The 18S sequences of *R. schellenbergi* and *R. antarctica* have GenBank accession nrs. KT808758 and KT808757, respectively while the 28S sequences have GenBank accession nrs. KT808739 and KT808738, respectively. COI sequences of *R. schellenbergi* and *R. antarctica* were retrieved from Verheye (2011). COI and COII sequences were aligned separately with MUSCLE (Edgar, 2004) in MEGA X (Kumar et al., 2018) and translated into amino acids to check for premature stop codons which could indicate pseudogenes. The 18S and 28S sequences were aligned with MAFFT version 7 (Katoh & Standley, 2013) (online server: http://mafft.cbrc.jp/alignment/server/) using the default settings. Aliscore version 2.0 (Misof & Misof, 2009) was used to identify poorly aligned regions and Alicut version 2.3 was used to remove any identified poorly aligned regions.

Phylogenetic reconstruction

The Xia et al. (2003) test implemented in DAMBE version 7.3.11 (Xia, 2018) was used to test for substitution saturation in the alignments of each gene using unambiguous sites only.

Sequences have experienced substitution saturation if the observed index of substitution saturation (I_{ss}) is significantly higher than the critical index of substitution saturation ($I_{ss.c}$) suggesting that they should not be utilized in phylogenetic reconstructions (Xia et al., 2003). Preliminary phylogenetic trees were constructed using Bayesian inference (BI) and Maximum likelihood (ML) methods for each dataset to evaluate the congruence between genes. Only sequences with complete 18S, 28S, COI, and COII sequences were used for these analyses. Three trees were constructed: from the 1) 18S dataset, 2) 28S dataset, and 3) a concatenated COI and COII dataset. COI and COII were concatenated using Geneious. Best-fitting evolutionary models were selected using the Bayesian Information Criterion (BIC) implemented in the jModelTest 2.1.7 (Darriba et al., 2012) for the 18S and 28S dataset. For the concatenated COI and COII dataset, BIC from Partitionfinder 2.1.1 (Lanfear et al., 2016) was used. The model selected for the 18S dataset was TIM3+G while K80+G was the best model for the 28S dataset. The SYM+I+G model was selected for codon position 1; the TRN+I+G model for codon position 2; and the GTR+G model for codon position 3 of the COI and COII data set.

Since the topologies of individual gene trees appeared to be congruent, DNA sequence data of the four molecular markers were concatenated to produce the best supported and resolved phylogeny using Bayesian inference (BI) and Maximum likelihood (ML) methods. Best-fitting evolutionary models were selected using the Bayesian Information Criterion (BIC) implemented in Partitionfinder.

ML trees were constructed using PhyML 3.0 (Guindon & Gascuel, 2003) with 1000 bootstrap replications for the 18S and 28S dataset and the model of molecular evolution identified by jModelTest. RAxML 8.2.12 (Stamatakis, 2014) in the CIPRES portal (Miller et al., 2010) was used for concatenated COI and COII dataset with the model identified with Partitionfinder and 1000 bootstrap replicates. RAxML was also used for the concatenated dataset consisting of four markers and using the model identified by Partitionfinder and 1000 bootstrap replicates. Nodes with bootstrap values (BV) ≥70 were regarded as well supported.

BI trees were constructed with MrBayes 3.2.7 (Ronquist & Huelsenbeck, 2003) in the CIPRES portal with 10 million generations. Trees were sampled every 1000th generation and 10% of the initial trees were discarded as burn-in. The convergence of parameters and effective sample size was examined with Tracer version 1.7.1 (Rambaut et al., 2018). Resulting trees

were viewed with FigTree version 1.4.4 (available at http://tree.bio.ed.ac.uk/software/figtree/0). Nodes were regarded as statistically supported if they had a posterior probability (PP) ≥ 0.95.

Molecular dating

Molecular dating was performed in BEAST version 2.6.7 (Bouckaert et al., 2014). A reduced dataset of one individual per phylogenetic clade with the most complete DNA sequence data concerning the number of markers each was used to improve computing efficiency and accuracy, similar to Copilaş-Ciocianu & Petrusek (2017) and Copilaş-Ciocianu et al. (2019). Cryptic diversity is known in polar *Eusirus* amphipods therefore, the phylogenetic clades were treated as putative genetic species. However, this was not statistically checked as this is beyond the scope of the thesis.

Each marker was treated as a separate partition with an unlinked site and clock model. The bModelTest version 1.2.1 package implemented in BEAST2 was used to estimate the parameters of the site model (including the substitution model defining the relative rates of different classes of substitutions, a model of rate heterogeneity across sites and/or a proportion of invariable sites). bModelTest uses a reversible jump Markov chain Monte Carlo (MCMC) that lets the Markov chain switch between substitution models in Bayesian MCMC inference. This allows the integration of all sampled substitution models while estimating the phylogeny and other model parameters (Bouckaert & Drummond, 2017).

The strict clock and uncorrelated relaxed clock models were used to investigate the clock-likeness of the data. The strict clock model assumes the same evolutionary rate for each branch in a phylogenetic tree. The uncorrelated relaxed molecular clock models assumes that each branch of the phylogenetic tree has its own independent rate drawn from a single shared parametric rate distribution (Drummond & Bouckaert, 2015). Both the uncorrelated log-normal relaxed molecular clock (UCLN) and uncorrelated exponential (UCED) models were implemented together with the Yule and Birth Death models as tree priors. The MCMC chain was run for 100 million generations, with a sampling frequency of 4000. Convergence of parameters and effective sample size was checked in Tracer version 1.7.1 (Rambaut et al., 2014). The maximum clade credibility tree with mean nodal height was produced with 10% of the trees discarded as burn-in in TreeAnnotator version 2.6.3.

A path-sampling analysis was used to select the best clock and tree models (Gelman & Meng, 1998; Lartillot & Philippe, 2006; Drummond & Bouckaert, 2015). The path-sampling analysis estimating the marginal likelihood (MLE) is implemented in the MODEL_SELECTION version 1.5.3 package in BEAST2 (Drummond & Bouckaert, 2015). For each path sampling analysis, 100 steps with a chain length of 1 million and a preburn-in of 100,000 were set. The relative support of the two models was assessed based on the log Bayes Factor (BF), calculated by taking the difference between the log marginal likelihoods of the two models expressed as $\log_e BF(M_0, M_1) = \log_e P(X|M_0) - \log_e P(X|M_1)$, where $\log_e P(X|M_i)$ is the marginal $\log_e$-likelihood estimate for the model Mi. According to the interpretation of Bayes Factors by Kass & Raftery (1995), the strength of support for a given model was determined based on the $2*\log_e(BF)$ and B_{10} values (see table 2 for details).

Table 2. Interpretation of Bayes Factors as indicated by Kass & Raftery (1995)

$2\log_e(BF)$	B_{10}	Evidence against the null model (M_0)
0 to 2	1 to 3	Barely worth a mention
2 to 6	3 to 20	Positive
6 to 10	20 to 150	Strong
>10	>150	Very strong

There are very few records of fossil amphipods (Zaddach, 1864; Lucks, 1927; Just, 1974; Karaman, 1984; Mukai & Takeda, 1987; Bousfield & Poinar, 1994; 1995; Jażdżewski & Kulicka, 2000; 2002; Coleman & Myers, 2001; Coleman & Ruffo, 2002; Weitschat et al., 2002; Coleman, 2004; 2006; Jażdżewski & Kupryjanowicz, 2010; McMenamin et al., 2013; Jażdżewski et al., 2014; Hegna et al., 2020; Jarzembowski et al., 2020) limiting the applicability of fossil data for molecular dating (Verheye et al., 2017). This scarcity can be attributed to their thin cuticle making amphipods difficult to fossilize well (Verheye et al., 2017; Jarzembowski et al., 2020). Moreover, most of the recorded aquatic amphipod fossils are from freshwater environments (Zaddach, 1864; Lucks, 1927; Just, 1974; Karaman, 1984; Coleman & Myers, 2001; Coleman & Ruffo, 2002; Jażdżewski & Kulicka, 2002; Jażdżewski et al., 2014; Arfianti et al., 2018) and are phylogenetically distant to *Eusirus* (Verheye et al., 2016; Copilaş-Ciocianu et al., 2020). In the absence of fossil data, geological events and dating results from other studies were used together with available substitution rates from existing publications. To account for

uncertainty, a normal distribution calibration prior was specified. The first calibration was placed at the node of the most recent common ancestor (MRCA) of the Antarctic clade; this was based on the opening of the Drake passage and the onset of the Antarctic Circumpolar Current (ACC) around 34-26 Ma. This geological event likely caused a marine biological barrier that prevented gene flow (Thornhill et al., 2008), which is a requirement for vicariance and subsequent allopatric speciation. The second calibration was set at the root where the *Eusirus* and *Rhachotropis* diverged. The age when the sister genera of *Eusirus* and *Rhachotropis* split was estimated as 66.9 Ma (HPD interval 37.2-99.7 Ma) by Copilaş-Ciocianu et al. (2020). The third calibration was based on the substitution rates of COI, 28S, and 18S as inferred for amphipods from the Crangonyctidae family in the study of Copilaş-Ciocianu et al. (2019). A normal distribution and a mean of 0.01773 substitutions/site/Ma (± 0.00441) was applied for the prior rate of COI, and a mean of 0.00161 substitutions/site/Ma (± 0.00036) and a normal distribution was set for the 28S prior. The prior rate for the 18S was set as a normal distribution with a mean of 0.00068 substitutions/site/Ma (± 0.00016). The same rate with a mean of 0.01773 substitutions/site/Ma (± 0.00441) and a normal distribution as for COI was also used for the COII rate prior since to our knowledge, no estimates of COII rates are currently available for amphipods.

Diversification rates analyses

Intraspecific polymorphisms have a significant impact on the diversification rate as they can cause a false increase in diversification rates during the most recent history of a clade (Mamos et al., 2016; Verheye et al., 2017). Consequently, a reduced dataset including only one individual per phylogenetic clade was used to explore the tempo of lineage diversification in *Eusirus*.

First, a lineage through time (LTT) plot was constructed by using the R-package phytools (Revell, 2012) to visualize the pattern of lineage accumulation during the evolutionary history of *Eusirus*. Then, speciation rate (λ) and extinction rates (μ) were estimated by fitting the empirical *Eusirus* phylogeny to the pure-birth and birth-death models, taking into account the incomplete sampling fraction. The estimates were then used to simulate 100 trees under the pure-birth and birth-death models and the mean LTT of these simulated trees were plotted with a 95% confidence interval along with the LTT plot of the empirical *Eusirus* phylogeny.

To test for deviations from a pure-birth model, the gamma (γ) statistic was computed and assessed using the Monte Carlo constant rates (MCCR) test, taking incomplete sampling into account (Pybus and Harvey 2000) by using the LASER R-package (Rabosky, 2006). A phylogeny's internal nodes are closer to its tips than would be expected under the pure birth process when gamma is positive, while a negative gamma value indicates that the internal nodes are closer to the root than expected by the pure birth model. The latter would support a deceleration in diversification rate through time, suggesting an early burst of diversification (Pybus and Harvey 2000; Fordyce, 2010).

Then, the fit of the four models for lineage accumulation was compared with the R-package LASER. The two constant-rate models consisted of pure-birth (PB) with a constant speciation rate (λ) and no extinction, and the birth-death (BD) model with a constant speciation rate (λ) and extinction rate (μ). Also, two density-dependent models were applied and compared: the density-dependent exponential (DDX) and density-dependent logistic (DDL) models. These density-dependent models predict declines in the diversification rates; in the DDX model, the divergence rate is influenced by the initial speciation rate, the number of lineages at a given time and the magnitude of rate change while in the DDL model, the divergence rate is influenced by the initial speciation, the number of lineages at a given time, and the carry capacity (Rabosky, 2006; Rabosky & Lovette, 2008). The Akaike Information Criterion (AIC) was used to compare the fit of these models (Burnham & Anderson, 2002). The delta AIC (dAIC) and the Aikaike weights (wAIC) were also calculated to check for the relative likelihood of each model.

Additionally, the fit of different models with time-varying rates and potentially missing extant species was performed following the method of Morlon et al. (2011) in the R package RPANDA (Morlon et al., 2016). Birth is denoted by B and death is denoted by D. The models compared were: 1) B constant: has constant speciation λ and no extinction μ (= PB model) ; 2) BD constant: both λ and μ are constant (= BD model); 3) B variable: exponential variation in λ through time and no μ; 4) B variable, D constant: constant μ and exponential variation in λ; 5) B constant, D variable: constant λ and exponential variation in μ; 6) BD variable: exponential variation in both λ and μ. These six models were also compared using AIC scores and weights. Finally, the Bayesian Analysis of Macroevolutionary Mixtures (BAMM) program (Rabosky, 2014) was applied to check if there was a more complex variation in the tempo of speciation during the evolution of *Eusirus*. Priors were generated with the BAMMtools R-package

(Rabosky et al., 2014) and the MCMC analysis was run for 10 million generations, sampling every 5000 generations. Convergence of the MCMC analysis was assessed after discarding 10% of the samples as burn-in, by checking the effective sample sizes (ESS) and the number of shifts in each sample using the R package CODA (Plummer et al., 2006). The outputs from BAMM analysis were used in BAMMtools.

Results

Data overview

The concatenated DNA sequences including the 18S and 28S ribosomal DNA and the mitochondrial genes COI and COII had a total length of 7,202 bp which. The length of each gene partition, the number of variable sites, and the best-fitting evolutionary model per gene partition and per codon position for the mitochondrial COI and COII genes are provided in Table 3.

Table 3. Length of each gene, number of variable sites, and the best-fitting evolutionary model for each gene partition with the coding genes COI and COII partitioned by codon position.

Gene Partition	Length (bp)	Variable sites	Model
18S	3421	1013	GTR+G
28S	1543	782	K80+G
COI_pos1			HKY+I+G
COI_pos2	1539	822	TRN+G
COI_pos3			HKY+I+G
COII_pos1			TRN+G
COII_pos2	699	360	TRN+G
COII_pos3			TRN+G

Phylogenetic reconstruction

No significant saturation was detected for all four markers (P<0.0001) (Supplementary table 4). Since the topologies of individual gene trees were congruent, the four markers were concatenated to reconstruct the phylogeny of *Eusirus*.

The BI and ML analyses based on the concatenated datasets both supported the monophyly of the Antarctic clade (posterior probability (PP) = 1; bootstrap value (BV) = 100) (Figure 1). The Arctic taxonomic group showed polyphyly with *Eusirus minutus* appearing as a sister lineage to a clade grouping non-polar species and the Arctic species *Eusirus propinqvuus* and *Eusirus cuspidatus* (Figure 1). The polyphyly of the Arctic *Eusirus* is consistently well supported by both BI and ML analyses (Figure 1).

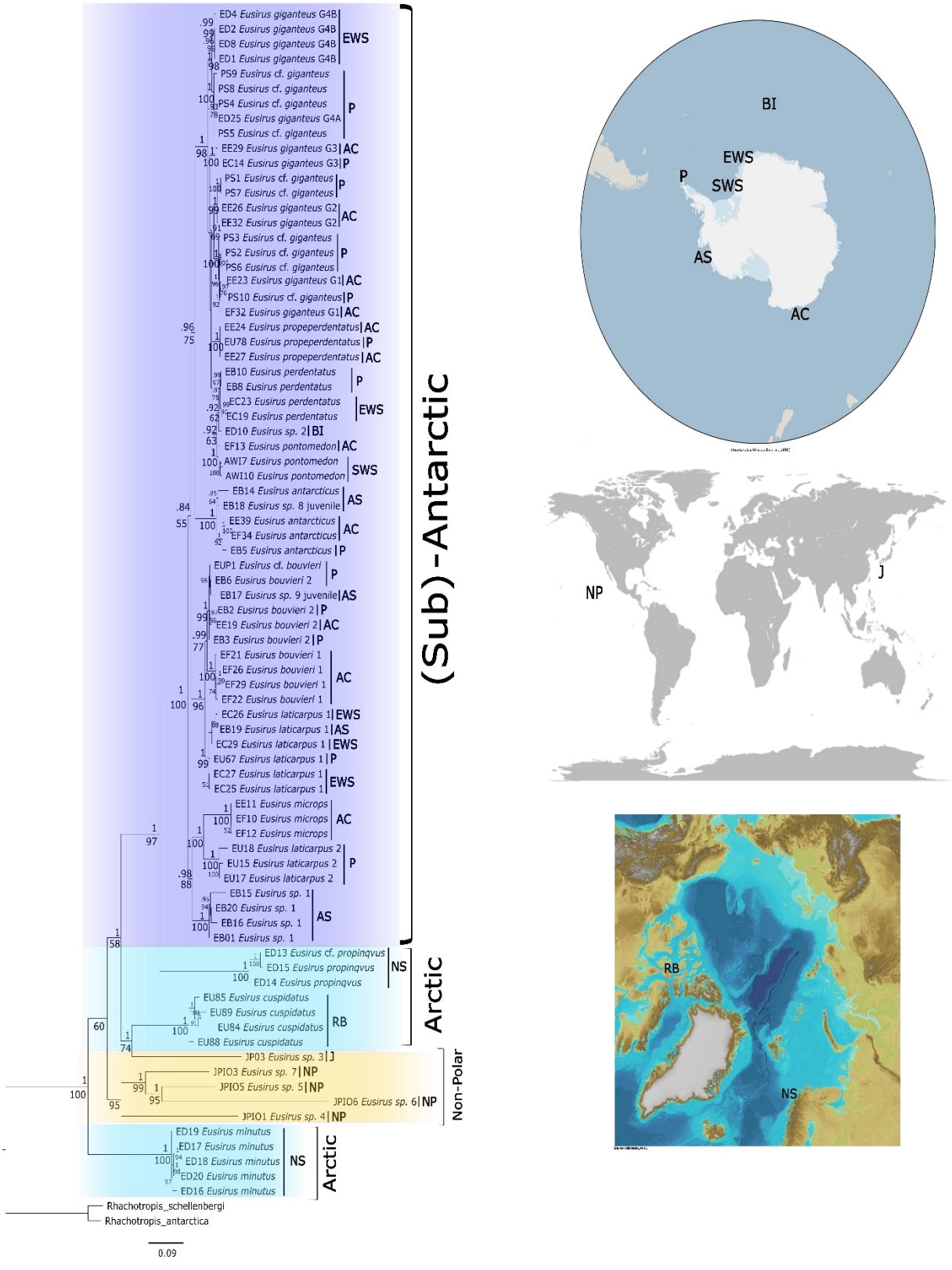

Figure 1. Phylogenetic tree obtained from the concatenated 18S, 28S, COI, and COII sequences using MrBayes and RAxML. Only bootstrap values of ≥50 (above the nodes) and posterior probabilities >0.80 (below the nodes) are shown. The scale bar corresponds to the number of substitutions per site. The maps show the geographical origins of the specimens which are also shown in the phylogenetic tree next to the names of the species. Antarctica: Peninsula (P); Amundsen Sea (AS); Adelie Coast (AC); East Weddell Sea (EWS); Southern Weddell Sea (SWS). Sub-Antarctic: Bouvet Island (BI). Arctic: Resolute Bay (RB); Norwegian Sea (NS). Non-Polar: Japan (J); North Pacific (NP).

Within the monophyletic Antarctic clade, the *Eusirus giganteus* complex, *Eusirus perdentatus*, *Eusirus pontomedon, and Eusirus propeperdentatus* formed a well-supported monophyletic clade (PP = 1; BV = 98) (Figure 1). Moreover, the presence of five putative species identified within the *Eusirus giganteus* complex is strongly supported by both ML and BI methods. The support for each putative species are as follows: *Eusirus giganteus* G4B (PP = 0.99; BV = 99); *Eusirus giganteus* G4A (PP = 1; BV = 100); *Eusirus giganteus* G3 (PP = 1 ; BV = 100); *Eusirus giganteus* G2 (PP = 1; BV = 99); and *Eusirus giganteus* G1 (PP = 1; BV = 100) (Figure 1). Two phylogenetic groups within the morphospecies *Eusirus bouvieri* and *Eusirus laticarpus* were also identified: *Eusirus bouvieri* 1 (PP = 1; BV = 100); *Eusirus bouvieri* 2 (PP = 1; BV = 100); *Eusirus bouvieri* 1 (PP = 1; BV = 99); *Eusirus laticarpus* 1 (PP = 1; BV = 99); *Eusirus laticarpus* 2(PP = 1; BV = 100) (Figure 1).

Molecular dating

Maximum likelihood estimates (MLE) from the path-sampling analysis and the log BF are provided in Table 4. Based on the BF, there is a very strong support for the uncorrelated lognormal clock (UCLN) as compared to the strict and uncorrelated exponential clock (UCED). For the two tree models: Birth-Death and Yule, there is a very strong support for the Yule model.

Table 4. Maximum likelihood estimates (MLE) retrieved from the path-sampling analysis and the log Bayes Factor (BF). The support for the three clock models (Strict, UCLN, and UCED) and the two tree models (Yule and Birth-death) was analysed by comparing the pairwise differences between the log marginal likelihoods of two models each (M1-M2). In the table, the alternative Model 2 (M2) for each comparison is given inside the brackets. A positive BF indicates support for Model 1 (M1) while a negative BF indicates support for Model 2 (M2). Interpretation of the strength of support for a given model is provided in Table 2.

	MLE	BF
Strict (UCLN)	-39312,0203	-5,70908823
UCLN (UCED)	-39306,3113	785,9727652
UCED (Strict)	-40092,284	-780,263677
Birth-death (Yule)	-39458,9592	-152,6479282

The mean age of the Antarctic clade was estimated at 29.51 million years (Ma) around the Oligocene (95% HPD: 25.78-33.29 Ma) (Figure 2). The divergence between the Antarctic clade and the Arctic *Eusirus propinqvuus* occurred during the Eocene at a mean 48.72 Ma (95% HPD: 35.71-62.9 Ma). Divergence between the two Arctic lineage, *Eusirus minutus* and *Eusirus*

cuspidatus was estimated at 63.47 Ma (95% HPD: 43.63-81.54 Ma), roughly during the Paleocene, even if this divergence is not strongly supported with a posterior probability being below 0.95. The polyphyly of the Arctic *Eusirus* observed in the time-calibrated tree (Figure 2) is consistent with the phylogenetic tree obtained by BI and ML analyses (Figure 1). The mean age of the speciation event between the non-polar *Eusirus* clade and the Arctic *Eusirus minutus* and *Eusirus cuspidatus* is estimated at 71.83 Ma (95% HPD: 55.69-88.99 Ma) around the late Cretaceous.

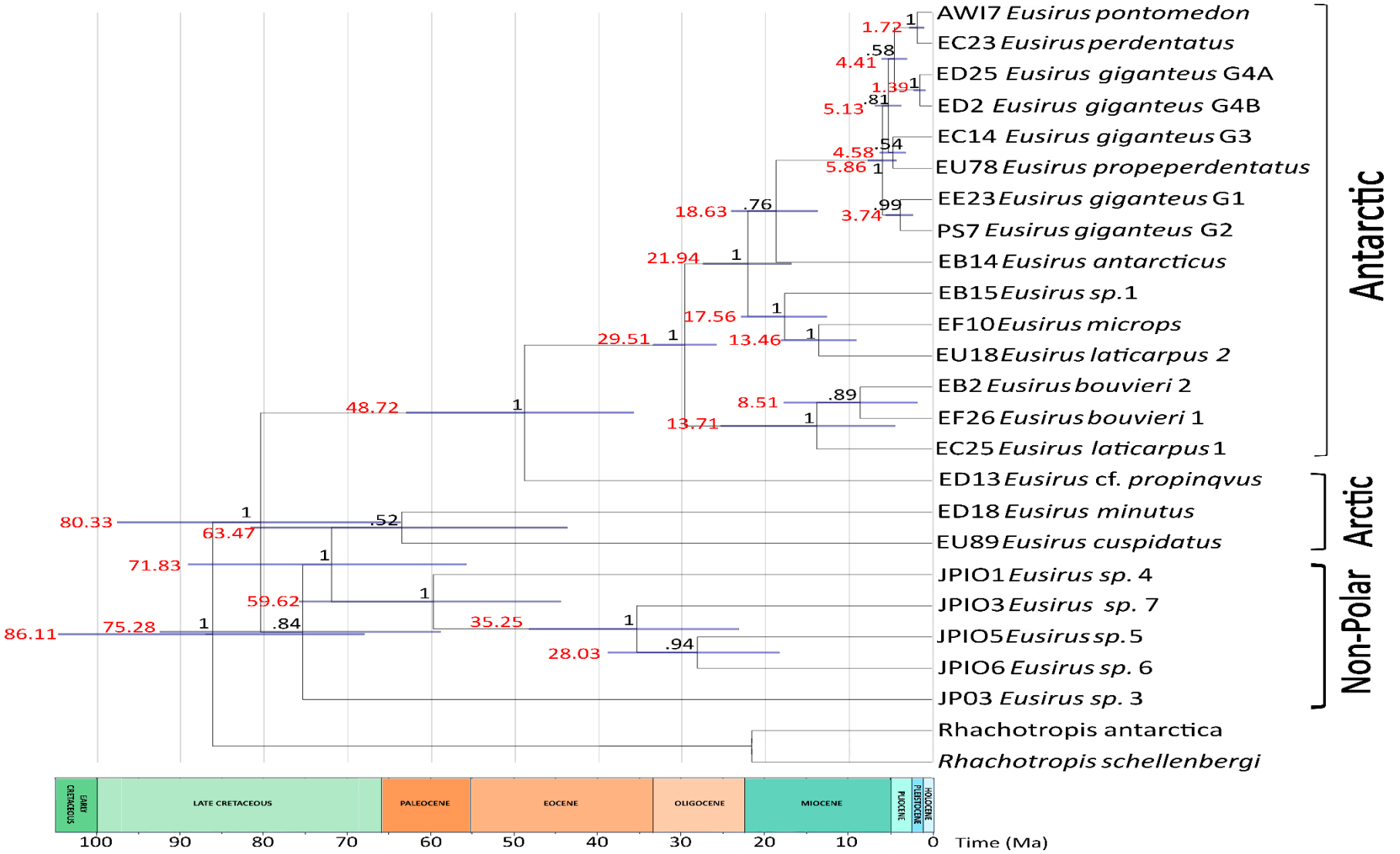

Figure 2. Maximum clade credibility chronogram generated from the BEAST analysis based on the full concatenated dataset (18S, 28S, COI, and COII) data set. The timescale is in million years (Ma). The posterior probabilities are shown on the nodes. Blue bars indicate the 95% HPD intervals. Mean nodes ages are indicated before the blue bars in red.

Diversification rates analyses

The lineage through time plot obtained from the empirical *Eusirus* phylogeny showed no deviations from the trees simulated under the pure-birth and birth-death models (Figure 3). We did not find any support for a deceleration or a burst of diversification in the *Eusirus* phylogeny with a positive gamma statistic (γ = 0.61), the null hypothesis of a constant rate of speciation was not rejected by the MCCR test (MCCR test: p-value= 0.89).

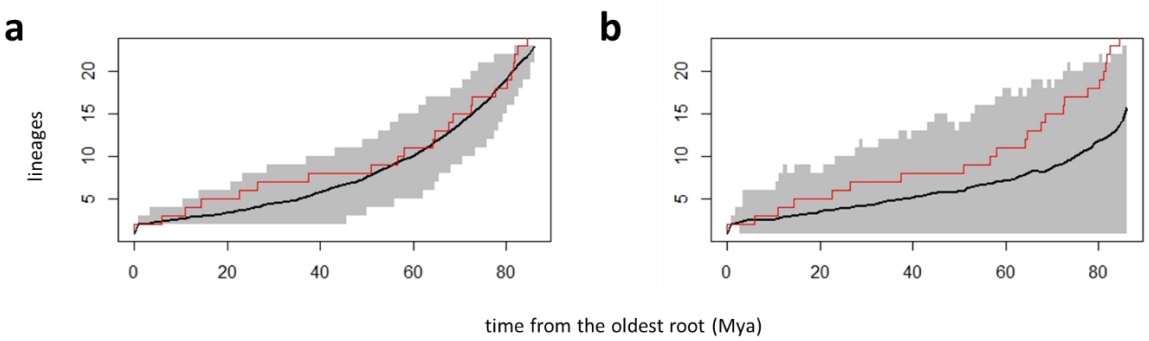

Figure 3. Lineage through time (LTT) plot obtained with the empirical *Eusirus* phylogeny (red line). Mean LTT plot (black line) and 95% confidence interval (gray shaded area) for 100 trees simulated under a) pure-birth and b) birth-death models.

Comparing lineage diversification models did not support a high rate of speciation early in the history of *Eusirus* followed by a decreasing speciation rate (Tables 5 & 6). Instead, the best fitting models were the ones considering a constant rate of speciation (PB in Laser and B constant in RPANDA). The dAIC between these best models and the others was not higher than four, indicating that more complex models including extinction cannot be rejected.

Table 5. Results of fitting diversification-process models using LASER. The best-fitting model is indicated in bold. The models compared were: pure-birth (PB), birth-death (BD), density-dependent exponential (DDX), and density-dependent logistic (DDL) models. The AIC of each model was calculated. dAIC is the delta AIC while the wAIC is the Aikaike weight. LHmax is the log-likelihood at the maximum. Parameters are abbreviated as: r1= the speciation rate, r= net diversification rate, a= extinction fraction, r0= initial speciation rate, xp= x parameter in the DDX model, and the kp= K parameter in the DDL model.

Model	AIC	dAIC	wAIC	LHmax	Parameters
PB	**102.058**	**0**	**0.45**	**-50.03**	**r1=0.03**
BD	103.575	1.52	0.21	-49.79	r=0.02; a=0.42
DDX	104.022	1.96	0.17	-50.01	r0=0.04; xp=0.07
DDL	104.058	2.00	0.17	-50.03	r0=0.029; kp=407768.3

Table 6. Results of fitting diversification-process models using RPANDA. The best-fitting model is indicated in bold. The models compared were: B constant: constant speciation rate and no extinction; BD constant: both speciation and extinction rates are constant; B variable: exponential variation in speciation rate through time and no extinction; B variable, D constant: constant extinction and exponential variation in speciation rate; B constant, D variable: constant speciation rate and exponential variation in extinction rate; 6) BD variable: exponential variation in both speciation and extinction rates. The AIC of each model was calculated. dAIC is the delta AIC while the wAIC is the Aikaike weight. LHmax is the log-likelihood at the maximum. Parameters are abbreviated as: λ= speciation rate when constant or the initial speciation rate when variable, μ= extinction rate when constant or the initial extinction rate when variable, α= rate of change parameter for the exponential variation of the speciation rate over time; β = rate of change parameter for the exponential variation of the extinction rate.

Model	AICc	dAICc	wAICc	LHmax	Parameters
B constant	**213.07**	**0**	**0.32**	**-105.45**	**λ=0.035**
BD constant	213.69	0.63	0.23	-104.57	λ=0.06; μ= 0.04
B variable	214.62	1.56	0.15	-105.04	λ=0.04; α= -0.01
B variable, D constant	214.58	1.52	0.15	-103.72	λ=0.08; α= 0.01; μ=0.11
B constant, D variable	215.07	2.00	0.12	-103.96	λ=0.08; μ=0.11; β= -0.02
BD variable	217.13	4.06	0.04	-103.56	λ=0.07; α=0.03; μ=0.10; β=0.02

Besides these results indicating a constant rate of speciation in *Eusirus*, BAMM allowed the refinement of our conclusions. Indeed, the results of BAMM analysis suggested the presence of speciation rate shifts along the time-calibrated phylogeny of *Eusirus* (Figure 4). The one rate shift model showed the highest probability (PP= 0.62) as compared to the others. Additional support for one rate shift as the best model was also obtained from the Bayes Factor (Table 7).

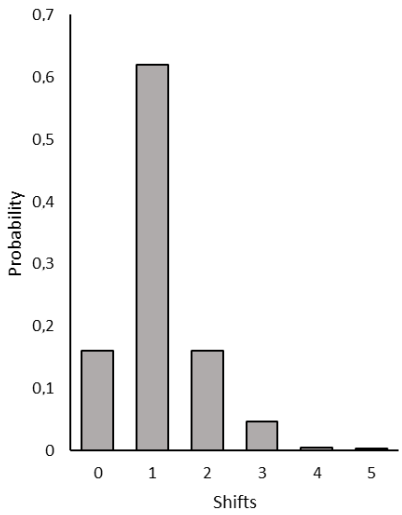

Figure 4. Posterior probability distribution of the number of rate shifts in the *Eusirus* data.

Table 7. Bayes factors (BF) of pairwise model comparisons. The best model is indicated in bold. Numerators are given as columns and the denominator model as rows. There is higher support for the numerator model if the BF is >1 while a BF <1 indicates higher support for the denominator model. Interpretation of the strength of support for a given model is provided in Table 2.

	1 shift	2 shifts	3 shifts	4 shifts	5 shifts
0 shift	**7.49**	3.99	2.27	0.54	0.76

The 95% credible sets from BAMM indicated that the Antarctic lineages did not follow the same pattern of speciation rates as the Artic and non-polar lineages. Indeed, Figures 5a, c & d show that 62% of the samples in the posterior can be assigned to a single shift configuration where an accelerated rate of diversification event is observed at the branch leading to the Antarctic clades. Specifically, 46% of the samples in the posterior had a core shift on the branch leading to the Antarctic clade diversification (Figure 5a) while 12% had one core shift on the branch leading to the diversification of *Eusirus giganteus* and *Eusirus perdentatus* complexes (Figure 5c) as well as to *Eusirus propeperdentatus* and 4.3% had a core shift on the branch which is proximate to the MRCA node of the Antarctic clade (Figure 5d). On the other hand, 34% of the samples in the posterior had zero core shifts (Figure 5b).

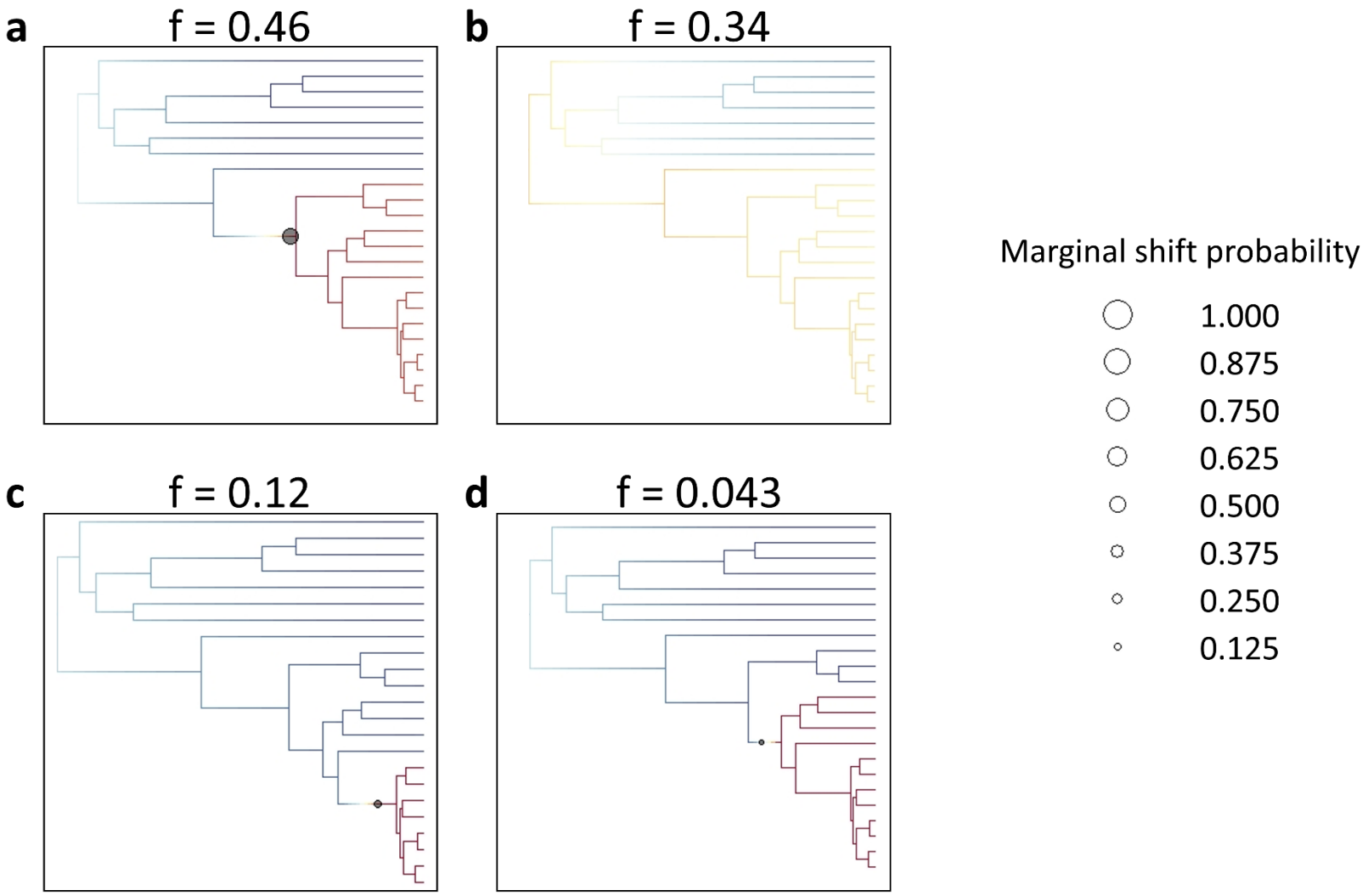

Figure 5. Phylorate plots (i.e. plots that show the instantaneous rates of diversification along the branches of the tree) for each shift configurations with the posterior probability indicated above each plot. Warmer colors indicate high rates of diversification while colder colors indicate low rates of diversification. Circles imply the location of rate shifts while the size of the circle is proportional to the overall marginal probability of the shift.

Discussion

The monophyly of the Antarctic component of the *Eusirus* genus has been previously suggested by Verheye (2011) based on DNA sequence data from COI and 28S. Our new phylogenies based on a much larger data set including the full COI and COII genes together with the 18S and 28S genes still support the monophyly of the (sub)-Antarctic clade (Figure 1). Our data demonstrate that *Eusirus* species occurring in the Arctic are a non-monophyletic group. Conversely to the scenario observed in Antarctic, *Eusirus* thus colonized the Arctic Ocean multiple times during its evolutionary history. A constant speciation rate model would explain the diversity of *Eusirus* at the largest phylogenetic scale. However, different regimes of speciation rate were detected with a burst of lineage diversification on the Antarctic clade and lower diversification rates on the Arctic and non-polar lineages (Figure 5).

Origin of the Polar *Eusirus*

Verheye (2011) suggested that Antarctic *Eusirus* diverged around 4-13.7 Ma setting the COI gene substitution rates to a minimum value of 1.4% and a maximum of 4.8%. Our dated phylogeny using three different calibrations as well as uncorrelated lognormal clock (UCLN) and the Yule models provided a much older age estimate of 29.51 Ma [95% HPD: 25.78-33.29 Ma] (Figure 2). The timing of Antarctic clade diversification coincides with the opening of the Drake passage around the late Eocene to Oligocene (34-26 Ma) after the separation of South America and Antarctica which subsequently caused the formation of the Antarctic circumpolar current (ACC) during the Oligocene (31-26 Ma) (Latimer & Filippelli, 2002; Lawver & Gahagan, 2003; Hodel et al., 2021; Vincze et al., 2021). The Eocene-Oligocene transition was also characterized by decreasing temperatures and increasing glaciation with the start of ice sheets expansion throughout the continent by the Oligocene around 34 Ma (Ingólfsson, 2004; Rogers, 2007; Lurcock & Florindo, 2017). The decreasing temperatures during the Eocene-Oligocene transition caused significant extinctions with warm-adapted taxa being replaced by species with cold adaptations (Coxall & Pearson, 2007; Hutchinson et al., 2021). Formerly occupied niches became available as a result of these extinctions and supplied surviving lineages with ecological opportunities (Brandt, 1999; Rogers, 2007; Verheye et al., 2017) which was assumed to have driven initial rapid lineage diversification (Rogers, 2007; Rabosky & Lovette, 2008; Yoder et al., 2010; Stroud & Losos, 2016; Verheye et al., 2017). A major marine biological

barrier was also established as a result of the opening of the Drake passage and the subsequent formation of the ACC which was followed by vicariant and subsequent allopatric speciation (Rogers, 2007; Thornhill et al., 2008). As observed in our time-calibrated tree (Figure 2), the *Eusirus* species radiated in the Antarctic when the temperatures were decreasing and when the Antarctic was already isolated from the other continents that were once part of the Gondwanaland.

The Arctic lineages followed different speciation events that took place at various times along the timeline, showing a varied history of lineage splitting with a mean age of 48.72 Ma [95% HPD: 35.71-62.9 Ma for *Eusirus propinqvus* (Figure 2). A mean age of around 63.47 Ma [95% HPD: 43.63-81.54 Ma] for the divergence between *Eusirus minutus* and *Eusirus cuspidatus* was observed (Figure 2). The varied origins suggest multiple adaptations to different ecological niches driven by dispersal events. During the late Cretaceous, a connection between the Arctic Ocean and two subtropical seaways was formed facilitating limited exchanges of species with evolutionary affinities to warm water along these seaways (Dunton, 1992; Dayton et al., 1994; Dayton, 2013). Around the end of the Cretaceous (80-100 Ma), the deep water connection of the North Pacific Ocean with the Arctic Ocean was closed (Marincovich et al., 1985; Dunton, 1992). It was also around this time when the Western Interior Seaway closed (about 65.5-70.6 ma), significantly isolating the Arctic Ocean (Marincovich et al., 1985; Dunton, 1992; Dayton et al., 1994; O'Regan et al., 2011; Dayton, 2013). Abyssal and bathyal fauna exchanges between the North Pacific and the Arctic ended when this connection closed (Dunton, 1992). Around 70 Ma, the higher latitudes of the Arctic Ocean were still ice-free and temperatures started to decrease around 65.5 Ma (O'Regan et al., 2011). Widening of the North Atlantic into the Arctic Ocean occurred around late Paleocene (about 56 Ma) (Brozena et al., 2003; Clarke & Crame, 2010; O'Regan et al., 2011). Exchanges between the Atlantic and the Arctic oceans started around 40 Ma which allowed species with Atlantic affinities to dominate the Arctic Ocean at this time (Clarke & Crame, 2010). During this period, the Arctic Ocean experienced increased temperatures (Sluijs et al., 2006; Zachos et al., 2008; Sluijs et al., 2009; O'Regan et al., 2011) with the seasonal absence of ice being a common occurrence in the marginal and central Arctic Ocean (Cronin & Cronin, 2015). The beginning of declining temperature was recorded around 48-45 ma which coincided with the onset of the winter sea ice formation (O'Regan et al., 2011; Cronin & Cronin, 2015). Deep waters of the Atlantic and Arctic oceans

were connect by the formation of the Fram Strait around 35-27 Ma (Dunton, 1992; Serreze & Barry, 2005; Kuklinski et al., 2013; Legezyñska et al., 2020). Cool temperate biota with origins from the Northern Atlantic thrived with declining temperatures (Wilce, 1990; Dunton, 1992). The differences in the timing suggest that distinct geological and climatic events have led to multiple diversification of the Arctic *Eusirus* species. The formation of these different connections provided various dispersal routes towards the Arctic Ocean as reflected by the varied origins of Arctic *Eusirus*. Moreover, the Arctic *Eusirus* species appear to have originated prior to the glacial/interglacial periods. However, there is no support in the node leading to the divergence of the *Eusirus minutus* and *Eusirus cuspidatus* indicating uncertainty in their divergence and similar age of origin. The non-polar *Eusirus* species seem to have originated earlier than the polar *Eusirus* species (Figure 2) with a mean age of 75.28 Ma [95% HPD: 58.82-92.41 Ma]. The basal position of the non-polar species suggests a non-polar origin of the genus *Eusirus* prior to the radiation of the genus to the polar environments. However, the precise origin of the *Eusirus* ancestors cannot be determined as additional data would be needed. It is recommended to include more species from additional locations of the non-polar regions for future phylogenetic reconstructions. Moreover, the main focus was to test for the monophyly of polar *Eusirus* species and not the non-polar ones.

Our results from *Eusirus* confirmed a general trend in the origin of the benthic fauna of Antarctica. Indeed, monophyly has also been observed in other Antarctic benthic taxa such as Antarctic Epimeria and Iphimediidae amphipods, isopods (Antarctic Serolidae), echinoderms (Antarctic Ctenocidarinae), decapods (Antarctic Notocangron), and fish (Antarctic Notothenioidei) (Held, 2000; David et al., 2005; Lockhart, 2006; Lecointre, 2012; Lecointre et al., 2013; Verheye, 2017; Verheye et al., 2017). Similarly, the polyphyly noted in the Arctic assemblage of *Eusirus* has also been found in other taxa like fishes (Stichaeidae) (Hotaling et al., 2021).

Diversification rates

When considering the entire dated tree, the tempo of speciation observed in *Eusirus* amphipods is constant but, in fact, quite heterogeneous among subclades. BAMM analyses allowed to identify different regimes of speciation rates; the Antarctic clade showed higher rates of speciation than the Arctic and the non-polar lineages. According to the observed burst of speciation, the evolution of the Antarctic clade seemed to follow a scenario of adaptive

radiation (Schluter, 2000). The initial diversification of Antarctic *Eusirus* clade occurred 29.51 ma [95% HPD: 25.78-33.29 Ma] around the Oligocene. Thermal isolation of the Antarctic as a result of the opening of the Drake passage and the formation of the ACC was then followed by vicariant events of some Antarctic taxa such as sea urchins (*Sterechinus neumayeri* and clades within the Ctenocidarines) and krill (*Euphausia superba* and *Euphausia crystallorophias*) (Patarnello et al., 1996; Lee et al., 2004; Lockhart, 2006; Pearse et al., 2009). An increase in diversification could have been driven by the extinction of competitors and/or the evolution of key innovations as response to ecological opportunities (Yoder et al., 2010; Stroud & Losos, 2016). Extinction events such as that of the decapods during the decreasing temperatures in the Tertiary could possibly have opened up previously occupied niches and decreased predation pressure which aided in the diversification of isopods and amphipods (Brandt, 1999; 2000; Aronson et al., 2007; Legezyñska et al., 2020). Moreover, Antarctic *Eusirus* could probably have been able to exploit different food items. Despite being primarily predators, these species can shift to opportunistic scavenging and even necrophagy which is presumed to be a highly adaptive trophic strategy (Klages & Gutt 1990; Dauby et al. 2001; Graeve et al., 2001; Nyssen et al., 2002; Nyssen, 2005; Krapp et al., 2008; Michel et al., 2020). The potential for niche expansion is higher for species that can shift their diets by taking advantage of the available resources (Stroud & Losos, 2016). Niche expansion occurring in reduced interspecific competitive pressures can lead to ecological release (Yoder et al., 2010; Stroud & Losos, 2016). Increased rates of lineage diversification may have been brought about by ecological opportunities through the ecological release mechanisms (Yoder et al., 2010).

The North Atlantic and Pacific connections to the Arctic could be attributed to the low rate of speciation observed in the Arctic lineages as these permitted exchanges of biota between oceans resulting in high gene flow (Dunton, 1992; Kuklinski et al., 2013). Indeed, molecular evidence showed high population connectivity between the Arctic and the North Atlantic and Pacific faunas sustaining high gene flow (Hardy et al., 2011). Higher gene flow could slow down speciation (Palumbi, 1994; Smadja & Butlin, 2011) which could be the case for the Arctic *Eusirus* lineages. The low diversification rates could also be explained by higher extinction rates, niche saturation, and maintenance of similar niches (Derryberry et al., 2011; Moen & Morlon, 2014; Schluter & Pennell, 2017) although these hypotheses should be explicitly tested.

Conclusions

This study provided first insights into the origin and lineage diversification of the genus *Eusirus*. Our results significantly increased a previous age estimate of Antarctic *Eusirus* and surprisingly show that the mean age of Arctic *Eusirus* is older than Antarctic *Eusirus* despite the older existence and longer geographic isolation of Antarctica. Moreover, contrasting tempos of diversification were observed between Antarctic and the Arctic *Eusirus.* The high diversification rates in the Antarctic clade could be attributed to the vicariant events that occurred following the Drake passage opening and the formation of the ACC and ecological opportunities brought about by the climatic and geological changes in the Antarctic. On the other hand, the contrasting slow diversification rates observed in the Arctic lineages could be explained by higher gene flow, higher extinction rates or niche saturation.

References

Altschul SF, Madden TL, Schäffer AA, Zhang J, Zhang Z, Miller W, Lipman DJ. 1997. Gapped BLAST and PSI-BLAST: a new generation of protein database search programs. Nucleic Acids Res. 25(17):810–3402.

Arfianti, T., Wilson, S., & Costello, M. J. 2018. Progress in the discovery of amphipod crustaceans. *PeerJ*, *6*, e5187.

Arntz, W. E., Brey, T., & Gallardo, V. A. 1995. Antarctic zoobenthos. *Oceanographic Literature Review*, *8*(42), 668.

Aronson, R. B., Thatje, S., Clarke, A., Peck, L. S., Blake, D. B., Wilga, C. D., & Seibel, B. A. 2007. Climate change and invasibility of the Antarctic benthos. Annu. Rev. Ecol. Evol. Syst., 38, 129-154.

Baird, H. P., Miller, K. J., & Stark, J. S. 2011. Evidence of hidden biodiversity, ongoing speciation and diverse patterns of genetic structure in giant Antarctic amphipods. *Molecular Ecology*, *20*(16), 3439-3454.

Barnes, D. K., Hodgson, D. A., Convey, P., Allen, C. S., & Clarke, A. 2006. Incursion and excursion of Antarctic biota: past, present and future. *Global Ecology and Biogeography*, *15*(2), 121-142.

Beu, A. G., Griffin, M., & Maxwell, P. A. 1997. Opening of Drake Passage gateway and Late Miocene to Pleistocene cooling reflected in Southern Ocean molluscan dispersal: evidence from New Zealand and Argentina. *Tectonophysics*, *281*(1-2), 83-97.

Bouckaert, R., Heled, J., Kühnert, D., Vaughan, T., Wu, C-H., Xie, D., Suchard, MA., Rambaut, A., & Drummond, A. J. 2014. BEAST 2: A Software Platform for Bayesian Evolutionary Analysis. PLoS Computational Biology, 10(4), e1003537.

Bouckaert, R. R., & Drummond, A. J. 2017. bModelTest: Bayesian phylogenetic site model averaging and model comparison. *BMC evolutionary biology*, *17*(1), 1-11.

Bousfield, E.L. & Poinar, G.O. 1994. A new terrestrial amphipod from Tertiary amber deposits of Chiapas Province, Southern Mexico. Hist. Biol. 7, 105–114.

Bousfield, E. L., & Poinar Jr. G. O. 1995. New terrestrial amphipod from Tertiary amber deposits of the Dominican Republic. Journal of Crustacean Biology, 15(4), 746-755.

Brandt, A. 1999. On the origin and evolution of Antarctic Peracarida (Crustacea, Malacostraca). Scientia Marina 63, 261-274.

Brandt, A. 2000. Hypotheses on Southern Ocean peracarid evolution and radiation (Crustacea, Malacostraca). Antarctic Science, 12(3), 269-275.

Brozena, J. M., Childers, V. A., Lawver, L. A., Gahagan, L. M., Forsberg, R., Faleide, J. I., & Eldholm, O. 2003. New aerogeophysical study of the Eurasia Basin and Lomonosov Ridge: Implications for basin development. Geology, 31(9), 825-828.

Burnham, K.P., Anderson, D.R. 2002. Model selection and multimodel inference: a practical information theroretical approach, second edition. Springer-Verlag, New York.

Clarke, A. & Crame, J. A. 1989. The origin of the Southern Ocean marine fauna. Geological Society, London, Special Publications, 47(1), 253–268.

Clarke, A., & Crame, J. A. 2010. Evolutionary dynamics at high latitudes: speciation and extinction in polar marine faunas. *Philosophical Transactions of the Royal Society B: Biological Sciences*, *365*(1558), 3655-3666.

Clarke, A., & Johnston, N. M. 2003. Antarctic marine benthic diversity. In *Oceanography and Marine Biology, An Annual Review. CRC Press. Volume 41*: pp. 55-57.

Coleman, C.O. 2004. Aquatic amphipods (Crustacea: Amphipoda: Crangonyctidae) in three pieces of Baltic amber. Organisms, Diversity & Evolution 4: 119-122.

Coleman, C.O. 2006. An amphipod of the genus Synurella Wrzesniowski, 1877 (Crustacea, Amphipoda, Crangonyctidae) found in Baltic amber. Org. Divers. Evol. 6, 103–108.

Coleman, H. O., & Myers, A. A. 2001. New Amphipoda from Baltic amber. Polskie Archiwum Hydrobiologii, 47(3/4), 457-464.

Coleman, C. O., & Ruffo, S. 2002. Another discovery of a niphargid amphipod (Crustacea) in Baltic amber. Mitteilungen aus dem Geologisch-Paläontologischen Institut der Universität Hamburg, 86, 239-244.

Copilaş-Ciocianu, D., & Petrusek, A. 2017. Phylogeography of a freshwater crustacean species complex reflects a long‐gone archipelago. *Journal of Biogeography*, *44*(2), 421-432.

Copilaş-Ciocianu, D., Sidorov, D., & Gontcharov, A. 2019. Adrift across tectonic plates: molecular phylogenetics supports the ancient Laurasian origin of old limnic crangonyctid amphipods. *Organisms Diversity & Evolution*, *19*, 191-207.

Copilaş-Ciocianu, D., Borko, Š., & Fišer, C. 2020. The late blooming amphipods: global change promoted post-Jurassic ecological radiation despite Palaeozoic origin. *Molecular Phylogenetics and Evolution*, *143*, 106664.

Coxall, H. K., & Pearson, P. N. 2007. The Eocene-Oligocene transition. *Deep time perspectives on climate change: Marrying the signal from computer models and biological proxies*, 351-387.

Crame, J. A. 1999. An evolutionary perspective on marine faunal connections between southernmost South America and Antarctica. *Scientia Marina*, *63*, 1-14.

Cronin, T. M., & Cronin, M. A. 2015. Biological response to climate change in the Arctic Ocean: the view from the past. arktos, 1, 1-18.

Darriba, D., Taboada G.L., Doallo R., Posada, D. 2012. jModelTest 2: more models, new heuristics and parallel computing. Nature Methods 9(8), 772.

Dauby, P., Scailteur, Y., & De Broyer, C. 2001. Trophic diversity within the eastern Weddell Sea amphipod community. Hydrobiologia, 443(1), 69-86.

David, B., Choné, T., Mooi, R., De Ridder, C. 2005. Antarctic Echinoidea.Synopses of the Antarctic benthos vol 10 (ed. by J. W. Wägele, and J. Sieg). Koeltz Scientific books Publishing, Königstein.

Dayton, P. K. 2013. 12 Polar Benthos. Polar Oceanography: Chemistry, Biology, and Geology, 631.

Dayton, P. K., Mordida, B. J., & Bacon, F. 1994. Polar marine communities. American Zoologist, 34(1), 90-99.

Derryberry, E. P., Claramunt, S., Derryberry, G., Chesser, R. T., Cracraft, J., Aleixo, A., Pérez-Emán, J., Remsen, J.V. Jr. & Brumfield, R. T. 2011. Lineage diversification and morphological evolution in a large‐scale continental radiation: the Neotropical ovenbirds and woodcreepers (Aves: Furnariidae). Evolution, 65(10), 2973-2986.

Donath, A., Jühling, F., Al-Arab, M., Bernhart, S. H., Reinhardt, F., Stadler, P. F., Middendorf, M, & Bernt, M. 2019. Improved annotation of protein-coding genes boundaries in metazoan mitochondrial genomes. *Nucleic acids research*, *47*(20), 10543-10552.

Drummond, A. J., & Bouckaert, R. R. 2015. *Bayesian evolutionary analysis with BEAST*. Cambridge University Press.

Dunton, K. 1992. Arctic biogeography: the paradox of the marine benthic fauna and flora. *Trends in Ecology & Evolution*, *7*(6), 183-189.

Eastman, J. T. 2005. The nature of the diversity of Antarctic fishes. *Polar biology*, *28*(2), 93-107.

Edgar, R. C. 2004. MUSCLE: multiple sequence alignment with high accuracy and high throughput, Nucleic Acids Research 32(5), 1792-97

Englisch, U. 2001. Analyse der Phylogenie der Amphipoda (Crustacea, Malacostraca) mit Hilfe von Sequenzen des Gens der RNA der kleinen ribosomalen Untereinheit. Ph.D. Dissertation. Fakultat fur Biologie. Bochum, Germany: RuhrUniversitat Bochum. pp. 1–158.

Fordyce, J. A. 2010. Interpreting the γ statistic in phylogenetic diversification rate studies: a rate decrease does not necessarily indicate an early burst. *PLoS One*, *5*(7), e11781.

Gelman, A. and X.-L. Meng. 1998. Simulating normalizing constants: from importance sampling to bridge sampling to path sampling. Statistical Science 13:163–185.

Golikov, A. N., & Scarlato, O. A. 1989. Evolution of Arctic ecosystems during the Neogene period. In *The Arctic Seas.* Springer, Boston, MA. 257-279.

Graeve, M., Dauby, P., & Scailteur, Y. 2001. Combined lipid, fatty acid and digestive tract content analyses: a penetrating approach to estimate feeding modes of Antarctic amphipods. Polar biology, 24(11), 853-862.

Guindon, S. & Gascuel, O. 2003. A simple, fast, and accurate algorithm to estimate large phylogenies by maximum likelihood. Syst Biol. 52(5): 696–704

Hardy, S. M., Carr, C. M., Hardman, M., Steinke, D., Corstorphine, E., & Mah, C. 2011. Biodiversity and phylogeography of Arctic marine fauna: insights from molecular tools. *Marine Biodiversity*, *41*(1), 195-210.

Hegna, T. A., Lazo-Wasem, E. A., de Lourdes Serrano-Sánchez, M., Barragán, R., & Vega, F. J. 2020. A new fossil talitrid amphipod from the lower early Miocene Chiapas amber documented with microCT scanning. Journal of South American Earth Sciences, 98, 102462.

Held, C. 2000. Phylogeny and biogeography of serolid isopods (Crustacea, Isopoda, Serolidae) and the use of ribosomal expansion segments in molecular systematics. Molecular phylogenetics and evolution, 15(2), 165-178.

Helmuth, B., Veit, R. R., & Holberton, R. 1994. Long-distance dispersal of a subantarctic brooding bivalve (Gaimardia trapesina) by kelp-rafting. *Marine biology*, *120*, 421-426.

Hodel, F., Grespan, R., de Rafélis, M., Dera, G., Lezin, C., Nardin, E., Rouby D., Aretz M., Steinnman M., Buatier M., Lacan F., Jeandel C., & Chavagnac, V. 2021. Drake Passage gateway opening and Antarctic Circumpolar Current onset 31 Ma ago: The message of foraminifera and reconsideration of the Neodymium isotope record. Chemical Geology, 570, 120171.

Hotaling, S., Borowiec, M. L., Lins, L. S., Desvignes, T., & Kelley, J. L. 2021. The biogeographic history of eelpouts and related fishes: Linking phylogeny, environmental change, and patterns of dispersal in a globally distributed fish group. Molecular phylogenetics and evolution, 162, 107211.

Hutchinson, D. K., Coxall, H. K., Lunt, D. J., Steinthorsdottir, M., de Boer, A. M., Baatsen, M., von der Heydt, A., Huber, M., Kennedy-Asser, A. T., Kunzmann, L., Ladant, J. B., Lear, C. H., Moraweck, K., Pearson, P. N., Piga, E., Pound, M. J., Salzmann, U., Scher, H. D., Sijp, W. P., Śliwińska, K.K., Wilson, P.A.,

Zhang, Z. 2021. The Eocene–Oligocene transition: a review of marine and terrestrial proxy data, models and model–data comparisons. Climate of the Past, 17(1), 269–315.

Ingólfsson, Ó. 2004. Quaternary glacial and climate history of Antarctica. Developments in Quaternary sciences, 2, 3-43.

Jarzembowski, E. A., Cheny, C., Fang, Y., & Wang, B. 2020. First Mesozoic amphipod crustacean from the Lower Cretaceous of SE England. Cretaceous Research, 112, 104429.

Jażdżewski, K., Kulicka, R. 2000. A note on amphipod crustaceans in a piece of Baltic amber. Ann. Zool. 50, 99–100.

Jażdżewski, K., & Kulicka, R. 2002. New fossil amphipod, Palaeogammarus polonicus sp. nov. from the Baltic amber. *Acta Geologica Polonica*, *52*(3), 379-383.

Jażdżewski, K., & Kupryjanowicz, J. 2010. One more fossil niphargid (Malacostraca: Amphipoda) from Baltic amber. *Journal of Crustacean Biology*, *30*(3), 413-416.

Jażdżewski, K., Grabowski, M., & Kupryjanowicz, J. 2014. Further records of Amphipoda from Baltic Eocene amber with first evidence of prae-copulatory behaviour in a fossil amphipod and remarks on the taxonomic position of Palaeogammarus Zaddach, 1864. Zootaxa, 3765(5), 401-417.

Jung, T. W.; Kim, M.-S.; Soh, H.-Y.; Yoon, S. M. 2016. A new species of *Eusirus* from Jeju Island, Korea (Crustacea, Amphipoda, Eusiridae). *ZooKeys.*(640), 19-35.

Just, J. 1974. On Palaeogammarus Zaddach, 1864, with a description of a new species from western Baltic amber (Crustacea, Amphipoda, Crangonyctidae). Steenstrupia 3, 93–99.

Karaman, G. S. 1984. Critical remarks to the fossil Amphipoda with description of some new taxa. Poljoprivreda i Sumarstvo 30: 87-104.

Kass, R. E. & Raftery, A. E. 1995. Bayes Factor. *Journal of the American Statistical Association*, *90*, 773-795.

Katoh, K., Standley, D.M. 2013. MAFFT multiple sequence alignment software version 7: improvements in performance and usability. Molecular Biology and Evolution 30, 772- 780.

Klages, M., & Gutt, J. 1990. Observations on the feeding behaviour of the Antarctic gammarid Eusirus perdentatus Chevreux, 1912 (Crustacea: Amphipoda) in aquaria. Polar Biology, 10(5), 359-364.

Knox, G.A. 2006. Biology of the Southern Ocean, Second Edition. CRC Press, Boca Raton.

Knox, G.A. & Lowry, J.K. 1977. A comparison between the benthos of the Southern Ocean and the North Polar Ocean with special reference to the Amphipoda and Polychaeta. In: Dunbar, M.J. (Ed.), Polar oceans. Proceedings of the Polar Ocean Conference, Calgary, pp. 432- 462.

Krapp, R.H., Berge, J., Flores, H., Gulliksen, B., Werner, I. 2008 Sympagic occurence of Eusirid and Lyssianassoid amphipods under Antarctic pack ice. Deep-Sea Research II, 55, 1015-1023.

Kuklinski, P., Taylor, P. D., Denisenko, N. V., & Berning, B. 2013. Atlantic origin of the Arctic biota? Evidence from phylogenetic and biogeographical analysis of the cheilostome bryozoan genus Pseudoflustra. *PLoS One*, *8*(3), e59152. 1-25.

Kumar, S., Stecher, G., Li, M., Knyaz, C., & Tamura, K. 2018. MEGA X: molecular evolutionary genetics analysis across computing platforms. *Molecular biology and evolution*, *35*(6), 1547.

Lanfear, R., Frandsen, P. B., Wright, A. M., Senfeld, T., Calcott, B. 2016. PartitionFinder 2: new methods for selecting partitioned models of evolution for molecular and morphological phylogenetic analyses. Molecular biology and evolution.

Lartillot, N., & Philippe, H. 2006. Computing Bayes factors using thermodynamic integration. *Systematic biology*, *55*(2), 195-207.

Latimer, J. C., & Filippelli, G. M. 2002. Eocene to Miocene terrigenous inputs and export production: geochemical evidence from ODP Leg 177, Site 1090. Palaeogeography, Palaeoclimatology, Palaeoecology, 182(3-4), 151-164.

Lawver, L. A., & Gahagan, L. M. 2003. Evolution of Cenozoic seaways in the circum-Antarctic region. Palaeogeography, Palaeoclimatology, Palaeoecology, 198(1-2), 11-37.

Lecointre, G. 2012. Phylogeny and Systematics of Antarctic Teleosts: Methodological and Evolutionary Issues. In: di Prisco, G., Verde, C. (eds) Adaptation and Evolution in Marine Environments, Volume 1. From Pole to Pole. Springer, Berlin, Heidelberg.

Lecointre, G., Améziane, N., Boisselier, M. C., Bonillo, C., Busson, F., Causse, R., Chenuil, A., Couloux, A., Coutanceau, J.P., Cruaud, C., d'Udekem d'Acoz, C., De Ridder, C., Denys, G., Dettaï, A., Duhamel, G., Eléaume, M., Féral, J.P., Gallut, C., Havermans, C., Held, C., Hemery, L., Lautrédou, A.C., Martin, P., Ozouf-Costaz, C., Pierra, B., Pruvost, P., Puillandre, N., Samadi, S., Saucède, T., Schubart, C., & David, B. 2013. Is the species flock concept operational? The Antarctic shelf case. *PloS one*, *8*(8), e68787.

Lee, Y. H., Song, M., Lee, S., Leon, R., Godoy, S. O., & Canete, I. 2004. Molecular phylogeny and divergence time of the Antarctic sea urchin (Sterechinus neumayeri) in relation to the South American sea urchins. Antarctic Science, 16(1), 29-36.

Legezyñska, J., De Broyer, C., & Wesławski, J. M. 2020. Invasion of the poles. *The Natural History of the Crustacea: Evolution and Biogeography of the Crustacea*, 216-246.

Lockhart, S. J. 2006. Molecular Evolution, Phylogenetics, and Parasitism in Antarctic Cidaroid Echinoids. Ph.D. diss., University of California, Santa Cruz.

Lucks, R. 1927. Palaeogammarus balticus, nov. spec., ein neuer Gammaride aus dem Bernstein. Schr. Naturforsch. Ges. Danzig, N. F. 18, 1–13.

Lurcock, P. C., & Florindo, F. 2017. Antarctic climate history and global climate changes. Oxford University Press.

Mamos, T., Wattier, R., Burzyński, A., & Grabowski, M. 2016. The legacy of a vanished sea: a high level of diversification within a European freshwater amphipod species complex driven by 15 My of Paratethys regression. *Molecular Ecology*, *25*(3), 795-810.

Marincovich Jr, L., Brouwers, E. M., & Carter, L. D. 1985. Early Tertiary marine fossils from northern Alaska: implications for Arctic Ocean paleogeography and faunal evolution. Geology, 13(11), 770-773.

Marincovich, L., & Gladenkov, A. Y. 1999. Evidence for an early opening of the Bering Strait. *Nature*, *397*(6715), 149-151.

McMenamin, M. A., Zapata, L. P., & Hussey, M. C. 2013. A Triassic giant amphipod from Nevada, USA. Journal of Crustacean Biology, 33(6), 751-759.

Michel, L. N., Nyssen, F. L., Dauby, P., & Verheye, M. 2020. Can mandible morphology help predict feeding habits in Antarctic amphipods?. Antarctic Science, 32(6), 496-507.

Miller, M.A., Pfeiffer, W., and Schwartz, T. 2010. "Creating the CIPRES Science Gateway for inference of large phylogenetic trees" in Proceedings of the Gateway Computing Environments Workshop (GCE), 14 Nov. 2010, New Orleans, LA pp 1 - 8.

Misof, B., & Misof, K. 2009. A Monte Carlo approach successfully identifies randomness in multiple sequence alignments: a more objective means of data exclusion. *Systematic biology*, *58*(1), 21-34.

Moen, D., & Morlon, H. 2014. Why does diversification slow down?. Trends in Ecology & Evolution, 29(4), 190-197.

Morlon, H., Parsons, T. L., & Plotkin, J. B. 2011. Reconciling molecular phylogenies with the fossil record. *Proceedings of the National Academy of Sciences*, *108*(39), 16327-16332.

Morlon, H., Lewitus, E., Condamine, F. L., Manceau, M., Clavel, J., & Drury, J. 2016. RPANDA: an R package for macroevolutionary analyses on phylogenetic trees. *Methods in Ecology and Evolution*, *7*(5), 589-597.

Mukai, K. & M. Takeda. 1987. A giant amphipod Crustacea from the Miocene Morozaki Group in the Chita Peninsula, Central Japan. Bulletin of the Natural Sciences Museum, Tokyo, ser. C 13: 35-39.

Nyssen, F. 2005. Role of benthic amphipods in Antarctic trophodynamics: a multidisciplinary study (Doctoral dissertation, Université de Liège).

Nyssen, F., Brey, T., Lepoint, G., Bouquegneau, J. M., De Broyer, C., & Dauby, P. 2002. A stable isotope approach to the eastern Weddell Sea trophic web: focus on benthic amphipods. Polar Biology, 25(4), 280-287.

O'Regan, M., Williams, C. J., Frey, K. E., & Jakobsson, M. 2011. A synthesis of the long-term paleoclimatic evolution of the Arctic. Oceanography, 24(3), 66-80.

Palerud, R., & Vader, W. 1991. *Marine Amphipoda Gammaridea in north-east Atlantic and Norwegian Arctic*. p. 1-54.

Palumbi, S.R. 1994. Genetic Divergence, Reproductive Isolation, and Marine Speciation. Annual Review of Ecology and Systematics, 25(1), 547–572.

Patarnello, T., Bargelloni, L., Varotto, V. & Battaglia, B. 1996. Krill evolution and the Antarctic ocean currents: evidence of vicariant speciation as inferred by molecular data. Mar. Biol. 126, 603–608.

Pearse, J. S., Mooi, R., Lockhart, S. J., & Brandt, A. 2009. Brooding and species diversity in the Southern Ocean: selection for brooders or speciation within brooding clades?. Smithsonian at the poles: contributions to international polar year science.

Peña Othaitz J. & Sorbe J.C. 2020. *Eusirus bonnieri* sp. nov. (Crustacea: Amphipoda: Eusiridae), a new deep species from the southeastern Bay of Biscay (NE Atlantic Ocean). *Zootaxa.* 4751(2): 238-256.

Piepenburg, D. 2005. Recent research on Arctic benthos: common notions need to be revised. *Polar Biology*, *28*(10), 733-755.

Plummer, M., Best, N., Cowles, K., & Vines, K. 2006. CODA: convergence diagnosis and output analysis for MCMC. *R news*, *6*(1), 7-11.

Pybus, O. G., and P. H. Harvey. 2000. Testing macro-evolutionary models using incomplete molecular phylogenies. *Proc. Biol. Sci.* 267:2267–72.

Rabosky, D. L. 2006. LASER: a maximum likelihood toolkit for detecting temporal shifts in diversification rates from molecular phylogenies. *Evolutionary Bioinformatics*, *2*, 117693430600200024.

Rabosky, D. L. 2014. Automatic detection of key innovations, rate shifts, and diversity-dependence on phylogenetic trees. *PloS one*, *9*(2), e89543.

Rabosky, D. L. 2022. Evolutionary time and species diversity in aquatic ecosystems worldwide. *Biological Reviews*, *97*(6), 2090-2105.

Rabosky, D. L., & Lovette, I. J. 2008. Density-dependent diversification in North American wood warblers. *Proceedings of the Royal Society B: Biological Sciences*, *275*(1649), 2363-2371.

Rabosky, D. L., Grundler, M., Anderson, C., Title, P., Shi, J. J., Brown, J. W., Huang, H., & Larson, J. G. 2014. BAMM tools: an R package for the analysis of evolutionary dynamics on phylogenetic trees. *Methods in Ecology and Evolution*, *5*(7), 701-707.

Rambaut, A., Suchard, M.A., Xie, D., Drummond, A.J. 2014. Tracer v1.6. Available from http://beast.bio.ed.ac.uk/Tracer.

Rambaut, A., Drummond, A. J., Xie, D., Baele, G., & Suchard, M. A. 2018. Posterior summarization in Bayesian phylogenetics using Tracer 1.7. *Systematic biology*, *67*(5), 901-904.

Revell, L. J. 2012. Phytools: an R package for phylogenetic comparative biology (and other things). *Methods in ecology and evolution*, (2), 217-223.

Rogers, A. D. 2007. Evolution and biodiversity of Antarctic organisms: a molecular perspective. Philosophical transactions of the royal society B: Biological sciences, 362(1488), 2191-2214.

Ronquist, F. & Huelsenbeck, J.P. 2003. MRBAYES 3: Bayesian phylogenetic inference under mixed models. Bioinformatics. 19(12):1572–1574.

Schluter, D. 2000. The ecology of adaptive radiation. OUP Oxford.

Schluter, D., & Pennell, M. W. 2017. Speciation gradients and the distribution of biodiversity. Nature, 546(7656), 48-55.

Serreze, M. C., & Barry, R. G. 2005. *The Arctic climate system*. Cambridge University Press.

Sirenko, B. I. 2009. Main differences in macrobenthos and benthic communities of the Arctic and Antarctic, as illustrated by comparison of the Laptev and Weddell Sea faunas. *Russian Journal of Marine Biology*, *35*(6), 445-453.

Sirenko, B.I.; Clarke, C.; Hopcroft, R.R.; Huettmann, F.; Bluhm, B.A.; Gradinger, R. (eds). 2022. The Arctic Register of Marine Species (ARMS) compiled by the Arctic Ocean Diversity (ArcOD). Accessed at https://www.marinespecies.org/arms on 2022-12-14.

Sluijs, A., Schouten, S., Pagani, M., Woltering, M., Brinkhuis, H., Damsté, J. S. S., Dickens, G. R., Huber, M., Reichart, G. J., Stein, R., Matthiessen, J., Lourens, L. J., Pedentchouk, N., Backman, J., & Moran, K. 2006. Subtropical Arctic Ocean temperatures during the Palaeocene/Eocene thermal maximum. Nature, 441(7093), 610–613.

Sluijs, A., Schouten, S., Donders, T. H., Schoon, P. L., Röhl, U., Reichart, G. J., Sangiorgi, F., Kim, J. H., Sinninghe Damsté, J. S., & Brinkhuis, H. 2009. Warm and wet conditions in the Arctic region during Eocene Thermal Maximum 2. Nature Geoscience, 2(11), 777–780.

Smadja, C. M., & Butlin, R. K. 2011. A framework for comparing processes of speciation in the presence of gene flow. Molecular ecology, 20(24), 5123-5140.

Smith, S. D. 2002. Kelp rafts in the Southern Ocean. *Global Ecology and Biogeography*, *11*(1), 67-69.

Stamatakis, A. 2014. RAxML version 8: a tool for phylogenetic analysis and post-analysis of large phylogenies. Bioinformatics, 30(9), 1312-1313.

Stroud, J. T., & Losos, J. B. 2016. Ecological opportunity and adaptive radiation. *Annual Review of Ecology, Evolution, and Systematics*, *47*, 507-532.

Strugnell, J. M., Rogers, A. D., Prodöhl, P. A., Collins, M. A., & Allcock, A. L. 2008. The thermohaline expressway: the Southern Ocean as a centre of origin for deep‐sea octopuses. *Cladistics*, *24*(6), 853-860.

Strugnell, J. M., Cherel, Y., Cooke, I. R., Gleadall, I. G., Hochberg, F. G., Ibáñez, C. M., Jorgensen, E., Laptikhovsky, V.V., Linse, K., Norman, M., Vecchione, M., Voight, J.R. & Allcock, A. L. 2011. The Southern Ocean: source and sink?. *Deep Sea Research Part II: Topical Studies in Oceanography*, *58*(1-2), 196-204.

Teske, P. R., McQuaid, C. D., Froneman, P. W., & Barker, N. P. 2006. Impacts of marine biogeographic boundaries on phylogeographic patterns of three South African estuarine crustaceans. *Marine Ecology Progress Series*, *314*, 283-293.

Thatje, S., Hillenbrand, C. D., & Larter, R. 2005. On the origin of Antarctic marine benthic community structure. *Trends in Ecology & Evolution*, *20*(10), 534-540.

Thatje, S., Hillenbrand, C. D., Mackensen, A., & Larter, R. 2008. Life hung by a thread: endurance of Antarctic fauna in glacial periods. *Ecology*, *89*(3), 682-692.

Thornhill, D. J., Mahon, A. R., Norenburg, J. L., & Halanych, K. M. 2008. Open‐ocean barriers to dispersal: A test case with the Antarctic Polar Front and the ribbon worm *Parborlasia corrugatus* (Nemertea: Lineidae). *Molecular ecology*, *17*(23), 5104-5117.

Thurston, M. 2009. Key to the genera and species of Eusiridae from the Arctic Ocean and Norwegian Sea. Deep-sea workshop. Skibotn: Unpublished.

Verheye ML. 2011. *Systématique et diversité génétique des Eusirus de l'Océan Austral (Crustacea, Amphipoda, Eusiridae). Mémoire présenté en vue de l'obtention du diplôme de Master en Biologie des Organismes et Ecologie*. Louvainla- Neuve: Université Catholique de Louvain-la-Neuve.

Verheye, M.L., Martin, P., Backeljau, T., d'Udekem D'Acoz, C. 2016. DNA analyses reveal abundant homoplasy in taxonomically important morphological characters of Eusiroidea (Crustacea, Amphipoda). Zoologica Scripta 45, 300-321.

Verheye, M.L. 2017. Systematics, phylogeography and historical biogeography of Eusiroidea (Crustacea, Amphipoda) from the Southern Ocean, with a special focus on the families Epimeriidae and Iphimediidae. PhD thesis, Université Catholique de Louvain-la-Neuve.

Verheye, M. L., Backeljau, T., & d'Acoz, C. D. U. 2017. Locked in the icehouse: evolution of an endemic Epimeria (Amphipoda, Crustacea) species flock on the Antarctic shelf. *Molecular phylogenetics and evolution*, *114*, 14-33.

Verheye, M. L., & D'Udekem D'Acoz, C. 2020. Integrative taxonomy of giant crested *Eusirus* in the Southern Ocean, including the description of a new species (Crustacea: Amphipoda: Eusiridae). *Zoological Journal of the Linnean Society*, *193*(1), 31-77.

Vincze, M., Bozóki, T., Herein, M., Borcia, I. D., Harlander, U., Horicsányi, A., Nyerges, A., Rodda, C., Pál, A., & Pálfy, J. 2021. The Drake Passage opening from an experimental fluid dynamics point of view. Scientific reports, 11(1), 1-11.

Wang, Y., Sha, Z., & Ren, X. 2021. A new species of *Eusirus* (Amphipoda, Amphilochidea, Eusiridae) described from a hydrothermal vent in the Okinawa Trough, North-West Pacific. *Crustaceana*, *94*(11-12), 1395-1405.

Waters, J. M. 2008. Driven by the West Wind Drift? A synthesis of southern temperate marine biogeography, with new directions for dispersalism. *Journal of Biogeography*, *35*(3), 417-427.

Weitschat, W., Brandt, A., Coleman, C. O., Møller-Andersen, N., Myers, A. A., & Wichard, W. 2002. Taphocoenosis of an extraordinary arthropod community in Baltic amber. *Mitteilungen aus dem Geologisch-Paläontologischen Institut der Universität Hamburg*, *86*, 189-210.

Wilce, R. T. 1990. Role of the Arctic Ocean as a bridge between the Atlantic and Pacific Oceans: fact and hypothesis. In *Evolutionary biogeography of the marine algae of the North Atlantic.* Springer, Berlin, Heidelberg. 323-347.

Williams, S. T., Reid, D. G., & Littlewood, D. T. J. 2003. A molecular phylogeny of the Littorininae (Gastropoda: Littorinidae): unequal evolutionary rates, morphological parallelism, and biogeography of the Southern Ocean. *Molecular phylogenetics and evolution*, *28*(1), 60-86.

Xia X. 2018. DAMBE7: New and improved tools for data analysis in molecular biology and evolution. Molecular Biology and Evolution 35:1550–1552.

Xia, X., Xie, Z., Salemi, M., Chen, L., Wang, Y. 2003. An index of substitution saturation and its application. Mol. Phylogenet. Evol. 26, 1–7.

Yoder, J. B., Clancey, E., Des Roches, S., Eastman, J. M., Gentry, L., Godsoe, W., Hagey, T.J., Jochimsen, D., Oswald., B.P., Robertson., J., Sarver., B.A.J., Schenk, J.J., Spear., S.F., & Harmon, L. J. 2010. Ecological opportunity and the origin of adaptive radiations. *Journal of evolutionary biology*, *23*(8), 1581-1596.

Zachos, J.C., G.R. Dickens, and R.E. Zeebe. 2008. An early Cenozoic perspective on greenhouse warming and carbon-cycle dynamics. Nature. 451:279–283

Zaddach, G. 1864. Ein Amphipode im Bernstein. Schriften der Koniglichen Physikalisch-Okonomischen Gesellschaft zu Konigsberg 5: 1-12.

Zenkevitch, L. 1963. BioLogy of the Seas of t h e U.S.S.R. George Allen and Unwin Ltd., London. pp. 1-968.

Chapter 5: Ecological and morphological diversification of the genus *Eusirus*: A comparative study of the polar oceans

Louraine Salabao[1,2], Isa Schön[2,4], Gilles Lepoint[3], Marie Verheye[4,5], & Bruno Frédérich[1]

Admiralty Bay, Antarctica (Photo taken by Louraine Salabao)

[1] Laboratory of Evolutionary Ecology, FOCUS, Department of Biology, Ecology & Evolution, University of Liège, B-4000 Liège, Belgium

[2] Centre for Environmental Sciences, Zoology: Toxicology and Biodiversity, Campus Diepenbeek, Agoralaan Gebouw D - B-3590 Diepenbeek

[3] Laboratoire d'Ecologie Trophique et Isotopique (LETIS), FOCUS, Université de Liège, B-4000 Liège, Belgium

[4] Royal Belgian Institute of Natural Sciences, OD Nature, Freshwater Biology, Vautierstraat 29, 1000 Brussels, Belgium

[5] Department of Biology, Ecology, Evolution and Biodiversity Conservation unit, Katholieke Universiteit Leuven, Charles Deberiotstraat 32, 3000, Leuven, Belgium

Abstract

Understanding the evolutionary processes that have shaped the current species diversity in the polar regions is essential to predict the possible responses of endemic taxa to future climate changes. The amphipod genus *Eusirus* can serve as a good model group for studying these eco-evolutionary processes due to its eco-morphological variability and worldwide distribution, including both polar oceans. By combining novel phylogenetic with ecological and trophic data generated by stable isotopes and morphological analyses, we aim to address the following questions: (1) Did the *Eusirus* species mainly originate through adaptive or non-adaptive radiation? (2) Is the pattern of ecological diversification of *Eusirus* the same in the Arctic and the Antarctic? (3) Is there a striking convergence in the Arctic and Antarctic *Eusirus* species? Our results suggest different evolutionary scenarios for Arctic and Antarctic *Eusirus*. In the Antarctic, a scenario of non-adaptive radiation could explain why there is no rate shift for morphological diversification while a high rate of lineage diversification was observed. Based on these patterns, allopatric speciation is the most likely evolutionary process driving diversity of *Eusirus* in Antarctica. However, we cannot fully rule out that some ecological diversification also occurred which was perhaps not captured by the investigated traits. As for Arctic *Eusirus*, the higher morphological and ecological diversity probably accumulated through the longer evolutionary history. These high level of morphological and ecological diversity in Arctic *Eusirus* are coupled with a relatively constant rate of lineage diversification and thus no speciation bursts. The highest level of eco-morphological diversity observed in the Arctic lineages could instead be linked to the polyphyletic origin of Arctic *Eusirus* and to the older age of these lineages. Allopatric speciation events and multiple extinction events could further have contributed to the high level of eco-morphological diversity in the Arctic.

Introduction

Patterns of species diversity in the polar regions have been shaped by various evolutionary processes, which can at least partly be linked to past environmental changes (Brandt, 2005; Clarke & Crame, 2010; Verheye et al., 2017; Hardy et al., 2011; Legezyñska et al., 2020). Around the Cretaceous-Palaeogene (K–Pg) boundary, the polar regions experienced global warmth (Brozena et al., 2003; O'Regan et al., 2011; Renne et al., 2013; Petersen et al., 2016)

causing extinctions of certain polar species and allowing more adaptable species to thrive (Sluijs et al., 2006; Sluijs et al., 2009; O'Regan et al., 2011; Crame et al., 2014; Crame, 2018). Subsequent cooling during the Eocene-Oligocene transition resulted in the extinction of warm-adapted marine taxa, which were replaced by cold-adapted species (Dunton, 1992; Keller et al., 1992; Prothero, 1994; Serreze & Barry, 2005; Coxall & Pearson, 2007; Hutchinson et al., 2021). Repeated ice expansions and retreats during the Quaternary caused shelf fauna assemblages to be almost eliminated (Dunton, 1992; Convey et al., 2009; Kuklinski et al., 2013; Legezyñska et al., 2020). Some surviving fauna found refuge in the ice-free shelf sites while others retreated into deeper waters and later reinvaded the continental shelves (Golikov & Scarlato, 1989; Dunton, 1992; Thatje et al., 2005; 2008; Strugnell et al., 2008; Strugnell et al., 2011; Dornburg et al., 2017; Legezyñska et al., 2020).

Adaptive radiation is one of the processes that could explain how species diversity could have evolved in the polar regions (and elsewhere) as a response to climate change (Brandt, 1999; Matschiner et al., 2011; Near et al., 2012; Daane et al., 2019; Doenz et al., 2019). The most common view of adaptive radiation is a scenario defined by the rapid diversification of lineages from a common ancestor that occupy a variety of ecological niches and have different traits to exploit those ecological niches (Schluter, 2000; Ridley, 2003; Gavrilets & Losos, 2009; Rundell & Price; 2009; Saupe & Myers, 2021; Matsubayashi & Yamaguchi, 2022). Ecological opportunity caused by the colonization of new areas, the evolution of key innovations, and/or the extinction of competitors are assumed to be vital for adaptive radiations to occur (Simpson, 1953; Ridley, 2003; Yoder et al., 2010; Stroud & Losos, 2016; Doenz et al., 2019). An alternative scenario to explain polar species diversity would be through non-adaptive radiation (Eastman, 2005; Eastman & Eakin, 2022), where lineages diversify without significant ecological and trait differentiation (Gittenberger, 1991; Schluter, 2000; Rundell & Price, 2009). This scenario of lineage diversification would be mainly driven by the isolation of populations (allopatry, parapatry) due to climate and/or geographic barriers. Another possible evolutionary scenario would be repeated convergence (Parker et al., 2022), where lineages evolve in response to similar selective pressures in the environment and/or as a consequence of constraints that can arise from developmental processes, shared pleiotropic or epistatic effects, competition, and biases in phenotypic variation (Losos, 2011; Frédérich et al., 2013). Confronted now with fast-paced environmental changes such as global warming (Rogers, 2007; Turner & Overland,

2009; Near et al., 2012; Gutt et al., 2015), understanding the evolutionary processes that have shaped the current diversity in the polar regions is essential to predict their possible response to future climate change (Near et al., 2012; Parker et al., 2022).

Amphipods are among the most diverse crustaceans in the polar regions (Sirenko, 2001; Węsławski & Legeżyńska, 2002; Thomas et al., 2008; Sirenko, 2009; Bodil et al., 2011; Legezyñska et al., 2020; Arfianti & Costello, 2020) and have different trophic types (Dauby et al., 2001; Nyssen, 2005; Legeżyńska et al., 2012). Amphipods also show high abundance and endemicity at both poles (Thomas et al., 2008; Meltofte et al., 2013; Legezyñska et al., 2020; Arfianti & Costello, 2020). Brooding behaviour, the absence of a free-swimming larval stage, and extended parental care all limit dispersal of amphipods (Baird et al., 2011: Copilaş-Ciocianu et al., 2020) resulting in reproductive isolation (Baird et al., 2011; Rogers, 2007; Legezyñska et al., 2020). As a result, populations can easily become genetically isolated, resulting in high species richness and recent distribution patterns that accurately depict past events (Copilaș-Ciocianu et al., 2019; Copilaş-Ciocianu et al., 2020).

The worldwide distribution of the amphipod *Eusirus*, its occurrence in both the Southern and the Arctic Ocean, and its ecological and morphological variability make it an ideal group to study eco-evolutionary patterns of polar taxa. The amphipod genus *Eusirus,* Krøyer, 1845 is composed of thirty-one described species (Verheye, 2011; Jung et al., 2016; Peña Othaitz & Sorbe, 2020; Wang et al., 2021) with ten described species from the Antarctic (Verheye, 2011; Jung et al., 2016; Peña Othaitz & Sorbe, 2020). The number of recognized Arctic species varies according to the authors. Here, the classification of Thurston (2009) and Palerud & Vader (1991) recognizing nine species will be followed. *Eusirus* occupies different habitats ranging from benthic to bentho-pelagic, with some being strictly pelagic (Weisshappel, 2000; Arndt & Swadling, 2006; De Broyer et al., 2007; Golovan et al., 2013; Peña Othaitz & Sorbe, 2020; Verheye & d'Udekem d'Acoz, 2020) and others being able to switch to a sympagic lifestyle (Arndt & Swadling, 2006; Macnaughton et al., 2007; Krapp et al., 2008; Kiko et al., 2008; Kosobokova et al., 2011; Peña Othaitz & Sorbe, 2020). *Eusirus* amphipods are mainly predators with different feeding habits ranging from deposit feeding, scavenging to necrophagous behaviour (Klages & Gutt, 1990; Dauby et al., 2001; Nyssen et al., 2002; Takeuchi et al., 2002; De Broyer et al., 2004; Nyssen, 2005; Michel et al., 2020).

The main objective of this study is to understand the eco-morphological diversification of the genus *Eusirus* by combining a novel, dated phylogeny with ecological information generated by stable isotope analyses and morphological data. The marine diversity of both polar regions has been shaped by their geological and climatic history; however, evolutionary history was found to differ between the two regions (Legezyñska et al., 2020). Hence, we hypothesize that the evolutionary scenario of the *Eusirus* would also be different in the Arctic and the Antarctic. We specifically aim to address the following issues: (1) Did the *Eusirus* species mainly originate through adaptive or non-adaptive radiation? (2) Is the pattern of ecological diversification of *Eusirus* the same in the Arctic and the Antarctic? (3) Is there a striking convergence in the Arctic and Antarctic *Eusirus* species?

Materials and methods

Taxon sampling

Amphipods were collected from different localities in the Arctic, Antarctic, and non-polar regions (Table 1 and Supplementary table 5). 21 of the 31 (67.7%) described *Eusirus* species were included in this study, together with 12 other species being tentatively identified as undescribed and denoted as "*Eusirus sp.*". The taxon sampling covered eight of the ten (80%) formally described species from the Antarctic and one undescribed *Eusirus* species, while all nine (100%) recognized species from the Arctic were also included here. Additionally, four of the twelve (33.3%) described non-polar *Eusirus* were analyzed in this study together with eleven undescribed non-polar *Eusirus* species. All specimens were preserved in 95-100% ethanol except for *Eusirus bonnieri*, which was fixed in formaldehyde. Vouchers were deposited at the Royal Belgian Institute of Natural Sciences (RBINS, Brussels, Belgium), Muséum National d'Histoire Naturelle (MNHN, Paris, France), Centre for Biodiversity Genomics (University of Guelph, Canada), The Civic Museum of Natural History of Verona (Italy), National Institute of Water and Atmospheric Research (NIWA, New Zealand), and Hiroshima University (Japan).

Morphological data

Stack photography is a digital image processing technique that takes several photos at various focus distances and combines those into a single image with a higher field depth (Brecko et al., 2014). This technique was used to produce images of each *Eusirus* specimen with an Olympus EM10 III and lenses 30 mm 1: 3.5 macro ED (extra-low dispersion) MSC (movie & still compatible). A minimum of three specimens per species were analyzed to collect morphological data from stack photography. Dissections of amphipod appendages were generally not allowed by museum curators. Instead, appendages were manipulated with clay mold before taking stack photos to reduce errors. The stack photos were imported into the ImageJ 1.53e software (Rasband, 2014), with which morphological traits were measured. The measured 24 traits and their reference points are shown in figure 1; all measurements were recorded in centimeters (cm). Measurements of each trait were replicated three times to ensure accuracy and reduce errors. The mean of those three measurements was used as raw measurement data point. The sex of the analysed specimen was not determined because sexual dimorphism in *Eusirus* is weak, and sex determination risks damaging morphological traits because of the required physical manipulations (Verheye & D'Udekem D'Acoz, 2020).

Table 1. Overview of the number of individuals per putative genetic species with their geographic identity and number of analyzed samples for each data type. "NA" indicates that no data were available. Detailed information of each specimen can be found in Supplementary Table 5.

Species name	Locality	Molecular data	Morphological data	δ13C data	δ15N data
Eusirus microps	Antarctica	3	6	10	9
Eusirus propeperdentatus	Antarctica	3	5	17	17
Eusirus laticarpus 1	Antarctica	6	2	4	4
Eusirus laticarpus 2	Antarctica	3	3	3	NA
Eusirus laticarpus	Antarctica	NA	2	3	2
Eusirus perdentatus	Antarctica	5	15	33	29
Eusirus pontomedon	Antarctica	3	12	16	16
Eusirus antarcticus	Antarctica	5	8	20	17
Eusirus bouvieri 1	Antarctica	4	2	3	3
Eusirus bouvieri 2	Antarctica	6	1	4	4
Eusirus bouvieri	Antarctica	NA	NA	12	12
Eusirus giganteus G1	Antarctica	6	2	5	5
Eusirus giganteus G2	Antarctica	4	3	5	5
Eusirus giganteus G3	Antarctica	2	2	2	2
Eusirus giganteus G4a	Antarctica	5	3	4	4
Eusirus giganteus G4b	Antarctica	4	3	4	4
Eusirus giganteus	Antarctica	NA	NA	21	21
Eusirus sp. 1	Antarctica	4	3	NA	NA
Eusirus holmii	Arctic	NA	7	16	16
Eusirus cuspidatus	Arctic	4	7	11	11
Eusirus propinqvus	Arctic	3	4	4	3
Eusirus minutus	Arctic	5	3	4	4
Eusirus longipes	Arctic	NA	7	22	4
Eusirus abyssi	Arctic	NA	1	NA	NA
Eusirus biscayensis	Arctic	NA	5	9	NA
Eusirus leptocarpus	Arctic	NA	3	2	1

Eusirus tjalfiensis	Arctic	NA	1	NA	NA
Eusirus sp. 10	Non-polar	NA	1	1	NA
Eusirus sp. 11	Non-polar	NA	NA	1	NA
Eusirus sp. 3	Non-polar	1	1	1	NA
Eusirus sp. 12	Non-polar	NA	1	1	NA
Eusirus sp. 13	Non-polar	NA	1	1	NA
Eusirus bonnieri	Non-polar	NA	6	6	6
Eusirus nevandis	Non-polar	NA	1	NA	NA
Eusirus sp. 5	Non-polar	1	1	NA	NA
Eusirus sp. 14	Non-polar	NA	1	NA	NA
Eusirus sp. 4	Non-polar	1	1	NA	NA
Eusirus sp. 15	Non-polar	NA	1	NA	NA
Eusirus sp. 7	Non-polar	1	1	NA	NA
*Eusirus sp.*6	Non-polar	1	NA	NA	NA
Eusirus bulbodigitus	Non-polar	NA	2	2	2
Eusirus parvus	Non-polar	NA	4	3	NA

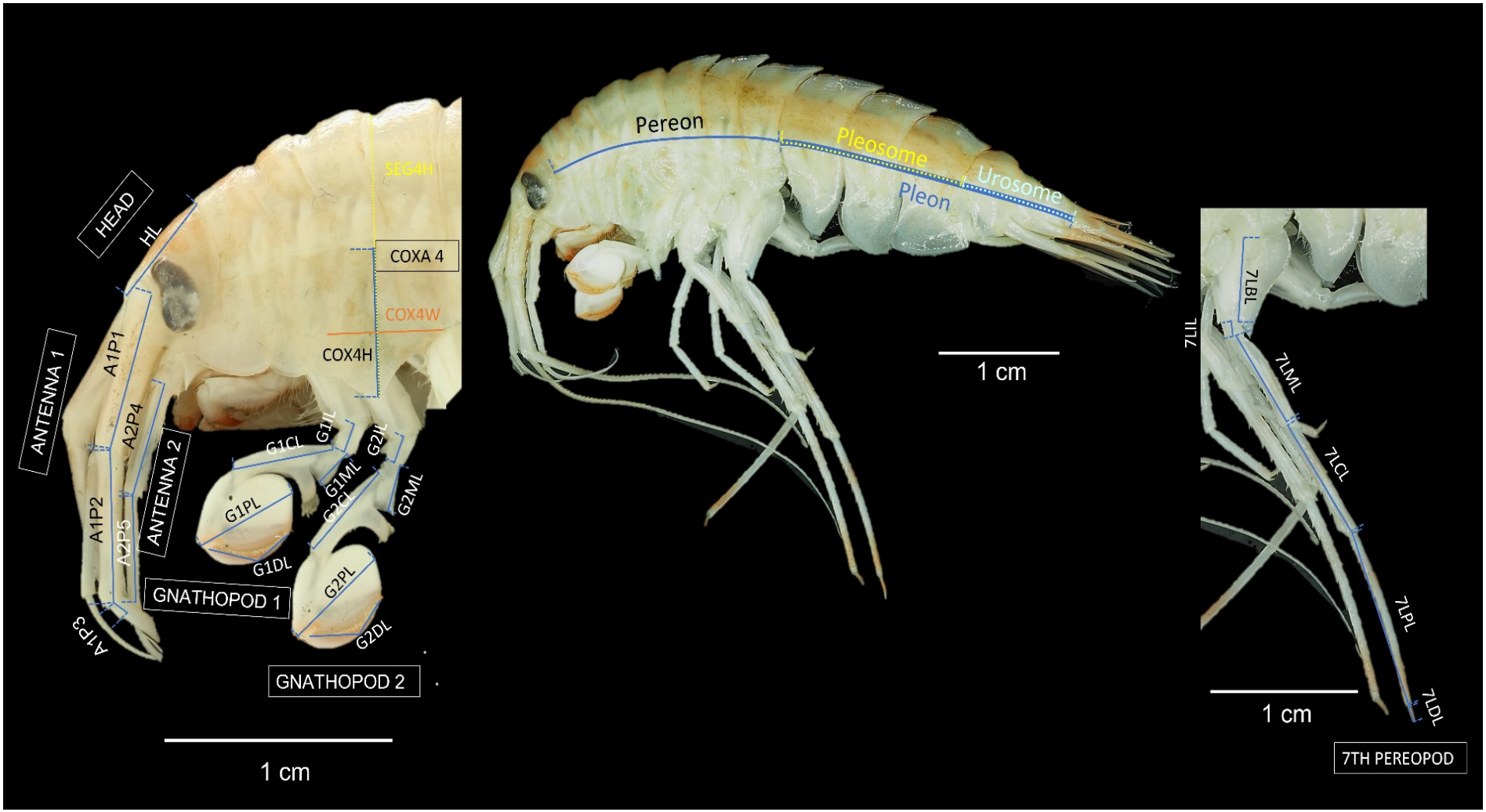

Figure 1. Analyzed morphological traits of *Eusirus* amphipods are abbreviated as: A1P1= peduncle 1 of antenna 1; A1P2= peduncle 2 of antenna 1; A1P3= peduncle 3 of antenna 1; A2P4= peduncle 4 of antenna 2; A2P5= peduncle 5 of antenna 2; COX4H= Height of coxa 4; COX4W= width of coxa 4; SEG4H= height of body segment 4; G1DL= gnathopod 1 dactylus length; G1PL= gnathopod 1 propodus length; G1CL= gnathopod 1 carpus length; G1ML= gnathopod 1 merus length; G1IL= gnathopod 1 ischium length; G2DL= gnathopod 2 dactylus length; G2PL= gnathopod 2 propodus length; G2CL= gnathopod 2 carpus length; G2ML= gnathopod 2 merus length; G2IL= gnathopod 2 ischium length; 7LDL= 7th pereopod dactylus length; 7LPL= 7th pereopod propodus length; 7LCL= 7th pereopod carpus length; 7LML= 7th pereopod merus length; 7LIL= 7th pereopod ischium length; 7LBL= 7th pereopod basis length.

Some morphological traits could not be measured due to damaged or missing appendages, resulting in missing data. Removal of missing data can decrease sample size and introduce bias, leading to erroneous conclusions (Penone et al., 2014). To address the missing data issue, imputations were performed on the raw measurement data using the missMDA R-package version 3.61 (R Core Team, 2019), which replaces missing values using a PCA model (Josse & Husson, 2016). To exclude the effect of size on morphological variation, we decided to produce 43 ratios of morphological traits to quantify the general morphology of *Eusirus* species. All these ratios are listed in table 2. To compute these ratios, total body length (TBL), total length of Antenna 1 (A1TL), total length of Antenna 2 (A2TL), Head length (HL), and Pleon length (Pleon) were also calculated. Total body length is the sum of the head, pereon, and pleon length. The total length of Antenna 1 is the sum of peduncles 1-3 of antenna 1, and the total length of Antenna 2 is the sum of peduncles 4-5. Head length is measured from the tip of the rostrum up to the edge of the first segment of the pereon. Pleon length is the sum of the lengths of both the pleosome and the urosome length.

To analyze the morphological diversity of *Eusirus*, a principal component analysis (PCA) on the 43 ratios was performed with the *princomp* function in the built-in R stats package (R Core Team, 2019). The R package factoextra (Kassambara & Mundt, 2017) was used to extract and visualize the results of PCA. PCA minimizes the dimensionality of a data set while retaining most of its variation and hence keeping most of the information (Jollife, 2002; Ringnér, 2008). The number of retained principal components is based on the cumulative explained variance, and usually, a common criterium is to retain the principal components that account for a cumulative variance of 70 to 90% (Jollife, 2002). To reduce the number of variables, the eight principal components that accounted for about 90% of the cumulative variance were retained here and used to identify the variables that contributed the highest variance to these components. This reduced data set, herewith referred to as the “reduced morphological dataset” contained 15 of the originally 43 calculated ratios.

Table 2. List of ratios/variables computed for morphological trait analyses. The 15 Ratios/variables that were retained based on the result from PCA in the "reduced morphological data set" are indicated in bold.

Ratio	Description
Head/TBL	Ratio of head length and total body length
Pereon/TBL	Ratio of pereon length and total body length
Pleon/TBL	Ratio of pleon length and total body length
Pereon/Pleon	Ratio of pereon length and pleon length
Pereon/Pleosome	Ratio of pereon length and pleosome length
A1TL/HL	Ratio of antenna 1 total length and head length
A2TL/HL	Ratio of antenna 2 total length and head length
A1TL/A2TL	Ratio of antenna 1 total length and antenna 2 total length
A1P2/A1P1	Ratio of peduncle 2 of antenna 1 length and peduncle 1 of antenna 1
A2P5/A2P4	Ratio of peduncle 5 of antenna 2 and peduncle 4 of antenna 2
COX4H/COX4W	Ratio of coxa 4 height and coxa 4 width
COX4H/Pereon	Ratio of coxa 4 height and pereon length
COX4W/Pereon	Ratio of coxa 4 width and pereon length
SEG4H/COX4H	Ratio of body segment 4 height and coxa 4 height
G1DL/G1PL	Ratio of dactylus length of gnathopod 1 and propodus length of gnathopod 1
G1PL/G1CL	Ratio of propodus length of gnathopod 1 and carpus length of gnathopod 1
G1CL/G1ML	Ratio of carpus length of gnathopod 1 and merus length of gnathopod 1
G1ML/G1IL	Ratio of merus length of gnathopod 1 and ischium length of gnathopod 1
G2DL/G2PL	Ratio of dactylus length of gnathopod 2 and propodus length of gnathopod 2
G2PL/G2CL	Ratio of propodus length of gnathopod 2 and carpus length of gnathopod 2
G2CL/G2ML	Ratio of carpus length of gnathopod 2 and merus length of gnathopod 2
G2ML/G2IL	Ratio of merus length of gnathopod 2 and ischium length of gnathopod 2
G1DL/Pereon	Ratio of dactylus length of gnathopod 1 and pereon length
G1PL/Pereon	Ratio of propodus length of gnathopod 1 and pereon length
G1CL/Pereon	Ratio of carpus length of gnathopod 1 and pereon length
G1ML/Pereon	Ratio of merus length of gnathopod 1 and pereon length
G1IL/Pereon	Ratio of ischium length of gnathopod 1 and pereon length
G2DL/Pereon	Ratio of dactylus length of gnathopod 2 and pereon length
G2PL/Pereon	Ratio of propodus length of gnathopod 2 and pereon length
G2CL/Pereon	Ratio of carpus length of gnathopod 2 and pereon length
G2ML/Pereon	Ratio of merus length of gnathopod 2 and pereon length
G2IL/Pereon	Ratio of ischium length of gnathopod 2 and pereon length
7LDL/7LPL	Ratio of dactylus length of the 7^{th} pereopod and propodus length of the 7^{th} pereopod
7LPL/7LCL	Ratio of propodus length of the 7^{th} pereopod and carpus length of the 7^{th} pereopod
7LCL/7LML	Ratio of carpus length of the 7^{th} pereopod and merus length of the 7^{th} pereopod
7LML/7LIL	Ratio of merus length of the 7^{th} pereopod and ischium length of the 7^{th} pereopod
7LIL/7LBL	Ratio of ischium length of the 7^{th} pereopod and basis length of the 7^{th} pereopod
7LDL/Pereon	Ratio of dactylus length of the 7^{th} pereopod and pereon length
7LPL/Pereon	Ratio of propodus length of the 7^{th} pereopod and pereon length
7LCL/Pereon	Ratio of carpus length of the 7^{th} pereopod and pereon length
7LML/Pereon	Ratio of merus length of the 7^{th} pereopod and pereon length
7LIL/Pereon	Ratio of ischium length of the 7^{th} pereopod and pereon length
7LBL/Pereon	Ratio of basis length of the 7^{th} pereopod and pereon length

Ecological data

In addition, we aimed to characterize the trophic diversity of *Eusirus* species. To do so, stable isotopes data were collected for each specimen with a minimum of ten specimens per species, if possible. Stable isotopes analyses use the ratio of heavy to light isotopes (R_x) typically measured with mass spectrometry (Newton, 2016; Hershey et al., 2017). Analyses of stable isotopes, specifically of carbon and nitrogen, are of particular interest in ecological and trophic studies (Hobson, 1999; Post, 2002; Layman et al., 2011; Le Bourg, 2020). This kind of analysis is based on the "you are what you eat" principle. Stable isotope ratios vary among food webs, and an animal's diet influences the ratios integrated into its tissue (Hobson, 1999; Le Bourg, 2020). These ratios provide long-term information on the organism's diet of the assimilated food as compared to its short-term diet of recent ingestions, as shown, for example, by stomach content analysis (Hood-Nowotny & Knols, 2007; Davis et al., 2012).

The ^{12}C and ^{13}C are the two stable isotopes of carbon commonly used in ecological and trophic studies (Newton, 2016). The carbon isotope ratio is typically used to identify the primary source of carbon in food webs or feeding areas since different carbon sources have different isotopic signatures (Post, 2002; Layman et al., 2011; Le Bourg, 2020). Between trophic levels, the carbon isotope ratios only slightly increase or become enriched, usually by 0-1‰ (Inger & Bearhop, 2008). The two isotopes of nitrogen commonly used in ecological and trophic studies are ^{14}N and ^{15}N (Newton, 2016). The ^{15}N goes through a stepwise increase of 2-4 ‰ with each trophic level, resulting in an increase in the heavy to light nitrogen isotope ratio (Layman et al., 2011; Hobson & Wassenaar, 2018). This increase is caused by the loss of the light ^{14}N to nitrogenous waste products during the assimilation of dietary proteins, resulting in an enrichment of ^{15}N in the organism's tissue relative to its diet (Inger & Bearhop, 2008). This ratio of nitrogen isotopes can thus be used to identify a species' trophic level or position in the food web (Post, 2002; Inger & Bearhop, 2008; Layman et al., 2011; Le Bourg, 2020).

Depending on the size, one or two pleopods of each amphipod specimen were dissected under a binocular microscope, stored in Eppendorf tubes, and oven-dried at 50°C for 48 hours. Samples were weighed in tin cups with a maximum of two mg and analyzed with an elemental analyzer (vario MICRO cube, Elementar Analysensysteme GMBH, Hanau, Germany) coupled to a continuous-flow IsoPrime100 isotope ratio mass spectrometer (Isoprime, Cheadle, United Kingdom). Isotope ratios of carbon and nitrogen were expressed as delta (δ) notations ($\delta^{13}C$

and $\delta^{15}N$, respectively), which are parts per thousand (‰) relative to their respective international standards (Peterson & Fry, 1987; Newton, 2016):

$$\delta X = \left(\frac{R_x}{R_{std}} - 1\right) \times 1000$$

where X is the sample name of the heavier isotope (^{13}C and ^{15}N, respectively) and R is the ratio of the heavy and light isotope ($^{13}C/^{12}C$ and $^{15}N/^{14}N$, respectively) of sample x (R_x) and an internationally agreed standard (R_{std}). The internationally accepted stable isotope for the carbon isotope is the Vienna-PeeDee Belemnite (vPDB) standard and for the nitrogen isotope (the standard Atmospheric Air (AIR) (Newton, 2016). Analytical standards with known stable isotope ratio values were used to account for potential drifts and improve accuracy during stable isotopes analysis. Procedural blanks, replicates (i.e., glycine, sea bass reference material), and certified reference material from the International Atomic Energy Agency (IAEA, Vienna, Austria): IAEA C-6 (sucrose; $\delta^{13}C$ = –10.8 ± 0.5 ‰; mean ± SD) and IAEA-N1 (ammonium sulphate; $\delta^{15}N$ = 0.4 ± 0.2‰; mean ± SD) were used as primary standards for carbon and nitrogen analysis, respectively. Since preservation methods were found to affect $\delta^{13}C$ values (Le Bourg et al., 2020), a correction factor of –0.6 ‰ was added to $\delta^{13}C$ values of samples stored in ethanol and of +0.8 ‰ for samples stored in formaldehyde (Le Bourg et al., 2020). Stable isotope ratio values were also standardized by comparing them to the values taken from isoscapes. Isoscapes are isotopic values across a landscape, can account for spatial variation and facilitate comparisons across different locations (Cheesman & Cernusak, 2016; Bowen, 2010; St John Glew et al., 2021; Espinasse et al., 2022). The isoscape values used to standardize the stable isotope ratio values of the *Eusirus* samples were collected from the available scientific literature. The corrected and standardized, stable isotope ratios were compiled and termed herewith as the "isotope dataset" containing the data of all *Eusirus* species with measured stable isotope ratios.

Phylogenetic Information

The time-calibrated phylogeny produced in Chapter 4 is used here. For phylogenetically-informed analyses, a perfect match among datasets (i.e., phylogeny, morphology, and ecology)

was required. The time-tree was thus pruned accordingly to match the species included in the morphological and ecological datasets by using the *drop.tip* function in the R package ape.

Datasets for analyses

The different datasets used in the subsequent analyses below are described here.

- The **"reduced morphological dataset"** contains 15 morphological ratios, which were reduced through PCA from the original 43 ratios.
- The **"isotope dataset"** includes the corrected and standardized, stable isotope ratios of $\delta^{13}C$ and $\delta^{15}N$.
- The **"mean morpho dataset"** contains the mean value of each species which was calculated from the "reduced morphological dataset".
- The **"mean isotope dataset"** represents the mean isotope ratios of each species, which were calculated from the "isotope dataset".
- The **"9sp dataset morpho"** is the same as the "reduced morphological dataset" except that species were categorized into Antarctic, Arctic, and non-polar groups.
- **"**The **9sp dataset SI"** is the same as the "isotope dataset" except that species were categorized into Antarctic, Arctic, and non-polar groups.

Taxonomic representation was optimized depending on the analysis. The highest number of species for which data were available was used for analyses exploring morphological traits. Only species being present in both datasets were used for analyses combining morphology and ecology.

Morphological and ecological traits association

To check for any possible links between morphology and ecology, the *phylo.integration* function and phylogenetic generalized least squares (PGLS) were used. Understanding this link is important because morphology can reflect the functional role of a species in an ecosystem (Sosiak & Barden, 2021). Moreover, in adaptive radiations, diversification is driven by niche specialization; hence, a strong correlation is expected between the species' occupied environment and the morphological features utilized to exploit these available resources (Ronco et al., 2021). Such a link could also provide insights in how functional roles shaped the

Eusirus diversity in the polar regions (Wong et al., 2019) and will also enable us to determine if phenotypic evolution was adaptive.

To check for a possible link between all morphological data and both stable isotopes, the function *phylo.integration* of the geomorph R-package, based on a permutation test of 9999 iterations, was used. This function uses partial least squares and takes the phylogenetic information into account by assuming a Brownian motion model of evolution (Adams & Felice, 2014). Brownian motion model characterizes the evolution of traits as a random walk along each lineage, using a normal distribution with a mean of 0 and a variance of β (or s^2) for the change that happens in each unit of time (Ackerly, 2009; Revell & Harmon, 2022). Such a partial least squares analysis can be utilized to evaluate the patterns of covariation between the morphological dataset and environmental dataset without any *a priori* directional relationship being assumed between these datasets (Adams & Felice, 2014). For this analysis, the "mean morpho dataset" and the "mean isotope dataset" were used together with the pruned time-tree.

To examine the same relationship by using a univariate framework (i.e. the coordinates of the observations on PC1 and PC2; as well as the isotopic data δ13C and δ15N) separately, a phylogenetic generalized least squares (PGLS) analysis was also performed. A PCA was performed on the "mean morpho dataset" to summarize the main axes of morphological variation using the function *princomp* in R. The PC scores of the PC1 and PC2 axes, together with the "mean isotope dataset" and the pruned dated tree, were used for the PGLS analysis. PGLS allowed us to explore possible correlations between morphological variation and their different PCs and trophic variables in four different models: model 1 (M1) tested the relationship between morphological variation and δ13C, a possible correlation between morphological variation in PC1 and δ15N was tested in model 2 (M2), a possible link between morphological variation in PC2 and δ13C was assessed in model 3 (M3), and the link between morphological variation in PC2 and δ13C was explored in model 4 (M4). PGLS was performed using the R packages ape (Paradis et al., 2004) and nlme (Pinheiro et al., 2007). A PGLS allows the fit of a linear model using the generalized least squares (Revell & Harmon, 2022) to assess the impact of the predictor variable (i.e. δ13C and δ15N) on the response variable (i.e. morphological data or PC scores) while controlling for the non-independence of the residuals (Mundry, 2014).

Phylogenetic signal of traits and ancestral state reconstructions

To explore how traits are dispersed across the phylogeny, ancestral states were reconstructed and tests of the phylogenetic signal were performed. These analyses provide insights into the distribution pattern of morphological variation across species and its association with the phylogeny (Adams, 2014). These analyses would also allow us to test for possible convergence in the polar regions and reveal the evolvability of morphological traits.

The phylogenetic signal is the tendency of closely related species to have comparable traits due to common ancestry (Blomberg et al., 2003; Adams, 2014). The phylogenetic signal is measured using the multivariate version of Blomberg et al.'s K statistic as described by Adams (2014), which also estimates the strength of the phylogenetic signal relative to what is expected under a Brownian motion model of evolution (Adams, 2014). The K values range from 0 to infinity and under Brownian motion, the expected K value is 1. Values of $K<1$ indicate less phylogenetic signal in the data than expected, while $K>1$ indicates more phylogenetic signal in the data than expected (Blomberg et al., 2003; Adams, 2014). The significance of the K statistics was assessed by comparing it to the values obtained from permutations of tree tips (Blomberg et al., 2003; Adams, 2014). The phylogenetic signal was analyzed using the *physignal* function in the R package geomorph with a permutation test of 9999 iterations. A PCA was conducted on the "mean morpho dataset" with the *princomp* function in R. The PC scores of all PC axes and the pruned time-tree were utilized for the analysis of the phylogenetic signal.

Several approaches of ancestral reconstructions of the morphological traits were applied. Ancestral states were reconstructed under Brownian motion using the function *fastAnc* in the R package phytools, which estimates the ancestral states with a maximum likelihood approach based on a Brownian motion model of evolution (Revell, 2013; Revell & Harmon, 2022). The "mean morpho dataset" was subjected to a PCA using the *princomp* function in R. Together with the pruned dated phylogeny, the PCA scores of the PC1 and PC2 axes were then used separately in ancestral state reconstructions. Besides the scores along PC1 and PC2, additional ancestral state reconstructions were also performed on four separated traits (i.e., ratios of Pereon/TBL, G1PL/G1CL, G2DL/G2PL, 7LIL/7LBL) as being representative for morphological diversity of each amphipod appendage. These traits are ecologically and functionally relevant and are related to locomotion and predation (Kralj-Fišer et al., 2020; Balázs et al., 2021).

Rate shifts of morphological diversification

The Bayesian Analysis of Macroevolutionary Mixtures (BAMM) tested for rate shifts in diversification of morphological trait. This method helps to reveal variations in the diversification rates through time (Rabosky, 2014). Under the scenario of adaptive radiation, organisms taking advantage of new ecological opportunities are predicted to go through rapid lineage and morphological diversification at the start of the radiation as they fill available adaptive zones (Schluter, 2000). In non-adaptive radiation, diversification is likely to occur in allopatric environments which results to insignificant ecological and morphological differentiation with consistent rate of speciation and morphological differentiation and no rapid morphological evolution (Schluter, 2000; Lambert et al., 2019). Exploring the evolutionary dynamics of morphological diversification of *Eusirus* will help reveal whether these amphipod species went through such adaptive radiations in both polar regions and whether the tempo of morphological evolution was similar in the Antarctic and the Arctic.

The "mean morpho dataset" was subjected to a PCA, and scores of the PC1 and PC2 axes combined with the pruned dated phylogeny, were subsequently used to test for shifts of morphological diversification using BAMM (Rabosky, 2014). Priors were generated with the R package BAMMtools (Rabosky et al., 2014), and the MCMC analysis was run for 10 million generations, sampling every 5000 generations. Convergence of the MCMC analysis was assessed after discarding 10% of the samples as burnin by checking the effective sample sizes (ESS) and the number of shifts in each sample with the R package CODA (Plummer et al., 2006). The Bayes factor (BF) was also calculated with BAMMtools to assess the relative support of the two different models being compared. The strength of support for a given model was based on the interpretation of the Bayes Factor as suggested by Kass & Raftery (1995) and shown in table 3.

Table 3. Interpretation of Bayes f=Factor as indicated by Kass & Raftery (1995)

B_{10}	Evidence as compared to the null model (M_0)
1 to 3	Barely worth a mention
3 to 20	Positive
20 to 150	Strong
>150	Very strong

Morphological and ecological disparity

Morphological disparity and ecological diversity were analyzed using the "9sp dataset morpho" and "9sp dataset SI" to check for the repetition of ecological and morphological diversity between Arctic and Antarctic regions. The "9sp dataset morpho" was subjected to a PCA using the *princomp* function in R to summarize the morphological variation in each group; the PCA was plotted using *ggplot* function in the R package ggplot2 (Wickham, 2016). To visualize the isotopic diversity of each group in the isospace, biplots of $\delta^{13}C$ and $\delta^{15}N$ were also done using the *ggplot* function in R and the "9sp dataset SI". The position and the size of each group (i.e., Antarctic, Arctic, and non-polar species) in the morphospace (i.e., morphological space) and the isospace (i.e., isotope space) were compared. By size, we refer to the estimates of the volume occupied by the groups in the phylogenetic space, while position refers to the location of the group in the morphospace and isospace (Guillerme et al., 2020a).

The level of disparity (i.e., size) was based on the Procrustes variance, a disparity metric, which is the relative sum of the diagonal elements of the covariance matrix of the ordination scores (Zelditch et al., 2012; Adams & Otárola-Castillo, 2013; Guillerme, 2018). Pairwise comparisons of disparity between groups were conducted with the *morphol.disparity* function in the geomorph R-package (Adams & Otárola-Castillo, 2013) with a permutation test of 9999 iterations. The position of the groups in the morpho- and isospaces was compared with the *procD.lm* function in the geomorph package, which performs a Procrustes ANOVA and a permutation test of 9999 iterations.

In parallel, the morphological and ecological diversity were also estimated and compared among the three groups using three indices: functional richness, functional evenness, and functional divergence. Functional richness calculates the volume occupied by a group in the functional trait space. Functional evenness estimates how evenly abundances are distributed in the functional trait space, and functional divergence approximates how abundance is spread along the range of the functional trait space (Villéger et al., 2008). Only eight of the original fifteen variables in the "9sp dataset morpho" were used to calculate the functional diversity indices because a hull volume of zero was returned when calculating the functional richness using all fifteen variables. The hull volume equals zero when species are distributed in a line (Villéger et al., 2008).

Disparity through time

Disparity through time (DTT) analyses explore the evolution of morphological diversity through time (Harmon et al., 2003; Guillerme et al., 2020b). It is expected in groups that undergo adaptive radiation to diverge into a variety of morphologically and ecologically distinct species, occupying available niches; DTT will eventually slow down as these niches are filled (Gavrilets & Losos, 2009; Colombo et al., 2015). DTT analysis illustrates the tempo of morphological changes, providing insights into whether clades went through adaptive radiations (Colombo et al., 2015; Guillerme et al., 2020b). DTT plots were generated with the *dtt* function of the R package geiger (Pennell et al., 2014). In this kind of analysis, the average relative disparity per subclade of a trait is computed at each node in the phylogeny and plotted against the age of each node. DTT plots were only interpreted for the first 80% of the relative time to provide a more accurate estimate and reduce the impact of incomplete sampling, as this tends to mask a possible pattern of slowdown of morphological evolution (Harmon et al., 2003). The morphological disparity index (MDI) was also determined to measure the difference between average observed relative disparity for each subclade through time as compared to the expected subclade disparity under the Brownian motion model (Harmon et al., 2003) with 1000 simulations. Under a Brownian motion model (Revell, 2012; Frédérich et al., 2013) morphological disparity uniformly increases through time. Similar to DTT plots, MDI was calculated for only the first 80% of the relative timeline. Only four selected traits (i.e., Pereon/TBL, G1PL/G1CL, G2DL/G2PL, 7LIL/7LBL) were subjected to DTT analysis using the pruned dated tree. These traits are ecologically and functionally relevant and are related to locomotion and predation (Kralj-Fišer et al., 2020; Balázs et al., 2021). Moreover, preliminary examinations of these traits have shown variability among species. PC scores of the morphological traits were not used for the DTT analysis; this can cause biased inferences as the first few principal components of traits that evolved under a constant-rate Brownian motion of evolution will seem to have evolved through an "early burst" process (Uyeda et al., 2015).

Results

Morphological and ecological disparity

In a PCA analysis based on the "9sp dataset morpho", the smallest morphospace and thus amount of morphological variation is observed in the Antarctic *Eusirus* group compared to the Arctic and non-polar groups (Figure 2). The first three PC axes explained 89.7% of the total variance. The first PC axis (PC1) explained 67.3% of the total variance and mainly described variation in the ratio of carpus length of gnathopod 1 and merus length of gnathopod 1 (G1CL/G1ML) (Figure 2). The second axis (PC2) explained 12.9% of the total variance and expressed mainly variation of the ratio of merus length of gnathopod 1 and ischium length of gnathopod 1 (G1ML/G1IL) (Figure 2). The third axis (PC3) described the ratio of pereon length and pleosome length (Pereon/Pleosome), explaining 9.5% of the total variance (Supplementary figure 5).

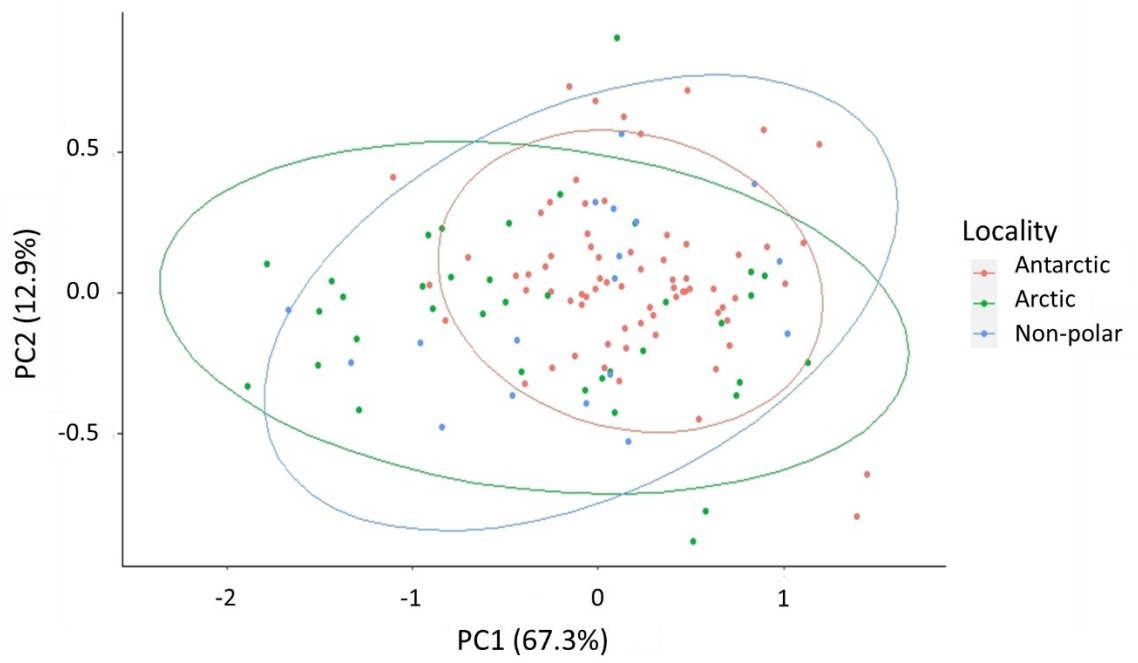

Figure 2. Principal component analysis (PCA) performed on the "9sp dataset morpho" showing PC1 (67.3%) and PC2 (12.9%). The three groups of *Eusirus* amphipods are indicated by colours with red for the Antarctic, green for the Arctic, and blue for the non-polar group.

Both Arctic and Antarctic *Eusirus* showed large variation of $\delta^{13}C$. However, the Arctic group furthermore had a wider isotopic distribution in the isospace for $\delta^{15}N$ as compared to the Antarctic group (Figure 3).

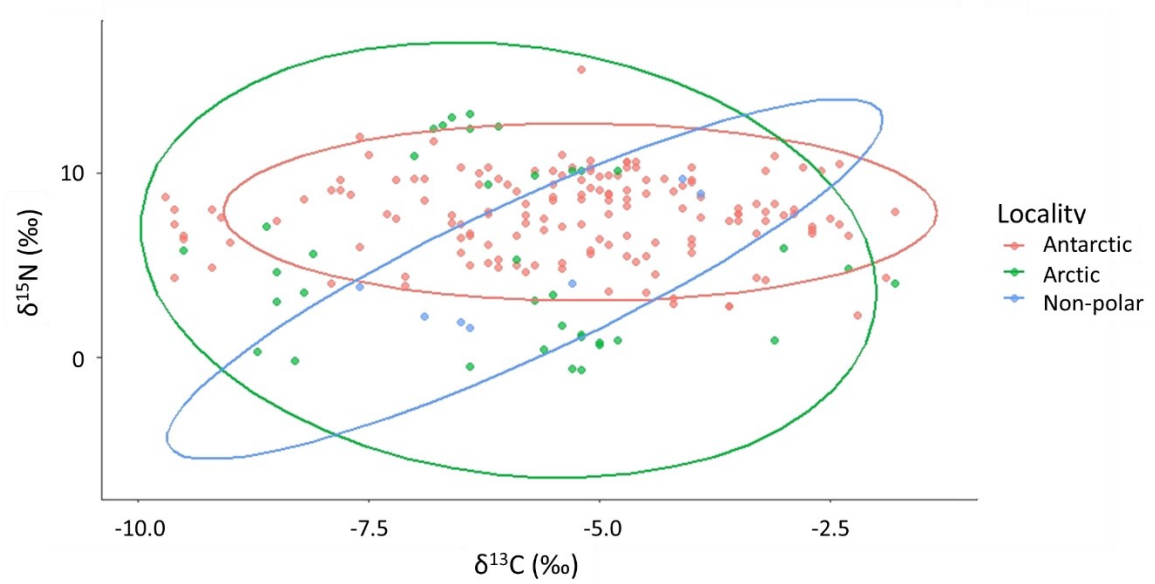

Figure 3. $\delta^{13}C$ versus $\delta^{15}N$ biplot illustrating the distribution of *Eusirus* in the isospace with 95% standard ellipses. The three groups are indicated by colours with red for the Antarctic, green for the Arctic, and blue for the non-polar group.

The level of disparity, i.e. the size of the subspace occupied by the group, was the highest for the Arctic group compared to the Antarctic and the non-polar groups (Figure 4a). This difference in the level of disparity was significant between the Antarctic and Arctic groups (p-value=0.0003) (Figure 4a).

Similarly, the Arctic group showed the highest level of isotopic diversity compared to the Antarctic and the non-polar groups (Figure 4b). Significant differences were observed between Antarctic and Arctic groups (p-value=0.0001), and between *Eusirus* from the Antarctic and non-polar regions (p-value=0.0439), as well as between Arctic and non-polar groups (p-value=0.0416) (Figure 4b).

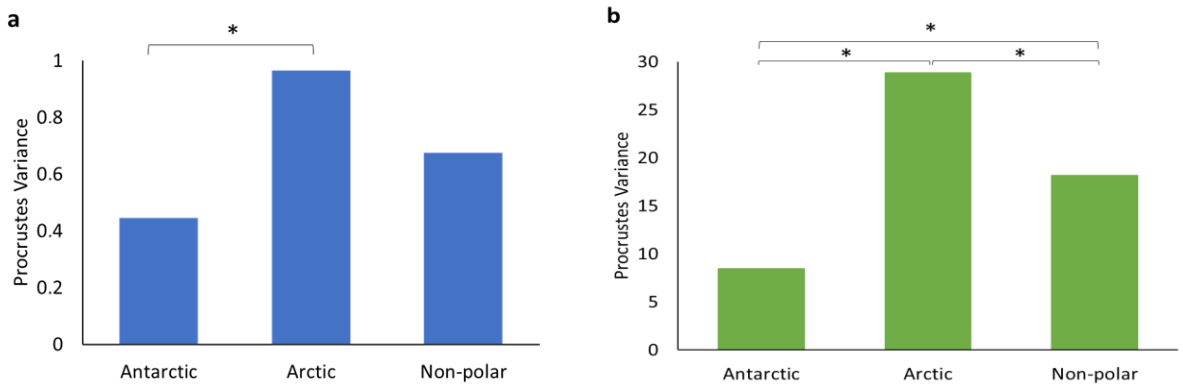

Figure 4. Procrustes variance of Antarctic, Arctic, and non-polar *Eusirus* groups based on a) the "9sp dataset morpho" (blue) and b) the "9sp dataset SI" (green). Significant differences ($p<0.05$) are indicated by *.

In addition to size variation of subspace occupation in the morphospace and isotopic space, the Procrustes ANOVA revealed that the three groups occupied different positions in both spaces (Table 6). In other words, the mean values of each group varied significantly.

Table 6. Comparison of the position of groups in the morphospace and the isospace based on the "9sp dataset morpho" and "9sp dataset SI". Significant differences ($p<0.05$) among groups (i.e., Antarctic, Arctic, and non-polar) are indicated by *. SS is the sums of squares, MS is the mean square, Rsq is the R-squared, F is the F values for each model term, Z is the Z-scores, and Pr(>F) is the p-value.

	SS	MS	Rsq	F	Z	Pr(>F)
"9sp dataset morpho" (group)	7.174	3.5870	0.09021	6.0981	3.0277	0.0007*
"9sp dataset SI" (group)	235.38	117.69	0.0923	10.016	4.3429	0.0001*

Functional diversity

Three different parameters were also analyzed to compare the functional diversity among the three *Eusirus* groups. Analyzing functional richness showed that the Arctic group occupied the largest functional trait space in morphology (1.9E-09) compared to the Antarctic (8.9E-10) and non-polar (4.9E-12) groups (Figure 5a). The Arctic group also had the largest occupancy in isospace (89.71) compared to Antarctic (67.11) and non-polar (10.33) *Eusirus* (Figure 5d). On the other hand, functional evenness for morphology was highest in the non-polar group (0.79), and the Antarctic group (0.73) showed a higher functional evenness than the Arctic group (0.67) (Figure 5b). Functional evenness for ecology was highest in the Antarctic group (0.63) compared to the Arctic (0.52) and the non-polar (0.59) groups (Figure 5e). Morphological functional divergence was higher in the non-polar group (0.68), while the same functional divergence value was observed for the two polar groups (0.67) (Figure 5c). For ecology, the highest functional divergence was found in Arctic *Eusirus* (0.79) compared to Antarctic (0.68) and non-polar (0.73) *Eusirus* (Figure 5f).

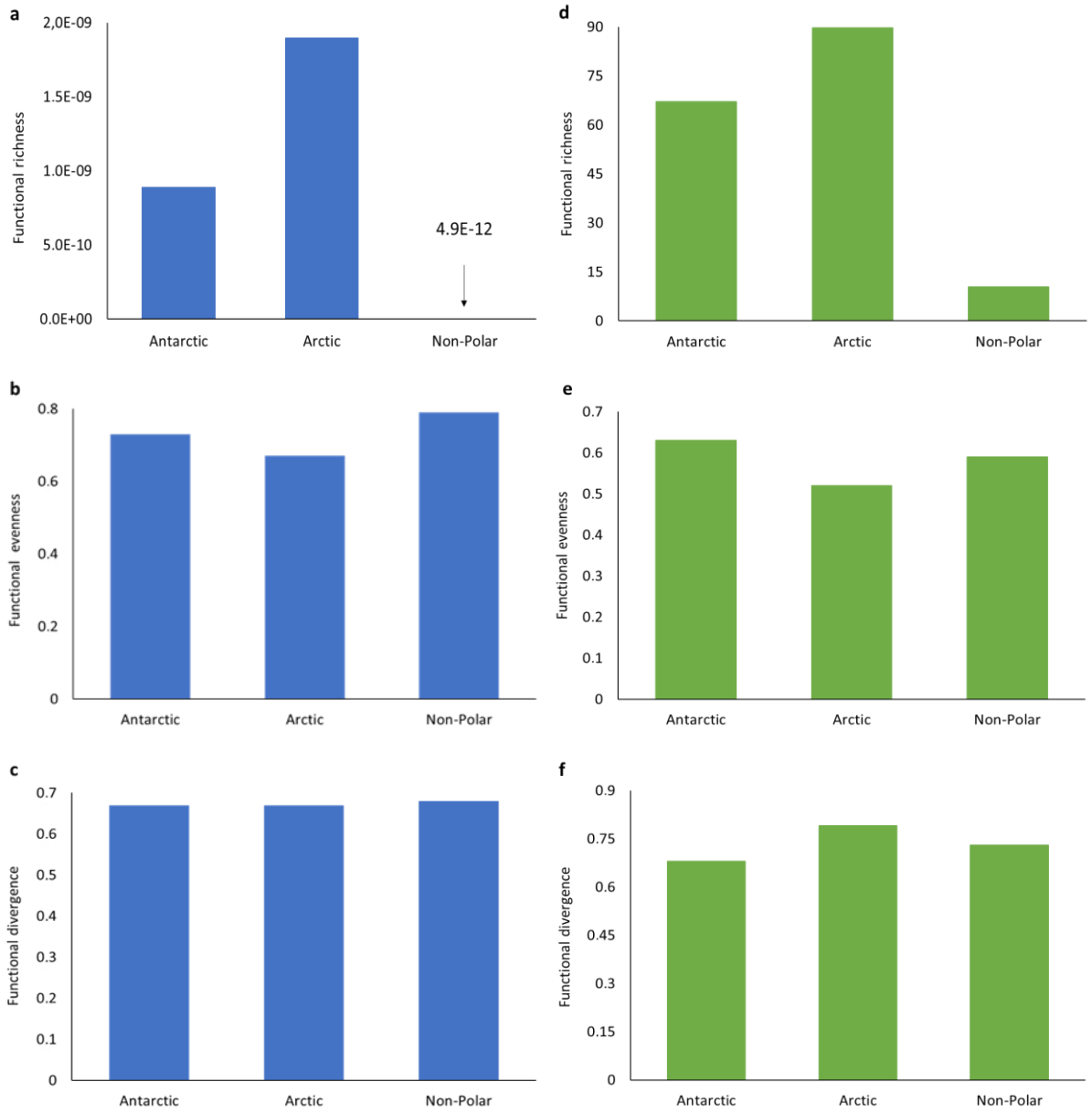

Figure 5. Values of functional richness, functional evenness, and functional divergence of morphological traits based on the "9sp dataset morpho" dataset (a-c; blue), and ecology using stable isotopes based on "9sp dataset SI" dataset (d-f; green) of Antarctic, FigureArtic and non-polar groups.

Association of morphological and ecological traits

Our phylogenetic-informed two-block PLS analysis showed a significant positive relationship between morphology and isotopy (r-PLS= 0.8945; p-value = 0.0001). The results of PGLS are summarized in table 4 showing the coefficients of each model. The PGLS analysis revealed a significant negative relationship between morphological traits and $\delta^{15}N$ based on the PC1 scores (p-value = 0.0002). A significant negative correlation was also observed between

morphological traits and the stable isotopes $\delta^{13}C$ (p-value = 0.0004) and $\delta^{15}N$ (p-value = 0.0001) based on the PC2 scores (Table 4).

Table 4. Summary of PGLS results showing the coefficients of each model. Model 1 (M1) tested the relationship between morphological variation and δ13C, a possible correlation between morphological variation in PC1 and δ15N was represented in model 2 (M2), a possible link between morphological variation in PC2 and δ13C was tested in model 3 (M3), and the link between morphological variation in PC2 and δ13C was explored in model 4 (M4). Significance (p<0.05) is indicated by *.

	Coefficients (M1)	Coefficients (M2)	Coefficients (M3)	Coefficients (M4)
Intercept	-0.32	1.285	-0,696	0.788*
δ13C	-0.057		-0.118*	
δ15N		-0.184*		-0.108*

Phylogenetic signal and ancestral state reconstructions of morphological traits

Morphological traits showed a significant phylogenetic signal (p-value= 0.0197) and the low K value (K=0.4265) indicated larger morphological variation between sister species than expected under a Brownian motion model of evolution.

The variation of the PC1 axis was mainly described by the ratio of carpus length of gnathopod 1 and merus length of gnathopod 1 (G1CL/G1ML), explaining 88% of the total variance. Reconstructing the ancestral state revealed a collectively low variation along PC1 within the Antarctic clade, while the Arctic group showed more variation along this axis (Figure 6a). The variation of the PC2 axis explained 7.1% of the total variance and was mainly described by the ratio of merus length of gnathopod 1 and ischium length of gnathopod 1 (G1ML/G1IL). Ancestral state reconstructions showed different results along the PC2 axis for the Antarctic and the Arctic groups (Figure 6b). The ratio of pereon length and total body length (Pereon/TBL) varied for both the Arctic and the Antarctic species, ranging from intermediate to higher Pereon/TBL ratios (Figure 6c). A similar pattern of intermediate to high values was observed for the ratio of propodus length of gnathopod 1 and carpus length of gnathopod 1 (G1PL/G1CL) (Figure 6d), and the ratio of dactylus length of gnathopod 2 and propodus length of gnathopod 2 (G2DL/G2PL) (Figure 6e). The ratio of ischium length of the 7th pereopod and basis length of the 7th pereopod (7LIL/7LBL) (Figure 6f) was low for the Arctic *species Eusirus minutus* and the Antarctic species *Eusirus laticarpus* 1 and *Eusirus sp.* 1.

Rate shifts of morphological diversification

Using PC1 scores, model 0, which had no rate shift in morphological diversification, showed the highest posterior probability (0.26) compared to the other models (Figure 7a). In contrast, based on the Bayes Factor analysis, model 13 with 13 rate shifts was strongest supported (Table 5). For the PC2 scores, model 0 including no rate shifts had the highest posterior probability (0.38) (Figure 7b), while the Bayes Factor analysis provided strong support for model 15 with 15 rate shifts (Table 5).

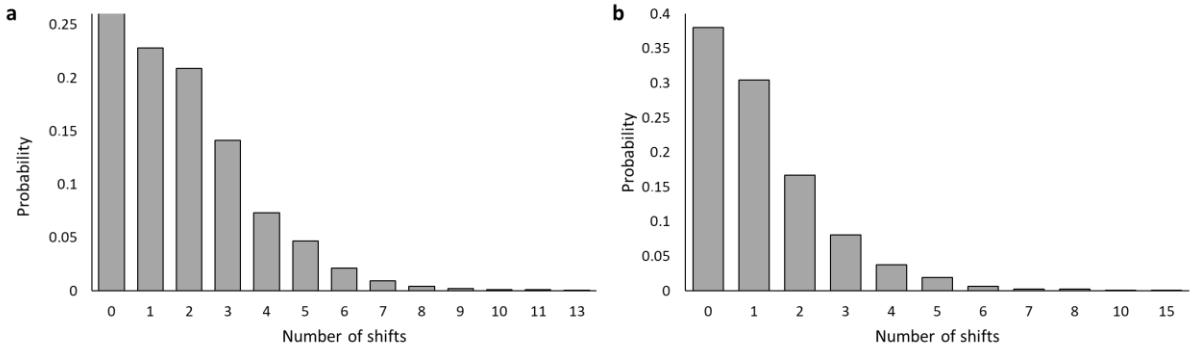

Figure 7. Distribution of posterior probability for the number of shifts of morphological diversification based on the a) PC1 scores and b) PC2 scores of morphological traits.

Table 5. Bayes factor (BF) of pairwise model comparisons using PC1 and PC2 scores. The best model is indicated in bold. Numerators are given as columns, and denominator models as rows. AThe numerator model is more supported if the Bayes factor is >1 while <1 indicates a higher support for the denominator model. The interpretation of the strength of support for a given model is based on table 3.

		Shifts												
		1	2	3	4	5	6	7	8	9	10	11	13	15
PC1	0	1.74	3.18	4.3	4.47	5.68	5.14	4.6	3.79	4.33	4.33	8.66	**17.32**	
PC2	0	1.6	1.75	1.69	1.59	1.59	1.03	0.75	1.49		1.49			**47.84**

The 95% credible set from the BAMM analysis identified five distinct shift configurations (i.e. a mapping of rate shifts to a certain phylogenetic topology illustrating positions of possible shifts in the tree) based on the PC1 scores (Figure 8a-e). The figure showed that 45% of the samples in the posterior had zero core shifts (Figure 8a), while 49.9% of the samples in the posterior can be assigned to a single shift configuration where an accelerated rate of

diversification events is observed at the phylogenetic branch leading to the Antarctic clades (Figure 8b-e). Specifically, 37% of the illustrating positions of possible shifts in the tree samples in the posterior showed a core shift on the branch leading to the diversification of *Eusirus giganteus* and *Eusirus perdentatus* complexes including *Eusirus propeperdentatus* (Figure 8b) and 5.5% had a core shift on the branch leading to the to the diversification of *Eusirus perdentatus* complexes and two putative genetic species of *Eusirus giganteus* (Figure 8c). Also, 3.8% had a core shift on the branch leading to the diversification of two putative genetic species of the *Eusirus giganteus* complexes (Figure 8d) while 3.6% had a core shift on the branch leading to the diversification of *Eusirus perdentatus* complexes, and three putative genetic species of the *Eusirus giganteus*, and *Eusirus propeperdentatus* (Figure 8e).

Based on the scores of the PC2 axis, the 95% credible set from the BAMM analysis indicated three distinct shift configurations (Figure 8f-h). The figure illustrated that 74% of the samples in the posterior had zero core shifts (Figure 8f), while 25% of the samples in the posterior showed a single rate shift with an increased rate of diversification observed at the branch leading to the Antarctic phylogenetic clades (Figure 8g-h). In particular, 17% of the samples in the posterior had a core shift on the branch leading to the diversification of *Eusirus giganteus* and *Eusirus perdentatus* complexes including *Eusirus propeperdentatus* (Figure 8g) and 8% had a core shift on the branch which is proximate to the MRCA node of the Antarctic clade (Figure 8h).

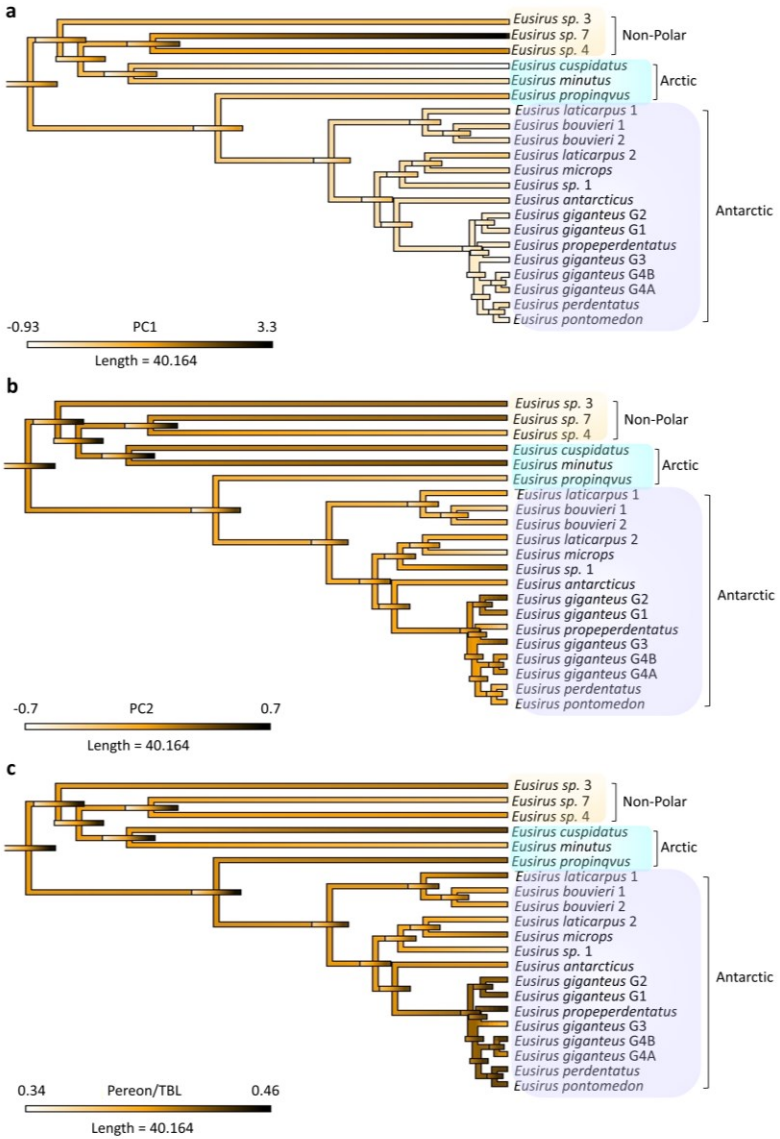
a
Eusirus sp. 3
Eusirus sp. 7
Eusirus sp. 4
Non-Polar
Eusirus cuspidatus
Eusirus minutus
Eusirus propinqvus
Arctic
Eusirus laticarpus 1
Eusirus bouvieri 1
Eusirus bouvieri 2
Eusirus laticarpus 2
Eusirus microps
Eusirus sp. 1
Eusirus antarcticus
Eusirus giganteus G2
Eusirus giganteus G1
Eusirus propeperdentatus
Eusirus giganteus G3
Eusirus giganteus G4B
Eusirus giganteus G4A
Eusirus perdentatus
Eusirus pontomedon
Antarctic
-0.93
PC1
3.3
Length = 40.164
b
Eusirus sp. 3
Eusirus sp. 7
Eusirus sp. 4
Non-Polar
Eusirus cuspidatus
Eusirus minutus
Eusirus propinqvus
Arctic
Eusirus laticarpus 1
Eusirus bouvieri 1
Eusirus bouvieri 2
Eusirus laticarpus 2
Eusirus microps
Eusirus sp. 1
Eusirus antarcticus
Eusirus giganteus G2
Eusirus giganteus G1
Eusirus propeperdentatus
Eusirus giganteus G3
Eusirus giganteus G4B
Eusirus giganteus G4A
Eusirus perdentatus
Eusirus pontomedon
Antarctic
-0.7
PC2
0.7
Length = 40.164
c
Eusirus sp. 3
Eusirus sp. 7
Eusirus sp. 4
Non-Polar
Eusirus cuspidatus
Eusirus minutus
Eusirus propinqvus
Arctic
Eusirus laticarpus 1
Eusirus bouvieri 1
Eusirus bouvieri 2
Eusirus laticarpus 2
Eusirus microps
Eusirus sp. 1
Eusirus antarcticus
Eusirus giganteus G2
Eusirus giganteus G1
Eusirus propeperdentatus
Eusirus giganteus G3
Eusirus giganteus G4B
Eusirus giganteus G4A
Eusirus perdentatus
Eusirus pontomedon
Antarctic
0.34
Pereon/TBL
0.46
Length = 40.164

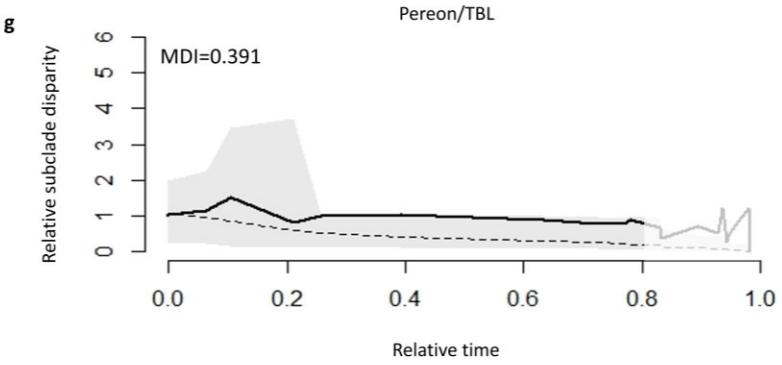
g
Pereon/TBL
MDI=0.391
Relative subclade disparity
0
1
2
3
4
5
6
0.0
0.2
0.4
0.6
0.8
1.0
Relative time

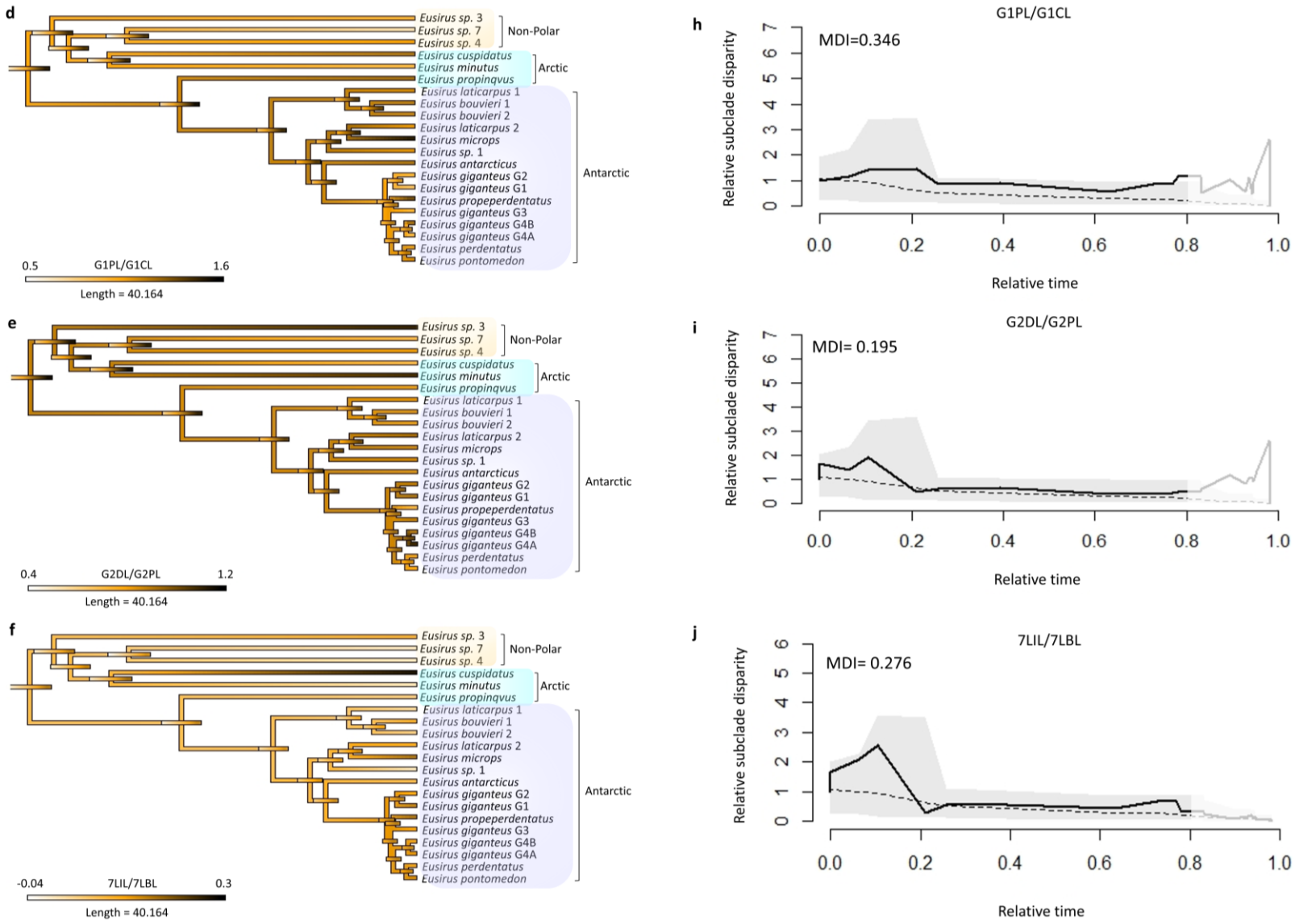
d
Eusirus sp. 3
Eusirus sp. 7
Eusirus sp. 4
Non-Polar
Eusirus cuspidatus
Eusirus minutus
Eusirus propinqvus
Arctic
Eusirus laticarpus 1
Eusirus bouvieri 1
Eusirus bouvieri 2
Eusirus laticarpus 2
Eusirus microps
Eusirus sp. 1
Eusirus antarcticus
Eusirus giganteus G2
Eusirus giganteus G1
Eusirus propeperdentatus
Eusirus giganteus G3
Eusirus giganteus G4B
Eusirus giganteus G4A
Eusirus perdentatus
Eusirus pontomedon
Antarctic
0.5
G1PL/G1CL
1.6
Length = 40.164
h
G1PL/G1CL
MDI=0.346
Relative subclade disparity
0 1 2 3 4 5 6 7
0.0 0.2 0.4 0.6 0.8 1.0
Relative time
e
Eusirus sp. 3
Eusirus sp. 7
Eusirus sp. 4
Non-Polar
Eusirus cuspidatus
Eusirus minutus
Eusirus propinqvus
Arctic
Eusirus laticarpus 1
Eusirus bouvieri 1
Eusirus bouvieri 2
Eusirus laticarpus 2
Eusirus microps
Eusirus sp. 1
Eusirus antarcticus
Eusirus giganteus G2
Eusirus giganteus G1
Eusirus propeperdentatus
Eusirus giganteus G3
Eusirus giganteus G4B
Eusirus giganteus G4A
Eusirus perdentatus
Eusirus pontomedon
Antarctic
0.4
G2DL/G2PL
1.2
Length = 40.164
i
G2DL/G2PL
MDI= 0.195
Relative subclade disparity
0 1 2 3 4 5 6 7
0.0 0.2 0.4 0.6 0.8 1.0
Relative time
f
Eusirus sp. 3
Eusirus sp. 7
Eusirus sp. 4
Non-Polar
Eusirus cuspidatus
Eusirus minutus
Eusirus propinqvus
Arctic
Eusirus laticarpus 1
Eusirus bouvieri 1
Eusirus bouvieri 2
Eusirus laticarpus 2
Eusirus microps
Eusirus sp. 1
Eusirus antarcticus
Eusirus giganteus G2
Eusirus giganteus G1
Eusirus propeperdentatus
Eusirus giganteus G3
Eusirus giganteus G4B
Eusirus giganteus G4A
Eusirus perdentatus
Eusirus pontomedon
Antarctic
-0.04
7LIL/7LBL
0.3
Length = 40.164
j
7LIL/7LBL
MDI= 0.276
Relative subclade disparity
0 1 2 3 4 5 6
0.0 0.2 0.4 0.6 0.8 1.0
Relative time

Figure 6. Left part: Ancestral state reconstructions and disparity through time (DTT) plots of morphological traits. Reconstructions of ancestral states were based on a)PC1 scores and b) PC2 scores of the morphological traits; c) Pereon/TBL ratio; d) G1PL/G1CL ratio; e) G2DL/G2PL ratio; f) 7LIL/7LBL ratio. Colours indicate the geographic origin of the different groups: Antarctic *Eusirus* are indicated in blue, Arctic *Eusirus* in aquamarine, and non-polar *Eusirus* in yellow. The color gradient indicates the estimated morphological trait values. The horizontal bars at each node indicate the 95% confidence intervals of each estimated state. The horizontal bars at the bottom left of each graph correspond to the colour gradient of each branch and also provide the scale for the branch lengths of the trees or the substitutions per site.
Right part: Disparity through time (DTT) plots of g) Pereon/TBL ratio; h) G1PL/G1CL ratio; i) G2DL/G2PL ratio; j) 7LIL/7LBL ratio. The morphological disparity index (MDI) is also provided for each DTT plot. The mean relative disparity for each subclade from the simulated datasets following the Brownian model of evolution is shown by dashed lines, and the actual data from this study are indicated as solid lines. The grey-shaded areas show the 95% confidence intervals of the simulated data.

Disparity through time

The analyses of disparity through time showed no clear departure from the expectations based on an evolutionary model of Brownian motion (Figures 6g-j). Also, the relative subclade disparity values were close to zero, and positive morphological disparity indices (MDI) were observed with 0.391 for Pereon/TBL, 0.346 for G1PL/G1CL, 0.195 for G2DL/G2PL, and 0.276 for 7LIL/7LBL, respectively. (Figures 6g-j).

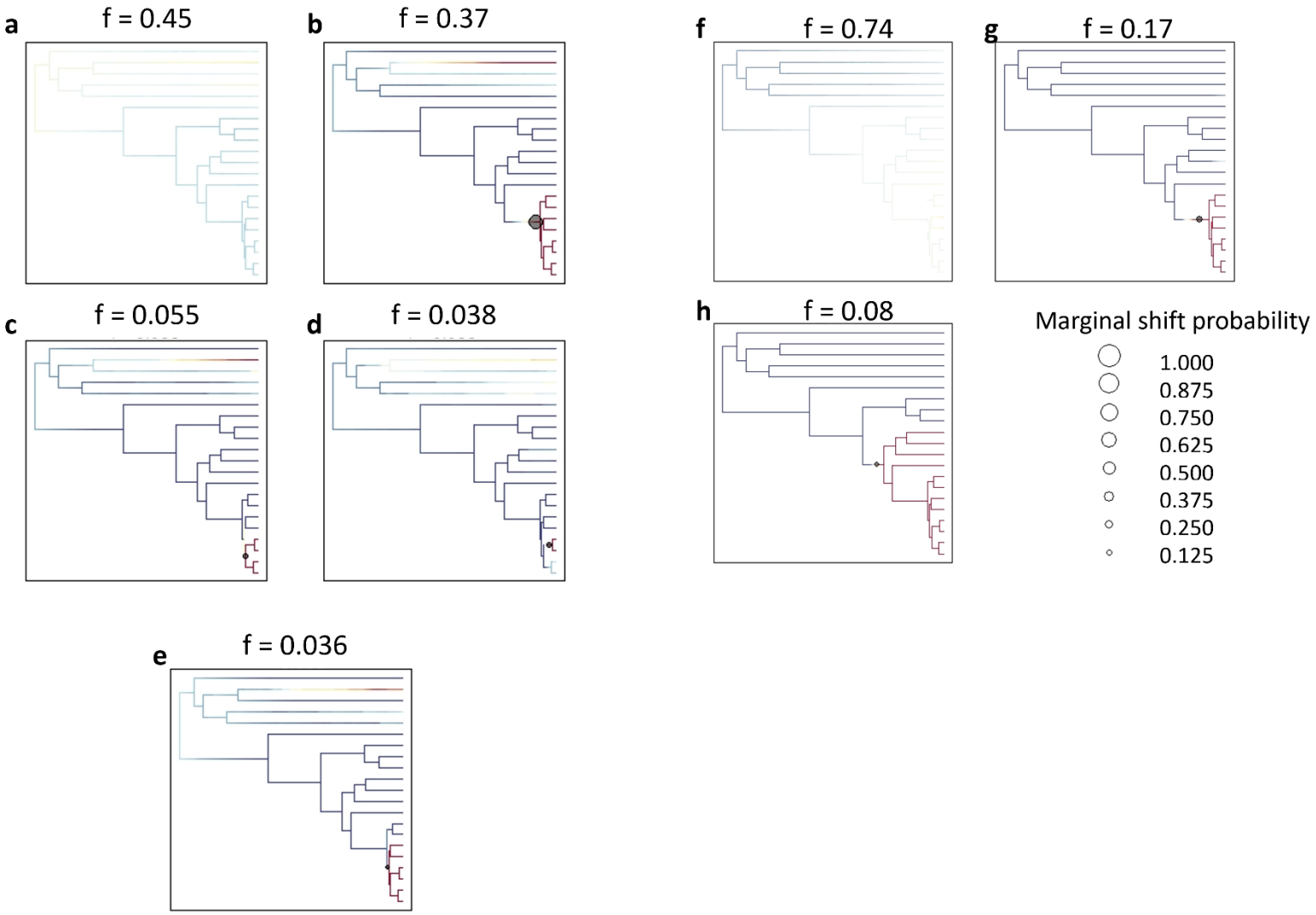

Figure 8. The 95% credibility set of rate shift configurations (i.e. a mapping of rate shifts to a certain phylogenetic topology illustrating positions of possible shifts in the tree) generated by the BAMM analyses is based on a-e) PC1 scores and f-h) PC2 scores of the morphological traits. The posterior probability is indicated above each plot. Warm colours indicate high diversification rates, while cold colours indicate low diversification rates. Circles show the locations of rate shifts, and the circle is sized according to the marginal probability of the shift.

Discussion

Isotopic diversity in *Eusirus*

The isotopic data revealed a clear difference in the trophic ecology diversity between the Arctic and the Antarctic groups with a higher isotopic diversity in Arctic *Eusirus* (Figure 3). The observed diversity in the Arctic and the Antarctic groups in the isospace can be associated with variation in their overall trophic ecology encompassing variation in feeding habits and locations. The wide range of $\delta^{13}C$ values in both Arctic and Antarctic *Eusirus* suggests wide variation in the origins of the consumed food resources (Post, 2002; Layman et al., 2011; Le Bourg, 2020). On the other hand, the Arctic group showed a larger variation along $\delta^{15}N$ than the Antarctic *Eusirus* which suggests that Arctic *Eusirus* may occupy different trophic levels than Antarctic relatives (Dauby et al., 2001; Post, 2002; Nyssen, 2005; Inger & Bearhop, 2008; Layman et al., 2011; Le Bourg, 2020).

Association of morphological and ecological traits

Globally, the results of two-block PLS as well as PGLS demonstrated a proportion of morphological variation in *Eusirus* is related to variation in trophic ecology. Variation along both PC's is mainly represented by change in the ratios of the gnathopod 1, an appendage used for feeding and capturing prey in *Eusirus* (Klages & Gutt 1990). Our results indicate that the morphology of gnathopods (especially size and shape) is informative about the trophic ecology of *Eusirus*. Analysis of the gut content of *Eusirus* amphipods revealed mainly crustaceans, mineral particles, unidentified organic matter, and polychaetes (Dauby et al., 2001; Nyssen, 2005) indicating that these amphipods prey on organisms from various trophic levels; this is confirmed by the wide range of isotope values of investigated *Eusirus* (Nyssen et al., 2001; Nyssen, 2005; Michel et al., 2020). The same pattern is revealed in the current study for both Antarctic and Arctic *Eusirus* groups showing a wide range of $\delta^{13}C$. However, Arctic *Eusirus* showed larger variation of $\delta^{15}N$ than Antarctic *Eusirus* (Figure 3). This difference suggests a trophic partitioning in Arctic *Eusirus* spanning different trophic levels. *Eusirus* amphipods were also found to have the ability to change their diet in response to food availability (Nyssen, 2005; Michel et al., 2020) which fits the wide range of isotopic distribution in the isospace found in the current study (Figure 3).

Phylogenetic signal and ancestral state reconstructions of morphological traits

A significant but low phylogenetic signal (K < 1) indicates that the studied morphological traits are evolutionary labile at the genus level (Blomberg et al., 2003; Revell et al., 2008; Kamilar & Cooper, 2013; Adams, 2014). In other words, large morphological divergences can be observed between two sister-species. This result suggests that events of speciation is generally associated with morphological variation, a pattern probably driven by ecological radiation (Kamilar & Cooper, 2013). Species with evolutionary labile morphological traits could possibly adapt to new environmental conditions (Cano-Barbacil et al., 2022). Interestingly, the ancestral state reconstructions (Figure 6) and levels of disparity (Figure 4a) revealed that the morphological variance among subclades is not evenly distributed across *Eusirus*. Indeed, morphological variation within the Antarctic clade is relatively limited in comparison with Arctic *Eusirus* species (Figure 4). This lower variation could be attributed to allopatric speciation (Rogers, 2007; Thornhill et al., 2008) and/or a reduced competition in the Antarctic (Brandt, 1999; Verheye, 2017). Examination of each trait (Figures 6c-f), however, showed more diverse results, which could imply that these individual traits have changed with different evolutionary rates.

Patterns of morphological diversification

A significant partition of trait disparity among subclades would suggest a scenario of adaptive radiation as rates of phenotypic evolution are expected to slow down through time as niches become saturated (Schluter 2000; Harmon et al. 2003). The DTT plots did not support such a scenario. Instead, we found low levels of relative subclade disparity in the DTT plots with values close to zero (Figures 6g-j) indicating that morphological trait disparity is rather partitioned within than among subclades (Harmon et al., 2003; Near et al., 2012). In addition, our BAMM analyses did not support a scenario where the speciation of Arctic and Antarctic *Eusirus* has been driven by bursts of morphological diversification (Figure 8a and f). Instead, morphological variation observed among species has accumulated continuously across the various events of speciation (Stroud & Losos, 2016). Some increase in the rate of lineage diversification was observed, particularly in the Antarctic clade (see chapter 4) and it appears that this high rate of speciation was obviously not associated with an increase in the rate of phenotypic evolution as expected for scenarios of adaptive radiation. One hypothesis to explain these results would be that the high rate of lineage diversification could be the result

of allopatric speciation, similar to the example of *Plethodon* salamanders, which showed a high rate of species diversification together with small changes in their ecological niches and morphology (Kozak et al., 2006). Allopatric speciation events could correspond with the diversification of the Antarctic *Eusirus* about 29.51 Ma [25.78-33.29 Ma] (chapter 4) which coincided with the opening of the Drake passage and the ACC formation, triggering vicariant events (Brandt, 1999; Verheye, 2017; Legezyńska et al., 2020). On the other hand, we cannot completely rule out the possibility that ecological diversification of Antarctic *Eusirus* was not captured by the studied traits. For example, we cannot reject the hypothesis that speciation event could be associated with physiological or behavioural adaptations, which would not be captured by our large morphological dataset. In contrary, higher level of morphological and isotopic variation despite the low rate of lineage diversification in the Arctic *Eusirus* could probably be related to the older phylogenetic origin of the Arctic *Eusirus* than the Antarctic *Eusirus*. Thus, it could be expected that they have accumulated more morphological divergence over time. The multiple origins of the Arctic lineages from 63.47 Ma [43.63-81.54 Ma] to 48.72 Ma [35.71-62.9 Ma] could also be attributed to the higher morphological and isotopic variation in the Arctic *Eusirus*. Connections to the Arctic ocean (Clarke & Crame, 2010) may have permitted the multiple invasions of the *Eusirus* ancestors to the Arctic as reflected by their polyphyletic origins. The large morphological and isotopic variation observed in the Arctic group (Figure 4a &b) sustains the scenario made of ecological speciation events. Finally, the relatively low species number of extant lineages in the Arctic might be related to different extinction events. It is likely that the multiple past invasions in the Arctic would be associated with pulse of speciation associated with ecological diversification. The current large disparity level would be thus a signature of such a scenario.

Conclusions

Combining phylogenetic information, trophic data generated by stable isotope analyses, as well as morphological data, provided insights into the eco-morphological diversification of the genus *Eusirus* in the Antarctic and Arctic Oceans. Our results suggest different evolutionary scenarios for Arctic and Antarctic *Eusirus*. A scenario of non-adaptive radiation could explain why rate shifts of morphological diversification were absent despite a burst of lineage

diversification in Antarctic group. Allopatric speciation would be the most adequate evolutionary scenario driving diversity of *Eusirus* in Antarctica. However, we cannot fully rule out an ecological diversification which was not captured by the studied traits. As for Arctic *Eusirus*, the accumulation of morphological and ecological diversity was probably produced more constantly through time and along speciation events. Despite the highest level of morphological and ecological diversity observed in Arctic *Eusirus*, this variation is coupled with a relatively constant rate of lineage diversification. The highest level of eco-morphological diversity observed in Arctic lineages could be linked to the polyphyletic origin of this assemblage and to their older age. Allopatric speciation associated with multiple extinction events could be additional explanations for the high level of eco-morphological diversity in the Arctic.

References

Ackerly, D. 2009. Conservatism and diversification of plant functional traits: evolutionary rates versus phylogenetic signal. Proceedings of the National Academy of Sciences, 106(supplement_2), 19699-19706.

Adams, D. C. 2014. A generalized K statistic for estimating phylogenetic signal from shape and other high-dimensional multivariate data. *Systematic biology*, *63*(5), 685-697.

Adams, D. C., & Otárola‐Castillo, E. 2013. geomorph: an R package for the collection and analysis of geometric morphometric shape data. *Methods in ecology and evolution*, *4*(4), 393-399.

Adams, D. C., & Felice, R. N. 2014. Assessing trait covariation and morphological integration on phylogenies using evolutionary covariance matrices. *PloS one*, *9*(4), e94335.

Arfianti, T., & Costello, M. J. 2020. Global biogeography of marine amphipod crustaceans: latitude, regionalization, and beta diversity. *Marine Ecology Progress Series*, *638*, 83-94.

Arndt, C. E., & Swadling, K. M. 2006. Crustacea in Arctic and Antarctic sea ice: distribution, diet and life history strategies. *Advances in marine biology*, *51*, 197-315.

Baird, H. P., Miller, K. J., & Stark, J. S. 2011. Evidence of hidden biodiversity, ongoing speciation and diverse patterns of genetic structure in giant Antarctic amphipods. Molecular Ecology, 20(16), 3439-3454.

Balázs, G., Biró, A., Fišer, Ž., Fišer, C., & Herczeg, G. 2021. Parallel morphological evolution and habitat‐dependent sexual dimorphism in cave‐vs. surface populations of the Asellus aquaticus (Crustacea: Isopoda: Asellidae) species complex. Ecology and Evolution, 11(21), 15389-15403.

Blomberg, S. P., Garland Jr, T., & Ives, A. R. 2003. Testing for phylogenetic signal in comparative data: behavioral traits are more labile. *Evolution*, *57*(4), 717-745.

Bodil, B. A., Ambrose, W. G., Bergmann, M., Clough, L. M., Gebruk, A. V., Hasemann, C., Iken, K., Klages, M., MacDonald, I.R., Renaud, P.E., Schewe, I., Soltwedel, T., & Włodarska-Kowalczuk, M. 2011. Diversity of the arctic deep-sea benthos. *Marine Biodiversity*, *41*, 87-107.

Bowen, G. J. 2010. Isoscapes: spatial pattern in isotopic biogeochemistry. Annual review of earth and planetary sciences, 38, 161-187.

Brandt, A. 1999. On the origin and evolution of Antarctic Peracarida (Crustacea, Malacostraca). *Scientia Marina*, *63*(S1), 261-274.

Brandt, A. 2005. Evolution of Antarctic biodiversity in the context of the past: the importance of the Southern Ocean deep sea. *Antarctic Science*, *17*(4), 509-521.

Brecko, J., Mathys, A., Dekoninck, W., Leponce, M., VandenSpiegel, D., & Semal, P. 2014. Focus stacking: Comparing commercial top-end set-ups with a semi-automatic low budget approach. A possible solution for mass digitization of type specimens. *ZooKeys*, (464), 1.

Brozena, J. M., Childers, V. A., Lawver, L. A., Gahagan, L. M., Forsberg, R., Faleide, J. I., & Eldholm, O. 2003. New aerogeophysical study of the Eurasia Basin and Lomonosov Ridge: Implications for basin development. *Geology*, *31*(9), 825-828.

Cano-Barbacil, C., Radinger, J., Grenouillet, G., & García‐Berthou, E. 2022. Phylogenetic signal and evolutionary relationships among traits of inland fishes along elevational and longitudinal gradients. Freshwater Biology, 67(5), 912-925.

Cheesman, A. W., & Cernusak, L. A. 2016. Isoscapes: a new dimension in community ecology. Tree Physiology, 1-4.

Clarke, A., & Crame, J. A. 2010. Evolutionary dynamics at high latitudes: speciation and extinction in polar marine faunas. *Philosophical Transactions of the Royal Society B: Biological Sciences*, *365*(1558), 3655-3666.

Colombo, M., Damerau, M., Hanel, R., Salzburger, W., & Matschiner, M. 2015. Diversity and disparity through time in the adaptive radiation of Antarctic notothenioid fishes. Journal of Evolutionary Biology, 28(2), 376-394.

Convey, P., Stevens, M. I., Hodgson, D. A., Smellie, J. L., Hillenbrand, C. D., Barnes, D. K., Clarke, A., Pugh, P.J.A., Linse, K., & Cary, S. C. 2009. Exploring biological constraints on the glacial history of Antarctica. *Quaternary Science Reviews*, *28*(27-28), 3035-3048.

Copilaş-Ciocianu, D., Borko, Š., & Fišer, C. 2020. The late blooming amphipods: global change promoted post-Jurassic ecological radiation despite Palaeozoic origin. *Molecular Phylogenetics and Evolution*, *143*, 106664.

Coxall, H. K., & Pearson, P. N. 2007. The Eocene-Oligocene transition. *Deep time perspectives on climate change: Marrying the signal from computer models and biological proxies*, 351-387.

Crame, J. A. 2018. Key stages in the evolution of the Antarctic marine fauna. *Journal of Biogeography*, *45*(5), 986-994.

Crame, J. A., Beu, A. G., Ineson, J. R., Francis, J. E., Whittle, R. J., & Bowman, V. C. 2014. The early origin of the Antarctic marine fauna and its evolutionary implications. *PloS one*, *9*(12), e114743. 1-22.

Daane, J. M., Dornburg, A., Smits, P., MacGuigan, D. J., Brent Hawkins, M., Near, T. J., H. Detrich, III, W., & Harris, M. P. 2019. Historical contingency shapes adaptive radiation in Antarctic fishes. *Nature ecology & evolution*, *3*(7), 1102-1109.

Dauby, P., Scailteur, Y., & De Broyer, C. 2001. Trophic diversity within the eastern Weddell Sea amphipod community. *Hydrobiologia*, *443*(1), 69-86.

Davis, A. M., Blanchette, M. L., Pusey, B. J., Jardine, T. D., & Pearson, R. G. 2012. Gut content and stable isotope analyses provide complementary understanding of ontogenetic dietary shifts and trophic relationships among fishes in a tropical river. Freshwater Biology, 57(10), 2156-2172.

De Broyer, C., Nyssen, F., & Dauby, P. 2004. The crustacean scavenger guild in Antarctic shelf, bathyal and abyssal communities. *Deep Sea Research Part II: Topical Studies in Oceanography*, *51*(14-16), 1733-1752.

De Broyer, C., Lowry, J. K., Jazdzewski, K., & Robert, H. 2007. *Census of Antarctic Marine Life. Synopsis of the Amphipoda of the Southern Ocean. Vol. 1. Part 1: Catalogue of the Gammaridean and Corophiidean Amphipoda of the Southern Ocean with Distribution and Ecological Data, by C. de Broyer, JK Lowry, K Jazdzewski and H. Robert*. Institut Royal des Sciences Naturelles de Belgique.

Doenz, C. J., Krähenbühl, A. K., Walker, J., Seehausen, O., & Brodersen, J. 2019. Ecological opportunity shapes a large Arctic charr species radiation. *Proceedings of the Royal Society B*, *286*(1913), 20191992.

Dornburg, A., Federman, S., Lamb, A. D., Jones, C. D., & Near, T. J. 2017. Cradles and museums of Antarctic teleost biodiversity. Nature ecology & evolution, 1(9), 1379-1384.

Dunton, K. 1992. Arctic biogeography: the paradox of the marine benthic fauna and flora. *Trends in Ecology & Evolution*, *7*(6), 183-189.

Eastman, J. T. 2005. The nature of the diversity of Antarctic fishes. *Polar biology*, *28*, 93-107.

Eastman, J. T., & Eakin, R. R. 2022. Decomplicating and identifying species in the radiation of the Antarctic fish genus Pogonophryne (Artedidraconidae). *Polar Biology*, *45*(5), 825-832.

Espinasse, B., Sturbois, A., Basedow, S. L., Hélaouët, P., Johns, D. G., Newton, J., & Trueman, C. N. 2022. Temporal dynamics in zooplankton δ13C and δ15N isoscapes for the North Atlantic Ocean: Decadal cycles, seasonality, and implications for predator ecology. Frontiers in Ecology and Evolution, 10, 986082.

Frédérich, B., Sorenson, L., Santini, F., Slater, G. J., & Alfaro, M. E. 2013. Iterative ecological radiation and convergence during the evolutionary history of damselfishes (Pomacentridae). *The American Naturalist*, *181*(1), 94-113.

Gavrilets, S., & Losos, J. B. 2009. Adaptive radiation: contrasting theory with data. *Science*, *323*(5915), 732-737.

Gittenberger, E. 1991. What about non-adaptive radiation?. *Biological Journal of the Linnean Society*, *43*(4), 263-272.

Golikov, A. N., & Scarlato, O. A. 1989. Evolution of Arctic ecosystems during the Neogene period. In *The Arctic Seas.* Springer, Boston, MA. 257-279.

Golovan, O. A., Błażewicz-Paszkowycz, M., Brandt, A., Budnikova, L. L., Elsner, N. O., Ivin, V. V., Lavrenteva, A. V., Malyutina, M. V., Petryashov, V. V., & Tzareva, L. A. 2013. Diversity and distribution of peracarid crustaceans (Malacostraca) from the continental slope and the deep-sea basin of the Sea of Japan. *Deep Sea Research Part II: Topical Studies in Oceanography*, *86–87*, 66–78.

Guillerme, T. 2018. dispRity: a modular R package for measuring disparity. Methods in Ecology and Evolution, 9(7), 1755-1763.

Guillerme, T., Puttick, M. N., Marcy, A. E., & Weisbecker, V. 2020a. Shifting spaces: Which disparity or dissimilarity measurement best summarize occupancy in multidimensional spaces?. *Ecology and evolution*, *10*(14), 7261-7275.

Guillerme, T., Cooper, N., Brusatte, S. L., Davis, K. E., Jackson, A. L., Gerber, S., Goswami, A., Healy, K., Hopkins, M.J., Jones, M.E.H., Lloyd, G.T., O'Reilly, J.E., Pate, A., Puttick, M.N., Rayfield, E.J., Saupe, E.E., Sherratt, E., Slater, G.J., Weisbecker, V., Thomas, G.H., & Donoghue, P. C. 2020b. Disparities in the analysis of morphological disparity. Biology letters, 16(7), 20200199.

Gutt, J., Bertler, N., Bracegirdle, T. J., Buschmann, A., Comiso, J., Hosie, G., Isla, E., Schloss, I.R., Smith, C.R., Tournadre, J., & Xavier, J. C. 2015. The Southern Ocean ecosystem under multiple climate change stresses ‐ an integrated circumpolar assessment. *Global Change Biology*, *21*(4), 1434-1453.

Hardy, S. M., Carr, C. M., Hardman, M., Steinke, D., Corstorphine, E., & Mah, C. 2011. Biodiversity and phylogeography of Arctic marine fauna: insights from molecular tools. *Marine Biodiversity*, *41*(1), 195-210.

Harmon, L. J., Schulte, J. A., Larson, A., & Losos, J. B. 2003. Tempo and mode of evolutionary radiation in iguanian lizards. *Science*, *301*(5635), 961-964.

Hershey, A. E., Northington, R. M., Finlay, J. C., & Peterson, B. J. 2017. Stable isotopes in stream food webs. In Methods in stream ecology (pp. 3-20). Academic Press.

Hobson, K. A. 1999. Tracing origins and migration of wildlife using stable isotopes: a review. Oecologia, 120(3), 314-326.

Hobson, K. A., & Wassenaar, L. I. (Eds.). 2018. Tracking animal migration with stable isotopes. Academic Press.

Hood-Nowotny, R., & Knols, B. G. 2007. Stable isotope methods in biological and ecological studies of arthropods. Entomologia Experimentalis et Applicata, 124(1), 3-16.

Hutchinson, D. K., Coxall, H. K., Lunt, D. J., Steinthorsdottir, M., de Boer, A. M., Baatsen, M., von der Heydt, A., Huber, M., Kennedy-Asser, A. T., Kunzmann, L., Ladant, J. B., Lear, C. H., Moraweck, K., Pearson, P. N., Piga, E., Pound, M. J., Salzmann, U., Scher, H. D., Sijp, W. P., Śliwińska, K.K., Wilson, P.A., Zhang, Z. 2021. The Eocene–Oligocene transition: a review of marine and terrestrial proxy data, models and model–data comparisons. *Climate of the Past*, *17*(1), 269–315.

Inger, R., & Bearhop, S. 2008. Applications of stable isotope analyses to avian ecology. Ibis, 150(3), 447-461.

Jollife, I. T. 2002. Principal Component Analysis, 2nd Edn. New York,NY: Springer-Verlag.

Josse, J., & Husson, F. 2016. missMDA: a package for handling missing values in multivariate data analysis. *Journal of statistical software*, *70*, 1-31.

Jung, T. W.; Kim, M.-S.; Soh, H.-Y.; Yoon, S. M. 2016. A new species of *Eusirus* from Jeju Island, Korea (Crustacea, Amphipoda, Eusiridae). *ZooKeys.*(640), 19-35.

Kamilar, J. M., & Cooper, N. 2013. Phylogenetic signal in primate behaviour, ecology and life history. *Philosophical Transactions of the Royal Society B: Biological Sciences*, *368*(1618), 20120341.

Kass, R. E. & Raftery, A. E. 1995. Bayes Factor. *Journal of the American Statistical Association*, *90*, 773-795.

Kassambara, A., & Mundt, F. 2017. Package 'factoextra'. *Extract and visualize the results of multivariate data analyses*, *76*(2).

Keller, G., MacLeod, N., & Barrera, E. 1992. Eocene-Oligocene Faunal Turnover in Planktic Foraminifera and Antarctic Glaciation. In D. R. Prothero & W. A. Berggren (Eds.), Eocene-Oligocene Climatic and Biotic Evolution. Princeton University Press. 218–244.

Kiko, R., Michels, J., Mizdalski, E., Schnack-Schiel, S. B., & Werner, I. 2008. Living conditions, abundance and composition of the metazoan fauna in surface and sub-ice layers in pack ice of the western Weddell Sea during late spring. *Deep Sea Research Part II: Topical Studies in Oceanography*, *55*(8-9), 1000-1014.

Klages, M., & Gutt, J. 1990. Observations on the feeding behaviour of the Antarctic gammarid *Eusirus perdentatus* Chevreux, 1912 (Crustacea: Amphipoda) in aquaria. *Polar Biology*, *10*(5), 359-364.

Kosobokova, K. N., Hopcroft, R. R., & Hirche, H. J. 2011. Patterns of zooplankton diversity through the depths of the Arctic's central basins. *Marine Biodiversity*, *41*(1), 29-50.

Kozak, K. H., Weisrock, D. W. & Larson, A. 2006 Rapid lineage accumulation in a non-adaptive radiation: phylogenetic analysis of diversification rates in eastern North American woodland salamanders (Plethodontidae: Plethodon). Proc. R. Soc. B 273, 539 –546.

Kralj-Fišer, S., Premate, E., Copilaş-Ciocianu, D., Volk, T., Fišer, Ž., Balázs, G., Herczeg, G., Delić, T., & Fišer, C. 2020. The interplay between habitat use, morphology and locomotion in subterranean crustaceans of the genus Niphargus. Zoology, 139, 125742.

Krapp, R. H., Berge, J., Flores, H., Gulliksen, B., & Werner, I. 2008. Sympagic occurrence of Eusirid and Lysianassoid amphipods under Antarctic pack ice. *Deep Sea Research Part II: Topical Studies in Oceanography*, *55*(8-9), 1015-1023.

Kuklinski, P., Taylor, P. D., Denisenko, N. V., & Berning, B. 2013. Atlantic origin of the Arctic biota? Evidence from phylogenetic and biogeographical analysis of the cheilostome bryozoan genus Pseudoflustra. *PLoS One*, *8*(3), e59152. 1-25.

Lambert, J. W., Reichard, M., & Pincheira-Donoso, D. 2019. Live fast, diversify non-adaptively: evolutionary diversification of exceptionally short-lived annual killifishes. BMC evolutionary biology, 19, 1-13.

Layman, C. A., Araujo, M. S., Boucek, R., Hammerschlag-Peyer, C. M., Harrison, E., Jud, Z. R., Matich, P., Rosenblatt, A. E., Vaudo, J. J., Yeager, L. A., Post, D. M., & Bearhop, S. 2011. Applying stable isotopes to examine food-web structure: an overview of analytical tools. Biological Reviews, 87(3), 545–562.

Le Bourg, B. 2020. Trophic ecology of Southern Ocean sea stars: Influence of environmental drivers on trophic diversity. University of Liege (Doctoral Thesis).

Le Bourg, B., Lepoint, G., & Michel, L. N. 2020. Effects of preservation methodology on stable isotope compositions of sea stars. Rapid Communications in Mass Spectrometry, 34(2), e8589.

Legeżyńska, J., Kędra, M., & Walkusz, W. 2012. When season does not matter: summer and winter trophic ecology of Arctic amphipods. *Hydrobiologia*, *684*(1), 189-214.

Legezyñska, J., De Broyer, C., & Wesławski, J. M. 2020. Invasion of the poles. *The Natural History of the Crustacea: Evolution and Biogeography of the Crustacea*, 216-246.

Losos, J. B. 2011. Convergence, adaptation, and constraint. *Evolution*, *65*(7), 1827-1840.

Macnaughton, M. O., Thormar, J., & Berge, J. 2007. Sympagic amphipods in the Arctic pack ice: redescriptions of *Eusirus holmii* Hansen, 1887 and *Pleusymtes karstensi* (Barnard, 1959). *Polar Biology*, *30*(8), 1013-1025.

Matschiner, M., Hanel, R., Salzburger, W. 2011. On the origin and trigger of the notothenioid adaptive radiation. PloS one 6, e18911.

Matsubayashi, K. W., & Yamaguchi, R. 2022. The speciation view: Disentangling multiple causes of adaptive and non‐adaptive radiation in terms of speciation. Population Ecology, 64(2), 95-107.

Meltofte, H., Barry, T., Berteaux, D., Bültmann, H., Christiansen, J. S., Cook, J. A., Dahlberg, A.,Daniëls, F.J.A., Ehrich, D., Fjeldså, J., Friðriksson, F., Ganter, B., Gaston, A.J., Gillespie, L.J., Grenoble, L., Hoberg, E.P., Hodkinson, I.D., Huntington, H.P., Ims, R.A., Josefson, A.B., Kutz, S.J., Kuzmin, S.L., Laidre, K.L., Lassuy, D.R., Lewis, P.N., Lovejoy, C., Michel, C., Mokievsky, V., Mustonen, T., Payer, D.C., Poulin, M., Reid, D.G., Reist, J.D., Tessler, D.F. & Wrona, F. J. 2013. *Arctic Biodiversity Assesment. Synthesis*. Conservation of Arctic Flora and Fauna (CAFF).

Michel, L. N., Nyssen, F. L., Dauby, P., & Verheye, M. 2020. Can mandible morphology help predict feeding habits in Antarctic amphipods?. *Antarctic Science*, *32*(6), 496-507.

Mundry, R. 2014. Statistical issues and assumptions of phylogenetic generalized least squares. Modern phylogenetic comparative methods and their application in evolutionary biology: concepts and practice, 131-153.

Near, T. J., Dornburg, A., Kuhn, K. L., Eastman, J. T., Pennington, J. N., Patarnello, T., Zane, L., Fernández, D.A., & Jones, C. D. 2012. Ancient climate change, antifreeze, and the evolutionary diversification of Antarctic fishes. *Proceedings of the National Academy of Sciences*, *109*(9), 3434-3439.

Newton, J. 2016. Stable isotopes as tools in ecological research. eLS, 1-8.

Nyssen, F. 2005. Role of benthic amphipods in Antarctic trophodynamics: a multidisciplinary study (Doctoral dissertation, Université de Liège).

Nyssen, F., Brey, T., Lepoint, G., Bouquegneau, J. M., De Broyer, C., & Dauby, P. 2001. Use of stable isotopes to delineate amphipod trophic status in Antarctic food webs. *Polskie Archiwum Hydrobiologii*, *47*(3-4).

Nyssen, F., Brey, T., Lepoint, G., Bouquegneau, J. M., De Broyer, C., & Dauby, P. 2002. A stable isotope approach to the eastern Weddell Sea trophic web: focus on benthic amphipods. *Polar Biology*, *25*(4), 280-287.

O'Regan, M., Williams, C. J., Frey, K. E., & Jakobsson, M. 2011. A synthesis of the long-term paleoclimatic evolution of the Arctic. *Oceanography*, *24*(3), 66-80.

Palerud, R., & Vader, W. 1991. *Marine Amphipoda Gammaridea in north-east Atlantic and Norwegian Arctic*. p. 1-54.

Paradis, E., Claude, J., & Strimmer, K. 2004. APE: analyses of phylogenetics and evolution in R language. Bioinformatics, 20(2), 289-290.

Parker, E., Zapfe, K. L., Yadav, J., Frédérich, B., Jones, C. D., Economo, E. P., Federman, S., Near, T.J. & Dornburg, A. 2022. Periodic Environmental Disturbance Drives Repeated Ecomorphological Diversification in an Adaptive Radiation of Antarctic Fishes. *The American Naturalist*, *200*(6), E221-E236.

Pennell, M. W., J. M. Eastman, G. J. Slater, J. W. Brown, J. C. Uyeda, R. G. FitzJohn, M. E. Alfaro, and L. J. Harmon. 2014. geiger v2.0: an expanded suite of methods for fitting macroevolutionary models to phylogenetic trees. Bioinformatics, 30, 2216-2218.

Penone, C., Davidson, A. D., Shoemaker, K. T., Di Marco, M., Rondinini, C., Brooks, T. M., Young, B.E., Graham, C.H., & Costa, G. C. 2014. Imputation of missing data in life‐history trait datasets: which approach performs the best?. *Methods in Ecology and Evolution*, *5*(9), 961-970.

Peña Othaitz J. & Sorbe J.C. 2020. *Eusirus bonnieri* sp. nov. (Crustacea: Amphipoda: Eusiridae), a new deep species from the southeastern Bay of Biscay (NE Atlantic Ocean). *Zootaxa.* 4751(2): 238-256.

Peterson, B. J., & Fry, B. 1987. Stable isotopes in ecosystem studies. Annual review of ecology and systematics. 293-320.

Petersen, S. V., Dutton, A., & Lohmann, K. C. 2016. End-Cretaceous extinction in Antarctica linked to both Deccan volcanism and meteorite impact via climate change. *Nature communications*, *7*(1), 1-9.

Pinheiro, J., Bates, D., DebRoy, S., Sarkar, D., & R Core Team. 2007. Linear and nonlinear mixed effects models. *R package version*, *3*(57), 1-89.

Plummer, M., Best, N., Cowles, K., & Vines, K. 2006. CODA: convergence diagnosis and output analysis for MCMC. *R news*, *6*(1), 7-11.

Post, D. M. 2002. Using stable isotopes to estimate trophic position: models, methods, and assumptions. Ecology, 83(3), 703-718.

Prothero, D. R. 1994. The late Eocene-Oligocene extinctions. *Annual Review of Earth and Planetary Sciences*, *22*, 145-165.

R Core Team. 2019. R: A language and environment for statistical computing. R Foundation for Statistical Computing, Vienna, Austria. URL (http://www.R-project.org/).

Rabosky, D. L. 2014. Automatic detection of key innovations, rate shifts, and diversity-dependence on phylogenetic trees. *PloS one*, *9*(2), e89543.

Rabosky, D. L., Grundler, M., Anderson, C., Title, P., Shi, J. J., Brown, J. W., Huang, H., & Larson, J. G. 2014. BAMM tools: an R package for the analysis of evolutionary dynamics on phylogenetic trees. *Methods in Ecology and Evolution*, *5*(7), 701-707.

Rasband, W. S. 2014. ImageJ, US National Institutes of Health, Bethesda, Maryland, USA, imagej. nih. gov/ij/, 1997-2012. JMP®, Versión, 7, 1989-2007

Renne, P. R., Deino, A. L., Hilgen, F. J., Kuiper, K. F., Mark, D. F., Mitchell, W. S., Morgan, L. E., Mundil, R., & Smit, J. 2013. Time Scales of Critical Events Around the Cretaceous-Paleogene Boundary. *Science*, *339*(6120), 684–687.

Revell, L. J. 2012. Phytools: an R package for phylogenetic comparative biology (and other things). *Methods in ecology and evolution*, (2), 217-223.

Revell, L. J. 2013. Two new graphical methods for mapping trait evolution on phylogenies. *Methods in Ecology and Evolution*, *4*(8), 754-759.

Revell, L. J., & Harmon, L. J. 2022. *Phylogenetic comparative methods in R*. Princeton University Press.

Revell, L. J., Harmon, L. J., & Collar, D. C. 2008. Phylogenetic signal, evolutionary process, and rate. *Systematic biology*, *57*(4), 591-601.

Ridley, M. 2003. Evolution (Third edition). Blackwell Science Limited. pp. 521-643.

Ringnér, M. 2008. What is principal component analysis?. Nature biotechnology, 26(3), 303-304.

Rogers, A. D. 2007. Evolution and biodiversity of Antarctic organisms: a molecular perspective. *Philosophical transactions of the royal society B: Biological sciences*, *362*(1488), 2191-2214.

Ronco, F., Matschiner, M., Böhne, A., Boila, A., Büscher, H. H., El Taher, A., Indermaur, A., Malinsky, M., Ricci, V., Kahmen, A., Jentoft, S. & Salzburger, W. 2021. Drivers and dynamics of a massive adaptive radiation in cichlid fishes. Nature, 589(7840), 76-81.

Rundell, R. J., & Price, T. D. 2009. Adaptive radiation, nonadaptive radiation, ecological speciation and nonecological speciation. *Trends in Ecology & Evolution*, *24*(7), 394-399.

Saupe, E. E., & Myers, C. E. 2021. Macroevolution. *Evolutionary Developmental Biology: A Reference Guide*, 149-167.

Schluter, D. 2000. *The ecology of adaptive radiation*. OUP Oxford.

Serreze, M. C., & Barry, R. G. 2005. *The Arctic climate system*. Cambridge University Press.

Simpson, G.G. 1953. *The Major Features of Evolution*. New York: Columbia Univ. Press.

Sirenko, B. I. (Ed.). 2001. *List of species of free-living invertebrates of Eurasian Arctic seas and adjacent deep waters*. Moscow: Russian Academy of Science, Zoological Institute.

Sirenko, B. I. 2009. Main differences in macrobenthos and benthic communities of the Arctic and Antarctic, as illustrated by comparison of the Laptev and Weddell Sea faunas. *Russian Journal of Marine Biology*, *35*, 445-453.

Sluijs, A., Schouten, S., Pagani, M., Woltering, M., Brinkhuis, H., Damsté, J. S. S., Dickens, G. R., Huber, M., Reichart, G. J., Stein, R., Matthiessen, J., Lourens, L. J., Pedentchouk, N., Backman, J., & Moran, K. 2006. Subtropical Arctic Ocean temperatures during the Palaeocene/Eocene thermal maximum. *Nature*, *441*(7093), 610–613.

Sluijs, A., Schouten, S., Donders, T. H., Schoon, P. L., Röhl, U., Reichart, G. J., Sangiorgi, F., Kim, J. H., Sinninghe Damsté, J. S., & Brinkhuis, H. 2009. Warm and wet conditions in the Arctic region during Eocene Thermal Maximum 2. *Nature Geoscience*, *2*(11), 777–780.

Sosiak, C. E., & Barden, P. 2021. Multidimensional trait morphology predicts ecology across ant lineages. Functional Ecology, 35(1), 139-152.

St John Glew, K., Espinasse, B., Hunt, B. P., Pakhomov, E. A., Bury, S. J., Pinkerton, M., Nodder, S.D., Gutiérrez-Rodríguez, A., Safi, K., Brown, J.C.S., Graham, L., Dunbar, R.B., Mucciarone, D.A., Magozzi, S., Somes, S., & Trueman, C. N. 2021. Isoscape models of the Southern Ocean: Predicting spatial and temporal variability in carbon and nitrogen isotope compositions of particulate organic matter. Global Biogeochemical Cycles, 35(9), e2020GB006901.

Stroud, J. T., & Losos, J. B. 2016. Ecological opportunity and adaptive radiation. *Annual Review of Ecology, Evolution, and Systematics*, *47*, 507-532.

Strugnell, J. M., Rogers, A. D., Prodöhl, P. A., Collins, M. A., & Allcock, A. L. 2008. The thermohaline expressway: the Southern Ocean as a centre of origin for deep‐sea octopuses. *Cladistics*, *24*(6), 853-860.

Strugnell, J. M., Cherel, Y., Cooke, I. R., Gleadall, I. G., Hochberg, F. G., Ibáñez, C. M., Jorgensen, E., Laptikhovsky, V.V., Linse, K., Norman, M., Vecchione, M., Voight, J.R. & Allcock, A. L. 2011. The Southern Ocean: source and sink?. *Deep Sea Research Part II: Topical Studies in Oceanography*, *58*(1-2), 196-204.

Takeuchi, I., Watanabe, K., Tanimura, A., & Fukuchi, M. 2002. Assemblages of necrophagous animals off Enderby Land, east Antarctica. In *Ecological Studies in the Antarctic Sea Ice Zone*. Springer, Berlin, Heidelberg. 97-103.

Thatje, S., Hillenbrand, C. D., & Larter, R. 2005. On the origin of Antarctic marine benthic community structure. *Trends in Ecology & Evolution*, *20*(10), 534-540.

Thatje, S., Hillenbrand, C. D., Mackensen, A., & Larter, R. 2008. Life hung by a thread: endurance of Antarctic fauna in glacial periods. *Ecology*, *89*(3), 682-692.

Thomas, D. N., Fogg, G. E., Convey, P., Fritsen, C. H., Gili, J. M., Gradinger, R., Laybourn-Parry, J., Reid, K. & Walton, D. W.H. 2008. *The biology of polar regions*. OUP Oxford.

Thornhill, D. J., Mahon, A. R., Norenburg, J. L., & Halanych, K. M. 2008. Open‐ocean barriers to dispersal: A test case with the Antarctic Polar Front and the ribbon worm *Parborlasia corrugatus* (Nemertea: Lineidae). *Molecular ecology*, *17*(23), 5104-5117.

Thurston, M. 2009. Key to the genera and species of Eusiridae from the Arctic Ocean and Norwegian Sea. Deep-sea workshop. Skibotn: Unpublished.

Turner, J., & Overland, J. 2009. Contrasting climate change in the two polar regions. *Polar Research*, *28*(2), 146-164.

Uyeda, J. C., Caetano, D. S., & Pennell, M. W. 2015. Comparative analysis of principal components can be misleading. *Systematic Biology*, *64*(4), 677-689.

Verheye M.L. 2011. *Systématique et diversité génétique des Eusirus de l'Océan Austral (Crustacea, Amphipoda, Eusiridae). Mémoire présenté en vue de l'obtention du diplôme de Master en Biologie des Organismes et Ecologie*. Louvainla- Neuve: Université Catholique de Louvain-la-Neuve.

Verheye, M.L. 2017. Systematics, phylogeography and historical biogeography of Eusiroidea (Crustacea, Amphipoda) from the Southern Ocean, with a special focus on the families Epimeriidae and Iphimediidae. PhD thesis, Université Catholique de Louvain-la-Neuve.

Verheye, M. L., Backeljau, T., & d'Acoz, C. D. U. 2017. Locked in the icehouse: evolution of an endemic Epimeria (Amphipoda, Crustacea) species flock on the Antarctic shelf. *Molecular phylogenetics and evolution*, *114*, 14-33.

Verheye, M. L., & D'Udekem D'Acoz, C. 2020. Integrative taxonomy of giant crested *Eusirus* in the Southern Ocean, including the description of a new species (Crustacea: Amphipoda: Eusiridae). *Zoological Journal of the Linnean Society*, *193*(1), 31-77.

Villéger, S., Mason, N. W., & Mouillot, D. 2008. New multidimensional functional diversity indices for a multifaceted framework in functional ecology. *Ecology*, *89*(8), 2290-2301.

Wang, Y., Sha, Z., & Ren, X. 2021. A new species of *Eusirus* (Amphipoda, Amphilochidea, Eusiridae) described from a hydrothermal vent in the Okinawa Trough, North-West Pacific. *Crustaceana*, *94*(11-12), 1395-1405.

Weisshappel, J. B. 2000. Distribution and diversity of the hyperbenthic amphipod family Eusiridae in the different seas around the Greenland-Iceland-Faeroe-Ridge. *Sarsia*, *85*(3), 227-236.

Węsławski, J. M., & Legeżyńska, J. 2002. Life cycles of some Arctic amphipods. *Polish Polar Research*, 253-264.

Wickham H 2016. ggplot2: Elegant Graphics for Data Analysis. Springer-Verlag New York. ISBN 978-3-319-24277-4, https://ggplot2.tidyverse.org.

Wong, M. K., Guénard, B., & Lewis, O. T. 2019. Trait-based ecology of terrestrial arthropods. Biological Reviews, 94(3), 999-1022.

Yoder, J. B., Clancey, E., Des Roches, S., Eastman, J. M., Gentry, L., Godsoe, W., Hagey, T.J., Jochimsen, D., Oswald., B.P., Robertson., J., Sarver., B.A.J., Schenk, J.J., Spear., S.F., & Harmon, L. J. 2010. Ecological opportunity and the origin of adaptive radiations. *Journal of evolutionary biology*, *23*(8), 1581-1596.

Zelditch, M. L., Swiderski, D. L., & Sheets, H. D. 2012. Geometric morphometrics for biologists: A primer. Waltham, MA: Academic Press.

Chapter 6: General discussions

The present work explored genetic adaptations (**Chapters 2 and 3**) and the tempo and mode of species diversification of the genus *Eusirus* in the Arctic and the Southern Oceans (**Chapters 4 and 5**). For this purpose, I assembled and published novel mitochondrial genomes (mitogenomes) of two *Eusirus* and one *Charcotia* amphipod species from the Southern Ocean (**Chapter 2**). These mitogenomes together with additional mitogenomes of other amphipods were used to investigate signatures of cold adaptations (**Chapter 3**). I also reconstructed a time-calibrated phylogeny to test for monophyly of Arctic and Antarctic *Eusirus* clades as well as their evolutionary age (**Chapter 4**). This time-calibrated phylogeny was utilized together with morphological and ecological data to test whether the genus *Eusirus* evolved through adaptive or non-adaptive radiations in the Arctic and Southern Ocean (**Chapter 5**).

6.1. Characteristics of Antarctic amphipod mitogenomes

The successfully assembled and annotated novel mitogenomes of Antarctic amphipods (Salabao et al. 2022) showed the same lengths as other mitogenomes from amphipods and contained the common metazoan gene composition of 13 protein-coding genes, 2 ribosomal RNA genes (rRNA), 22 transfer RNA genes (tRNA), and a non-coding control region (CR). Aberrant tRNA and short rRNA genes were found in these novel mitogenomes which is a common feature shared with other amphipod mitogenomes and possibly linked to the minimalization of mitogenomes in general (Yamazaki et al., 1997). Distinct features included a lower AT-richness in the entire mitogenomes, negative GC- skews on both strands of the protein coding genes and unique gene rearrangements. Moreover, the most variable protein coding genes were *nad6* and *atp8* while *cox1* showed the least genetic variability among closely and more distantly related species; this might have important implications for the wide use of this gene for DNA barcoding (Hebert et al., 2003; Witt et al., 2006; Romanova et al., 2016), also of amphipods. Amino-acid sequences of mitochondrial protein coding genes seemed to be suitable markers for phylogenetic reconstructions as amphipod species belonging to the same superfamilies clustered together in the phylogenetic tree based on mitochondrial amino-acids. With the development of next-generation sequencing, information of amphipod mitogenomes has been increasing in public databases (Pons et al., 2014; Li et al., 2019b) with 89 mitogenomes currently available in the GenBank database as

of 2023. These mitogenomes are becoming a popular tool for research on population genetics, phylogenetics, adaptation, and evolution (Ballard & Whitlock, 2004; Fontanillas et al., 2005; Carapelli et al., 2019; Pons et al., 2014; Li et al., 2019b; Sun et al., 2020; Bauzà-Ribot et al., 2012). Despite the increasing availability of amphipod mitogenomes, mitogenomic data of polar amphipod are still poorly represented with only one published mitogenome from the Antarctic (Shin et al., 2012) and one from the Arctic (Ki et al., 2010). The novel mitogenomes of the Antarctic amphipods presented in **chapter 2** are thus valuable additions to the genetic resources of amphipods from the polar regions. Notably, the data of the novel mitogenomes were obtained through a cost-efficient low coverage skimming sequencing approach. Despite the lower depth of coverage, this approach produced complete mitogenomes with less than 0.01% of ambiguities illustrating that this approach was successful and affordable. The novel and complete mitogenomes provided additional insights into the features of Antarctic amphipod mitogenomes and showed that they are suitable tools for the reconstruction of phylogenetic relationships with other amphipods.

6.2. Signatures for cold adaptations from amphipod mitogenomes

Evidence for purifying selection was observed in all analysed amphipod mitogenomes. Mitogenomes of amphipods from cold regions showed signatures of molecular adaptations to cold environments including significantly lower proportions of charged amino acid and higher average ratios of non-synonymous to synonymous substitutions (ω). In contrast, species from cold regions did not cluster together in the phylogenetic tree and did not share similar patterns of gene translocations. It is possible that these features of mitogenomes are not adaptive. The conducted analysis was based on a lower number of amphipod species from cold and warm regions as compared to species from temperate regions which could have reduced the statistical power. Hence, there is a need to include more representatives from these regions for more balanced comparisons in future research.

The survival and success of organisms in different environments are greatly influenced by their molecular adaptations (Somero, 2010; Fox et al., 2019; Sebastian et al., 2020). Some of the most extreme environments are characterized by very low temperatures where organisms must survive (Peck, 2018; Peck, 2020). Cold adaptation is driven by several cellular processes and adjustments permitting survival (Lipaeva et al., 2021). Certain molecular adaptations

allow the maintenance of cellular processes and an optimized metabolic efficiency under cold stress (Ballard & Whitlock, 2004; Fontanillas et al., 2005; Stier et al., 2014; Consuegra et al., 2015; Berthelot et al., 2019; Carapelli et al., 2019; Lipaeva et al., 2021). Understanding the molecular mechanisms driving these adaptations provides important insights into the fundamental processes that allow organisms to survive in the cold. Resources that have been used to study molecular adaptations in low temperatures are mitogenomes (Melo-Ferreira et al., 2014; Consuegra et al., 2015; Carapelli et al., 2019; Sokolova, 2023). Mitogenomes contain genes that are involved in energy production, and it is expected that selection on these genes may be driven by environmental factors (Melo-Ferreira et al., 2014; Consuegra et al., 2015; Sun et al., 2020). Moreover, fitness and metabolic processes of an organism may significantly be impacted by mutations in its mitogenome (Melo-Ferreira et al., 2014; Consuegra et al., 2015; Carapelli et al., 2019). Mitogenomes of several taxa have already been utilized to test for molecular adaptations in cold temperatures including hexapods (Carapelli et al., 2019), fishes (Consuegra et al., 2015), and amphipods (**chapter 3**). Signatures of adaptations at low temperatures in amphipods were identified such as significantly lower proportions of charged amino acid and higher average ratios of non-synonymous to synonymous substitutions (ω) than what was observed in amphipods living in temperate or warm regions. These notable signatures of cold adaptations unraveled in **chapter 3** provide more insights on how amphipods adapt to cold environments and highlight molecular mechanisms that allow amphipods to keep important mitochondrial gene functioning under low temperature stress (Ballard & Whitlock, 2004; Castellana et al., 2011; Carapelli et al., 2019). Lower proportions of charged amino acids increase protein flexibility which is necessary for cold adaptations (Gianese et al., 2001; Huang et al., 2023). The lower proportion of charged amino acid is in line with previous studies where abyssal and hadal amphipods, living in deep-sea habitats with low temperatures showed similar patterns (Li et al. 2019a and b). Another study showed the reduced abundance of charged amino acids in psychrophiles or organisms that can endure cold temperatures (Gianese et al., 2001; Methé et al., 2005; Goldstein, 2007; Metpally et al., 2009). Interestingly, the current study is the first (**chapter 3**) to have recorded higher average ratios of non-synonymous to synonymous substitutions (ω) in amphipods from cold regions. The higher average ω could be due to lower average synonymous substitutions (ds) (Parker et al., 2018); this could possibly suggest that weaker purifying selection (Jeffares et al., 2015)

acts on the mitochondrial genes of amphipods from cold regions as compared to the amphipods from temperate and warm regions.

6.3. Origin and diversification patterns of the genus *Eusirus* in the polar regions

The molecular phylogeny supported the monophyly of the Antarctic *Eusirus* clade while the Arctic clade was found to be polyphyletic. The time-calibrated phylogeny suggested that the diversification of the Antarctic clade coincided with the opening of the Drake passage and the formation of the Antarctic circumpolar current (ACC) as well as with lower temperatures and the onset of ice sheet expansions. There may have been a burst of diversification in the Antarctic clade, possibly as a result of vicariant events and ecological opportunities provided by the changes of Antarctic climate and geology. Arctic *Eusirus* species showed varying diversification ages which appeared to correspond to pre-glacial/interglacial periods. Moreover, the age variations imply that distinct geological and climatic events led to multiple diversification events of Arctic *Eusirus* species. The initial diversification of the Arctic *Eusirus* occurred prior to the diversification of the Antarctic clade; however, no evidence for an increase of diversification rates was observed in Arctic *Eusirus*.

Understanding the origins of species and the diversification patterns that shaped their diversity are important topics in biodiversity and its conservation (Colombo, 2015; Panero & Crozier, 2016). The Arctic and the Antarctic regions serve as natural laboratories to study the diversification of species due to their long histories, the high abundance of endemic taxa (Hardy et al., 2011; Saucède et al., 2014) and the well-known past major climate changes that have shaped the current diversity (Aronson & Blake, 2001; Clarke & Crame, 2010; Near et al., 2012). With the recent fast rise in temperatures experienced by the polar regions due to global warming (Turner & Overland, 2009; Turner & Marshall, 2011), it is highly relevant to understand the origins and diversification patterns of polar endemic species. The Arctic is thought to be evolutionary young, species-poor, and has fewer endemic species in comparison to the Antarctic (Gutt et al., 2004; Piepenburg, 2005; Hardy et al., 2011). Characterized by its connections with North Pacific and Atlantic Oceans (Thomas et al., 2008; Clarke and Crame, 2010; Legezyñska et al., 2020), the current Arctic fauna is composed of a mixture of taxa from different origins, including faunas from the North Atlantic, North Pacific, deep sea cosmopolitans, and endemic species of native origin (Knox & Lowry, 1977; Sirenko, 2009;

Gradinger et al., 2010; Josefson & Mokievsky, 2013; Renaud et al., 2015; Legezyñska et al., 2020). As suggested by the novel phylogenetic results (**chapter 4**)**,** Arctic *Eusirus* amphipods seem to have undergone a varied evolutionary history of lineage splitting, which is reflected in the polyphyly of the group with origins prior to the glacial/interglacial periods. The mean ages of the Arctic lineages splitting ranged from 48.72 to 63.47 Ma [95% HPD: 35.71-81.54 Ma] (**chapter 4**) coinciding with events that facilitated dispersal of ancestors into the Arctic and the other oceans (Dunton, 1992; Dayton, 2013). In the late Cretaceous, connections between the two subtropical seaways and the Arctic Ocean facilitated species exchanges. Abyssal and bathyal fauna exchanges also occurred through the connections between North Pacific and the Arctic oceans around this time while the Arctic Ocean later closed at the end of the Cretaceous (80-100 Ma) (Dunton, 1992; O'Regan et al., 2011). Around the middle Paleogene (about 40 Ma), connections between the Atlantic and the Arctic oceans permitted species to become exchanged between these oceans (Clarke & Crame, 2010); exchange was further facilitated by the formation of the deep-water connections during the late Paleogene (about 35-27 Ma) through the Fram Strait (Serreze & Barry, 2005; Kuklinski et al., 2013; Legezyñska et al., 2020).

In contrast, the Antarctic Southern Ocean is isolated from the South Pacific, Atlantic, and Indian oceans by the ACC (Thomas et al., 2008; Clarke and Crame, 2010; Legezyñska et al., 2020). The marine Antarctic fauna is comprised of taxa from different origins (Knox & Lowry, 1977; Brandt, 1999; Clarke, 2008; Sirenko, 2009; Clarke & Crame, 2010; Legezyñska et al., 2020) with the Antarctic *Eusirus* clade (see **chapter 4**) most likely having originated *in situ* when Antarctica was already geographically isolated (Rogers, 2007; Thornhill et al., 2008) as exemplified by the monophyly of the Antarctic *Eusirus* group. Indeed, the mean age estimate of the Antarctic was 29.51 Ma [95% HPD: 25.78-33.29 Ma] coinciding with the opening of the Drake passage during the late Eocene to Oligocene (34-26 Ma) followed by the formation of the ACC around the Oligocene (31-26 Ma) (Hodel et al., 2021; Vincze et al., 2021). The opening of Drake passage and the formation of the ACC were followed by vicariant and subsequent allopatric speciation (Rogers, 2007; Thornhill et al., 2008). Extinctions also occurred around the Eocene-Oligocene transition creating ecological opportunities for surviving lineages which might have driven initial rapid lineage diversification (Stroud & Losos, 2016; Verheye, 2017); this could also be the case for Antarctic *Eusirus* (**chapter 4**). Extinction of decapods in the Tertiary could possibly have opened up previously occupied niches and decreased predation

pressure aiding in the diversification of Antarctic amphipods (Brandt, 1999; Legezyñska et al., 2020) including *Eusirus* (**chapter 4**).

6.4. Evolutionary diversification processes of the genus *Eusirus* in the polar regions

The Antarctic and Arctic *Eusirus* species were found to follow different evolutionary patterns. The burst of lineage diversification in the Antarctic *Eusirus* was not coupled with a rate shift for the morphological diversification which could be attributed to non-adaptive radiation of the Antarctic *Eusirus*. Diversity of Antarctic *Eusirus* could be mainly driven by allopatric speciation but, as suggested by the eco-morphological diversity present in the Antarctic clade, ecological diversification has also operated. The tempo of morphological and ecological accumulation during speciation events of the Arctic *Eusirus* appeared as constant in BAMM analyses. Moreover, the constant rate of lineage diversification in Arctic *Eusirus* was coupled with high levels of morphological and ecological diversity. This pattern could be attributed to the polyphyletic origin and the older age of Arctic lineages. The high levels of morphological and ecological diversity in the Arctic group are signature of ecological radiation probably smoothed by multiple extinction events.

The success of taxa that are morphologically and ecologically diverse is usually explained by adaptive radiations (Rutschmann et al., 2011; Matschiner et al., 2011; Colombo et al., 2015; Hu et al., 2016; Doenz et al., 2019). Adaptive radiation is driven by ecological opportunities which could originate through colonization of new habitats, key innovations, and extinction of competitors (Schluter, 2000; Stroud & Losos, 2016). These ecological opportunities could drive rapid lineage diversification coupled with morphological and ecological variation, occupying available niches (Schluter, 2000; Saupe & Myers, 2021) and adaptive radiation will eventually slow down as these niches are filled through time (Schluter, 2000; Gavrilets & Losos, 2009; Colombo et al., 2015). However, these patterns were not observed in either Arctic or Antarctic *Eusirus*. In the Arctic region, adaptive radiations have only been recorded in freshwater fishes such as the Artic charr species (Doenz et al., 2019; Østbye et al., 2020; Peris Tamayo et al., 2020) and whitefish (Kahilainen et al., 2011) with no evidence in marine taxa. On the other hand, in the Antarctic, adaptive radiations of several marine taxa have been described including gastropods of the families Buccinidae, Naticidae, and Turridae (Crame, 1997) and the notothenioid fishes (Rutschmann et al., 2011; Near et al., 2012; Colombo et al.,

2015; Daane et al., 2019). The documented adaptive radiations in the polar regions were attributed to ecological opportunities brought about by adaptations to different environments and key innovations like for example the antifreeze glycoproteins in fishes (Crame, 1997; Kahilainen et al., 2011; Rutschmann et al., 2011; Near et al., 2012; Colombo et al., 2015; Daane et al., 2019; Doenz et al., 2019; Østbye et al., 2020; Peris Tamayo et al., 2020). However, the diversification of the Antarctic icefish *Pogonophryne* was not accompanied with significant ecological differentiation suggesting non-adaptive radiation (Eastman, 2005). During non-adaptive radiations, species typically evolve in allopatry or peripatry and exhibit minimal morphological variation and no clear niche differentiation (Gittenberger, 1991; 2004; Wilke et al., 2010). Habitat fragmentation during geological events and low dispersal ability can cause allopatric speciation resulting in non-adaptive radiation (Gittenberger, 1991; Wiens, 2004; Rundell & Price, 2009). Unlike adaptive radiations, a diversity-dependent lineage and eco-morphological diversification in the most recent evolutionary history is not observed during non-adaptive radiations (Landeira et al., 2023). In Antarctic *Eusirus*, no rate shift of morphological evolution was observed although we found a burst of lineage diversification (**chapter 5**); this pattern support a scenario of non-adaptive radiation (Schluter, 2000; Rundell & Price, 2009; Ramirez-Reyes et al., 2022). A high number of endemic *Eusirus* species is found in the Antarctic and this is coupled with low morphological and isotopic diversity suggesting that evolution has been driven by allopatric speciation (Rundell & Price, 2009). It should, however, be noted that some speciation events might also be related to ecological diversification in the Antarctic as suggested by the morphological and isotopic diversity present in this group. The origin of the Antarctic *Eusirus* clade coincided with the opening of the Drake passage and the formation of the ACC which created a natural marine barrier preventing genetic exchange and consequently, providing opportunities for vicariant speciation events (Bargelloni et al., 2000; Lee et al., 2004). This was later followed by repeated glaciations and deglaciations, providing additional opportunities for allopatric speciation especially for less dispersive organisms such as brooding amphipods (Thatje et al., 2005; Rogers, 2007; Thornhill et al., 2008; Verheye, 2017; Legezyñska et al., 2020). Isolated habitats and low dispersal capabilities are conditions where genetic drift may play a significant role (Wilke et al., 2010) as populations in allopatry can speciate through genetic drift if they are isolated for a sufficiently long period (Coyne & Orr, 2004; Heinicke et al., 2017). In such examples of allopatric speciation, genetic drift can lead to divergence and potentially to

speciation without clear niche differentiation (Gittenberger, 2004) or significant morphological changes (Verheye, 2017).

A different scenario could be observed for the evolution of Arctic *Eusirus*, where a relatively constant rate of lineage diversification (**chapter 4**) was coupled with high levels of morphological and ecological diversity (**chapter 5**). Moreover, accumulation of morphological and ecological diversity probably occurred more constantly along speciation events. The high morphological and ecological diversity in the Arctic *Eusirus* could be explained by their polyphyletic origin and their older age to the Antarctic *Eusirus*. Arctic *Eusirus* originated 63.47 Ma [43.63-81.54 Ma] to 48.72 Ma [35.71-62.9 Ma] when connections between the Arctic and the other oceans permitted dispersal into the Arctic (Dayton, 2013). Moreover, with its older origin, it could be expected that the Arctic *Eusirus* have accumulated more morphological divergence. Another explanation could be attributed to the events of speciation associated with niche partitioning which reflects the high morphological and ecological diversity in the Arctic *Eusirus*. The lower species diversity in the Arctic may be explained from multiple extinction events in the past and multiple invasions that triggered speciation and ecological diversification, leaving a signature of high morphological diversity.

This study has unraveled evolutionary scenarios of speciation in the polar regions using the genus *Eusirus* amphipods as model organisms. To our knowledge, similar studies utilizing taxa with bipolar distributions to compare the evolutionary scenarios between both polar regions have not been conducted yet. Given that these polar species had different origins and took millions of years to evolve, these species may be at a high risk to become extinct because of climate change (Peck, 2005; Clarke & Crame, 2010; Gilg et al., 2012), even more so because they have evolved specific molecular mechanisms for cold adaptations. These adaptations makes these species more susceptible to temperature changes as they are more constricted to temperature boundaries compared to non-polar relatives (Peck et al., 2004; Cheung et al., 2009). Consequently, these constricted temperature boundaries suggest that they are the least likely to be able to resist change and will have limited scope to escape unfavourable conditions (Peck et al., 2004; Peck, 2018). The long evolutionary history along with the specific cold adaptations of these species leading to restricted temperature boundaries may give these species insufficient time to evolve to new environmental conditions (Cheung et al., 2009; Peck, 2018) resulting in their extinction (Constable et al., 2014).

6.5. Future perspectives

With only one Antarctic amphipod mitogenome available prior to this thesis, the novel mitogenomes of Antarctic amphipods (**chapter 2**) contributed a significant addition to the database. These new molecular data also provided information on the distinct features of Antarctic amphipod mitogenomes. These mitogenomes can be used for future studies including primer design, reconstruction of phylogenetic relationships, population genetics, and unraveling phylogeographic patterns and evolutionary histories (Bauzà-Ribot et al., 2012; Keis et al., 2013; Meimberg et al., 2016; Romanova et al., 2016). Moreover, genetic adaptations can also be successfully studied utilizing mitogenomes in other taxa (similar to the ones in **chapter 3**). For future studies, increasing the number of mitogenomes for amphipod species, especially from cold and warm regions could improve the strengths of statistical analyses for possible signals of thermal adaptations and provide a more balanced dataset for comparisons.

Mitogenomic data (full length sequences of the mitochondrial COI and COII genes) together with nuclear ribosomal data generated a well-supported phylogeny and unraveled the origins and evolutionary diversification processes of *Eusirus* amphipods in the polar regions (as in **chapter 4 and 5**). Similar analyses could be conducted on other polar organisms for which large scale genomic data are not yet available. Origins and diversification processes of both polar regions were unraveled by using *Eusirus* amphipods as model organisms (**chapters 4 and 5**). This is the first study that compared evolutionary scenarios at both poles using taxa with bipolar distributions. In the future, utilizing the most recent third generation sequencing techniques which produce long reads (average sequencing reads of about 2–10 Kb) such as the “single-molecule real-time” sequencing techniques (SMRT-seq using Pacific Biosystems and Oxford Nanopore Technologies) would also be promising to use for studies of genetic adaptations and evolutionary processes. These sequencing methods have successfully generated genomes of Antarctic species such as Antarctic krill *Euphausia superba* and Antarctic blackfin icefish *Chaenocephalus aceratus* (Kelley et al., 2014; Kim et al., 2019; Shao et al., 2023). The application of similar methods to polar amphipods is currently still complicated by the large variation in genome size of amphipods, ranging from 3 to 64 pg (Rees et al. 2007). There are no data on genome sizes of *Eusirus* species but published chromosome-level genomes of for example the red claw crayfish with a genome size of 5 Gb (Chen et al.

2023) indicate that it is becoming possible to assemble high quality genomes of polar amphipods in the future. Such complete genomic assemblies would provide more insights into adaptations to cold environments and extensive molecular data for phylogenetic reconstructions. Moreover, additional studies based on full taxon sampling of *Eusirus* species is advisable to identify the origin of the polar *Eusirus*. It would also be recommended to analyse additional phenotypic traits such as the mouthparts (Michel et al., 2020) and link their variation to the ecology of *Eusirus* which might provide additional information to explain the successful diversification of *Eusirus*. The different subspace occupations of morphospace and isospace between Arctic and Antarctic group provide substantial evidence that the product of both radiations in polar regions is not strictly similar. Additional works should be achieved to check the amplitude and degree of phenotypic convergence in polar regions. It would be also be interesting to repeat our work in other biological systems with bipolar distributions and different biology or ecologies such as for example the fish family Liparidae which is one of the dominant taxa at both poles (Eastman, 1997; Di Prisco et al., 1998). This would allow us to test if similar evolutionary patterns and evolutionary age estimates as for *Eusirus* will be obtained.

References

Aronson, R. B., & Blake, D. B. 2001. Global climate change and the origin of modern benthic communities in Antarctica. *American Zoologist*, *41*(1), 27-39.

Ballard, J. W. O., & Whitlock, M. C. 2004. The incomplete natural history of mitochondria. *Molecular ecology*, *13*(4), 729-744.

Bauzà-Ribot, M. M., Juan, C., Nardi, F., Oromí, P., Pons, J., & Jaume, D. 2012. Mitogenomic phylogenetic analysis supports continental-scale vicariance in subterranean thalassoid crustaceans. *Current Biology*, *22*(21), 2069-2074.

Bargelloni, L., Marcato, S., Zane, L., Patarnello, T., 2000. Mitochondrial phylogeny of notothenioids: a molecular approach to Antarctic fish evolution and biogeography. Systematic Biology 49,114-129.

Berthelot, C., Clarke, J., Desvignes, T., William Detrich III, H., Flicek, P., Peck, L. S., Flicek, P., Peck, L.S., Peters, M., Postlethwait, J.H., & Clark, M. S. 2019. Adaptation of proteins to the cold in Antarctic fish: a role for methionine?. *Genome biology and evolution*, *11*(1), 220-231.

Brandt, A. 1999. On the origin and evolution of Antarctic Peracarida (Crustacea, Malacostraca). Scientia Marina 63, 261-274

Carapelli, A., Fanciulli, P. P., Frati, F., & Leo, C. 2019. Mitogenomic data to study the taxonomy of Antarctic springtail species (Hexapoda: Collembola) and their adaptation to extreme environments. *Polar Biology*, *42*, 715-732.

Castellana, S., Vicario, S., & Saccone, C. 2011. Evolutionary patterns of the mitochondrial genome in Metazoa: exploring the role of mutation and selection in mitochondrial protein-coding genes. *Genome biology and evolution*, *3*, 1067-1079.

Chen, H., Zhang, R., Liu, F., Shao, C., Liu, F., Li, W., ... & Lou, B. 2023. The chromosome-level genome of Cherax quadricarinatus. Scientific data, 10(1), 215.

Cheung, W. W., Lam, V. W., Sarmiento, J. L., Kearney, K., Watson, R., & Pauly, D. 2009. Projecting global marine biodiversity impacts under climate change scenarios. Fish and fisheries, 10(3), 235-251.

Clarke, A. 2008. Antarctic marine benthic diversity: patterns and processes. *Journal of Experimental Marine Biology and Ecology*, *366*(1-2), 48-55.

Clarke, A., & Crame, J. A. 2010. Evolutionary dynamics at high latitudes: speciation and extinction in polar marine faunas. *Philosophical Transactions of the Royal Society B: Biological Sciences*, *365*(1558), 3655-3666.

Colombo, M. 2015. *Morphology and ecology during the course of teleost adaptive radiations* (Doctoral dissertation, University of Basel).

Colombo, M., Damerau, M., Hanel, R., Salzburger, W., & Matschiner, M. 2015. Diversity and disparity through time in the adaptive radiation of Antarctic notothenioid fishes. *Journal of Evolutionary Biology*, *28*(2), 376-394.

Constable, A. J., Melbourne‐Thomas, J., Corney, S. P., Arrigo, K. R., Barbraud, C., Barnes, D. K., ... & Ziegler, P. 2014. Climate change and Southern Ocean ecosystems I: how changes in physical habitats directly affect marine biota. Global change biology, 20(10), 3004-3025.

Consuegra, S., John, E., Verspoor, E., & de Leaniz, C. G. 2015. Patterns of natural selection acting on the mitochondrial genome of a locally adapted fish species. *Genetics Selection Evolution*, *47*(1), 1-10.

Coyne J.A. & Orr, H.A. 2004. Speciation. Sinauer Associates, Inc., Sunderland, Massachusetts.

Crame, J. A. 1997. An evolutionary framework for the polar regions. *Journal of Biogeography*, *24*(1), 1-9.

Daane, J. M., Dornburg, A., Smits, P., MacGuigan, D. J., Brent Hawkins, M., Near, T. J., Detrich IIII. H.M., & Harris, M. P. 2019. Historical contingency shapes adaptive radiation in Antarctic fishes. *Nature ecology & evolution*, *3*(7), 1102-1109.

Dayton, P. K. 2013. 12 Polar Benthos. Polar Oceanography: Chemistry, Biology, and Geology, 631.

Di Prisco, G., Pisano, E., Clarke, A., Eastman, J. T., & Clarke, A. 1998. A comparison of adaptive radiations of Antarctic fish with those of nonAntarctic fish. Fishes of Antarctica: a biological overview, 3-26.

Doenz, C. J., Krähenbühl, A. K., Walker, J., Seehausen, O., & Brodersen, J. 2019. Ecological opportunity shapes a large Arctic charr species radiation. *Proceedings of the Royal Society B*, *286*(1913), 20191992.

Dunton, K. 1992. Arctic biogeography: the paradox of the marine benthic fauna and flora. *Trends in Ecology & Evolution*, *7*(6), 183-189.

Eastman, J. T. 1997. Comparison of the Antarctic and Arctic fish faunas. Cybium (Paris), 21(4), 335-352.

Eastman, J. T. 2005. The nature of the diversity of Antarctic fishes. *Polar biology*, *28*, 93-107.

Fontanillas, P., Depraz, A., Giorgi, M. S., & Perrin, N. 2005. Nonshivering thermogenesis capacity associated to mitochondrial DNA haplotypes and gender in the greater white‐toothed shrew, Crocidura russula. Molecular Ecology, 14(2), 661-670.

Fox, R. J., Donelson, J. M., Schunter, C., Ravasi, T., & Gaitán-Espitia, J. D. 2019. Beyond buying time: the role of plasticity in phenotypic adaptation to rapid environmental change. *Philosophical Transactions of the Royal Society B*, *374*(1768), 20180174.

Gavrilets, S., & Losos, J. B. 2009. Adaptive radiation: contrasting theory with data. Science, 323(5915), 732-737.

Gilg, O., Kovacs, K. M., Aars, J., Fort, J., Gauthier, G., Grémillet, D., Ims, R.A., Meltofte, H., Moreau, J., Post, E., Schmidt, N.M., Yannic, G., & Bollache, L. 2012. Climate change and the ecology and evolution of Arctic vertebrates. Annals of the New York Academy of Sciences, 1249(1), 166-190.

Gittenberger, E. 1991. What about non-adaptive radiation?. *Biological Journal of the Linnean Society*, *43*(4), 263-272.

Gittenberger, E. 2004. Radiation and adaptation, evolutionary biology and semantics. Organisms Diversity & Evolution, 4(3), 135-136.

Goldstein, R. A. 2007. Amino‐acid interactions in psychrophiles, mesophiles, thermophiles, and hyperthermophiles: insights from the quasi‐chemical approximation. *Protein science*, *16*(9), 1887-1895.

Gradinger, R., Bluhm, B. A., Hopcroft, R. R., Gebruk, A. V., Kosobokova, K., Sirenko, B., & Wesławski, J. M. 2010. Marine life in the Arctic. *Life in the World's Oceans: Diversity, Distribution and Abundance. Wiley-Blackwell, Oxford*, 183-202.

Gutt, J., Sirenko, B. I., Smirnov, I. S., & Arntz, W. E. 2004. How many macrozoobenthic species might inhabit the Antarctic shelf?. *Antarctic Science*, *16*(1), 11-16.

Hardy, S. M., Carr, C. M., Hardman, M., Steinke, D., Corstorphine, E., & Mah, C. 2011. Biodiversity and phylogeography of Arctic marine fauna: insights from molecular tools. *Marine Biodiversity*, *41*, 195-210.

Hebert, P. D., Cywinska, A., Ball, S. L., & DeWaard, J. R. 2003. Biological identifications through DNA barcodes. Proceedings of the Royal Society of London. Series B: Biological Sciences, 270(1512), 313-321.

Heinicke, M. P., Jackman, T. R., & Bauer, A. M. 2017. The measure of success: geographic isolation promotes diversification in Pachydactylus geckos. BMC Evolutionary Biology, 17(1), 1-17.

Hodel, F., Grespan, R., de Rafélis, M., Dera, G., Lezin, C., Nardin, E., Rouby D., Aretz M., Steinnman M., Buatier M., Lacan F., Jeandel C., & Chavagnac, V. 2021. Drake Passage gateway opening and Antarctic Circumpolar Current onset 31 Ma ago: The message of foraminifera and reconsideration of the Neodymium isotope record. Chemical Geology, 570, 120171.

Hu, Y., Ghigliotti, L., Vacchi, M., Pisano, E., Detrich, H. W., & Albertson, R. C. 2016. Evolution in an extreme environment: developmental biases and phenotypic integration in the adaptive radiation of antarctic notothenioids. *BMC evolutionary biology*, *16*, 1-13.

Huang, A., Lu, F., & Liu, F. 2023. Discrimination of psychrophilic enzymes using machine learning algorithms with amino acid composition descriptor. Frontiers in Microbiology, 14, 1130594.

Jeffares, D. C., Tomiczek, B., Sojo, V., & Reis, M. D. 2015. A beginners guide to estimating the non-synonymous to synonymous rate ratio of all protein-coding genes in a genome. In Parasite genomics protocols. Humana Press, New York, NY. pp. 65-90.

Josefson, A. B. & Mokievsky, V. 2013. Marine invertebrates. In Arctic Biodiversity Assessment: Status and Trends in Arctic Biodiversity (ed. H. MELTOFTE), pp. 224–257. CAFF, Tromsø, Norway.

Kahilainen, K. K., Siwertsson, A., Gjelland, K. Ø., Knudsen, R., Bøhn, T., & Amundsen, P. A. 2011. The role of gill raker number variability in adaptive radiation of coregonid fish. *Evolutionary Ecology*, *25*, 573-588.

Keis, M., Remm, J., Ho, S. Y., Davison, J., Tammeleht, E., Tumanov, I. L., Saveljev, A.P., Männil, P., Kojola, I., & Abramov A.V. 2013. Complete mitochondrial genomes and a novel spatial genetic method reveal cryptic phylogeographical structure and migration patterns among brown bears in north‐western Eurasia. *Journal of Biogeography*, *40*(5), 915-927.

Kelley, J. L., Peyton, J. T., Fiston-Lavier, A. S., Teets, N. M., Yee, M. C., Johnston, J. S., Bustamante, C.D., Lee, R.E., & Denlinger, D. L. 2014. Compact genome of the Antarctic midge is likely an adaptation to an extreme environment. Nature communications, 5(1), 4611.

Ki, J. S., Hop, H., Kim, S. J., Kim, I. C., Park, H. G., & Lee, J. S. 2010. Complete mitochondrial genome sequence of the Arctic gammarid, Onisimus nanseni (Crustacea; Amphipoda): Novel gene structures and unusual control region features. *Comparative Biochemistry and Physiology Part D: Genomics and Proteomics*, *5*(2), 105-115.

Kim, B. M., Amores, A., Kang, S., Ahn, D. H., Kim, J. H., Kim, I. C., Lee, J.H., Lee, S.G., Lee, H., Lee, J., Kim, H., Desvignes, T., Batzel, P., Sydes, J., Titus, T., Wilson, C.A., Catchen, J.M., Warren, W.C., Schartl, M., Detrich, H.W. III, Postlethwait, J.H., & Park, H. 2019. Antarctic blackfin icefish genome reveals adaptations to extreme environments. Nature ecology & evolution, 3(3), 469-478.

Knox, G.A. & Lowry, J.K. 1977. A comparison between the benthos of the Southern Ocean and the North Polar Ocean with special reference to the Amphipoda and Polychaeta. In: Dunbar, M.J. (Ed.), Polar oceans. Proceedings of the Polar Ocean Conference, Calgary, pp. 432- 462.

Kuklinski, P., Taylor, P. D., Denisenko, N. V., & Berning, B. 2013. Atlantic origin of the Arctic biota? Evidence from phylogenetic and biogeographical analysis of the cheilostome bryozoan genus Pseudoflustra. *PLoS One*, *8*(3), e59152. 1-25.

Landeira, J. M., Deville, D., Fatira, E., Zhang, Z., Thatje, S., Lin, Q., Hernández-León, S., & Wakabayashi, K. 2023. Diversification of cephalic shield shape and antenna in phyllosoma I of slipper and spiny lobsters (Decapoda: Achelata). Frontiers in Marine Science, 10, 1070296.

Gianese, G., Argos, P., & Pascarella, S. 2001. Structural adaptation of enzymes to low temperatures. Protein engineering, 14(3), 141-148.

Lee, Y.-H., Song, M., Lee, S., Leon, R., Godoy, S.O., Canete, I. 2004. Molecular phylogeny and divergence time of the Antarctic sea urchin (Sterechinus neumayeri) in relation to the South American sea urchins. Antarctic Science 16, 29-36.

Legezyñska, J., De Broyer, C., & Wesławski, J. M. 2020. Invasion of the poles. The Natural History of the Crustacea: Evolution and Biogeography of the Crustacea, 216-246.

Li, J. Y., Zeng, C., Yan, G. Y., & He, L. S. 2019a. Characterization of the mitochondrial genome of an ancient amphipod Halice sp. MT-2017 (Pardaliscidae) from 10,908 m in the Mariana Trench. Scientific reports, 9(1), 1-15.

Li, J. Y., Song, Z. L., Yan, G. Y., & He, L. S. 2019b. The complete mitochondrial genome of the largest amphipod, Alicella gigantea: Insight into its phylogenetic relationships and deep sea adaptive characters. International journal of biological macromolecules, 141, 570-577.

Lipaeva, P., Vereshchagina, K., Drozdova, P., Jakob, L., Kondrateva, E., Lucassen, M., Bedulina, D., Timofeyev, M., Stadler, P., & Luckenbach, T. 2021. Different ways to play it cool: Transcriptomic analysis sheds light on different activity patterns of three amphipod species under long‐term cold exposure. *Molecular ecology*, *30*(22), 5735-5751.

Matschiner, M., Hanel, R., & Salzburger, W. 2011. On the origin and trigger of the notothenioid adaptive radiation. *PLoS one*, *6*(4), e18911.

Meimberg, H., Schachtler, C., Curto, M., Husemann, M., & Habel, J. C. 2016. A new amplicon based approach of whole mitogenome sequencing for phylogenetic and phylogeographic analysis: An example of East African white-eyes (Aves, Zosteropidae). *Molecular phylogenetics and evolution*, *102*, 74-85.

Melo-Ferreira, J., Vilela, J., Fonseca, M. M., da Fonseca, R. R., Boursot, P., & Alves, P. C. 2014. The elusive nature of adaptive mitochondrial DNA evolution of an arctic lineage prone to frequent introgression. *Genome biology and evolution*, *6*(4), 886-896.

Methé, B. A., Nelson, K. E., Deming, J. W., Momen, B., Melamud, E., Zhang, X., ... & Fraser, C. M. 2005. The psychrophilic lifestyle as revealed by the genome sequence of Colwellia psychrerythraea 34H through genomic and proteomic analyses. *Proceedings of the National Academy of Sciences*, *102*(31), 10913-10918.

Metpally, R. P. R., & Reddy, B. V. B. 2009. Comparative proteome analysis of psychrophilic versus mesophilic bacterial species: Insights into the molecular basis of cold adaptation of proteins. *BMC genomics*, *10*(1), 1-10.

Michel, L. N., Nyssen, F. L., Dauby, P., & Verheye, M. 2020. Can mandible morphology help predict feeding habits in Antarctic amphipods?. Antarctic Science, 32(6), 496-507.

Near, T. J., Dornburg, A., Kuhn, K. L., Eastman, J. T., Pennington, J. N., Patarnello, T.,Zane, L., Fernández, D.A., & Jones, C. D. 2012. Ancient climate change, antifreeze, and the evolutionary diversification of Antarctic fishes. *Proceedings of the National Academy of Sciences*, *109*(9), 3434-3439.

O'Regan, M., Williams, C. J., Frey, K. E., & Jakobsson, M. 2011. A synthesis of the long-term paleoclimatic evolution of the Arctic. Oceanography, 24(3), 66-80.

Østbye, K., Hagen Hassve, M., Peris Tamayo, A. M., Hagenlund, M., Vogler, T., & Præbel, K. 2020. "And if you gaze long into an abyss, the abyss gazes also into thee": four morphs of Arctic charr adapting to a depth gradient in Lake Tinnsjøen. *Evolutionary Applications*, *13*(6), 1240-1261.

Parker, D. J., Wiberg, R. A. W., Trivedi, U., Tyukmaeva, V. I., Gharbi, K., Butlin, R. K., Hoikkala, A., Kankare, M., & Ritchie, M. G. 2018. Inter and intraspecific genomic divergence in Drosophila montana shows evidence for cold adaptation. Genome Biology and Evolution, 10(8), 2086-2101.

Panero, J. L., & Crozier, B. S. 2016. Macroevolutionary dynamics in the early diversification of Asteraceae. *Molecular Phylogenetics and Evolution*, *99*, 116-132.

Peck, L. S. 2005. Prospects for survival in the Southern Ocean: vulnerability of benthic species to temperature change. Antarctic Science, 17(4), 497-507.

Peck, L. S. 2018. Antarctic marine biodiversity: adaptations, environments and responses to change. *Oceanography and Marine Biology*.

Peck, L. S. 2020. The ecophysiology of responding to change in polar marine benthos. *Life in Extreme Environments: Insights in Biological Capability*, 184.

Peck, L. S., Webb, K. E., & Bailey, D. M. 2004. Extreme sensitivity of biological function to temperature in Antarctic marine species. *Functional Ecology*, *18*(5), 625-630.

Peris Tamayo, A. M., Devineau, O., Præbel, K., Kahilainen, K. K., & Østbye, K. 2020. A brain and a head for a different habitat: Size variation in four morphs of Arctic charr (Salvelinus alpinus (L.)) in a deep oligotrophic lake. *Ecology and Evolution*, *10*(20), 11335-11351.

Piepenburg, D. 2005. Recent research on Arctic benthos: common notions need to be revised. *Polar Biology*, *28*(10), 733-755.

Pons, J., Bauzà-Ribot, M. M., Jaume, D., & Juan, C. 2014. Next-generation sequencing, phylogenetic signal and comparative mitogenomic analyses in Metacrangonyctidae (Amphipoda: Crustacea). *BMC genomics*, *15*, 1-16.

Ramirez-Reyes, T., Velasco, J. A., Flores-Villela, O., & Piñero, D. 2022. Decoupling in diversification and body size Rates during the Radiation of Phyllodactylus: Evidence suggests minor role of Ecology in shaping phenotypes. Evolutionary Biology, 49(3), 373-387.

Rees, D. J., Dufresne, F., Glemet, H., & Belzile, C. 2007. Amphipod genome sizes: first estimates for Arctic species reveal genomic giants. Genome, 50(2), 151-158.

Renaud, P. E., Sejr, M. K., Bluhm, B. A., Sirenko, B., & Ellingsen, I. H. 2015. The future of Arctic benthos: expansion, invasion, and biodiversity. *Progress in Oceanography*, *139*, 244-257.

Rogers, A. D. 2007. Evolution and biodiversity of Antarctic organisms: a molecular perspective. Philosophical transactions of the royal society B: Biological sciences, 362(1488), 2191-2214.

Romanova, E. V., Aleoshin, V. V., Kamaltynov, R. M., Mikhailov, K. V., Logacheva, M. D., Sirotinina, E. A., Gornov, A.Y., Anikin, A.S., & Sherbakov, D. Y. 2016. Evolution of mitochondrial genomes in Baikalian amphipods. *BMC genomics*, *17*(14), 1016.

Rundell, R. J., & Price, T. D. 2009. Adaptive radiation, nonadaptive radiation, ecological speciation and nonecological speciation. *Trends in Ecology & Evolution*, *24*(7), 394-399.

Rutschmann, S., Matschiner, M., Damerau, M., Muschick, M., Lehmann, M. F., Hanel, R., & Salzburger, W. 2011. Parallel ecological diversification in Antarctic notothenioid fishes as evidence for adaptive radiation. *Molecular Ecology*, *20*(22), 4707-4721.

Salabao, L., Plevoets, T., Frédérich, B., Lepoint, G., Kochzius, M., & Schön, I. 2022. Describing novel mitochondrial genomes of Antarctic amphipods. Mitochondrial DNA Part B, 7(5), 810-818.

Saucède, T., Pierrat, B., Danis, B., & David, B. 2014. Biogeographic processes in the Southern Ocean.

Saupe, E. E., & Myers, C. E. 2021. Macroevolution. Evolutionary Developmental Biology: A Reference Guide, 149-167.

Schluter, D. 2000. *The ecology of adaptive radiation*. OUP Oxford.

Sebastian, W., Sukumaran, S., Zacharia, P. U., Muraleedharan, K. R., Dinesh Kumar, P. K., & Gopalakrishnan, A. 2020. Signals of selection in the mitogenome provide insights into adaptation mechanisms in heterogeneous habitats in a widely distributed pelagic fish. *Scientific Reports*, *10*(1), 9081.

Serreze, M. C., & Barry, R. G. 2005. *The Arctic climate system*. Cambridge University Press.

Shao, C., Sun, S., Liu, K., Wang, J., Li, S., Liu, Q., Deagle, B.E., Seim, I., Biscontin, A., Wang, Q., Liu, X., Kawaguchi, S., Liu, Y., Jarman, S., Wang, Y., Wang, H., Huang, G., Hu, J., Feng, B., De Pittà, C., & Fan, G. 2023. The enormous repetitive Antarctic krill genome reveals environmental adaptations and population insights. Cell, 186(6), 1279-1294.

Shin, S. C., Cho, J., Lee, J. K., Ahn, D. H., Lee, H., & Park, H. 2012. Complete mitochondrial genome of the Antarctic amphipod Gondogeneia antarctica (Crustacea, amphipod). *Mitochondrial DNA*, *23*(1), 25-27.

Sirenko, B. I. 2009. Main differences in macrobenthos and benthic communities of the Arctic and Antarctic, as illustrated by comparison of the Laptev and Weddell Sea faunas. Russian Journal of Marine Biology, 35(6), 445-453.

Sokolova, I. M. 2023. Ectotherm mitochondrial economy and responses to global warming. *Acta Physiologica*, *237*(4), e13950.

Somero, G. N. 2010. The physiology of climate change: how potentials for acclimatization and genetic adaptation will determine 'winners' and 'losers'. *Journal of Experimental Biology*, *213*(6), 912-920.

Stier, A., Massemin, S., & Criscuolo, F. 2014. Chronic mitochondrial uncoupling treatment prevents acute cold-induced oxidative stress in birds. *Journal of Comparative Physiology B*, *184*, 1021-1029.

Stroud, J. T., & Losos, J. B. 2016. Ecological opportunity and adaptive radiation. *Annual Review of Ecology, Evolution, and Systematics*, *47*, 507-532.

Sun, S., Wu, Y., Ge, X., Jakovlić, I., Zhu, J., Mahboob, S., Al-Ghanim, K.A., Al-Misned, F., & Fu, H. 2020. Disentangling the interplay of positive and negative selection forces that shaped mitochondrial genomes of Gammarus pisinnus and Gammarus lacustris. *Royal Society open science*, *7*(1), 190669.

Thatje, S., Hillenbrand, C. D., & Larter, R. 2005. On the origin of Antarctic marine benthic community structure. Trends in Ecology & Evolution, 20(10), 534-540.

Thomas, D. N., Fogg, G. E., Convey, P., Fritsen, C. H., Gili, J. M., Gradinger, R., Laybourn-Parry, J., Reid, K. & Walton, D. W.H. 2008. The biology of polar regions. OUP Oxford.

Thornhill, D. J., Mahon, A. R., Norenburg, J. L., & Halanych, K. M. 2008. Open ocean barriers to dispersal: A test case with the Antarctic Polar Front and the ribbon worm Parborlasia corrugatus (Nemertea: Lineidae). Molecular ecology, 17(23), 5104-5117.

Turner, J., & Overland, J. 2009. Contrasting climate change in the two polar regions. *Polar Research*, *28*(2), 146-164.

Turner, J., & Marshall, G. J. 2011. *Climate change in the polar regions*. Cambridge University Press.

Verheye, M.L. 2017. Systematics, phylogeography and historical biogeography of Eusiroidea (Crustacea, Amphipoda) from the Southern Ocean, with a special focus on the families Epimeriidae and Iphimediidae. PhD thesis, Université Catholique de Louvain-la-Neuve.

Vincze, M., Bozóki, T., Herein, M., Borcia, I. D., Harlander, U., Horicsányi, A., Nyerges, A., Rodda, C., Pál, A., & Pálfy, J. 2021. The Drake Passage opening from an experimental fluid dynamics point of view. Scientific reports, 11(1), 1-11.

Wang, C., Zhang, M., Zhou, J., Gao, X., Zhu, S., Yuan, L.,Hou, X., Liu, T., Chen, G., Tang, X., Shan, G., & Hou, J. 2022. Transcriptome analysis and differential gene expression profiling of wucai (Brassica campestris L.) in response to cold stress. BMC genomics, 23(1), 1-16.

Wiens, J. J. 2004. Speciation and ecology revisited: phylogenetic niche conservatism and the origin of species. *Evolution*, *58*(1), 193-197.

Wilke, T., Benke, M., Brändle, M., Albrecht, C., & Bichain, J. M. 2010. The neglected side of the coin: non-adaptive radiations in spring snails (Bythinella spp.). Evolution in action: case studies in adaptive radiation, speciation and the origin of biodiversity, 551-578.

Witt, J. D., Threloff, D. L., & Hebert, P. D. 2006. DNA barcoding reveals extraordinary cryptic diversity in an amphipod genus: implications for desert spring conservation. Molecular ecology, 15(10), 3073-3082.

Yamazaki, N., Ueshima, R., Terrett, J. A., Yokobori, S. I., Kaifu, M., Segawa, R., Kobayashi, T., Numachi, K., Ueda, T., & Nishikawa, K. 1997. Evolution of pulmonate gastropod mitochondrial genomes: comparisons of gene organizations of Euhadra, Cepaea and Albinaria and implications of unusual tRNA secondary structures. Genetics, 145(3), 749-758.

Supplementary Figures

a

Family diagram for Pancrustacean ground pattern

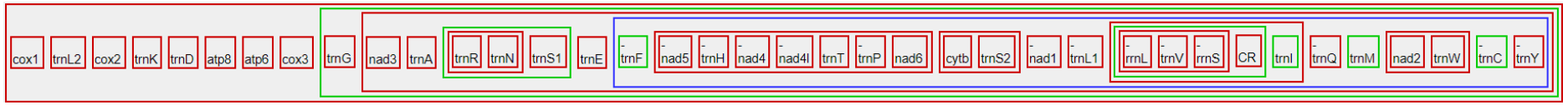

Family diagram for *Eusirus giganteus* (G1) and *Eusirus giganteus* (G2)

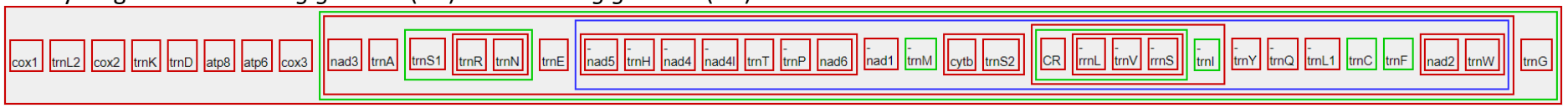

Scenario:

transposition

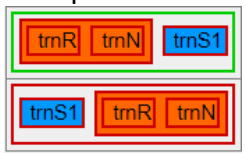

transposition

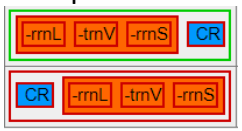

Supplementary Figures

transposition

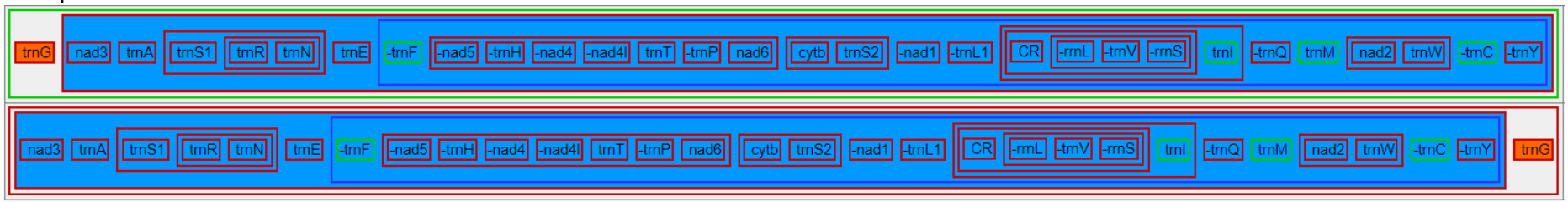

reversal

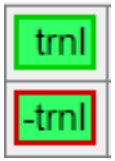

reversal

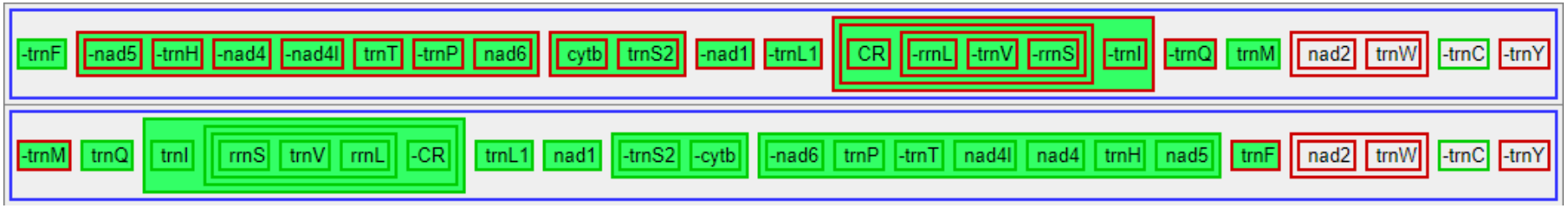

reversal

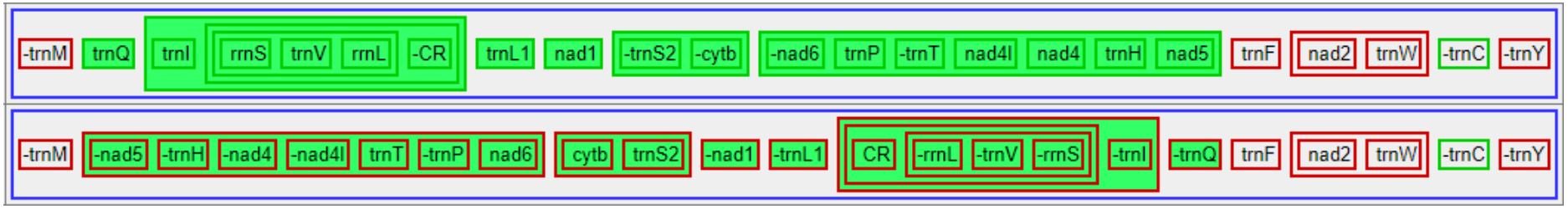

Supplementary Figures

reversal

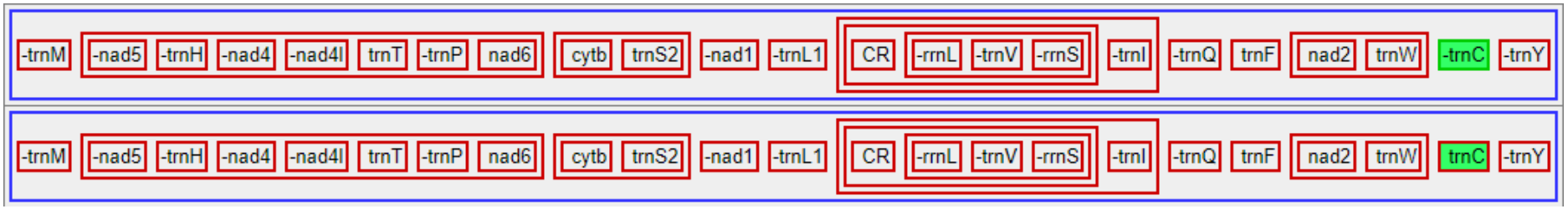

tdrl

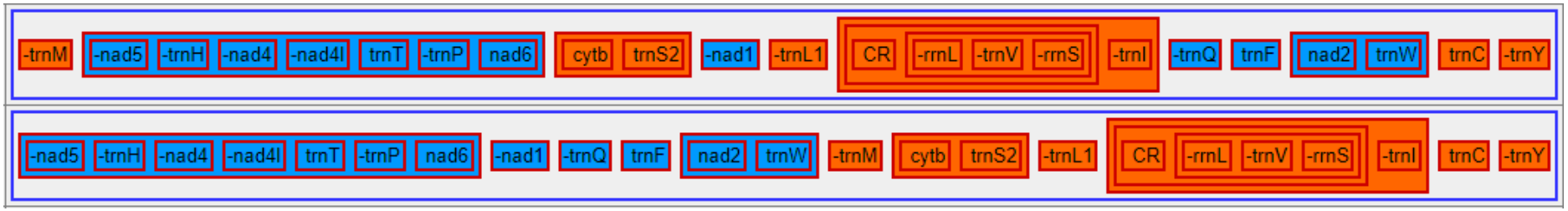

tdrl

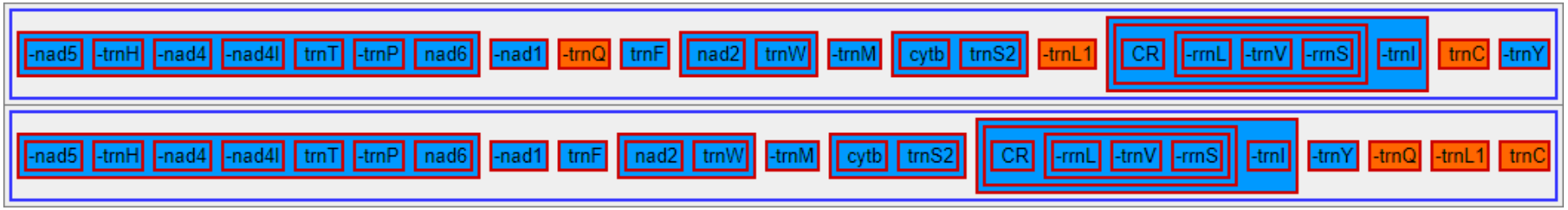

transposition

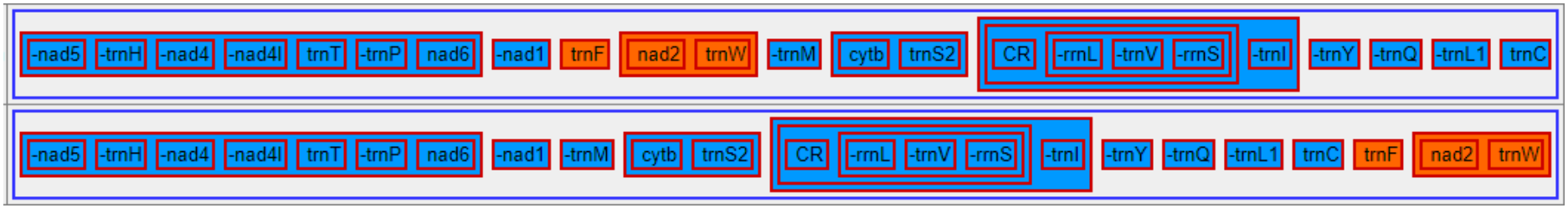

b

Family diagram for Pancrustacean ground pattern

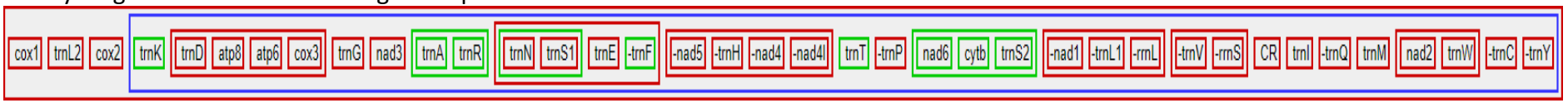

Family diagram for Charcotia amundseni

Scenario:

transposition

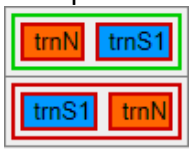

Supplementary Figures

reversal

reversal

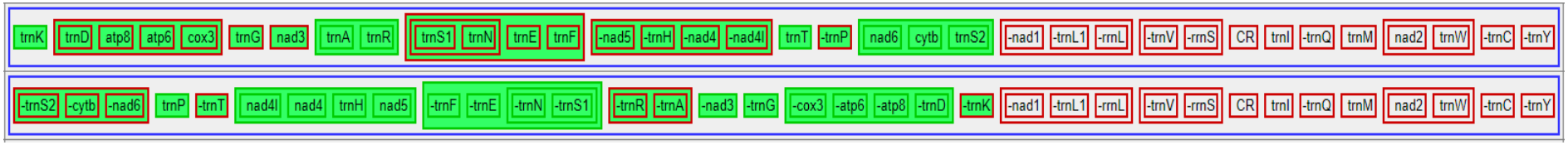

reversal

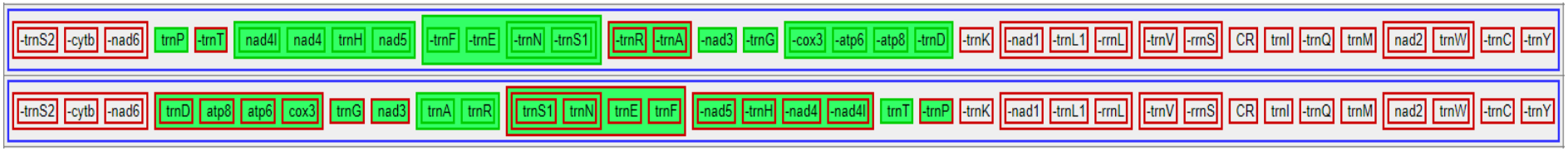

reversal

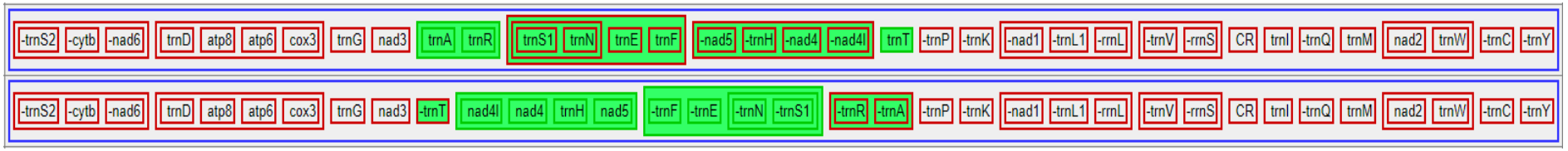

reversal

Supplementary Figures

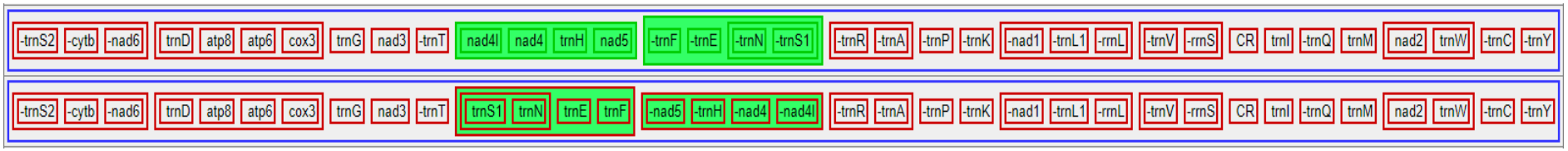

tdrl

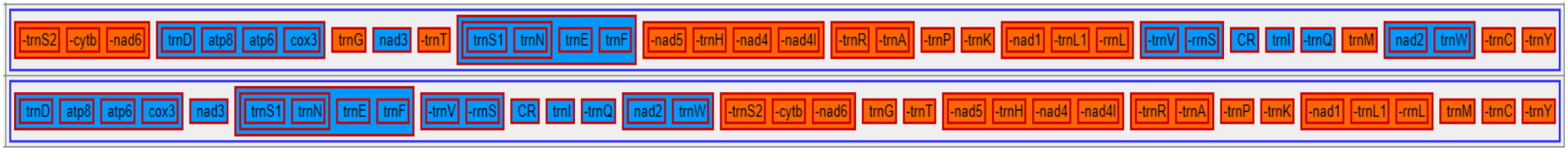

tdrl

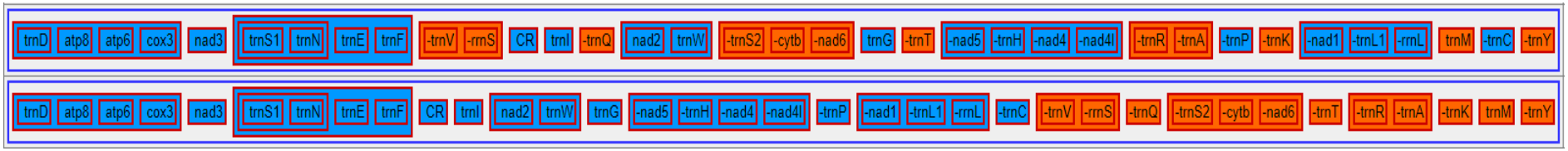

transposition

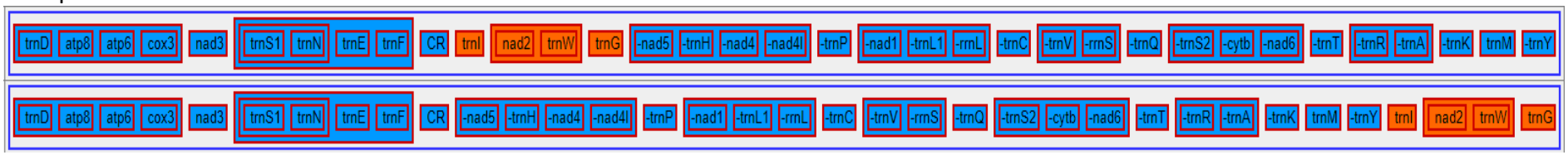

Supplementary figure 1. Overview of the mitochondrial rearrangement scenarios of **a** *Eusirus* cf. *giganteus* (G1 and G2) and **b** *Charcotia amundseni* as deduced by CREx (see discussion for details). Colours indicate which genes undergo rearrangements. The orange color indicates genes with tandem duplications and subsequent random gene loss (tdrl) and transpositions. Blue indicates genes without rearrangements, green indicates gene reversals.

a

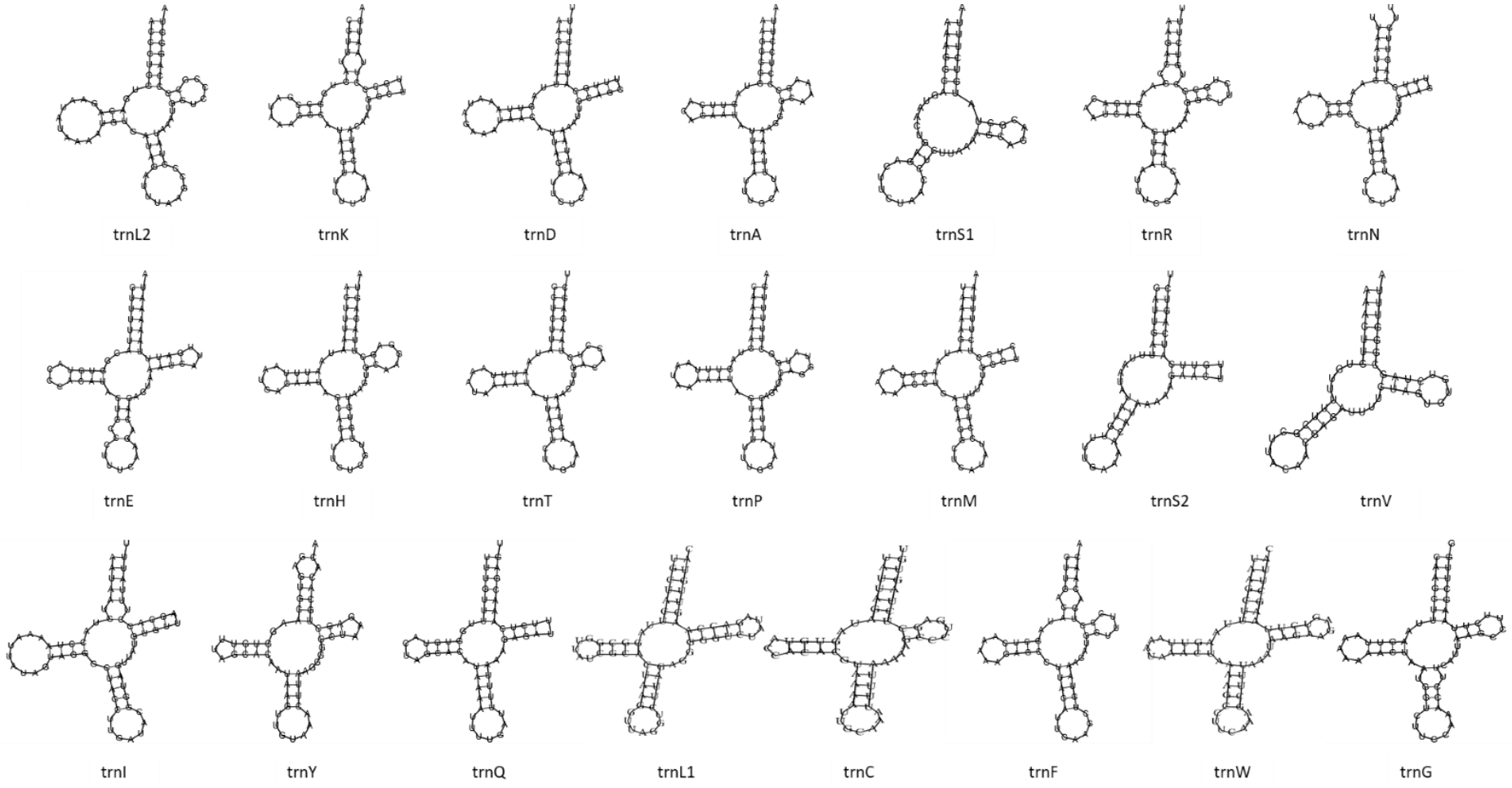
trnL2
trnK
trnD
trnA
trnS1
trnR
trnN
trnE
trnH
trnT
trnP
trnM
trnS2
trnV
trnI
trnY
trnQ
trnL1
trnC
trnF
trnW
trnG

b

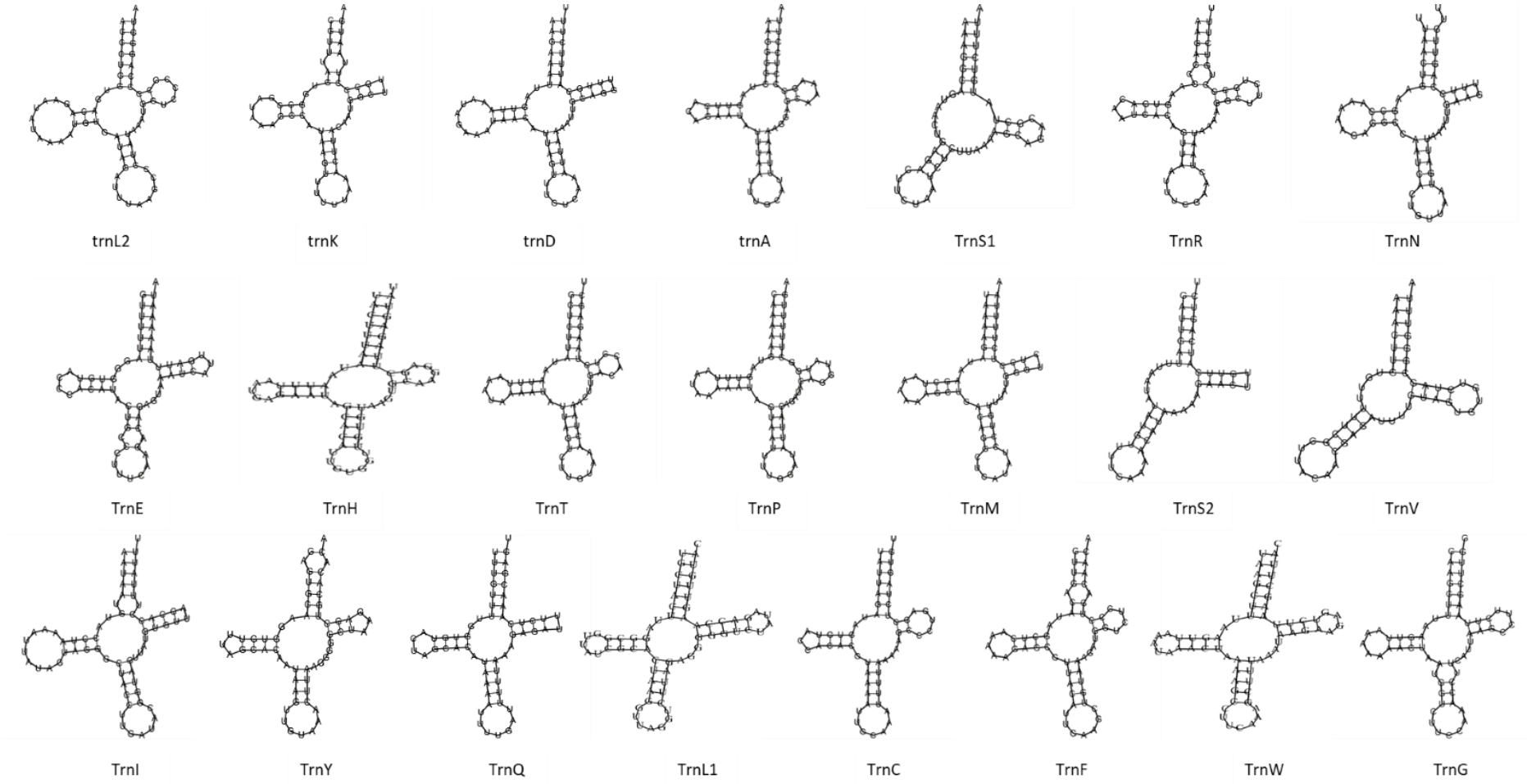
trnL2
trnK
trnD
trnA
TrnS1
TrnR
TrnN
TrnE
TrnH
TrnT
TrnP
TrnM
TrnS2
TrnV
TrnI
TrnY
TrnQ
TrnL1
TrnC
TrnF
TrnW
TrnG

c

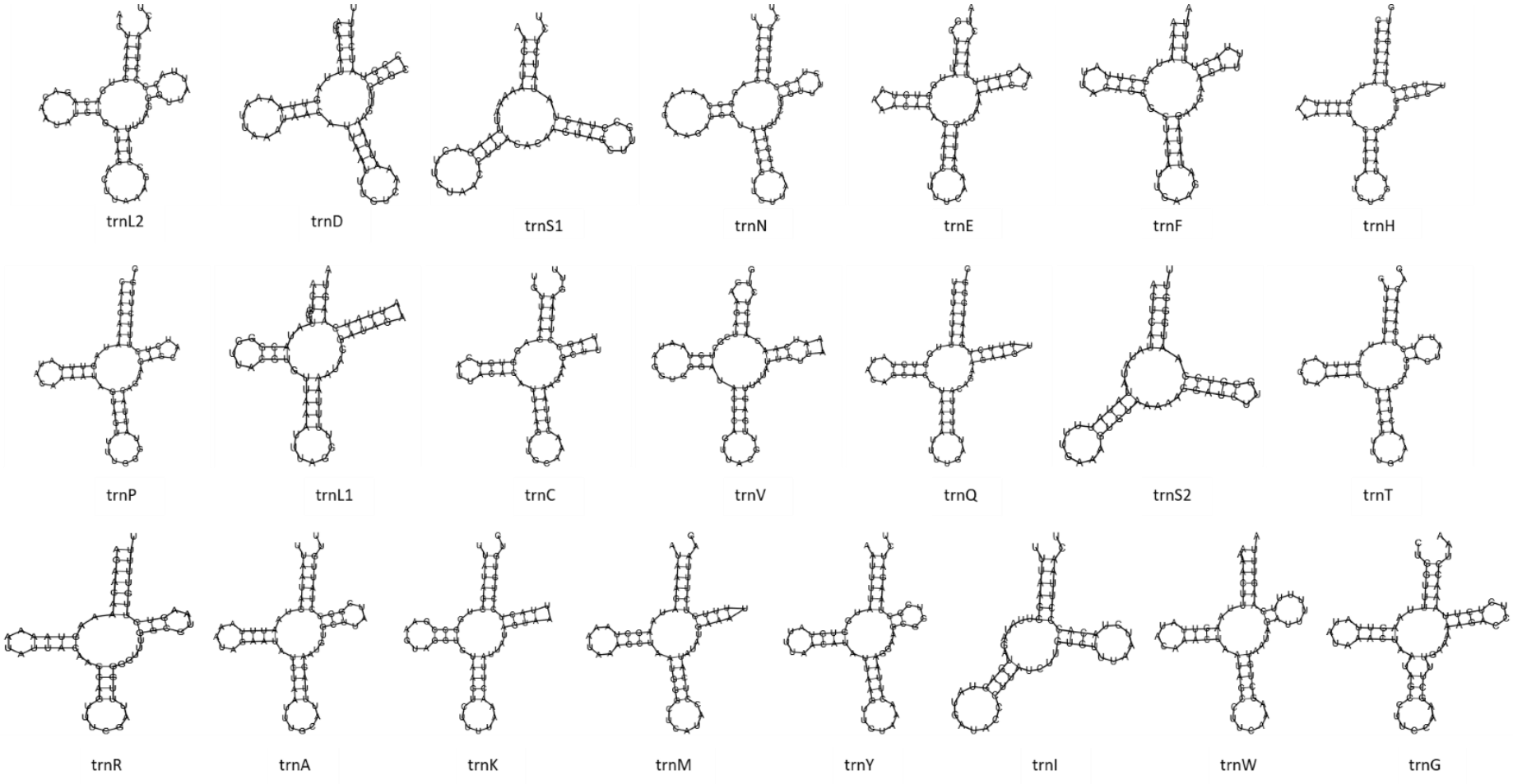

Supplementary figure 2. Putative secondary structures of the 22 tRNAs in **a** Eusirus cf. giganteus (G1) **b** Eusirus cf. giganteus (G2) **c** Charcotia amundseni mitogenomes.

Pancrustacean ground pattern

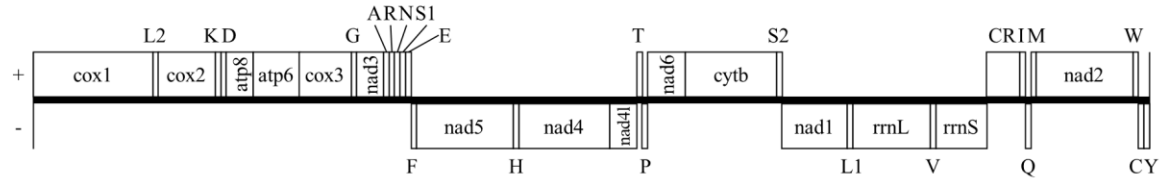

Alicella gigantea

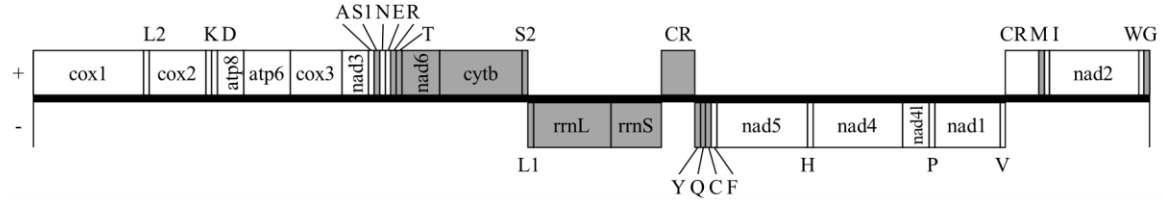

Ampithoe lacertosa

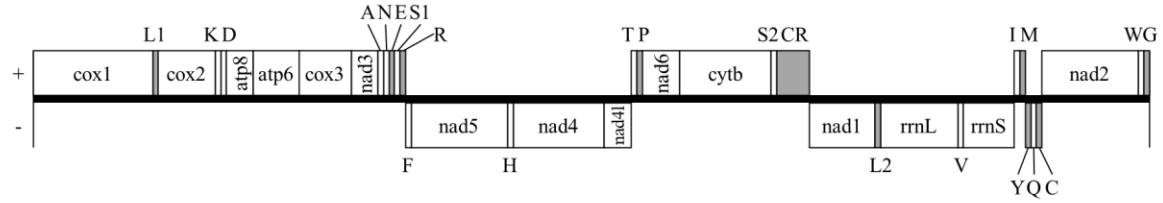

Bahadzia jaraguensis

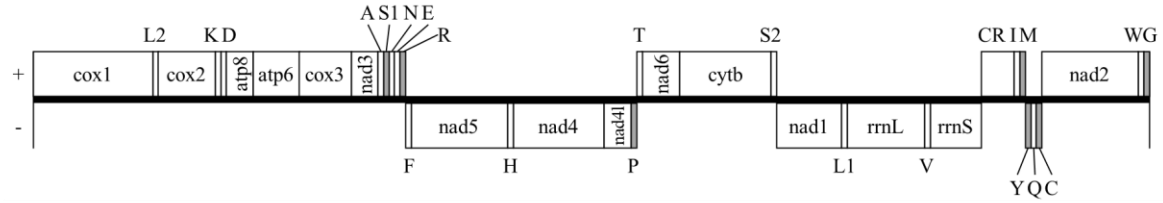

Brachyuropus grewingkii

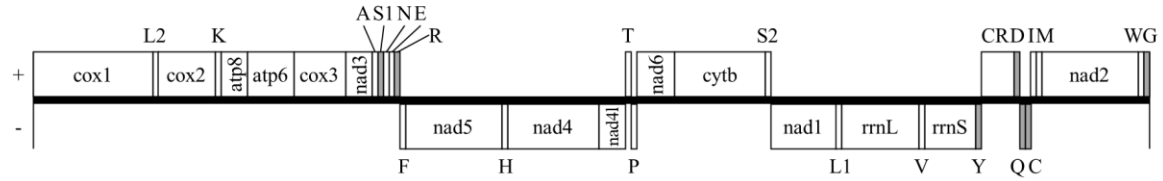

Caprella mutica

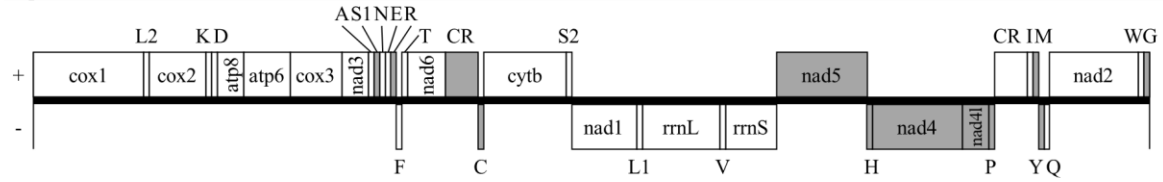

Caprella scaura

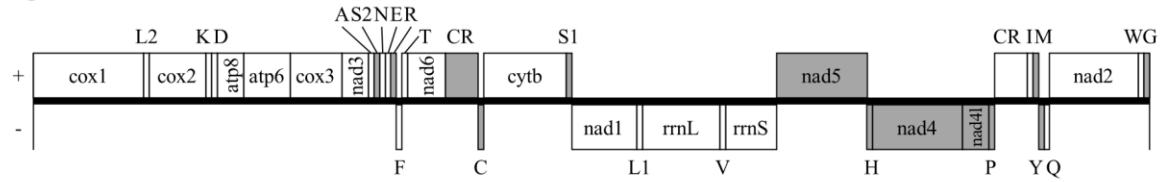

Charcotia amundseni

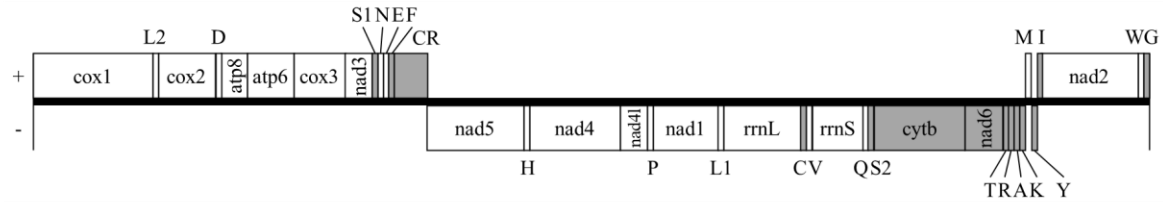

Supplementary Figures

Epimeria cornigera

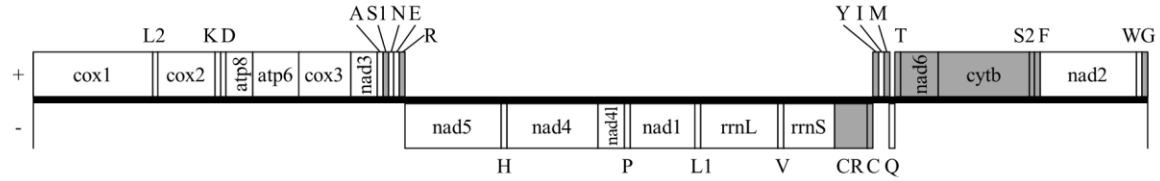

Eulimnogammarus cyaneus, Gammarus duebeni, Gammarus pisinnus, Gammarus lacustris, Gammarus fossarum

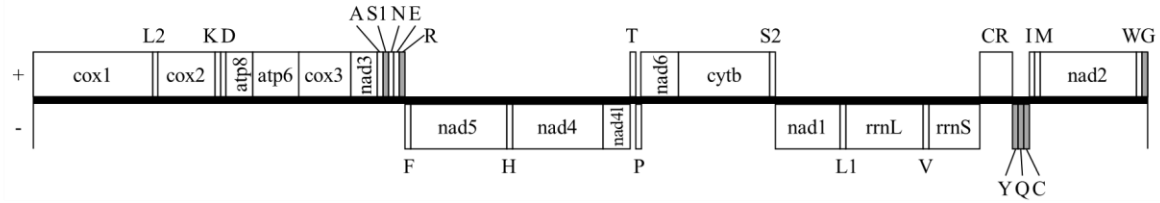

Eulimnogammarus verrucosus

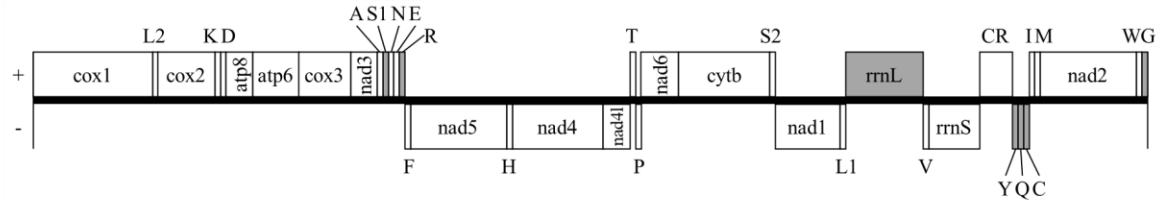

Eulimnogammarus vittatus

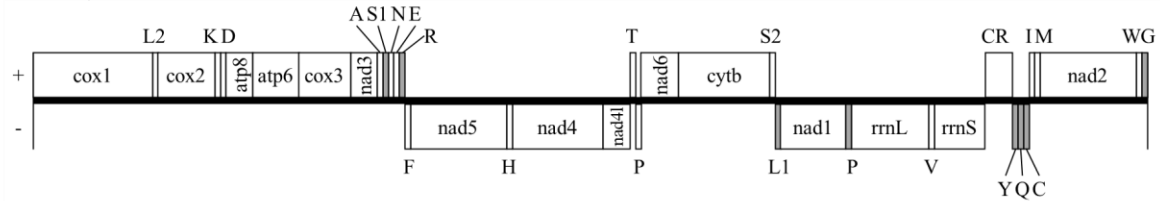

Eurythenes magellanicus

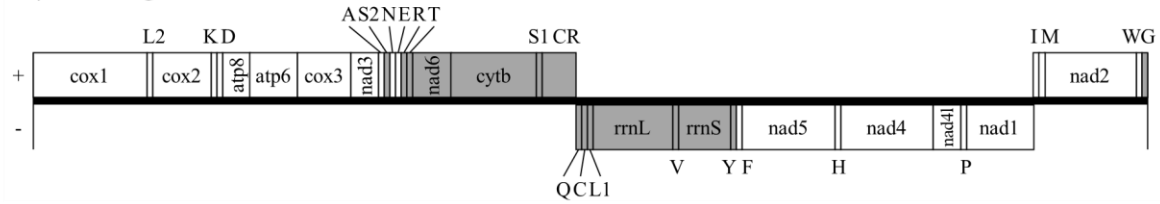

Eusirus cf. *giganteus* G1 and G2

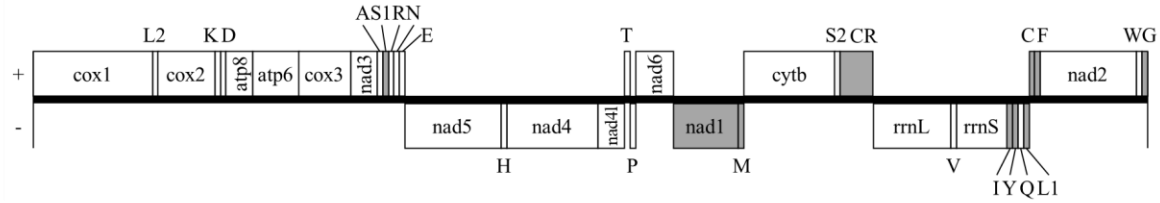

Gammarus roeselii

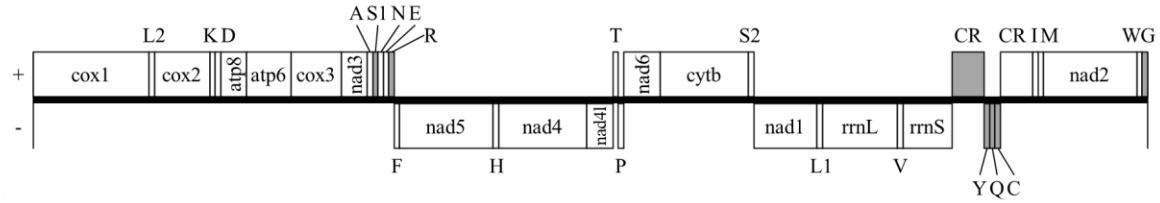

Gmelinoides fasciatus

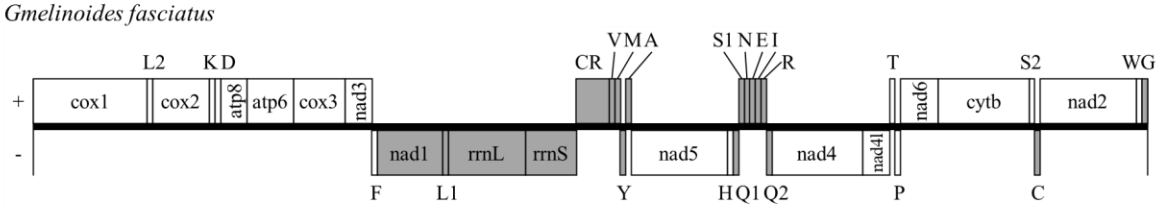

Gondogeneia antarctica

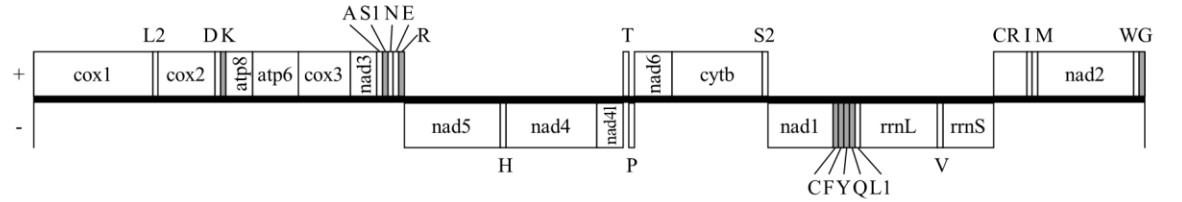

Grandidierella fasciata

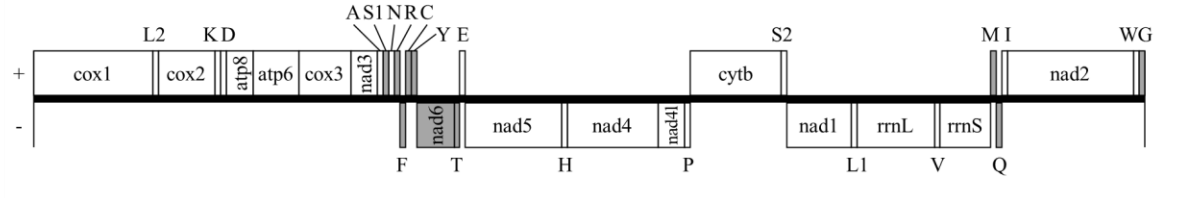

Grandidierella osakaensis

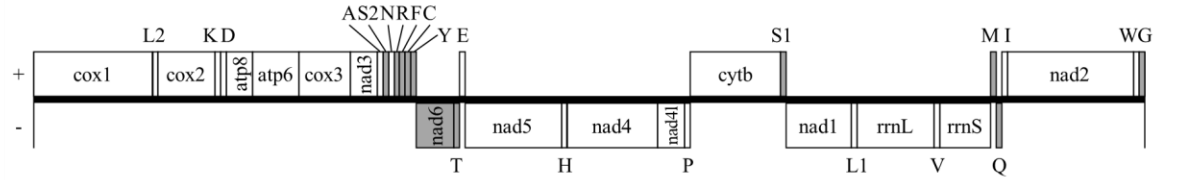

Grandidierella rubroantennata

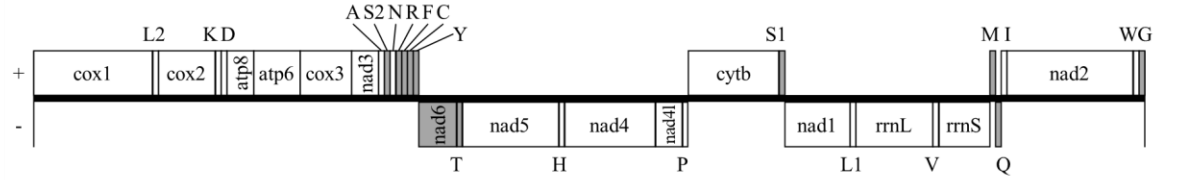

Metacrangonyx repens, *Metacrangonyx spinicaudatus,* "Metacrangonyx boveei', "Metacrangonyx nicoleae tamri"

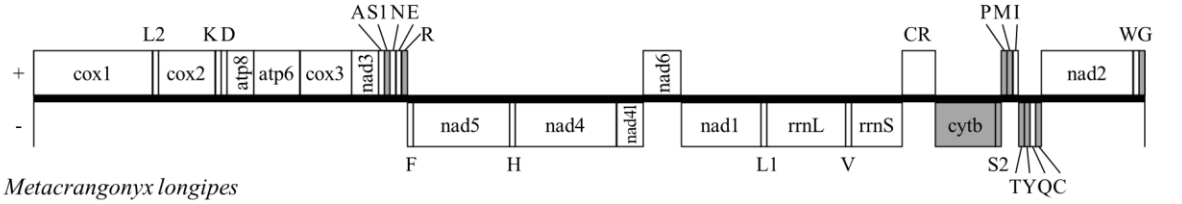

Metacrangonyx longipes

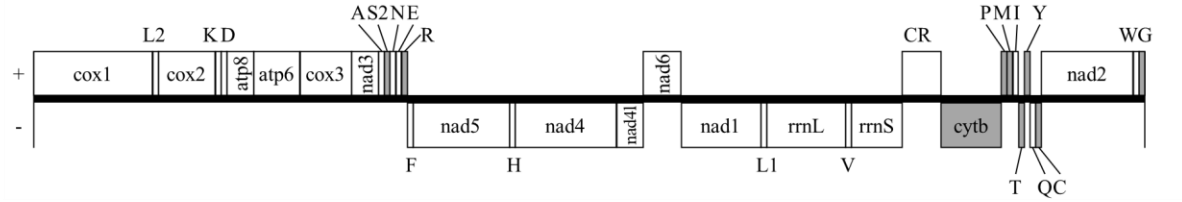

Metacrangonyx panousei , Metacrangonyx dominicanus, Metacrangonyx goulmimensis, Metacrangonyx ilvanus, Metacrangonyx longicaudus, Metacrangonyx remyi, "Metacrangonyx notenboomi"

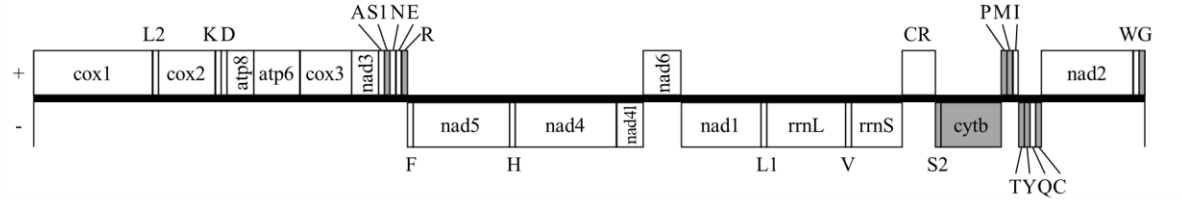

Onisimus nanseni

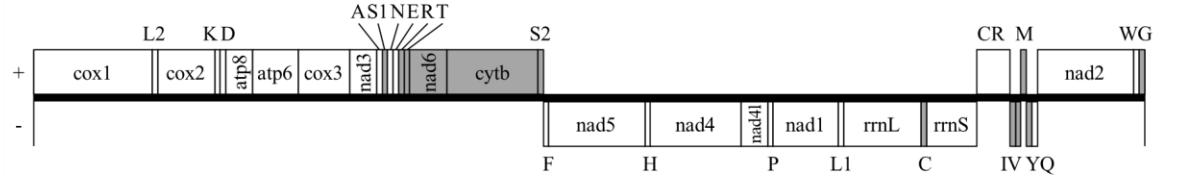

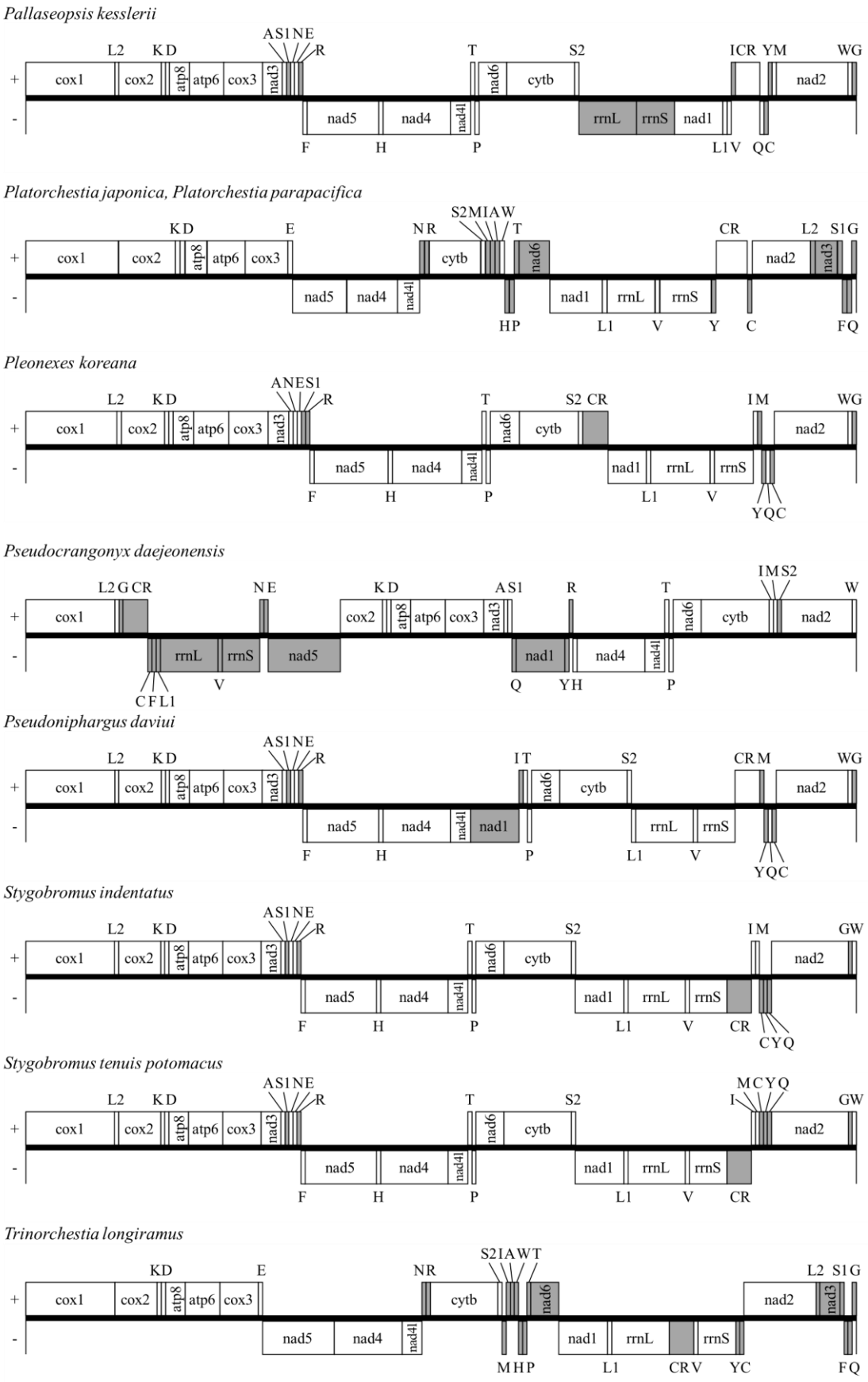

Supplementary figure 3. Gene order of amphipods with complete mitogenomes in comparison to the putative pancrustacean ground pattern (Boore et al., 1998). Grey-colored genes indicate changes of gene order relative to the putative

pancrustacean ground pattern. Genes on the (+) strand are found above the line while genes on the (-) strand are found below the line. Species from the cold regions are indicated in blue while species from the temperate regions are indicated in black. Species names that are not in italics and are in quotes indicate taxa that are not formally described yet as specified by Bauzà-Ribot et al. (2012). Control region is indicated by CR. tRNA genes are labeled using their single-letter amino acid code: G - Glycine, P - Proline, A - Alanine, V - Valine, L1 - Leucine1, L2 - Leucine2 , I - Isoleucine, M - Methionine, C - Cysteine, F - Phenylalanine, Y - Tyrosine, W - Tryptophan, H - Histidine, K - Lysine, R - Arginine, Q - Glutamine, N - Asparagine, E - Glutamic Acid, D - Aspartic Acid, S1 - Serine 1, S2 - Serine2, T - Threonine.

	Pgp	Ag	Al	Bj	Bg	Cm	Cs	Ca	Ec	Ec	Ev	Ev	Em	EgG	EgG	Gd	Gf	Gl	Gp	Gr	Gf	Ga	Gf	Go	Gr	Mb	Md	Mg	Mi	Ml	Ml	Mnt	Mn	Mp	Mr	Mr	Ms	On	Pk	Pj	Pp	Pk	Pd	Pd	Si	Stp	Tl
Pancrustacean ground pattern	1400	118	216	462	342	152	110	58	144	464	464	392	116	150	150	464	464	464	464	426	140	208	198	154	162	190	192	192	192	192	144	190	192	192	192	190	190	170	362	70	70	342	100	212	456	456	68
Alicella gigantea	118	1326	158	354	174	332	212	142	348	380	380	392	322	258	258	380	380	380	380	380	176	332	296	232	234	334	334	334	334	334	214	334	334	334	334	334	334	508	334	54	54	276	114	348	304	304	54
Ampithoe lacertosa	216	158	1400	462	302	182	116	60	156	458	458	420	116	168	168	458	458	458	458	534	124	188	108	102	110	296	298	298	298	298	176	296	298	298	298	296	296	180	450	60	60	734	124	324	464	464	56
Bahadzia jaraguensis	462	354	462	1400	564	414	244	108	396	1062	1062	998	236	314	314	1062	1062	1062	1062	998	236	390	302	222	232	684	686	686	686	686	356	684	686	686	686	684	684	522	822	76	76	892	146	732	1124	1124	72
Brachyuropus grewingkii	342	174	302	564	1400	198	118	82	164	730	730	638	156	148	148	730	730	730	730	728	120	260	150	106	118	260	260	260	260	260	152	260	260	260	260	260	260	236	454	64	64	352	102	268	596	596	42
Caprella mutica	152	332	182	414	198	1326	812	100	356	396	396	388	220	264	264	396	396	396	396	396	184	308	304	222	226	380	382	382	382	382	228	380	382	382	382	380	380	446	362	70	70	338	120	370	434	434	70
Caprella scaura	110	212	116	244	118	812	1326	94	234	226	226	222	340	202	202	226	226	226	226	226	174	188	222	304	368	228	228	228	228	228	378	228	228	228	228	228	228	302	208	68	68	226	102	220	254	254	68
Charcotia amundseni	58	142	60	108	82	100	94	1400	142	90	90	94	114	78	78	90	90	90	90	98	82	92	106	102	102	86	86	86	86	86	80	86	86	86	86	86	86	158	86	30	30	92	44	88	80	80	30
Epimeria cornigera	144	348	156	396	164	356	234	142	1400	376	376	372	234	432	432	376	376	376	376	364	186	446	286	226	228	362	362	362	362	362	242	362	362	362	362	362	362	418	340	84	84	300	124	350	360	360	76
Eulimnogammarus cyaneus	464	380	458	1062	730	396	226	90	376	1400	1400	1256	280	312	312	1400	1400	1400	1400	1326	218	454	292	212	224	548	550	550	550	550	272	548	550	550	550	548	548	490	876	84	84	732	156	548	1062	1062	76
Eulimnogammarus verrucosus	464	380	458	1062	730	396	226	90	376	1400	1400	1256	280	312	312	1400	1400	1400	1400	1326	218	454	292	212	224	548	550	550	550	550	272	548	550	550	550	548	548	490	876	84	84	732	156	548	1062	1062	76
Eulimnogammarus vittatus	392	392	420	998	638	388	222	94	372	1256	1256	1326	276	296	296	1256	1256	1256	1256	1186	202	410	284	208	218	538	540	540	540	540	264	538	540	540	540	538	538	456	818	74	74	674	138	540	938	938	68
Eurythenes magellanicus	116	322	116	236	156	220	340	114	234	280	280	276	1400	204	204	280	280	280	280	288	162	246	212	272	304	220	220	220	220	220	340	220	220	220	220	220	220	288	240	68	68	218	104	222	196	196	56
Eusirus giganteus G1	150	258	168	314	148	264	202	78	432	312	312	296	204	1400	1400	312	312	312	312	310	184	490	278	214	206	290	294	294	294	294	206	290	294	294	294	290	290	256	300	66	66	306	144	290	284	284	68
Eusirus giganteus G2	150	258	168	314	148	264	202	78	432	312	312	296	204	1400	1400	312	312	312	312	310	184	490	278	214	206	290	294	294	294	294	206	290	294	294	294	290	290	256	300	66	66	306	144	290	284	284	68
Gammarus duebeni	464	380	458	1062	730	396	226	90	376	1400	1400	1256	280	312	312	1400	1400	1400	1400	1326	218	454	292	212	224	548	550	550	550	550	272	548	550	550	550	548	548	490	876	84	84	732	156	548	1062	1062	76
Gammarus fossarum	464	380	458	1062	730	396	226	90	376	1400	1400	1256	280	312	312	1400	1400	1400	1400	1326	218	454	292	212	224	548	550	550	550	550	272	548	550	550	550	548	548	490	876	84	84	732	156	548	1062	1062	76
Gammarus lacustris	464	380	458	1062	730	396	226	90	376	1400	1400	1256	280	312	312	1400	1400	1400	1400	1326	218	454	292	212	224	548	550	550	550	550	272	548	550	550	550	548	548	490	876	84	84	732	156	548	1062	1062	76
Gammarus pisinnus	464	380	458	1062	730	396	226	90	376	1400	1400	1256	280	312	312	1400	1400	1400	1400	1326	218	454	292	212	224	548	550	550	550	550	272	548	550	550	550	548	548	490	876	84	84	732	156	548	1062	1062	76
Gammarus roeselii	426	380	534	998	728	396	226	98	364	1326	1326	1186	288	310	310	1326	1326	1326	1326	1326	216	446	292	212	224	538	540	540	540	540	262	538	540	540	540	538	538	488	876	82	82	938	156	540	998	998	82
Gmelinoides fasciatus	140	176	124	236	120	184	174	82	186	218	218	202	162	184	184	218	218	218	218	216	1326	190	182	178	178	206	206	206	206	206	200	206	206	206	206	206	206	182	210	58	58	236	98	232	196	196	68
Gondogeneia antarctica	208	332	188	390	260	308	188	92	446	454	454	410	246	490	490	454	454	454	454	446	190	1400	274	210	220	308	308	308	308	308	196	308	308	308	308	308	308	302	378	54	54	300	142	324	374	374	52
Grandidierella fasciata	198	296	108	302	150	304	222	106	286	292	292	284	212	278	278	292	292	292	292	292	182	274	1326	644	618	280	284	284	284	284	214	280	284	284	284	280	280	266	264	74	74	234	120	272	266	266	74
Grandidierella osakaensis	154	232	102	222	106	222	304	102	226	212	212	208	272	214	214	212	212	212	212	212	178	210	644	1326	1254	212	214	214	214	214	278	212	214	214	214	212	212	206	200	72	72	212	102	212	190	190	72
Grandidierella rubroantennata	162	234	110	232	118	226	368	102	228	224	224	218	304	206	206	224	224	224	224	224	178	220	618	1254	1254	216	218	218	218	218	344	216	218	218	218	216	216	208	212	70	70	220	100	216	202	202	70
Metacrangonyx boveei	190	334	296	684	260	380	228	86	362	548	548	538	220	290	290	548	548	548	548	538	206	308	280	212	216	1400	1328	1328	1328	1328	656	1400	1328	1328	1328	1400	1400	334	512	80	80	588	120	672	550	550	74
Metacrangonyx dominicanus	192	334	298	686	260	382	228	86	362	550	550	540	220	294	294	550	550	550	550	540	206	308	284	214	218	1328	1400	1400	1400	1400	668	1328	1400	1400	1400	1328	1328	334	512	80	80	592	120	674	552	552	74
Metacrangonyx goulmimensis	192	334	298	686	260	382	228	86	362	550	550	540	220	294	294	550	550	550	550	540	206	308	284	214	218	1328	1400	1400	1400	1400	668	1328	1400	1400	1400	1328	1328	334	512	80	80	592	120	674	552	552	74
Metacrangonyx ilvanus	192	334	298	686	260	382	228	86	362	550	550	540	220	294	294	550	550	550	550	540	206	308	284	214	218	1328	1400	1400	1400	1400	668	1328	1400	1400	1400	1328	1328	334	512	80	80	592	120	674	552	552	74
Metacrangonyx longicaudus	192	334	298	686	260	382	228	86	362	550	550	540	220	294	294	550	550	550	550	540	206	308	284	214	218	1328	1400	1400	1400	1400	668	1328	1400	1400	1400	1328	1328	334	512	80	80	592	120	674	552	552	74
Metacrangonyx longipes	144	214	176	356	152	228	378	80	242	272	272	264	340	206	206	272	272	272	272	262	200	196	214	278	344	656	668	668	668	668	1326	656	668	668	668	656	656	214	242	78	78	348	102	346	272	272	72
Metacrangonyx nicoleae tamri	190	334	296	684	260	380	228	86	362	548	548	538	220	290	290	548	548	548	548	538	206	308	280	212	216	1400	1328	1328	1328	1328	656	1400	1328	1328	1328	1400	1400	334	512	80	80	588	120	672	550	550	74
Metacrangonyx notenboomi	192	334	298	686	260	382	228	86	362	550	550	540	220	294	294	550	550	550	550	540	206	308	284	214	218	1328	1400	1400	1400	1400	668	1328	1400	1400	1400	1328	1328	334	512	80	80	592	120	674	552	552	74
Metacrangonyx panousei	192	334	298	686	260	382	228	86	362	550	550	540	220	294	294	550	550	550	550	540	206	308	284	214	218	1328	1400	1400	1400	1400	668	1328	1400	1400	1400	1328	1328	334	512	80	80	592	120	674	552	552	74
Metacrangonyx remyi	192	334	298	686	260	382	228	86	362	550	550	540	220	294	294	550	550	550	550	540	206	308	284	214	218	1328	1400	1400	1400	1400	668	1328	1400	1400	1400	1328	1328	334	512	80	80	592	120	674	552	552	74
Metacrangonyx repens	190	334	296	684	260	380	228	86	362	548	548	538	220	290	290	548	548	548	548	538	206	308	280	212	216	1400	1328	1328	1328	1328	656	1400	1328	1328	1328	1400	1400	334	512	80	80	588	120	672	550	550	74
Metacrangonyx spinicaudatus	190	334	296	684	260	380	228	86	362	548	548	538	220	290	290	548	548	548	548	538	206	308	280	212	216	1400	1328	1328	1328	1328	656	1400	1328	1328	1328	1400	1400	334	512	80	80	588	120	672	550	550	74
Onisimus nanseni	170	508	180	522	236	446	302	158	418	490	490	456	288	256	256	490	490	490	490	488	182	302	266	206	208	334	334	334	334	334	214	334	334	334	334	334	334	1400	376	54	54	312	110	338	542	542	54
Pallaseopsis kesslerii	362	334	450	822	454	362	208	86	340	876	876	818	240	300	300	876	876	876	876	876	210	378	264	200	212	512	512	512	512	512	242	512	512	512	512	512	512	376	1400	54	54	716	142	624	822	822	54
Platorchestia japonica	70	54	60	76	64	70	68	30	84	84	84	74	68	66	66	84	84	84	84	82	58	54	74	72	70	80	80	80	80	80	78	80	80	80	80	80	80	54	54	1400	1400	74	72	64	70	70	1192
Platorchestia parapacifica	70	54	60	76	64	70	68	30	84	84	84	74	68	66	66	84	84	84	84	82	58	54	74	72	70	80	80	80	80	80	78	80	80	80	80	80	80	54	54	1400	1400	74	72	64	70	70	1192
Pleonexes koreana	342	276	734	892	352	338	226	92	300	732	732	674	218	306	306	732	732	732	732	938	236	300	234	212	220	588	592	592	592	592	348	588	592	592	592	588	588	312	716	74	74	1400	138	632	782	782	68
Pseudocrangonyx daejeonensis	100	114	124	146	102	120	102	44	124	156	156	138	104	144	144	156	156	156	156	98	142	120	102	100	120	120	120	120	120	120	102	120	120	120	120	120	120	110	142	72	72	138	1400	132	156	156	62
Pseudoniphargus daviui	212	348	324	732	268	370	220	88	350	548	548	540	222	290	290	548	548	548	548	540	232	324	272	212	216	672	674	674	674	674	346	672	674	674	674	672	672	338	624	64	64	632	132	1400	594	594	62
Stygobromus indentatus	456	304	464	1124	596	434	254	80	360	1062	1062	938	196	284	284	1062	1062	1062	1062	998	196	374	266	190	202	550	552	552	552	552	272	550	552	552	552	550	550	542	822	70	70	782	156	594	1400	1400	68
Stygobromus tenuis potomacus	456	304	464	1124	596	434	254	80	360	1062	1062	938	196	284	284	1062	1062	1062	1062	998	196	374	266	190	202	550	552	552	552	552	272	550	552	552	552	550	550	542	822	70	70	782	156	594	1400	1400	68
Trinorchestia longiramus	68	54	56	72	42	70	68	30	76	76	76	68	56	68	68	76	76	76	76	82	68	52	74	72	70	74	74	74	74	74	72	74	74	74	74	74	74	54	54	1192	1192	68	62	62	68	68	1400

Supplementary figure 4. Common interval matrix values inferred using gene orders of the analysed amphipod mitogenomes. A high number of common intervals or bright colour means similar gene orders while a high number of breakpoints or reversals, or dark colours, mean dissimilar gene orders. Identical gene orders result to a value of 1,400. The characters found in the on the header represent the first characters of the amphipod species names found in the first column.

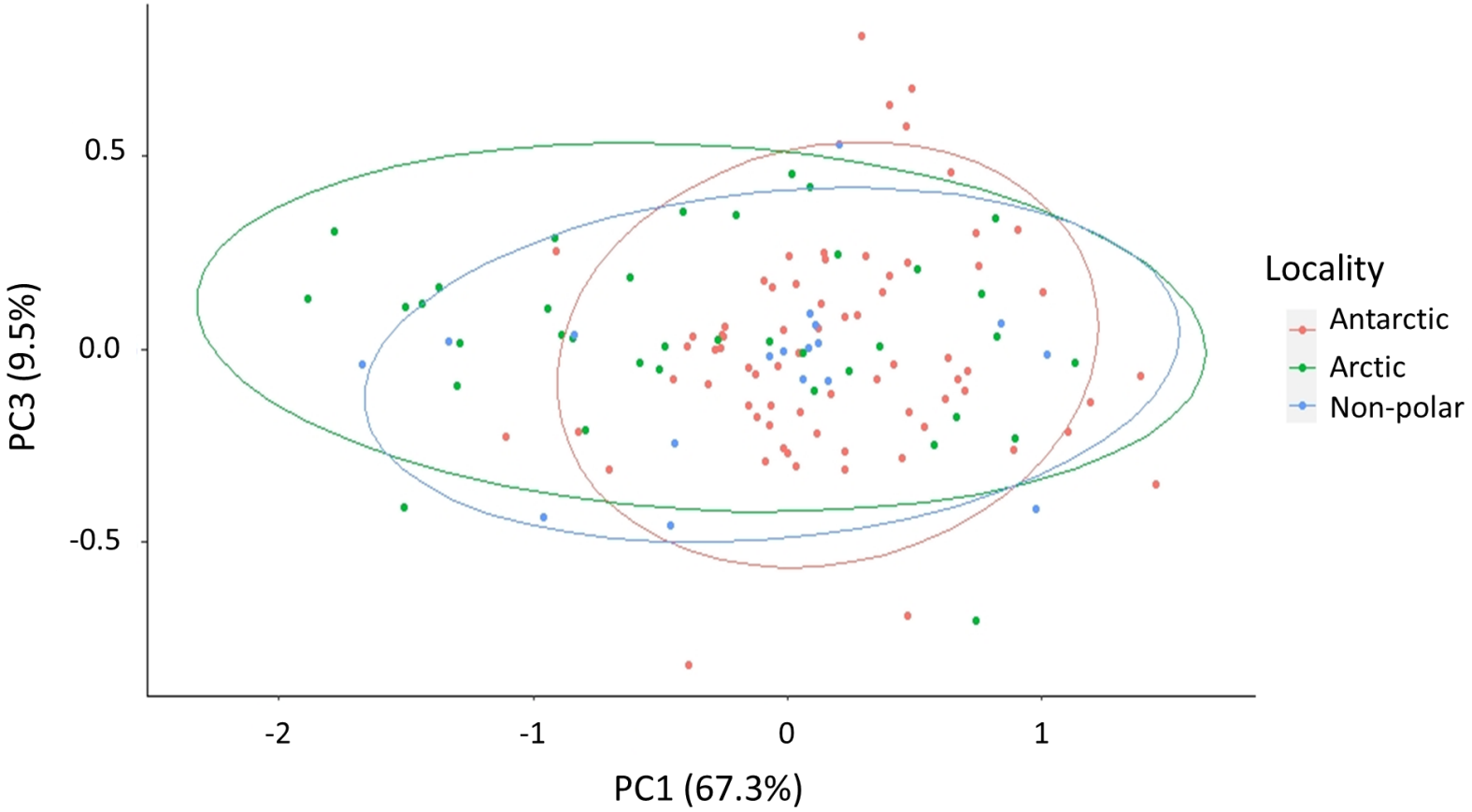

Supplementary figure 5. Principal component analysis (PCA) performed on the "9sp dataset morpho" showing PC1 and PC3. The three localities are indicated in colours with red for the Antarctic, green for the Arctic, and blue for the Non-polar.

Supplementary Tables

Supplementary table 1. List of amphipod species species analysed for their AT and GC skew of mitogenomes. Target species of the current study are indicated in bold.

Species	Family	Genbank No.	Publication
Eusirus* cf. *giganteus (G1)	**Eusiridae**	**OK489458**	**This study**
Eusirus* cf. *giganteus (G2)	**Eusiridae**	**OK489459**	**This study**
Charcotia amundseni	**Lysianassidae**	**OK489457**	**This study**
Alicella gigantea	Alicellidae	MK215211	Li et al., 2019
Ampithoe lacertosa	Ampithoidae	MK215645	Lee et al, 2019
Bahadzia jaraguensis	Hadziidae	FR872382	Bauzà et al., 2012
Brachyuropus grewingkii	Acanthogammaridae	KP161875	Romanova et al., 2016
Caprella mutica	Caprellidae	GU130250	Kilpert et al., 2010
Caprella scaura	Caprellidae	AB539699	Ito et al., 2010
Epimeria cornigera	Epimeriidae	MF361127	Beerman, et al, 2018
Eulimnogammarus cyaneus	Eulimnogammaridae	KX341964	Romanova et al., 2016
Eulimnogammarus verrucosus	Eulimnogammaridae	KF690638	Rivarola-Duarte et al., 2014
Eulimnogammarus vittatus	Eulimnogammaridae	KM287572	Romanova et al., 2016
Eurythenes magellanicus	Eurytheneidae	MN688221	Li et al., 2020
Eurythenes maldoror	Eurytheneidae	NC036429	Cheng et al., unpublished
Gammarus duebeni	Gammaridae	NC_017760	Krebes et al., 2012
Gammarus fossarum	Gammaridae	NC_034937	Macher et al., 2017
Gammarus lacustris	Gammaridae	MK354235	Sun et al, 2020
Gammarus pisinnus	Gammaridae	MK354236	Sun et al, 2020
Gammarus roeselii	Gammaridae	MG779536	Cormier et al, 2018
Gmelinoides fasciatus	Micruropodidae	NC_033361	Romanova et al., 2016
Gondogeneia antarctica	Pontogeneiidae	JN827386	Shin et al., 2012
Grandidierella fasciata	Aoridae	LC500464	Hiki et al, 2020

Grandidierella japonica	Aoridae	LC500462	Hiki et al, unpublished
Grandidierella osakaensis	Aoridae	LC546828	Hiki et al., 2020
Grandidierella rubroantennata	Aoridae	LC500463	Hiki et al, 2020
Haploginglymus sp.	Niphargidae	LT594768	Pons et al., unpublished
Hyalella azteca	Hyalellidae	NC_039403	Patra et al., unpublished
Metacrangonyx boveei	Metacrangonyctidae	HE860498	Bauzà-Ribot et al., 2012
Metacrangonyx longipes	Metacrangonyctidae	AM944817	Bauzà-Ribot et al., 2009
Metacrangonyx nicoleae tamri	Metacrangonyctidae	HE860504	Bauzà-Ribot et al., 2012
Metacrangonyx repens	Metacrangonyctidae	HE860495	Bauzà-Ribot et al., 2012
Metacrangonyx spinicaudatus	Metacrangonyctidae	HE860506	Bauzà-Ribot et al., 2012
Onisimus nanseni	Uristidae	FJ555185	Ki et al., 2010
Pallaseopsis kesslerii	Pallaseidae	KX341968	Romanova et al., 2016
Platorchestia japonica	Talitridae	MG010370	Yang et al., 2017
Platorchestia parapacifica	Talitridae	MG010371	Yang et al., 2017
Pleonexes koreana	Ampithoidae	MK265245	Lee et al, 2019
Pseudocrangonyx daejeonensis	Pseudocrangonyctidae	MH229998	Lee et al., 2018
Pseudoniphargus daviui	Pseudoniphargidae	FR872383	Stokkan et al., 2016
Stygobromus indentatus	Crangonyctidae	KU869711	Aunins et al., 2016
Stygobromus tenuis potomacus	Crangonyctidae	KU869712	Aunins et al., 2016
Trinorchestia longiramus	Talitridae	MH542431	Patra et al., 2019

Supplementary table 2. Annotation of the complete mitogenomes of *Eusirus* cf. *giganteus* (G1 and G2) and *Charcotia amundseni*

***Eusirus* cf. *giganteus* (G1)**						
Gene	**Strand**	**From**	**To**	**Length (bp)**	**Start**	**Stop**
cox1	+	1	1537	1537	ATT	T(AA)
trnL2	+	1538	1601	64		
cox2	+	1602	2279	678	ATC	TAA
Intergenic spacer 1		2280	2280	1		
trnK	+	2281	2339	59		
Intergenic spacer 2		2340	2412	73		
trnD	+	2413	2477	65		
atp8	+	2478	2636	159	ATC	TAA
atp6	+	2630	3300	671	ATG	TA(A)
cox3	+	3300	4088	789	ATG	TAA
Intergenic spacer 3		4089	4100	12		
nad3	+	4101	4448	348	ATT	TAA
trnA	+	4447	4504	58		
trnS1	+	4504	4555	52		
Intergenic spacer 4		4556	4559	4		
trnR	+	4560	4619	60		
Intergenic spacer 5		4620	4627	8		
trnN	+	4628	4688	61		
trnE	+	4686	4747	62		
Intergenic spacer 6		4748	4798	51		
nad5	-	4799	6511	1713	ATG	TAA
trnH	-	6512	6572	61		
nad4	-	6573	7878	1306	ATG	T(AA)
Intergenic spacer 8		7879	7883	5		
nad4l	-	7884	8177	294	ATG	TAA
Intergenic spacer 9		8178	8182	5		
trnT	+	8183	8242	60		
trnP	-	8242	8303	62		
Intergenic spacer 10		8304	8305	2		
nad6	+	8306	8881	576	ATG	TAA
nad1	-	8843	9763	921	ATT	TAA
Intergenic spacer 11		9764	9860	97		
trnM	-	9861	9920	60		
Intergenic spacer 12		9921	9933	13		
cytb	+	9934	11067	1134	ATG	TAG

trnS2	+	11067	11118	52		
Intergenic spacer 13		11119	11204	86		
Putative control region		11205	11458	254		
Intergenic spacer 14		11459	12306	848		
rrnL	-	12307	13177	871		
Intergenic spacer 15		13178	13201	24		
trnV	-	13202	13254	53		
rrnS	-	13255	13935	681		
Intergenic spacer 16		13936	13976	41		
trnI	-	13977	14042	66		
Intergenic spacer 17		14043	14051	9		
trnY	-	14052	14110	59		
trnQ	-	14107	14165	59		
Intergenic spacer 18		14166	14189	24		
trnL1	-	14190	14253	64		
Intergenic spacer 19		14254	14280	27		
trnC	+	14281	14339	59		
trnF	+	14338	14397	60		
Intergenic spacer 20		14398	14445	48		
nad2	+	14446	15433	988	ATC	T(AA)
trnW	+	15434	15497	64		
trnG	+	15497	15558	62		

***Eusirus* cf. *giganteus* (G2)**						
Gene	**Strand**	**From**	**To**	**Length (bp)**	**Start**	**Stop**
cox1	+	1	1537	1537	ATT	T(AA)
trnL2	+	1538	1601	64		
cox2	+	1602	2279	678	ATC	TAA
Intergenic spacer 1		2280	2280	1		
trnK	+	2281	2339	59		
Intergenic spacer 2		2340	2412	73		
trnD	+	2413	2477	65		
atp8	+	2478	2636	159	ATC	TAA
atp6	+	2630	3300	671	ATG	TA(A)
cox3	+	3300	4088	789	ATG	TAA
Intergenic spacer 3		4089	4100	12		
nad3	+	4101	4448	348	ATT	TAA
trnA	+	4447	4504	58		
trnS1	+	4504	4555	52		
Intergenic spacer 4		4556	4559	4		

trnR	+	4560	4619	60		
Intergenic spacer 5		4620	4626	7		
trnN	+	4627	4687	61		
trnE	+	4685	4746	62		
Intergenic spacer 6		4747	4797	51		
nad5	-	4798	6507	1710	ATG	TAA
Intergenic spacer 7		6508	6509	2		
trnH	-	6510	6572	63		
nad4	-	6571	7853	1283	ATG	TA(A)
Intergenic spacer 8		7854	7858	5		
nad4l	-	7859	8152	294	ATG	TAA
Intergenic spacer 9		8153	8157	5		
trnT	+	8158	8217	60		
trnP	-	8217	8278	62		
Intergenic spacer 10		8279	8280	2		
nad6	+	8281	8818	538	ATG	T(AA)
nad1	-	8818	9738	921	ATT	TAA
Intergenic spacer 11		9739	9835	97		
trnM	-	9836	9895	60		
Intergenic spacer 12		9896	9908	13		
cytb	+	9909	11042	1134	ATG	TAG
trnS2	+	11042	11093	52		
Intergenic spacer 13		11094	11179	86		
Putative control region		11180	11433	254		
Intergenic spacer 14		11434	12282	849		
rrnL	-	12283	13153	871		
Intergenic spacer 15		13154	13177	24		
trnV	-	13178	13230	53		
rrnS	-	13231	13911	681		
Intergenic spacer 16		13912	13952	41		
trnI	-	13953	14018	66		
Intergenic spacer 17		14019	14027	9		
trnY	-	14028	14086	59		
trnQ	-	14083	14141	59		
Intergenic spacer 18		14142	14165	24		
trnL1	-	14166	14229	64		
Intergenic spacer 19		14230	14256	27		
trnC	+	14257	14315	59		
trnF	+	14314	14373	60		
Intergenic spacer 20		14374	14421	48		

nad2	+	14422	15409	988	ATC	T(AA)
trnW	+	15410	15473	64		
trnG	+	15473	15534	62		

Charcotia amundseni						
Gene	**Strand**	**From**	**To**	**Length (bp)**	**Start**	**Stop**
cox1	+	1	1534	1534	ATA	T(AA)
trnL2	+	1535	1596	62		
cox2	+	1597	2275	679	ATG	T(AA)
trnD	+	2276	2336	61		
Intergenic spacer 2		2337	2338	2		
atp8	+	2339	2497	159	ATA	TAA
atp6	+	2491	3162	672	ATG	TAA
cox3	+	3162	3950	789	ATG	TAA
Intergenic spacer 3		3951	3963	13		
nad3	+	3964	4305	342	ATT	TAA
Intergenic spacer 4		4306	4307	2		
trnS1	+	4308	4362	55		
trnN	+	4362	4428	67		
trnE	+	4426	4485	60		
trnF	+	4485	4538	54		
Intergenic spacer 5		4539	5273	735		
Putative control region		5274	5839	566		
nad5	-	5840	7558	1719	ATG	TAA
trnH	-	7559	7617	59		
nad4	-	7618	8923	1306	ATC	T(AA)
Intergenic spacer 7		8924	8928	5		
nad4l	-	8929	9219	291	ATA	TAG
Intergenic spacer 8		9220	9222	3		
trnP	-	9223	9283	61		
Intergenic spacer 9		9284	9596	313		
nad1	-	9597	10514	918	ATG	TAA
Intergenic spacer 10		10515	10516	2		
trnL1	-	10517	10575	59		
Intergenic spacer 11		10576	10587	12		
rrnL	-	10588	11326	739		
Intergenic spacer 12		11327	11589	263		
trnC	-	11590	11648	59		
trnV	-	11647	11711	65		
rrnS	-	11699	12227	529		

Intergenic spacer 13		12228	12335	108		
trnQ	-	12336	12398	63		
trnS2	-	12397	12449	53		
Intergenic spacer 14		12450	12456	7		
cytb	-	12457	13596	1140	ATG	TAA
nad6	-	13596	14075	480	ATG	TAA
Intergenic spacer 15		14076	14076	1		
trnT	-	14077	14137	61		
trnR	-	14132	14192	61		
Intergenic spacer 16		14193	14194	2		
trnA	-	14195	14256	62		
Intergenic spacer 17		14257	14259	3		
trnK	-	14260	14320	61		
Intergenic spacer 18		14321	14339	19		
trnM	+	14340	14401	62		
trnY	-	14400	14459	60		
trnI	+	14458	14515	58		
nad2	+	14516	15496	981	ATA	TAA
trnW	+	15495	15555	61		
trnG	+	15556	15619	64		

Supplementary table 3. List of species used in this study including information on their sampling locality and expedition, the sample area, station, geographical coordinates and voucher IDs.

Specimen ID code	Species	Locality	Expedition	Area	Station	Latitude	Longitude	Voucher ID
EB14	*Eusirus antarcticus*	Antarctica	JR179	Amundsen Sea	BIO4-EBS-3A-EPI	74°23'54.4"S	104°37'55.7"W	INV.159925
EB5	*Eusirus antarcticus*	Antarctica	JR144 (BIOPEARL I)	Elephant Islands	EI-AGT-4	61°20'02.2"S	55°11'42.3"W	INV. 138482
EF34	*Eusirus antarcticus*	Antarctica	CEAMARC	Adelie Coast	87 (lot 3532)	65°30'22.7"S	139°21'31.5"E	No voucher
EE39	*Eusirus antarcticus*	Antarctica	CEAMARC	Adelie Coast	87 (lot 3532)	65°30'22.7"S	139°21'31.5"E	No voucher
EB6	*Eusirus bouvieri* 2	Antarctica	JR144 (BIOPEARL I)	Elephant Islands	EI-AGT-4	61°20'02.2"S	55°11'42.3"W	INV.159926
EF21	*Eusirus bouvieri* 1	Antarctica	CEAMARC	Adelie Coast	13A (lot 2969)	66°08'53.8"S	140°38'59.7"E	No voucher
EB2	*Eusirus bouvieri* 2	Antarctica	JR144 (BIOPEARL I)	Elephant Islands	EI-AGT-4	61°20'02.2"S	55°11'42.3"W	INV.159927
EF22	*Eusirus bouvieri* 1	Antarctica	CEAMARC	Adelie Coast	13A (lot 2969)	66°08'53.8"S	140°38'59.7"E	No voucher
EF29	*Eusirus bouvieri* 1	Antarctica	CEAMARC	Adelie Coast	11 (lot 2519)	66°33'42.5"S	141°15'43.0"E	No voucher
EE19	*Eusirus bouvieri* 2	Antarctica	CEAMARC	Adelie Coast	04 (lot 631)	66°18'59.0"S	142°00'01.3"E	No voucher
EB3	*Eusirus bouvieri* 2	Antarctica	JR144 (BIOPEARL I)	Elephant Islands	EI-AGT-4	61°20'02.2"S	55°11'42.3"W	INV.159928
EF26	*Eusirus bouvieri* 1	Antarctica	CEAMARC	Adelie Coast	11 (lot 2519)	66°33'42.5"S	141°15'43.0"E	No voucher
EUP1	*Eusirus* cf. *bouvieri*	Antarctica	PS118	Weddel Sea	12_10	63°50'14.8"S	55°35'09.7"W	INV.159949
EB01	*Eusirus sp.* 1	Antarctica	JR179	Amundsen Sea	BIO6-EBS-3D-EPI	71°20'56.2"S	109°57'53.2"W	INV.159929
EB20	*Eusirus sp.* 1	Antarctica	JR179	Amundsen Sea	BIO4-EBS-3D-EPI	74°23'27.2"S	104°46'02.1"W	INV.159930
EB17	*Eusirus sp.* juvenile	Antarctica	JR179	Amundsen Sea	BIO4-EBS-3A-EPI	74°23'54.4"S	104°37'55.7"W	INV.159931
EB18	*Eusirus sp.* 8 juvenile	Antarctica	JR179	Amundsen Sea	BIO4-EBS-3A-EPI	74°23'54.4"S	104°37'55.7"W	INV.159932
EB15	*Eusirus sp.* 1	Antarctica	JR179	Amundsen Sea	BIO4-EBS-3A-EPI	74°23'54.4"S	104°37'55.7"W	INV.159933
EB16	*Eusirus sp.* 1	Antarctica	JR179	Amundsen Sea	BIO4-EBS-3A-EPI	74°23'54.4"S	104°37'55.7"W	INV.159934
ED10	*Eusirus sp.* 2	Antarctica	ANT-XXII-3 (ANDEEP III)	North of Bouvet Island	21–7	47°38'43.8"S	4°15'12.0"E	INV.159935
PS1	*Eusirus* cf. *giganteus*	Antarctica	PS118	Weddel Sea	9_5	64°01'13.9"S	55°54'27.0"W	INV.159936
PS2	*Eusirus* cf. *giganteus*	Antarctica	PS118	Weddel Sea	12_10	63°50'14.8"S	55°35'09.7"W	INV.159937
PS3	*Eusirus* cf. *giganteus*	Antarctica	PS118	Weddel Sea	12_10	63°50'14.8"S	55°35'09.7"W	INV.159938
PS4	*Eusirus* cf. *giganteus*	Antarctica	PS118	Weddel Sea	12_10	63°50'14.8"S	55°35'09.7"W	INV.159939
PS5	*Eusirus* cf. *giganteus*	Antarctica	PS118	Weddel Sea	12_10	63°50'14.8"S	55°35'09.7"W	INV.159940

PS6	*Eusirus* cf. *giganteus*	Antarctica	PS118	Weddel Sea	12_10	63°50'14.8"S	55°35'09.7"W	INV.159941
PS7	*Eusirus* cf. *giganteus*	Antarctica	PS118	Weddel Sea	12_10	63°50'14.8"S	55°35'09.7"W	INV.159942
PS8	*Eusirus* cf. *giganteus*	Antarctica	PS118	Weddel Sea	12_10	63°50'14.8"S	55°35'09.7"W	INV.159943
PS9	*Eusirus* cf. *giganteus*	Antarctica	PS118	Weddel Sea	12_10	63°50'14.8"S	55°35'09.7"W	INV.159944
PS10	*Eusirus* cf. *giganteus*	Antarctica	PS118	Weddel Sea	9_5	64°01'13.9"S	55°54'27.0"W	INV.159945
EE23	*Eusirus giganteus* G1	Antarctica	CEAMARC	Adelie Coast	08 (lot 766)	66°33'51.4"S	142°23'13.9"E	MNHN-IU-2019-3362
EF32	*Eusirus giganteus* G1	Antarctica	CEAMARC	Adelie Coast	66 (lot 300)	66°00'14.2"S	143°42'57.9"E	Specimen missing
EE32	*Eusirus giganteus* G2	Antarctica	CEAMARC	Adelie Coast	19 (lot 3083)	66°10'14.3"S	139°21'11.3"E	MNHN-IU-2019-3365
EE26	*Eusirus giganteus* G2	Antarctica	CEAMARC	Adelie Coast	19 (lot 3103)	66°10'14.3"S	139°21'11.3"E	MNHN-IU-2019-3363
EC14	*Eusirus giganteus* G3	Antarctica	ANT-XXIII/8	End of the Antarctic Peninsula	683-1/684-1	62°57'46.2"S	57°57'53.4"W	INV. 138481
EE29	*Eusirus giganteus* G3	Antarctica	CEAMARC	Adelie Coast	38 (lot 1974)	66°18'55.9"S	143°18'05.1"E	MNHN-IU-2019-3366
ED25	*Eusirus giganteus* G4A	Antarctica	ANT-XXIII/8	Larsen B	700-2	65°55'04.2"S	60°20'09.0"W	INV. 132515
ED1	*Eusirus giganteus* G4B	Antarctica	ANT-XXIV/2 (ANDEEP SYSTCO)	East Weddell	48-1	70°23'56.4"S	8°19'08.4"W	INV. 138477
ED2	*Eusirus giganteus* G4B	Antarctica	ANT-XXIV/2 (ANDEEP SYSTCO)	East Weddell	48-1	70°23'56.4"S	8°19'08.4"W	INV. 132514
ED8	*Eusirus giganteus* G4B	Antarctica	ANT-XXIV/2 (ANDEEP SYSTCO)	East Weddell	48-1	70°23'56.4"S	8°19'08.4"W	INV. 138479
ED4	*Eusirus giganteus* G4B	Antarctica	ANT-XXIV/2 (ANDEEP SYSTCO)	East Weddell	48-1	70°23'56.4"S	8°19'08.4"W	INV. 138478
EE11	*Eusirus microps*	Antarctica	CEAMARC	Adelie Coast	49A (lot 1263)	67°02'48.9"S	145°09'03.0"E	IU-2008-787
EF10	*Eusirus microps*	Antarctica	CEAMARC	Adelie Coast	19 (lot 3103)	66°10'14.3"S	139°21'11.3"E	No voucher
EF12	*Eusirus microps*	Antarctica	CEAMARC	Adelie Coast	19 (lot 3103)	66°10'14.3"S	139°21'11.3"E	IU-2008-855
EC23	*Eusirus perdentatus* P2	Antarctica	ANT-XXI/2 (BENDEX)	East Weddell	253-1	71°04'53.4"S	11°32'12.6"W	INV. 132568
EC19	*Eusirus perdentatus* P2	Antarctica	ANT-XXI/2 (BENDEX)	East Weddell	253-1	71°04'53.4"S	11°32'12.6"W	INV. 132562
EB8	*Eusirus perdentatus* P2	Antarctica	JR144 (BIOPEARL I)	Elephant Islands	EI-EBS-4-Supra	61°20'07.6"S	55°12'13.6"W	INV. 138473
EB10	*Eusirus perdentatus* P2	Antarctica	JR144 (BIOPEARL I)	Elephant Islands	EI-EBS-4-Supra	61°20'07.6"S	55°12'13.6"W	INV. 138471
EF13	*Eusirus pontomedon*	Antarctica	CEAMARC	Adelie Coast	79 (lot 3678)	65°42'24.9"S	140°35'50.6"E	MNHN-IU-2019-3358
AWI10	*Eusirus pontomedon*	Antarctica	ANT-XXIX-9	Southern Weddell Sea	88-1	76° 57.98‘ S	32° 56.67‘ W	INV. 138471
AWI7	*Eusirus pontomedon*	Antarctica	ANT-XXIX-9	Southern Weddell Sea	88-1	76° 57.98‘ S	32° 56.67‘ W	INV. 138470

EU78	*Eusirus propeperdentatus*	Antarctica	ANTXXIX-3	Southeast of Clarence Island	135-1	61°30'01.8"S	53°43'34.8"W	INV. 122804
EE27	*Eusirus propeperdentatus*	Antarctica	CEAMARC	Adelie Coast	19 (lot 3103)	66°10'14.3"S	139°21'11.3"E	MNHN-IU-2019-3355
EE24	*Eusirus propeperdentatus*	Antarctica	CEAMARC	Adelie Coast	19 (lot 3103)	66°10'14.3"S	139°21'11.3"E	MNHN-IU-2019-3354
EU17	*Eusirus laticarpus* 2	Antarctica	ANTXXIX-3	Joinville island	152-2	63°50'48.6"S	50°51'39.6"W	INV.159946
EB19	*Eusirus laticarpus* 1	Antarctica	JR179	Amundsen Sea	BIO4-EBS-3D-EPI	74°23'27.2"S	104°46'02.1"W	INV.159947
EU67	*Eusirus laticarpus* 1	Antarctica	ANTXXIX-3	Drake Passage	234-5	62°17'21.6"S	61°12'03.6"W	INV. 122856
EU15	*Eusirus laticarpus* 2	Antarctica	ANTXXIX-3	Joinville Island	147-1	62°46'03.0"S	51°43'03.6"W	INV.159948
EU18	*Eusirus laticarpus* 2	Antarctica	ANTXXIX-3	Joinville island	152-2	63°50'48.6"S	50°51'39.6"W	INV.159950
EC25	*Eusirus laticarpus* 1	Antarctica	ANT-XXI/2 (BENDEX)	East Weddell	259-1	70°56'34.2"S	10°31'58.8"W	INV. 132572
EC26	*Eusirus laticarpus* 1	Antarctica	ANT-XXI/2 (BENDEX)	East Weddell	245-1	70°56'44.4"S	10°32'36.0"W	INV.132573
EC29	*Eusirus laticarpus* 1	Antarctica	ANT-XXI/2 (BENDEX)	East Weddell	248-1	71°05'30.6"S	11°30'27.6"W	INV.132564
EC27	*Eusirus laticarpus* 1	Antarctica	ANT-XXI/2 (BENDEX)	East Weddell	259-1	70°56'34.2"S	10°31'58.8"W	INV.132574
EU88	*Eusirus cuspidatus*	Arctic	not indicated	Resolute Bay, Canada	nd	74°41'02.4"N	94°51'25.2"W	NUN-0011
EU85	*Eusirus cuspidatus*	Arctic	not indicated	Resolute Bay, Canada	nd	74°41'02.4"N	94°51'25.2"W	NUN-0008
EU84	*Eusirus cuspidatus*	Arctic	not indicated	Resolute Bay, Canada	nd	74°41'02.4"N	94°51'25.2"W	NUN-0007
EU89	*Eusirus cuspidatus*	Arctic	not indicated	Resolute Bay, Canada	nd	74°41'02.4"N	94°51'25.2"W	NUN-0012
ED18	*Eusirus minutus*	Arctic	Cruise without a specific name	Malangen, Norway	726-02	69°33'26.4"N	18°00'02.4"E	INV. 132590
ED20	*Eusirus minutus*	Arctic	Cruise without a specific name	Malangen, Norway	726-02	69°33'26.4"N	18°00'02.4"E	INV.159951
ED16	*Eusirus minutus*	Arctic	Cruise without a specific name	Malangen, Norway	726-02	69°33'26.4"N	18°00'02.4"E	INV.132593
ED17	*Eusirus minutus*	Arctic	Cruise without a specific name	Malangen, Norway	726-02	69°33'26.4"N	18°00'02.4"E	INV.132587
ED19	*Eusirus minutus*	Arctic	Cruise without a specific name	Malangen, Norway	726-02	69°33'26.4"N	18°00'02.4"E	INV. 132585
ED13	*Eusirus* cf. *propinquus*	Arctic	Cruise without a specific name	Kvalsund,Norway	734-02	69°52'02.4"N	18°52'49.2"E	INV. 132592
ED15	*Eusirus propinquus*	Arctic	Cruise without a specific name	Kvalsund,Norway	734-02	69°52'02.4"N	18°52'49.2"E	INV.132591
ED14	*Eusirus propinquus*	Arctic	Cruise without a specific name	Kvalsund,Norway	734-02	69°52'02.4"N	18°52'49.2"E	INV.132586
JPIO1	*Eusirus sp.* 4	Non-polar	SO239-171	North Pacific Ocean	not indicated	14°02'32.4"N	130°06'05.4"W	INV.159952

Supplementary Tables

JPIO3	*Eusirus sp.* 7	Non-polar	SO239-133	North Pacific Ocean	not indicated	13°50'56.4"N	123°15'12.6"W	INV.159953
JPIO5	*Eusirus sp*. 5	Non-polar	SO239-118	North Pacific Ocean	not indicated	13°52'22.8"N	123°15'05.4"W	INV.159954
JPIO6	*Eusirus sp.*6	Non-polar	SO239-20	North Pacific Ocean	not indicated	11°49'45.0"N	117°00'29.4"W	INV.159955
JP03	*Eusirus sp.* 3	Non-polar	TRV Toyoshio-maru (Hiroshima University)	Off Cape Toi (the southern tip of Kyushu), Japan		31°14.54'N	131° 32.20'E	EUJP-003
KT808758 & KT808739	*Rhachotropis schellenbergi*	Antarctica	ANTXXVII/3	Larsen A	226-7	64°54.84'S	60°36.63'W	RBINS INV. 132660
KT808757 & KT808738	*Rhachotropis antarctica*	Antarctica	ANTXXVII/3	East Weddell Sea	284-1	70°58.34'S	10°29.99'W	RBINS INV. 132649
ED11	*Rhachotropis schellenbergi*	Antarctica	ANT-XIX/5 (LAMPOS)	Between South Sandwich and South Orkney	223	60°08'09.6"S	34°55'54.6"W	INV.159956
ED40	*Rhachotropis antarctica*	Antarctica	JR144 (BIOPEARL I)	South Georgia	SG-EBS-E3	53°35'50.8"S	37°54'11.1"W	INV.159957

Supplementary table 4. Results of the Xia's test for substitution saturations of each gene as implemented in DAMBE version 7.3.11.

Gene	Num OTU	Iss	Iss.cSym	P	Iss.cAsym	P
18S	4	0.194	0.820	0.0000	0.788	0.0000
	8	0.200	0.788	0.0000	0.682	0.0000
	16	0.217	0.771	0.0000	0.573	0.0000
	32	0.219	0.748	0.0000	0.441	0.0000
28s	4	0.077	0.791	0.0000	0.758	0.0000
	8	0.066	0.745	0.0000	0.634	0.0000
	16	0.073	0.709	0.0000	0.499	0.0000
	32	0.074	0.695	0.0000	0.367	0.0000
COI 1st and 2nd codon positions	4	0.170	0.948	0.0000	1.104	0.0000
	8	0.171	1.047	0.0000	1.113	0.0000
	16	0.168	0.560	0.0000	0.700	0.0000
	32	0.169	1.226	0.0000	1.313	0.0000
COI 3rd codon position	4	0.166	1.400	0.0000	1.798	0.0000
	8	0.168	1.788	0.0000	2.141	0.0000
	16	0.164	0.647	0.0002	1.416	0.0000
	32	0.169	2.454	0.0000	3.381	0.0000
COII 1st and 2nd codon positions		0.1007	0.6929	0.0000	0.3784	0.0000
COII 3rd codon position		0.2900	0.7167	0.0000	0.4016	0.0000

Supplementary table 5. List of putative genetic species used in this study including the locality, geographical coordinates, and voucher ID. The presence of molecular data (Mol), morphological data (Mor) and stable isotope data for δ13C (13C) and δ15N (15N) are indicated for each specimen. Coordinates with * indicate approximate coordinates based on the known locality for standardization of stable isotopes analysis.

SampleID	Species name	Locality	Latitude	Longitude	Voucher ID	Mol	Mor	13C	15N
EX48	*Eusirus microps*	Larsen A	64°54.79' S	60°30.80' W	INV.159962		X(#sp)	x	x
EF12	*Eusirus microps*	Adelie Coast	66.17064°S	139.353133°E	IU-2008-855	x	x	x	x
EF10	*Eusirus microps*	Adelie Coast	66.17064°S	139.353133°E	No voucher	x	x	x	x
EF11	*Eusirus microps*	Adelie Coast	66.17064°S	139.353133°E	No voucher			x	x
EC30	*Eusirus microps*	East Weddell	72.85867°S	19.61317°W	INV.159960		x	x	x
EU11	*Eusirus microps*	Adelie Coast	66°37.1'S	140°00'E	MNHN-IU-2016-6623		x	x	x
EU3	*Eusirus microps*	no locality recorded	71.5306702°S	171.3005066°E	NIWA NO. 20290		x	x	x
EU2	*Eusirus microps*	no locality recorded	72.2788315°S	171.4136658°E	NIWA NO. 20289			x	x
EA2	*Eusirus microps*	East Weddell	67.97683°S	3.00433°E	INV.159961			x	x
DMSI27	*Eusirus microps*	St. 125 Antarctica, Peter I Island, off Anderssen Point	68°49’50”S*	90°44’46”W*	NHMD-672539			x	
EE11	*Eusirus microps*	Adelie Coast	67°02'48.9"S	145°09'03.0"E	IU-2008-787	x			
EU78	*Eusirus propeperdentatus*	Southeast of Clarence Island	61°30'01.8"S	53°43'34.8"W	INV. 122804	x	x	x	x
EU77	*Eusirus propeperdentatus*	no locality recorded	62°39'07.8"S	52°25'19.8"W	INV.159964		x	x	x
EU4	*Eusirus propeperdentatus*	Site C3, shelf, Western Ross Sea	75.6330000°S	169.8500000°E	NIWA NO. 36115		x	x	x
EU5	*Eusirus propeperdentatus*	Site C3, shelf, Western Ross Sea	75.6330000°S	169.8500000°E	NIWA NO. 36140			x	x
EU19	*Eusirus propeperdentatus*	Site C5, shelf, Western Ross Sea	76.5940000°S	176.8280000°E	NIWA NO. 36603		x	x	x
EU20	*Eusirus propeperdentatus*	Site C2, shelf, Western Ross Sea	74.7262000°S	167.0132000°E	NIWA NO. 35955		x	x	x
SI01	*Eusirus propeperdentatus*	Site C3, shelf, Western Ross Sea	75.6330000°S	169.8500000°E	NIWA NO. 36115			x	x
SI02	*Eusirus propeperdentatus*	Site C3, shelf, Western Ross Sea	75.6330000°S	169.8500000°E	NIWA NO. 36115			x	x
SI03	*Eusirus propeperdentatus*	Site C3, shelf, Western Ross Sea	75.6330000°S	169.8500000°E	NIWA NO. 36115			x	x
SI04	*Eusirus propeperdentatus*	Site C3, shelf, Western Ross Sea	75.6330000°S	169.8500000°E	NIWA NO. 36115			x	x
EE24/EE25	*Eusirus propeperdentatus*	Adelie Coast	66.17064°S	139.353133°E	MNHN-IU-2019-3354	x		x	x
EE27/EE28	*Eusirus propeperdentatus*	Adelie Coast	66.17064°S	139.353133°E	MNHN-IU-2019-3355	x		x	x
SI05	*Eusirus propeperdentatus*	Site D4, shelf, Southern Ross Sea	76.7750000°S	167.8360000°E	NIWA NO. 36440			x	x
SI06	*Eusirus propeperdentatus*	Site D4, shelf, southern Ross Sea	76.7750000°S	167.8360000°E	NIWA NO. 36440			x	x

SI08	*Eusirus propeperdentatus*	Site D4, shelf, southern Ross Sea	76.7750000°S	167.8360000°E	NIWA NO. 36440			x	x
SI09	*Eusirus propeperdentatus*	Site C3, shelf, Western Ross Sea	75.6330000°S	169.8500000°E	NIWA NO. 36140			x	x
EU6	*Eusirus propeperdentatus*	Site D4, shelf, southern Ross Sea	76.7750000°S	167.8360000°E	NIWA NO. 36440			x	x
EC27	*Eusirus laticarpus* 1	East Weddell	70.94283°S	10.53300°W	INV.132574	x	x	x	x
EC25	*Eusirus laticarpus* 1	East Weddell	70.94283°S	10.53300°W	INV. 132572	x	x	x	x
EU15	*Eusirus laticarpus* 2	Joinville Island	62°46'03.0"S	51°43'03.6"W	INV.159948	x	x	x	
EU17	*Eusirus laticarpus* 2	Joinville Island	63°50'48.6"S	50°51'39.6"W	INV.159946	x	x	x	
EU18	*Eusirus laticarpus* 2	Joinville Island	63°50'48.6"S	50°51'39.6"W	INV.159950	x	x	x	
EB19	*Eusirus laticarpus* 1	Amundsen Sea	74.39088°S	104.76726°W	INV.159963	x		x	x
EC26	*Eusirus laticarpus* 1	East Weddell	70.94567°S	10.54333°W	INV.132573	x		x	x
EU67	*Eusirus laticarpus* 1	Drake Passage	62°17'21.6"S	61°12'03.6"W	INV. 122856	x			
EC29	*Eusirus laticarpus* 1	East Weddell	71°05'30.6"S	11°30'27.6"W	INV.132564	x			
EU12	*Eusirus laticarpus*	Adelie Coast	66°38.4'S	139°53.7'E	MNHN-IU-2019-2163			x	x
EU16	*Eusirus laticarpus*	Joinville Island	62°46'03.0"S	51°43'03.6"W	INV.159997			x	
EU1	*Eusirus laticarpus*	Ross sea	71.7549973°S	171.1425018°E	NIWA NO. 20288			x	x
EU29	*Eusirus perdentatus*	no locality recorded	71.7549973°S	171.1425018°E	NIWA NO. 20221		x	x	x
EU28	*Eusirus perdentatus*	no locality recorded	71.7549973°S	171.1425018°E	NIWA NO. 20221		x	x	x
EU36	*Eusirus perdentatus*	no locality recorded	71.3098297°S	170.4771729°E	NIWA NO. 20233		x	x	x
EU33	*Eusirus perdentatus*	no locality recorded	72.2768326°S	171.4490051°E	NIWA NO. 20228		x	x	x
EU30	*Eusirus perdentatus*	no locality recorded	71.7549973°S	171.1425018°E	NIWA NO. 20223		x	x	x
EU26	*Eusirus perdentatus*	no locality recorded	71.8010025°S	170.9413300°E	NIWA NO. 20217		x	x	x
EU46	*Eusirus perdentatus*	no locality recorded	71.6015015°S	170.8804932°E	NIWA NO. 20246		x	x	x
EU44	*Eusirus perdentatus*	no locality recorded	71.5120010°S	171.4251709°E	NIWA NO. 20243		x	x	x
EU45	*Eusirus perdentatus*	no locality recorded	71.5475006°S	171.1111603°E	NIWA NO. 20244		x	x	x
EU48	*Eusirus perdentatus*	no locality recorded	71.6206665°S	170.8665009°E	NIWA NO. 20248		x		
EU32	*Eusirus perdentatus*	no locality recorded	72.1279984°S	172.7006683°E	NIWA NO. 20226			x	x
EU27	*Eusirus perdentatus*	no locality recorded	71.7546692°S	171.4170074°E	NIWA NO. 20222			x	x
EU31	*Eusirus perdentatus*	no locality recorded	72.3418350°S	170.4429932°E	NIWA NO. 20224			x	x
EU34	*Eusirus perdentatus*	no locality recorded	71.2988358°S	170.5404968°E	NIWA NO. 20231			x	x

EU35	*Eusirus perdentatus*	no locality recorded	71.2935028°S	170.5766602°E	NIWA NO. 20230				x	x
EU37	*Eusirus perdentatus*	Cape Adare	71.3091670°S	170.450330°E	NIWA NO. 20234				x	x
EU39	*Eusirus perdentatus*	no locality recorded	71.3300018°S	170.4593353°E	NIWA NO. 20236				x	
EU41	*Eusirus perdentatus*	no locality recorded	72.0134964°S	170.7745056°E	NIWA NO. 20239				x	x
EU40	*Eusirus perdentatus*	no locality recorded	71.6446686°S	170.2188263°E	NIWA NO. 20238				x	
EU42	*Eusirus perdentatus*	no locality recorded	71.9811707°S	171.9665070°E	NIWA NO. 20241				x	
EU43	*Eusirus perdentatus*	no locality recorded	71.5296707°S	171.3008270°E	NIWA NO. 20242				x	
EU47	*Eusirus perdentatus*	no locality recorded	71.6220016°S	170.9230042°E	NIWA NO. 20247				x	x
EU48	*Eusirus perdentatus*	no locality recorded	71.6206665°S	170.8665009°E	NIWA NO. 20248				x	x
EUBV1	*Eusirus perdentatus*	no locality recorded	62°12.1942'S	58°23.4483'W	INV.159996				x	x
EB8	*Eusirus perdentatus*	Elephant Islands	61°20'07.6"S	55°12'13.6"W	INV. 138473	x	x	x	x	
EB10	*Eusirus perdentatus*	Elephant Islands	61°20'07.6"S	55°12'13.6"W	INV. 138471	x	x	x	x	
EB9	*Eusirus perdentatus*	Elephant Islands	61°20.13’ S	55°12.23’ W	INV. 138474		x	x	x	
EC19	*Eusirus perdentatus*	East Weddell	71°04'53.4"S	11°32'12.6"W	INV. 132562	x	x	x	x	
EC23	*Eusirus perdentatus*	East Weddell	71°04'53.4"S	11°32'12.6"W	INV. 132568	x	x	x	x	
EC22	*Eusirus perdentatus*	East Weddell	71.08150°S	11.53683°W	INV. 132571			x	x	
EE21	*Eusirus perdentatus*	Adelie Coast	66.003882°S	142.313777°E	MNHN-IU-2019-3361			x	x	
MH3	*Eusirus perdentatus*	Bransfield Strait	62°43'43.8"S	57°29'02.4"W	INV. 138476			x	x	
ED28	*Eusirus perdentatus*	Elephant Islands	61.07300°S	55.99683°W	INV. 132539			x	x	
ED7	*Eusirus perdentatus*	East Weddell	71.10733°S	11.46267°W	INV. 138475			x	x	
ED10	*Eusirus sp.* 2	North of Bouvet Island	47°38'43.8"S	4°15'12.0"E	INV.159935	x				
AWI6	*Eusirus pontomedon*	South-East Weddell Sea	76°57.98’ S	32°56.67’ W	INV. 138464		x	x	x	
AWI10	*Eusirus pontomedon*	Southern Weddell Sea	76° 57.98‘ S	32° 56.67‘ W	INV. 138471	x	x	x	x	
AWI11	*Eusirus pontomedon*	South-East Weddell Sea	76°57.98’ S	32°56.67’ W	INV. 138466		x	x	x	
AWI7	*Eusirus pontomedon*	Southern Weddell Sea	76°57.98‘ S	32°56.67‘ W	INV. 138470	x	x	x	x	
AWI12	*Eusirus pontomedon*	South-East Weddell Sea	76°57.98’ S	32°56.67’ W	INV. 138467		x	x	x	
EE31	*Eusirus pontomedon*	Adelie Coast	67°04.06’ S	144°39.71’ E	MNHN-IU-2019-3355		x	x	x	
HE4	*Eusirus pontomedon*	Bransfield Strait	62°55.83’ S	58°41.09’ W	INV.122811		x	x	x	
EE6	*Eusirus pontomedon*	Adelie Coast	65°42.41’ S	140°35.84’ E	MNHN-IU-2019-3356		x	x	x	

EF14	*Eusirus pontomedon*	Adelie Coast	65°42.41’ S	140°35.84’ E	MNHN-IU-2019-3359		x	x	x
EF13	*Eusirus pontomedon*	Adelie Coast	65°42.41’ S	140°35.84’ E	MNHN-IU-2019-3358	x	x	x	x
EF7/EC3	*Eusirus pontomedon*	North-East Weddell Sea	72°50.18’ S	19°35.94’ W	INV. 138465		x	x	x
ED5	*Eusirus pontomedon*	North-East Weddell Sea	70°23.94’ S	8°19.14’ W	INV. 132512		x	x	x
AWI19	*Eusirus pontomedon*	Southern Weddell Sea	76° 57.98’ S	32° 56.67’ W	INV. 138469			x	x
AWI13	*Eusirus pontomedon*	Southern Weddell Sea	76° 57.98’ S	32° 56.67’ W	INV. 138468			x	x
ED6	*Eusirus pontomedon*	NE of King George Island	61.63617°S	57.54433°W	INV. 132513			x	x
EE7	*Eusirus pontomedon*	Adelie Coast	65.706925°S	140.597385°E	MNHN-IU-2019-3357			x	x
EU76	*Eusirus antarcticus*	Bendex	70°50.69' S	10°35.51' W	INV.159984		x	x	x
EU23	*Eusirus antarcticus*	no locality recorded	71.9971695°S	172.1239929°E	NIWA NO. 20286		x	x	
EU70	*Eusirus antarcticus*	Bransfield Strait	62°45'03.0"S	57°26'40.8"W	INV.159985		x	x	x
EU69	*Eusirus antarcticus*	Weddell Sea	63°50'55.2"S	55°37'39.6"W	INV.159986		x	x	x
EU66	*Eusirus antarcticus*	Bransfield Strait	62°55'49.8"S	58°41'05.4"W	INV.159989		x	x	x
EF35	*Eusirus antarcticus*	Adelie Coast	65.5063°S	139.358743°E	No voucher		x	x	x
EB14	*Eusirus antarcticus*	Amundsen Sea	74°23'54.4"S	104°37'55.7"W	INV.159925	x	x	x	x
ED24	*Eusirus antarcticus*	King Haakon VII Sea	70.39900°S	8.31900°W	INV.159980		x	x	x
EB5	*Eusirus antarcticus*	Elephant Islands	61.33394°S	55.19509°W	INV. 138482	x		x	x
EE39	*Eusirus antarcticus*	Adelie Coast	65.5063°S	139.358743°E	No voucher	x		x	x
EF34	*Eusirus antarcticus*	Adelie Coast	65.5063°S	139.358743°E	No voucher	x		x	x
EE12	*Eusirus antarcticus*	Adelie Coast	66.148263°S	140.649927°E	No voucher			x	
EU21	*Eusirus antarcticus*	no locality recorded	71.8010025°S	170.9413300°E	NIWA NO. 20283			x	x
EU24	*Eusirus antarcticus*	no locality recorded	71.5005035°S	171.6069946°E	NIWA NO. 20287			x	x
EU25	*Eusirus antarcticus*	Cape Adare	71.3091670°S	170.4503330°E	NIWA NO. 20285			x	
EA7	*Eusirus antarcticus*	East Weddell	70.39900°S	8.31900°W	INV.159981			x	x
EU68	*Eusirus antarcticus*	Weddell Sea	63°51'31.8"S	55°40'44.4"W	INV.159982			x	x
EU73	*Eusirus antarcticus*	Bendex	70° 56.40' S	10° 32.60' W	INV.159983			x	x
EU55	*Eusirus antarcticus*	Shag Rocks	53° 23.94' S	42° 40.10' W	14.02.2011			x	x
EU56	*Eusirus antarcticus*	Bendex	70° 51.30' S,	10° 35.35' W	INV.159988			x	x
EB18	*Eusirus sp.* 8 juvenile	Amundsen Sea	74°23'54.4"S	104°37'55.7"W	INV.159932	x			

EB6	*Eusirus bouvieri* 2	Elephant Islands	61.33394°S	55.19509°W	INV.159926	x		x	x
EB7	*Eusirus bouvieri*	Elephant Islands	61.33394°S	55.19509°W	INV.159990			x	x
EU79	*Eusirus bouvieri*	Adelie Coast	66°39.6'S	140°02'E	MNHN-IU-2016-6246			x	x
EU62	*Eusirus bouvieri*	Weddell Sea	63°51'31.8"S	55°40'44.4"W	INV.159993			x	x
EU63	*Eusirus bouvieri*	Bransfield Strait	62°53'38.4"S	58°12'31.2"W	INV.159994			x	x
EF26	*Eusirus bouvieri* 1	Adelie Coast	66°33'42.5"S	141°15'43.0"E	No voucher	x	x	x	x
EB2	*Eusirus bouvieri* 2	Elephant Islands	61°20'02.2"S	55°11'42.3"W	INV.159927	x	x	x	x
EF29	*Eusirus bouvieri* 1	Adelie Coast	66°33'42.5"S	141°15'43.0"E	No voucher	x	x		
EU80	*Eusirus bouvieri*	Adelie Coast	66°37.1'S	140°00'E	MNHN-IU-2016-6227			x	x
EE19	*Eusirus bouvieri* 2	Adelie Coast	66.316385°S	142.000365°E	No voucher	x		x	x
EF22	*Eusirus bouvieri* 1	Adelie Coast	66.148263°S	140.649927°E	No voucher	x		x	x
EF21	*Eusirus bouvieri* 1	Adelie Coast	66.148263°S	140.649927°E	No voucher	x		x	x
EB3	*Eusirus bouvieri* 2	Elephant Islands	61.33394°S	55.19509°W	INV.159928	x		x	x
EB4	*Eusirus bouvieri*	Elephant Islands	61.33394°S	55.19509°W	INV.159927			x	x
EE36	*Eusirus bouvieri*	Adelie Coast	66.000305°S	142.0143°E	No voucher			x	x
EU74	*Eusirus bouvieri*	Larsen A	64° 54.75' S	60° 39.01' W	INV.159991			x	x
EU57	*Eusirus bouvieri*	Bendex	70° 50.64' S	10° 36.11' W	INV.159992			x	x
EU82	*Eusirus bouvieri*	Adelie Coast	66°36.7'S	140°04.3'E	MNHN-IU-2016-6454			x	x
EE22	*Eusirus bouvieri*	Adelie Coast	66.564283°S	142.387202°E	No voucher			x	x
EU65	*Eusirus bouvieri*	Bransfield Strait	62°45'03.0"S	57°26'40.8"W	INV.159995			x	x
EUP1	*Eusirus* cf. *bouvieri*	Weddel Sea	63°50'14.8"S	55°35'09.7"W	INV.159949	x			
EB17	*Eusirus sp.* 9 juvenile	Amundsen Sea	74°23'54.4"S	104°37'55.7"W	INV.159931	x			
EU64	*Eusirus giganteus*	Bransfield Strait	62°56'04.2"S	57°58'08.4"W	INV.159976			x	x
EU53	*Eusirus giganteus*	Bendex	70°47.34' S	10°40.39' W	INV.159970			x	x
PS7	*Eusirus giganteus* G2	Weddell Sea	63°50'14.8"S	55°35'09.7"W	INV.159942	x	x	x	x
PS8	*Eusirus giganteus* G4a	Weddell Sea	63°50'14.8"S	55°35'09.7"W	INV.159943	x	x	x	x
PS9	*Eusirus giganteus* G4a	no locality recorded	63°50'14.8"S	55°35'09.7"W	INV.159944	x		x	x
PS10	*Eusirus giganteus* G1	Weddell Sea	64°01'13.9"S	55°54'27.0"W	INV.159945	x	x	x	x
PS6	*Eusirus giganteus* G1	no locality recorded	63°50'14.8"S	55°35'09.7"W	INV.159941	x		x	x

PS5	*Eusirus giganteus* G4a	Weddell Sea	63°50'14.8"S	55°35'09.7"W	INV.159940	x	x	x	x	
PS4	*Eusirus giganteus* G4a	Weddell Sea	63°50'14.8"S	55°35'09.7"W	INV.159939	x	x	x	x	
PS3	*Eusirus giganteus* G1	no locality recorded	63°50'14.8"S	55°35'09.7"W	INV.159938	x		x	x	
PS2	*Eusirus giganteus* G1	Weddell Sea	63°50'14.8"S	55°35'09.7"W	INV.159937	x	x	x	x	
PS1	*Eusirus giganteus* G2	no locality recorded	64°01'13.9"S	55°54'27.0"W	INV.159936	x		x	x	
EU49	*Eusirus giganteus*	King George Island	62° 18.15' S	58° 40.50' W	INV.159967			x	x	
EU50	*Eusirus giganteus*	King George Island	62° 18.21' S	58° 39.90' W	INV.159968			x	x	
EU51	*Eusirus giganteus*	Larsen A	64° 54.79' S	60° 30.80' W	INV.159969			x	x	
EU52	*Eusirus giganteus*	Bendex	70° 47.34' S,	10° 40.39' W	INV.159971			x	x	
EU71	*Eusirus giganteus*	King George Island	66° 11.53' S	60° 8.10' W	INV.159972			x	x	
EU61	*Eusirus giganteus*	Bransfield Strait	62°53'27.0"S	58°13'03.6"W	INV.159973			x	x	
EU58	*Eusirus giganteus*	Bransfield Strait	62°55'49.8"S	58°41'05.4"W	INV.159974			x	x	
EU59	*Eusirus giganteus*	Bransfield Strait	62°47'48.0"S	57°05'21.0"W	INV.159975			x	x	
EU94	*Eusirus giganteus*	Site C2, shelf, western Ross Sea	74.7340000°S	167.1245000°E	NIWA NO. 36072			x	x	
SI10	*Eusirus giganteus*	Site C25, slope 1, Ross Sea	72.0755000°S	172.9043333°E	NIWA NO. 37701			x	x	
EE23	*Eusirus giganteus* G1	Adelie Coast	66.564283°S	142.387202°E	MNHN-IU-2019-3362	x		x	x	
EU72	*Eusirus giganteus*	King George Island	62° 18.21' S	58° 39.90' W	INV.159977			x	x	
EU75	*Eusirus giganteus*	Bendex	70° 47.34' S	10° 40.39' W	INV.159978			x	x	
EU95	*Eusirus giganteus*	Site C3, shelf, Western Ross Sea	75.6216667°S	169.8045000°E	NIWA NO. 42764			x	x	
EU99	*Eusirus giganteus*	Site C3, shelf, Western Ross Sea	75.6330000°S	169.8500000°E	NIWA NO. 36141			x	x	
EU60	*Eusirus giganteus*	Bransfield Strait	62°25'57.0"S	56°17'15.6"W	INV.159979			x	x	
EU92	*Eusirus giganteus*	Site C25, slope 1, Ross Sea	72.0755000°S	172.9043333°E	NIWA NO. 37701			x	x	
EU93	*Eusirus giganteus*	Site C4, shelf, western Ross Sea	76.1930556°S	176.2961111°E	NIWA NO. 36740			x	x	
EU96	*Eusirus giganteus*	Site C16, Ross Sea, slope 2	72.3168333°S	175.4738333°E	NIWA NO. 42767			x	x	
EU98	*Eusirus giganteus*	site C1, shelf, eastern Ross Sea	73.1245000°S	174.3205000°E	NIWA NO. 35351			x	x	
EF32	*Eusirus giganteus* G1	Adelie Coast	66°00'14.2"S	143°42'57.9"E	Specimen missing	x				

EE29	*Eusirus giganteus* G3	Adelie Coast	66.315523°S	143.301408°E	MNHN-IU-2019-3366	x	x	x	x	
EC14	*Eusirus giganteus* G3	End of the Antarctic Peninsula	62.96283°S	57.96483°W	INV. 138481	x	x	x	x	
EE32	*Eusirus giganteus* G2	Adelie Coast	66°10'14.3"S	139°21'11.3"E	MNHN-IU-2019-3365	x	x	x	x	
EE30	*Eusirus giganteus* G2	Adelie Coast	66°19.99’ S	143°21.42’ E	MNHN-IU-2019-3364		x	x	x	
EE26	*Eusirus giganteus* G2	Adelie Coast	66.17064°S	139.353133°E	MNHN-IU-2019-3363	x		x	x	
ED25	*Eusirus giganteus* G4a	Larsen B	65°55'04.2"S	60°20'09.0"W	INV. 132515	x				
ED1	*Eusirus giganteus* G4b	East Weddell	70°23'56.4"S	8°19'08.4"W	INV. 138477	x	x	x	x	
ED2	*Eusirus giganteus* G4b	East Weddell	70°23'56.4"S	8°19'08.4"W	INV. 132514	x	x			
ED3	*Eusirus giganteus* G4b	Eastern Weddell Sea	70°23.94’ S	8°19.14’ W	INV. 138480		x	x	x	
ED4	*Eusirus giganteus* G4b	East Weddell	70.39900°S	8.31900°W	INV. 138478	x		x	x	
ED8	*Eusirus giganteus* G4b	East Weddell	70.39900°S	8.31900°W	INV. 138479	x		x	x	
EB01	*Eusirus sp.* 1	Amundsen Sea	71°20'56.2"S	109°57'53.2"W	INV.159929	x	x			
EB15	*Eusirus sp.* 1	Amundsen Sea	74°23'54.4"S	104°37'55.7"W	INV.159933	x	x			
EB16	*Eusirus sp.* 1	Amundsen Sea	74°23'54.4"S	104°37'55.7"W	INV.159934	x	x			
EB20	*Eusirus sp.* 1	Amundsen Sea	74°23'27.2"S	104°46'02.1"W	INV.159930	x				
EU83	*Eusirus holmii*	Baffin Bay	73°22’26”N*	70°48’04”W*	BIOUG00940-C12		x	x	x	
DMEU11	*Eusirus holmii*	Amerloq Fjord near Sisimiut, West Greenland	66°47’46”N*	53°48’05”W*	NHMD-672529		x	x	x	
DMSI13	*Eusirus holmii*	Amerloq Fjord near Sisimiut, West Greenland	66°47’46”N*	53°48’05”W*	NHMD-672529		x	x	x	
DMSI20	*Eusirus holmii*	Amerloq Fjord near Sisimiut, West Greenland	66°47’46”N*	53°48’05”W*	NHMD-672529			x	x	
DMSI21	*Eusirus holmii*	Amerloq Fjord near Sisimiut, West Greenland	66°47’46”N*	53°48’05”W*	NHMD-672529		x	x	x	
DMSI16	*Eusirus holmii*	Amerloq Fjord near Sisimiut, West Greenland	66°47’46”N*	53°48’05”W*	NHMD-672529			x	x	
DMSI23	*Eusirus holmii*	Amerloq Fjord near Sisimiut, West Greenland	66°47’46”N*	53°48’05”W*	NHMD-672529		x	x	x	
DMSI10	*Eusirus holmii*	Amerloq Fjord near Sisimiut, West Greenland	66°47’46”N*	53°48’05”W*	NHMD-672529			x	x	
DMSI15	*Eusirus holmii*	Amerloq Fjord near Sisimiut, West Greenland	66°47’46”N*	53°48’05”W*	NHMD-672529			x	x	
DMSI14	*Eusirus holmii*	Amerloq Fjord near Sisimiut, West Greenland	66°47’46”N*	53°48’05”W*	NHMD-672529		x	x	x	
DMSI12	*Eusirus holmii*	Amerloq Fjord near Sisimiut, West Greenland	66°47’46”N*	53°48’05”W*	NHMD-672529		x	x	x	
DMSI22	*Eusirus holmii*	Amerloq Fjord near Sisimiut, West Greenland	66°47’46”N*	53°48’05”W*	NHMD-672529			x	x	
DMSI24	*Eusirus holmii*	Amerloq Fjord near Sisimiut, West Greenland	66°47’46”N*	53°48’05”W*	NHMD-672529			x	x	
DMSI17	*Eusirus holmii*	Amerloq Fjord near Sisimiut, West Greenland	66°47’46”N*	53°48’05”W*	NHMD-672529			x	x	

DMSI18	*Eusirus holmii*	Amerloq Fjord near Sisimiut, West Greenland	66°47’46”N*	53°48’05”W*	NHMD-672529			x	x
DMSI19	*Eusirus holmii*	Amerloq Fjord near Sisimiut, West Greenland	66°47’46”N*	53°48’05”W*	NHMD-672529			x	x
EU84	*Eusirus cuspidatus*	Resolute Bay	74°41'02.4"N	94°51'25.2"W	NUN-0007	x	x	x	x
EU86	*Eusirus cuspidatus*	Resolute Bay	74°41'02.4"N	94°51'25.2"W	NUN-0009		x	x	x
EU87	*Eusirus cuspidatus*	Resolute Bay	74°41'02.4"N	94°51'25.2"W	NUN-0010			x	x
EU88	*Eusirus cuspidatus*	Resolute Bay	74°41'02.4"N	94°51'25.2"W	NUN-0011	x		x	x
EU89	*Eusirus cuspidatus*	Resolute Bay	74°41'02.4"N	94°51'25.2"W	NUN-0012	x	x	x	x
EU90	*Eusirus cuspidatus*	Resolute Bay	74°41'02.4"N	94°51'25.2"W	NUN-0013		x	x	x
DMEU2	*Eusirus cuspidatus*	Davis Strait	67°57'00.0"N	55°30'00.0"W	NHMD-672524		x		
DMSI1	*Eusirus cuspidatus*	North of Iceland	66°33'00.0"N	20°05'00.0"W	NHMD-672525			x	x
DMSI2	*Eusirus cuspidatus*	Davis Strait	67°57'00.0"N	55°30'00.0"W	NHMD-672524			x	x
DMSI26	*Eusirus cuspidatus*	Fyllas Bank, West of Nuuk, West Greenland	64°00'00.0"N*	53°00'00.0"W*	NHMD-672526		x	x	x
DMSI25	*Eusirus cuspidatus*	Sermilik Fjord, Katek, East Greenland	66°12’25”N*	37°37’36”W*	NHMD-672527		x	x	x
EU85	*Eusirus cuspidatus*	Resolute Bay	74°41'02.4"N	94°51'25.2"W	NUN-0008	x		x	x
ED14	*Eusirus propinqvus*	Kvalsund Kårvik, Norway	69.86733°N	18.88033°E	INV.132586	x	x	x	x
DMSI41	*Eusirus propinqvus*	Finnmark, Norway	70°35’09”N*	25°42’15”E*	NHMD-672540		x	x	
DMEU9	*Eusirus propinqvus*	Finnmark, Norway	no coordinates	no coordinates	NHMD-672540		x		
DMSI42	*Eusirus propinqvus*	Finnmark, Norway	70°35’09”N*	25°42’15”E*	NHMD-672540		x		
ED13	*Eusirus propinqvus*	Kvalsund Kårvik, Norway	69.86733°N	18.88033°E	INV. 132592	x		x	x
ED15	*Eusirus propinqvus*	Kvalsund Kårvik, Norway	69.86733°N	18.88033°E	INV.132591	x		x	x
EF3/ED16	*Eusirus minutus*	Malangen Torsnes, Norway	69.55733°N	18.00067°E	INV.132593	x	x	x	x
ED17/EF2	*Eusirus minutus*	Malangen Torsnes, Norway	69.55733°N	18.00067°E	INV.132587	x	x	x	x
EF4/ED18	*Eusirus minutus*	Malangen Torsnes, Norway	69.55733°N	18.00067°E	INV. 132590	x	x	x	x
EF5/ED19	*Eusirus minutus*	Malangen Torsnes, Norway	69.55733°N	18.00067°E	INV. 132585	x		x	x
ED20	*Eusirus minutus*	Malangen, Norway	69°33'26.4"N	18°00'02.4"E	INV.159951	x			
EUI2	*Eusirus longipes*	Ancona, Adriatic Sea	no coordinates	no coordinates	no voucher		x		
EUI3	*Eusirus longipes*	Golfo di Napoli, Vervece	40°37'07.7"N*	14°19'29.0"E*	No voucher			x	x
EUI4	*Eusirus longipes*	Les Embiez, Toulon	43°07'13.3"N*	6°55'15.3"E*	no voucher		x	x	x
EUI5	*Eusirus longipes*	Les Embiez - Toulon	43°07'13.3"N*	6°55'15.3"E*	no voucher			x	x

EUI8	*Eusirus longipes*	Bergen, Norway	60°18'47.4"N*	5°11'10.6"E*	no voucher	x	x	x
DMEU4	*Eusirus longipes*	Trindelen, Denmark	57°22″53″N*	10°36′55″E*	NHMD-672536	x	x	
DMSI5	*Eusirus longipes*	West of Gothenburg, 4½ miles West of Vinga Lighthouse, West Sweden	57°38′16″N*	11°26′54″E*	NHMD-672538		x	
DMSI47	*Eusirus longipes*	Trindelen, Denmark	57°22″53″N*	10°36′55″E*	NHMD-672536		x	
DMEU3	*Eusirus longipes*	Lusitanean	35°50'00.0"N	6°03'00.0"W	NHMD-672532	x	x	
DMSI29	*Eusirus longipes*	South of West Sicily, Italy	36°25'14.8"N*	14°33'22.9"E*	NHMD-672533	x	x	
DMSI52	*Eusirus longipes*	West Norway	61°57'59.5"N*	4°09'12.8"E*	NHMD-672535	x	x	
DMSI53	*Eusirus longipes*	West Norway	61°57'59.5"N*	4°09'12.8"E*	NHMD-672535		x	
DMSI54	*Eusirus longipes*	West Norway	61°57'59.5"N*	4°09'12.8"E*	NHMD-672535		x	
DMSI55	*Eusirus longipes*	West Norway	61°57'59.5"N*	4°09'12.8"E*	NHMD-672535		x	
DMSI56	*Eusirus longipes*	West Norway	61°57'59.5"N*	4°09'12.8"E*	NHMD-672535		x	
DMSI57	*Eusirus longipes*	West Norway	61°57'59.5"N*	4°09'12.8"E*	NHMD-672535		x	
DMSI59	*Eusirus longipes*	West Norway	61°57'59.5"N*	4°09'12.8"E*	NHMD-672535		x	
DMSI43	*Eusirus longipes*	Lusitanean	35°50'00.0"N	6°03'00.0"W	NHMD-672532		x	
DMSI44	*Eusirus longipes*	Lusitanean	35°50'00.0"N	6°03'00.0"W	NHMD-672532		x	
DMSI46	*Eusirus longipes*	Lusitanean	35°50'00.0"N	6°03'00.0"W	NHMD-672532		x	
DMSI49	*Eusirus longipes*	Christianssund, Norway	63°06′34″N*	7°42′29″E*	NHMD-672534		x	
DMSI50	*Eusirus longipes*	West Norway	61°57'59.5"N*	4°09'12.8"E*	NHMD-672535		x	
DMSI51	*Eusirus longipes*	West Norway	61°57'59.5"N*	4°09'12.8"E*	NHMD-672535		x	
NE	*Eusirus abyssi*	Southwest of Iceland	60°37'00.0"N	27°52'00.0"W	ZMUC CRU-005028	x		
DMEU6	*Eusirus biscayensis*	Southwest of Faroes	61°07'00.0"N	9°30'00.0"W	NHMD-672523	x	x	
DMEU7	*Eusirus biscayensis*	Southwest of Faroes	61°15'00.0"N	9°35'00.0"W	NHMD-672497	x	x	
DMSI32	*Eusirus biscayensis*	Southwest of Faroes	61°15'00.0"N	9°35'00.0"W	NHMD-672497	x	x	
DMSI33	*Eusirus biscayensis*	Southwest of Faroes	61°15'00.0"N	9°35'00.0"W	NHMD-672497		x	
DMSI34	*Eusirus biscayensis*	Southwest of Faroes	61°15'00.0"N	9°35'00.0"W	NHMD-672497		x	
DMSI35	*Eusirus biscayensis*	Southwest of Faroes	61°15'00.0"N	9°35'00.0"W	NHMD-672497		x	
DMSI36	*Eusirus biscayensis*	Southwest of Faroes	61°15'00.0"N	9°35'00.0"W	NHMD-672497		x	
DMSI37	*Eusirus biscayensis*	Southwest of Faroes	61°15'00.0"N	9°35'00.0"W	NHMD-672497	x	x	

DMSI30	*Eusirus biscayensis*	Southwest of Faroes	61°07'00.0"N	9°30'00.0"W	NHMD-672523		x			
DMSI38	*Eusirus biscayensis*	Southwest of Faroes	61°15'00.0"N	9°35'00.0"W	NHMD-672497			x		
DMSI40	*Eusirus leptocarpus*	West Norway	no coordinates	no coordinates	NHMD-6725430		x			
DMSI8	*Eusirus leptocarpus*	West Norway	no coordinates	no coordinates	NHMD-6725430		x			
ED21	*Eusirus leptocarpus*	Vestfjorden East of Skrova, Norway	68.17200°N	14.95083°E	INV.159959		x	x		
ED22	*Eusirus leptocarpus*	Vestfjorden East of Skrova, Norway	68.17200°N	14.95083°E	INV.159958			x	x	
NE	*Eusirus tjalfiensis*	Greenland (Arctic)	70°41'00.0"N	52°07'00.0"W	ZMUC CRU-008396		x			
JP01	*Eusirus sp.* 10	Off Cape Toi (Southern tip of Kyushu), Japan	31°14.54'N	131°32.20'E	EUJP-001		x	x		
JPSI2	*Eusirus sp.* 11	Off Cape Toi (Southern tip of Kyushu), Japan	31°14.54'N	131°32.20'E	EUJP-002			x		
JP03	*Eusirus sp.* 3	Off Cape Toi (Southern tip of Kyushu), Japan	31°14.54'N	131°32.20'E	EUJP-003	x	x	x		
JP04	*Eusirus sp.* 12	Off Amami-Oshima Island (Northwestern Pacific Ocean), Kagoshima Prefecture, Japan	28.277150°N	129.634300°E	EUJP-004		x	x		
JP05	*Eusirus sp.* 13	Off Amami-Oshima Island (Northwestern Pacific Ocean), Kagoshima Prefecture, Japan	28.277150°N	129.634300°E	EUJP-005		x	x		
NE	*Eusirus bonnieri*	Capbreton canyon	43°36.05'N	1°46.97'W	IU-2013-5721		x			
NE	*Eusirus bonnieri*	Capbreton canyon	43°36.05'N	1°46.97'W	IU-2013-5720		x			
NE	*Eusirus bonnieri*	Capbreton canyon	43°36.05'N	1°46.97'W	IU-2013-5720		x			
NE	*Eusirus bonnieri*	Capbreton canyon	43°36.05'N	1°46.97'W	IU-2013-5720		x			
NE	*Eusirus bonnieri*	Capbreton canyon	43°36.05'N	1°46.97'W	IU-2013-5718		x			
NE	*Eusirus bonnieri*	Capbreton canyon	43°36.05'N	1°46.97'W	IU-2013-5718		x			
EBSI5707	*Eusirus bonnieri*	Capbreton canyon	43°36.05'N	1°46.97'W	IU-2013-5707			x	x	
EBSI5708	*Eusirus bonnieri*	Capbreton canyon	43°36.05'N	1°46.97'W	IU-2013-5708			x	x	
EBSI5709	*Eusirus bonnieri*	Capbreton canyon	43°36.05'N	1°46.97'W	IU-2013-5709			x	x	
EBSI5710	*Eusirus bonnieri*	Capbreton canyon	43°36.05'N	1°46.97'W	IU-2013-5710			x	x	
EBSI5718	*Eusirus bonnieri*	Capbreton canyon	43°36.05'N	1°46.97'W	IU-2013-5718			x	x	
EBSI5718 (2)	*Eusirus bonnieri*	Capbreton canyon	43°36.05'N	1°46.97'W	IU-2013-5718			x	x	
NE	*Eusirus nevandis*	Kenya	4°00'00.0"S	41°27'00.0"E	ZMUC CRU-007517		x			
JPIO5	*Eusirus sp.* 5	North Pacific Ocean	13°52'22.8"N	123°15'05.4"W	INV.159954	x	x			
JPIO2	*Eusirus sp.* 14	North Pacific Ocean	11°49'45.0"N	117°00'29.4"W	INV.159998		x			
JPIO1	*Eusirus sp.* 4	North Pacific Ocean	14°02'32.4"N	130°06'05.4"W	INV.159952	x	x			

JPIO4	*Eusirus sp.* 15	North Pacific Ocean	11°49'45.0"N	117°00'29.4"W	INV.159999		x		
JPIO3	*Eusirus sp.* 7	North Pacific Ocean	13°50'56.4"N	123°15'12.6"W	INV.159953	x	x		
JPIO6	*Eusirus sp.*6	North Pacific Ocean	11°49'45.0"N	117°00'29.4"W	INV.159955	x			
EU13	*Eusirus bulbodigitus*	Jeju Island, South Korea	33°29'12"N	126°57'17"E	INV.159965		x	x	x
EU14	*Eusirus bulbodigitus*	Jeju Island, South Korea	33°29'12"N	126°57'17"E	INV.159966		x	x	x
NE	*Eusirus parvus*	Salomon Sea Budibudi I. N Archipel Laughlan I.	9°11'24.6"N	153°55'18.0"E	MNHN-IU-2015-749		x		
EU10	*Eusirus parvus*	Salomon Sea Budibudi I. N Archipel Laughlan I.	9°10'47.4"N	153°54'27.0"E	MNHN-IU-2015-885		x	x	
EU8	*Eusirus parvus*	Salomon Sea Budibudi I. N Archipel Laughlan I.	9°11'24.6"N	153°55'18.0"E	MNHN-IU-2015-749		x	x	
EU7	*Eusirus parvus*	Salomon Sea Budibudi I. N Archipel Laughlan I.	9°11'24.6"N	153°55'18.0"E	MNHN-IU-2015-749		x	x	